Siemens Power Corporation

EMF-2055
Revision 9

Issue Date:

Consolidated Safety Analysis Report (SAR) for the Use of the ANF-250 Packaging for the Transport of Fissile Radioactive Materials

Certificate of Compliance 9217
Docket No. 71-9217

January 2000

Siemens Power Corporation

EMF-2055
Revision 9

Consolidated Safety Analysis Report (SAR) for the Use of the ANF-250 Packaging for the Transport of Fissile Radioactive Materials

Prepared: _____ 25 Jan. 00
P. C. Rieke, Transportation and Packaging Engineer
Regulatory Compliance
Date

Concurred: _____ 1-26-00
B. F. Bentley, Manager
Plant Operations
Date

Concurred: _____ 1/26/00
S. F. Gaines, Manager
Materials and Scheduling
Date

Concurred: RRF _____ 1-26-00
T. M Howe, Manager
Product Mechanical Engineering
Date

Concurred: _____ 1/26/00
D. A. Adkisson, Manager
Quality Engineering
Date

Concurred: _____ 1-26-00
C. M. Powers, Vice President
Quality and Regulatory Affairs
Date

Approved: _____ 1/25/00
L. J. Maas, Manager
Regulatory Compliance
Date

Nature of Changes

Item	Section or Page(s)	Description and Justification

EMF-2055 is a consolidated Safety Analysis Report (SAR) that has been reformatted to consolidate all referenced documents on the current USNRC certificate. This consolidated SAR was requested by the USNRC as a result of the certificate expiring at the end of January 2000 and the need for a renewal of the certificate. All changes have been identified by shading and are of editorial and format nature only.

Contents

Distribution

Controlled Distribution

NRC-HQ (6)

Notification List

D. A. Adkisson
B. F. Bentley
J. K. Davis
R. L. Foresman
S. F. Gaines
R. L. Gentz
T. M. Howe
L. J. Maas
C. D. Manning
R. D. Norman
C. M. Powers
P. C. Rieke
D. Steinigeweg
R. E. Vaughan

1. General Information

1.1 *Introduction*

1.1.1 Purpose of Application

This document is provided as the basis for a renewed certificate for continued approval for Siemens Power Corporation's (SPC's) use of the ANF-250 packaging for the transport of fissile radioactive materials. This consolidated Safety Analysis Report (SAR) is identified as SPC document EMF-2055, Revision 9 and represents the most current and applicable information contained in all references identified in NRC Certificate of Compliance (CoC) Number 9217 – Revision 8. The purpose of this document is to respond appropriately to the letter dated December 1, 1999 from C.R. Chappell to J.B. Edgar requesting this consolidated SAR.

1.1.2 Summary Information

This document includes all drawing changes and editorial modifications identified in the supplemental application letter dated June 30, 1999 from P.C. Rieke (SPC) to C.R. Chappell (NRC). Those changes were made in response to and completion of the Compensatory Action Plan agreed upon by the United States Nuclear Regulatory Commission (NRC) and SPC involving this packaging.

1.2 *Package Description*

1.2.1 Containment Boundary

The ANF-250 package consists of a 16-gauge steel inner container approximately 295 mm (11-5/8 in) outer diameter by 1454 mm (57-1/4 in) long with a bolted and gasketed top flange closure and steel welded bottom plate. The inner container is centered and supported in an approximately 571.5 mm (22-1/2 in) inner diameter by 1737 mm (68-3/8 in) long, 16-gauge steel drum by twelve 6.4 mm (1/4 in) diameter steel springs welded to the outside of the inner container near the top flange and near the bottom of the vessel. The space between the inner and outer containers is filled with vermiculite. Closure of the inner container is maintained by a lid, gasket and six 12.7 mm (1/2 in) hex-head bolts and nuts connected to a flange. The outer containment closure is made with a lid, a 12-gauge bolt locking ring with drop-forged lugs, one of which is threaded, having a 15.9 mm (5/8 in) diameter bolt and lock nut.

1.2.2 Contents

For the shipment of pellets, the pellets will be packed in pellet shipping suitcases (drawing EMF-304,306) in which the packing volume is about 124 mm (4.87 in) by 200 mm (7.87 in) by 635 mm (25 in). Two suitcases may be placed inside the inner container described above. These suitcases serve to confine the pellets to the geometry of the box. For criticality analysis, flooding within the suitcases has been assumed.

For the shipment of powder, the powder will be placed in plastic jugs within the cylindrical steel shipping container insert (see drawing EMF-306,176 for the insert) with an approximately 243

mm (9.56 in) inside diameter and 1256 mm (49.44 in) length. The insert has a bolted and gasketed top flange closure and a steel-welded bottom plate. The insert has been shown by the accident condition tests to prevent the in-leakage of water should a breach of the inner container of the ANF-250 occur during an accident condition. Water in-leakage into the insert, however, has been assumed for criticality analysis purposes.

1.2.3 Operational Features

The ANF-250 is a simple drum design with no complex operational features.

1.3 *Regulatory Requirements*

This package is identified for fissile radioactive material contents. As such it will be identified as an AF packaging. The maximum gross weight of the package is 616 pounds. The packaging is identified as the ANF-250 and is built and used as described previously in subsection 1.2. The smallest overall dimension of this package is 574 mm (22.6 in.).

The contents of the packaging will be comprised of solid uranium oxide pellets in suitcases or solid uranium oxide powder in plastic jugs, both as described in subsection 1.2.

The packages are maintained and used according to SPC's NRC approved EMF-1 Quality Assurance Manual. Appropriate measures and procedures to be followed for testing, maintenance, operational use, and ensuring the package is not tampered with during use are all identified in Sections 7 and 8 of this SAR. This includes always using a tamper indicating seal on the ring bolt.

As a result of this package being designed, constructed and used for fissile radioactive materials, a criticality transport index (TI) has been determined for each of the packages intended contents. It is as follows:

- For solid uranium oxide powder enriched to a maximum 5.0 weight percentage of U-235 in plastic jugs, a criticality TI of 1.8 is assigned.
- For solid uranium oxide pellets enriched to a maximum 5.0 weight percentage of U-235 in suitcases, a criticality TI of 0.6 is assigned.
- For solid uranium oxide powder in plastic jugs or solid uranium oxide pellets in suitcases, enriched to a maximum of 1.0 weight percentage of U-235, a criticality TI of 0.4 is assigned.

1.4 *Appendix*

[redacted]EMF-306,175 Revision 16 – Shipping Container Model ANF-250

[redacted]EMF-304,306 Revision 8 – Pellet Shipping Suit Case

[redacted]EMF-306,176 (2 sheets) Revision 5 (both sheets) – Shipping Container Inserts

2. Structural Evaluation

This section presents the structural information and evaluations showing that the ANF-250 package meets the applicable package requirements of 10 CFR 71 and IAEA Safety Standards to ensure safe and reliable shipment of its radioactive contents. The normal conditions of transport and the hypothetical accident conditions of 10 CFR 71.71 and 71.73, of IAEA Safety Standards 1973 709-714 and 719-724, and of IAEA 1985 619-624, 626-629, and 631-633 have been addressed by evaluation or testing.

2.1 *Structural Design*

The ANF-250 package consists of an inner container centered and supported inside of an outer drum structure. The space between inner and outer container is filled with vermiculite. Details of the construction are shown in Drawing EMF-306,175. The inner container functions as the containment boundary for the payload for all normal conditions of transport. In the hypothetical accident condition, the pellet shipping suitcase (Drawing EMF-304,306) and the container insert (Drawing EMF-306,176) serve to confine the payload geometry to that assumed in the criticality analysis in the case of pellet shipments, or the shipping container insert (Drawing EMF-306,176) serves to confine the payload geometry and to prevent the in-leakage of water in the case of powder shipments.

The outer drum (Drawing EMF-306,175) consists of two 55-gallon (0.21 m^3) Type DOT 17C 16-gauge or equivalent drums welded together end-to-end to form a container roughly 1750 mm (69 in) long. Closure of the drum is with a 16 gauge lid Type DOT 17C and a ring (12-gauge) with a 15.9 mm (5/8 in) bolt and nut.

The outer drum provides protection from the elements and in handling. It also provides spacing between the fissile material payloads of the containers for determining nuclear interaction in criticality safety.

The inner containment of the package is the 292 mm (11-1/2 in) inner diameter by 1454 mm (57-1/4 in) long 16-gauge steel inner container. The inner container closure is achieved by securing a 12.7 m (1/2 in) steel lid to an external flange by means of six 12.7 mm (1/2 in) hex head bolts and nuts. A seal is provided by means of a 6.4 m (1/4 in) thick silicon rubber gasket rated for 260°C (500°F) service.

2.1.1 Design Criteria

The series of evaluations and tests performed on the ANF-250 package were designed to demonstrate compliance with the current requirements for packaging as set forth in 10 CFR Part 71 and the IAEA Safety Series No. 6. The references for these requirements are listed in Table 2.1, where 10 CFR Part 71 has been used as the basis and comparable requirements from the IAEA Safety Series No. 6 are referenced. Table 2.2 is a listing of IAEA standards which are not specifically stated in 10 CFR Part 71 and are thus in addition to 10 CFR Part 71 requirements, or are different from the stated requirements of 10 CFR Part 71.

2.1.2 Weights and Center of Gravity

The ANF-250 package will weigh up to approximately 277 kg (610 lbs) when fully loaded with containers of uranium oxide which weigh about 141 kg (310 lbs). The empty ANF-250 package weighs about 136 kg (300 lbs). The container is approximately symmetrical; the center of gravity is near the geometrical center of the container.

2.2 *Mechanical Properties of Materials*

Standard commercial materials are used in the construction of the ANF-250 containers. A listing of the materials and the standards, as appropriate, appears on Drawing EMF-306,175.

2.2.1 General Standards for All Packages

The ANF-250 package complies with all of the general standards for all packaging specified in 10 CFR 71.43.

2.2.2 Minimum Package Size

The minimum dimension of the overall ANF-250 package is the 574 mm (22.6 in) diameter of the type DOT 17C drum.

2.2.3 Tamper-Proof Feature

A metal cable tamper proof seal is applied to each ANF-250 package prior to shipment. The seal (called Easy Lock) is applied using a loop method around the bolt on the closure ring of the drum so the bolt cannot be loosened without breaking the seal.

2.2.4 Positive Closure

Positive closure of the ANF-250 containers is assured by: 1) The inner container is gasketed and sealed with six hex head bolts and nuts, and 2) The outer container is sealed by a standard 17H 12-gauge bolt locking ring with drop forged lugs, one of which is threaded, having a 15.9 mm (5/8 in) bolt and lock nut. Both of these closure systems assure that the container cannot be inadvertently opened. Each package is provided with a tamper-proof seal prior to shipment with radioactive contents.

2.2.5 Chemical and Galvanic Reactions

There are no significant chemical, galvanic or other reactions among the packaging components and the package contents. The ANF-250 package structural components are mainly fabricated from carbon steel. Other components include vermiculite for insulation between the inner and outer containers and silicon rubber gasketing material. The U02 contents are packaged in plastic, aluminum or steel (or combinations thereof) containers.

2.3 *Lifting and Tie-Down Devices*

No lifting or tie-down devices are incorporated as a structural part of this container. Normally, two individual packages are steel banded to a special pallet and lifting and handling is with a

forklift. For transportation, conventional rigging is used to strap the pallets to the bed of the vehicle.

2.4 *Normal Conditions of Transport*

2.4.1 Heat

The ambient heat condition of up to 38°C (100°F) in 10 CFR 71 is to define an upper temperature preceding and following the tests which may be most unfavorable for the feature under consideration. A higher limit 70°C (158°F) is the upper limit design condition for type A packages in the IAEA Standards. In either case, these temperatures are not expected to appreciably affect the performance of the ANF-250 package due to the construction of the package. The package is made of thin section materials with good insulation between inner and outer containers and the contents of the inner package do not generate perceptible heat. Large temperature gradients or thermal stresses would not occur. Furthermore, the gasket material rated for 260°C (500°F) service would experience no deterioration at these maximum specified temperatures.

2.4.2 Cold

Steady-state ambient temperature of –40°C (-40°F) will not result in freezing of the U02 pellets or powder payload. The construction of the container is of thin sections [<10 mm (0.4 in)] for which no fracture toughness criteria are specified for Category III steels[1].

2.4.3 Reduced External Pressure

To assess the effects of external pressure equal to 24.5 kPa (3.5 psia), the inner containers of two packages (Nos. 35 and 42) were subjected to an increased internal differential pressure of 96.5 kPa (14 psig) which is in excess of the 77.2 kPa (11.2 psi) differential bursting pressure at an external pressure of 24.5 kPa. The test configuration is shown in Figure 2.1. In this test, a 3.2 mm (1/8 in) thick silicone rubber gasket was utilized to seal the inner container and the six lid bolts were torqued to 6.9 kgfm (50 ft-lbs). In each case, the inner container was pressurized to 96.5 kPa (14 psig) above atmospheric and monitored for one hour. There was no detectable reduction in internal pressure in either case. Figures 2.2.1 and 2.2.2 show pictures of the pressurization tests.

The 15.2 m (50 ft). immersion test of the Hypothetical Accident Conditions, should the outer drum leak, would subject the inner container to an excess external differential pressure of 145 kPa (21 psig). To test the integrity of the inner containers to this more severe condition, five containers were subjected to an internal , differential pressure of 172 kPa (25 psig) and monitored for one hour. Again, the silicone rubber gasket was 3.2 mm (1/8 in) thick and the closure bolts were torqued to 6.9 kgfm (50 ft-lbs). The results are shown in Table 2.3. Two of the five containers indicated slight leakage over the monitoring period.

---

[1] Holman, W.R. and R.T. Langland, "Recommendations for Protecting Against Brittle Fracture in Ferritic Steel Shipping Containers Up to Four Inches Thick,' NUREG/CR-1815.

A further experiment was conducted to test the reduction in torque on the closure bolts of the inner container which could be obtained with a thicker silicone rubber gasket. A 6.4 mm (1/4 in) thick gasket was utilized and for 3.5 kgfm (25 ft-lbs) and 172 kPa (25 psig), the internal differential pressure decreased by approximately 3.4 kPa (0.5 psig) in a period of 15 minutes. The torque was increased to 4.2 kgfm (30 ft-lbs) and no decrease from an initial differential pressure of 172 kPa (25 psig) was observed after 15 minutes.

2.4.4 Increased External Pressure

The test setup shown in Figure 2.1 was also used for tests of the effects of increased external pressure. This was simulated by partial evacuation of the inner container. The inner containers of packages Nos. 35 and 42 were evacuated to 67.6 kPa (20 in Hg) representing a differential crushing pressure of 67.6 kPa (9.8 psi) versus the 36.5 kPa (5.3 psi) to be assessed per CFR 71.71(c)(4). The tests were performed with a 3.2 mm (1/8 in) silicone rubber gasket and the closure bolts were torqued to 6.9 kgfm (50 ft-lbs). Both containers maintained the differential pressure over the monitoring period of one hour. This test verifies that no water in-leakage is expected for normal conditions of transport.

2.4.5 Vibration

The ANF-250, and its forerunner CE-250-2, have been utilized by SPC for nearly 20 years in transport of pellets to its subsidiary in Lingen, Federal Republic of Germany. The shipments involved truck, ship and airplane. There has not been a single case of damage to the packages by the vibrations incurred in normal conditions of transport, adequately demonstrating the package is resistant to damage from this source.

2.4.6 Water Spray

A water spray test was performed on a package (container #18) as a preconditioner to the free drop tests. The spray test simulated a rainfall of approximately 5 cm (2 in) per hour for greater than one hour. The test configuration is shown schematically in Figure 2.3. The nozzles were directed to spray at 45° angle to the underside of the ring closure for the outer drum lid. Figures 2.4.1 and 2.4.2 are photographs of the actual test.

2.4.7 Free Drop

Container #18, preconditioned by the water spray test described in 2.4.6, was submitted to the free drop tests listed in 10 CFR 71.71(7). The inner container had been loaded with dry sand and steel pieces to a total container weight of 261 kg (575 lbs) prior to the spray test. The series of 0.3 m (1 ft) drops on each of the quarters of each rim shown schematically in Figure 2.5.1 preceded the 1.2 m (4 ft) drop tests shown in Figure 2.5.2. The tests were begun shortly after two hours had elapsed from the end of the spray tests. Figure 2.5.2 shows the container orientation and the contact orientation; in each case, the drop distance was 1.2 m (4 ft) measured from the lowest point of the container to the top of the steel plate on a concrete pad acting as the unyielding surface. All fourteen of the drops shown in Figures 2.5.1 and 2.5.2 were performed using the single container #18. The drops were performed using a quick release mechanism with the container suspended from a crane. Figures 2.6.1 through 2.6.10 are photographs taken during the series of 0.3 m (1 ft) edge drops. Figure 2.6.1 shows the

contact on the locking lug during the first drop. Figure 2.6.2 shows the very minimal damage that the initial drop caused. Figure 2.6.3 shows contact for the second 0.3 m drop and Figure 2.6.4 shows the third drop. Figure 2.6.5 shows the cumulative effect of the four 0.3 m drops on the four quarters of the upper rim. The damage is only minor and more deformation occurred to the bottom of the container as a result of the toppling after the contacts. This is shown in Figure 2.6.6. Figures 2.6.7, 2.6.8 and 2.6.9 are photographs taken during the series of 0.3 m drops on the bottom rim, while Figure 2.6.10 is a picture of the bottom of the container after the completion of all eight 0.3 m drops. The damage to the outer drum is relatively minimal.

Figure 2.7.1 is a photograph of container #18 prior to the initial 1.2 m (4 ft) free drop onto the ring closure bolt. Figures 2.7.2 and 2.7.3 are photos from different angles showing the deformation resulting from this 1.2 m drop. Figure 2.7.4 shows the container suspended for the second 1.2 m drop, and also shows the deformation at the ring closure lug resulting from the first 1.2 m drop. Figure 2.7.5 shows the upper end of the container after completion of the series of six 1.2 m drops. The outer drum lid was removed subsequent to these tests to examine the inner container. The inner container showed no evidence of deformation or other damage as a result of the series of testing, and there was no evidence of water in-leakage into the drum from the spray testing.

The tests described above were performed on a container prior to the modification of Part 5 of Drawing EMF-306,175 from 16-gauge (0.152 mm, 0.060 in) to 0.95 mm (0.375 in) and for a gross container weight of 261 kg (575 lbs). This application is for a gross container weight of 277 kg (610 lb), approximately six percent more than in the above described tests. To demonstrate that the containment of the package would not be breached due to the added weight, container #951 was loaded with two pellet shipping suitcases (Drawing EMF-304,306) loaded with 110.4 kg (243.5 lbs) of steel and lead to simulate payload weight. With the shipping container insert (Drawing EMF-306,176), the gross container weight was 279 kg (616 lbs). This container was then subjected to the series of eight rim drops as shown in Figure 2.5.1, followed by the six 1.2m (4 ft.) drops shown in Figure 2.5.2. Figures 2.7.6 and 2.7.7 show the cumulative effects of the fourteen drop tests on the upper end of the container. Although, as previously, there was some distortion of the outer container due to these tests, the lid remained in place and containment was maintained. The inner container showed essentially no damage as a result of this test series.

2.4.8 Corner Drop

The corner drop testing is not applicable to the ANF-250 package.

2.4.9 Compression

The compression test for packages weighing up to 5000 kg calls for the package to be subjected, for a period of 24 hours, to a compressive load applied uniformly to the top and bottom of the package in the position in which the package would normally be transported. The compressive load must be the greater of the following:

(i) The equivalent of five times the weight of the package; or

(ii) The equivalent of 12.75 kPa (1.85 lb/in^2) multiplied by the vertically projected area.

For the ANF-250, the normal position during transport is horizontal and the vertically projected area is about 1.78 m x 0.58 m = 1.03 m^2 (70 in x 23 in = 1610 in^2). Thus, the second condition for compressive force is applicable and a container loading of about 1350 kg (approximately 3000 lbs) is required. To perform the test, two shipping containers were placed side by side on a 1.2 m x 2.6 m x 12.7 mm thick (4 ft x 8 ft x 1/2 in) steel plate with sufficient gap between them to enable deformation to take place without contact between the containers. A second steel plate of the same size was placed on top of the two containers to distribute the weight between them and five calibrated nominal 454 kg (1000 lbs) and one 227 kg (500 lbs) weight were placed on top of the upper plate. The total compressive load, including the upper steel plate, was 2790 kg (6152 lbs); thus, exceeding the 1350 kg (3000 lbs) required weight for each container. Figures 2.8.1. and 2.8.2 show the loaded containers during the test. The weights remained the required 24 hours and were removed. There was no detectable permanent deformation as a result of the test, and the two containers were subsequently used in the Hypothetical Accident testing.

2.4.10 Penetration

The penetration test calls for the impact of the hemispherical end of a vertical steel cylinder of 3.2 cm (1-1/4 in) diameter and 6 kg (13.2 lbs) mass, dropped from a height of 1 m (40 in) onto the exposed surface of the package which is expected to be most vulnerable to puncture with the long axis of the cylinder perpendicular to the package surface.

A bar was machined to the required specifications and weighed 6 kg (13.2 lbs) prior to affixing an eyelet to the flat end of the bar to enable suspending the bar in a vertical attitude over the container. The bar was dropped 1 m (40 in) onto both ends and the side of container #18 after being submitted to the water spray and free drops described in Sections 2.6.6 and 2.6.7. Only very minor deformation of approximately 6 mm (0.25 in) occurred in the drop to the side of the container.

2.5 *Hypothetical Accident-Conditions*

Four containers were used in a series of tests described in the following sections to determine the effects of the Hypothetical Accident Conditions sequence on the container. The free drop and puncture tests were recorded on video tape. A fifth container was subjected to a simulated 15 m (50 ft) immersion test, also described below.

2.5.1 Free Drop

Each of four empty packages was placed on a scale and the inner containers were loaded with dry sand and pieces of metal (lead or steel) until a total weight of 261 kg (575 lbs) was attained. Prior to filling, each inner container was marked with commercially available temperature-indicating substances which melt to indicate a temperature of at least the amount calibrated for each had been attained. Temperature indicators of 38 °C (100 °F), 93 °C (200 °F), 149 °C (300 °F), 204 °C (400 °F), 260 °C (500 °F), 315 °C (600 °F), 371 °C (700 °F), and 454°C (850°F) were utilized. The inner containers were marked on the inside bottom, the inside side, and the inside of the closure lid. The containers were numbers 14, 35, 42 and 57

selected randomly from a group of 96 containers. The inner containers were closed utilizing a 3.2 mm (1/8 in) thick silicon rubber gasket rated for 260°C (500°F) service and the closure bolts were torqued to 6.9 kgfm (50 ft-lb). A check of the vermiculite level in the space between the outer drum and the inner container showed that container #57 was not completely full, and 2.7 kg (6 lbs) of vermiculite were added to make the final test weight of this container 264 kg (581 lbs).

To assess several impact configurations, four containers were subjected to the 9 m (30 ft) free drop test as shown schematically in Figure 2.9. For the angled drops onto the top edge of the container, the center of gravity was located over the point of impact. Each container was dropped once from the 9 m (30 ft) height and the effects were recorded by photographs. Each container was then submitted to penetration tests discussed in the following section. Figures 2.10.1 and 2.10.2 show container #57 suspended 9 m over the steel drop pad in an orientation to provide impact on the closure lug of the outer drum closure ring. The post impact photographs, Figures 2.10.3, 2.10.4 and 2.10.5, show the deformation of the drum at the point of impact. There was no tearing of metal of the outer drum and the lid remained on the drum.

Container #35 dropped in a similar orientation as container #57, but to impact on the closure ring opposite the closure lug, received a similar deformation as container #57.

Container #14 was dropped from 9 m (30 ft) in a horizontal attitude and while very nearly horizontal at impact, impact did occur very slightly earlier on the top end of the container. Figure 2.11.1 shows the container suspended 9 m over the contact pad. Figures 2.11.2 and 2.11.3 show the results of the impact. The contact side of the container was flattened by the impact and the container showed a slight swayback on the top side. The drum closure lid remained in place; however, there was sufficient deformation of the lid and structure to enable a small amount of vermiculite to leak from the gap between the inner container and the outer drum.

Container #42 was dropped to receive impact in a vertical attitude on the bottom of the container. Figure 2.12.1 shows the container having bounced from the impact plate. The container came to rest standing in a vertical attitude on the bottom of the container. Figure 2.12.2 shows that the lowest stiffening corrugation was collapsed to a sharp ring-like structure and there was a minor amount of deformation at the bottom rim of the drum. Figure 2.12.3 shows the bottom of the container. An imprint the size of the bottom of the inner container can be seen as well as evidence of minor deformations caused by the support springs at the lower end of the container.

2.5.2 Puncture

For the puncture tests performed on each container subjected to the 9 m (30 ft) free drop described in Section 2.5.1., two 152 mm (6 in) diameter bars were welded and firmly fixed to steel base plates. One bar was 152 cm (60 in) length and was used to obtain an oblique strike on the closure ring for the drum lid to assess whether such a strike would knock the lid off the drum. The other bar was 30.5 cm (1 ft) long and was used for puncture tests on the surfaces of container.

Figure 2.13.1 shows container #57 suspended over the 152 cm bar. The first drop from 1 m (40 in) was not successful in contacting the closure ring and a second attempt that was successful was made. The lid remained on the drum; Figure 2.13.2 shows the damage resulting from these drops. The container was then dropped from 1 m onto the bottom of the container. The bottom was dented to a depth of about 3.8 cm (1-1/2 in) as shown in Figure 2.13.3. This container was also dropped 1 m onto the shorter bar so that impact occurred approximately at the center of the container. This resulted in a deformation of maximum depth of about 6.4 cm (2-1/2 in) as shown in Figures 2.13.4 and 2.13.5.

A similar series of puncture tests were performed on container #35. Figure 2.14.1 shows container #35 shortly after the oblique impact attempting to knock the lid from the drum. Very little damage resulted from this drop as can be seen in Figure 2.14.2. Figure 2.14.3 shows preparations for a drop onto the lid of the container and Figure 2.14.4 shows the container just after impact. The damage resulting is shown in Figure 2.14.5, where again the depth of the dent is about 3.8 cm (1-1/2 in). A further puncture test was performed dropping the container in a horizontal attitude 1 m onto the bar and impacting a few inches below the closure ring on the side of the container. Figure 2.14.6 shows the container just prior to impact. On impact, the container remained atop the bar as shown in Figure 2.14.7. Two views of the resulting damage are shown in Figures 2.14.8 and 2.14.9.

Figure 2.15.1 shows container #14 at about the time of contact with the taller vertical bar again attempting to dislodge the lid. Figure 2.15.2 shows the damage from this strike and Figure 2.15.3 shows the additional amount of vermiculite that leaked from the upper lid as the container toppled to ground and was rolled to be put in position to be lifted again. None of the lost vermiculite was replaced prior to the thermal tests discussed in Section 2.7.3.

For container #42 dropped from 9 m in a vertical attitude, and which was from outward appearances the least damaged of the four submitted to the free drop of 9 m, a puncture drop onto the shorter 15 cm diameter bar was performed to impact the bottom of the container. The damage is shown in Figure 2.16.1; the dent caused by the bar was about 3.8 cm (1-1/2 in) deep.

2.5.3 Thermal

The thermal tests of the four containers previously submitted to a free drop of 9 m (30 ft) followed by puncture tests were accomplished by means of gasoline/air fire. The test setup is shown in Figure 2.17.1 which shows container #42 just prior to the start of the thermal test. A steel pan 3 m (10 ft) x 1.8 m (6 ft) x 30 cm (12 in) deep was embedded in the ground and a steel cradle which supported the container 1 m (40 in) above a source of flames from the ignition of gasoline floating on water in the pan was placed at the center of the pan. The gasoline floated to the surface of the water at the center of the pan directly beneath the container. The flow of gasoline was not metered, but was controlled by valving to provide a fire to completely engulf the shipping container being tested. The support cradle was instrumented with four thermocouples attached in close proximity to the container. Thermocouple voltages were recorded throughout the test period for each container. The flame temperatures were also monitored by an optical pyrometer directed at the base of the flames. Pyrometer indications were also recorded throughout the test period for each container. Figure 2.17.2 shows the pyrometer and recorder. A shield constructed of steel

sheets was placed in the predominant wind direction; however, the tests were conducted on days with very little wind. Two of the four thermal tests were recorded on video tape.

Container #57 was the first of the four subjected to the thermal test. The container was placed on the cradle with the top towards north (away from the wind shield). The gasoline was ignited and flow continued for 30 minutes at which time the gasoline flow was valved off. The flames extinguished approximately 45 seconds later. The pyrometer traces indicated flame temperatures which averaged between 900 and 1000°C (1652 and 1832°F). The thermocouples at the north end of the cradle ranged from 725°C (1335°F) to 850°C (1560°F); those at the south end from 790°C (1450°F) to 1070°C (1960°F). Figures 2.18.1 through 2.18.3 are photographs taken during the test. Figures 2.18.4 and 2.18.5 are two views of the container subsequent to the test.

Container #42 which had been subjected to the 9 m (30 ft) drop onto the bottom in a vertical attitude was the second submitted to the thermal test. The gasoline flow was increased slightly from that of the prior test. The pyrometer indicated flame temperatures which averaged about 1050°C (1920°F). Thermocouple indications ranged from 840°C (1550°F) to 1050°C (1920°F) at the north location and 740°C (1360°F) to 1040°C (1900°F) at the south locations. Figures 2.18.6 and 2.18.7 were taken during the test. Figure 2.18.8 shows the container resting on the cradle subsequent to extinguishing the flames. The cradle structure glowed cherry red and the temperature at the underside of the container was sufficient to decrease the mechanical strength so that the weight of the container resulted in deformation of the container at the contact points on the cradle.

Containers #35 and #14 were submitted to the thermal test on subsequent days. The temperature recordings from the pyrometer and the thermocouples on the cradle were similar to the prior tests, although thermocouple #3 (south end closest to windbreak) was inoperative during the test of container #14, the last to be tested.

2.5.4 Immersion - Fissile Material

The four containers subjected to the thermal test described in Section 2.5.3 were subjected to an immersion test under a head of water of at least 0.9 m (3 ft) equivalent to 9 kPa (1.3 psi) for a period of greater than eight hours. The tests were performed in the immersion chamber shown in Figure 2.19.1. For the 0.9 m immersion tests, the pressure within the tank was established and maintained by an open vertical standpipe fitted to the fill pipe at the top of the chamber. The containers were placed in the chamber in a vertical attitude with the closure lid at the top. Each container was placed into the chamber in the afternoon and remained in the chamber under pressure until the following morning, or a period of about 16 hours. As a result of mechanical deformation from the drop tests and/or consumption of the lid closure gaskets in the thermal test, all four containers leaked water into the outer drum into the volume surrounding the inner container. None of the four containers, however, showed any evidence of water in-leakage into the inner container, and there was no evidence of damage to the gasket material forming the seal between the inner lid and the inner container.

Figure 2.19.2 shows the inner container of container #57 after removal from the outer drum and having removed the upper positioning flange with a cutting torch. External water was blown away with compressed air. Figure 2.19.3 shows the inside of the container after

removal of the lid. Figure 2.19.4 shows a laborer demonstrating the dryness of the sand used to load the container. Figure 2.19.5 shows that the gasket material is intact and undamaged and Figure 2.19.6 is a photograph of the temperature indicators on the inside of the inner container lid. None of the temperature indicators showed that they had melted.

In container #42, the polyethylene bags which held the vermiculite insulation in the volume between the outer drum lid and the inner drum lid had deteriorated. Figure 2.19.7 shows the inside of the inner container after opening. The temperature indicators for 38°C (100°F), 93°C (200°F), 149°C (300°F) and 204°C (400°F) on the inside of the lid had melted, those for 260°C (500°F) and above had not.

Figure 2.19.8 shows container #35 prior to opening the outer drum subsequent to the immersion test. The outer drum clearly shows the areas where yielding had occurred at the contact spots on the support cradle during the thermal test. Figure 2.19.9 shows the water/vermiculite mixture pouring from the outer drum; this was typical of all four containers tested. Figure 2.19.10 shows the inside of the closure lid of the inner container. As for container #42, the polyethylene bags holding vermiculate were deteriorated and temperature indicators through 204°C (400°F) had melted; 260°C (500°F) and above had not. Figure 2.19.11 shows the dry interior of the inner container.

In container #14, the polyethylene bags had not completely deteriorated and the temperature indicators for 38 °C, 93 °C, 148°C (100 °F, 200 °F, 300°F) had melted; 204°C (400°F) and above had not. Figure 2.19.12 shows the inside of the lid. Figures 2.19.13, 2.19.14, and 2.19.15 show the dry interior of the container and the undamaged condition of the gasket.

2.5.5 Immersion - All Packages

An undamaged container was subjected to a simulated 15 m (50 ft) water immersion test in the test chamber described in the previous section. The container was weighed and placed in the test chamber and the pressure gradually increased toward the 246 kPa (21 psig) required test pressure. At about 226 kPa (17 psig), two successive, loud, audible reports were heard from the test chamber. The pressure was increased to the required 246 kPa (21 psig) and maintained until the next day, a period of about 16 hours. Figures 2.20.1 and 2.20.2 show the removal of the container from the test chamber. The container bobbed to the surface indicating that in-leakage of water had not occurred. This was confirmed by re-weighing the container after blowing away water from the external surfaces with compressed air. The container weighed the same as before the test. The cause of the two audible reports was also apparent on viewing the collapsed drums. At the joining line of the two drums where the material overlaps and is reinforced by welding, there was sufficient strength to prevent collapse. The collapse of one of the drums resulted in enough deformation that instability and collapse occurred in the other drum as well. The roughly equilateral triangle shape of the collapsed drums are rotated about 90° to each other. In this configuration, array spacing for criticality analysis would be maintained.

Figure 2.20.3 shows the lid of the inner container on removal of the drum lid indicating no in-leakage of water into the outer drum despite the deformation of the drum. Figures 2.20.4 and 2.20.5 show the inside of the inner container again showing no in-leakage of water. In Figure

2.20.5, a slight inward dent of the inner container is visible near the bottom caused by the force of the collapse of the outer drum.

2.5.6 Summary of Damage

The performance of the test program and the results described in the prior sections are evidence that the ANF-250 is a safe and reliable package for transport of uranium oxide powder and pellets. While deformation was varied depending upon impact angle during the 9 m (30 ft) drops, the lids remained on all containers and the thermal tests did not result in deterioration of the sealing gasket for the inner container. All inner containers remained leak-tight to water penetration.

2.5.7 Additional Free Drop and Puncture Testing

As a result of the free drop from 9 m (30 ft) in a horizontal attitude, the lid on container #14 was distorted sufficiently so that a minor amount of vermiculite insulation leaked from the annulus between the inner container and the outer drum. In order to avoid this leakage of insulation and to provide additional safety against loss of the drum lid, a modification of the upper end of the container was designed and modified containers were subjected to testing as described in this section. The modification was to replace Part 5 of Drawing EMF-306,175, previously 16 gauge, with a 0.95 mm (0.375 in) flange. Seven containers were modified and tested; one was subjected to the drops of normal conditions of transport as described in Section 2.4.7.

Two pellet shipping suitcases (Drawing EMF-304,306) were loaded with lead and steel pieces totaling 55.8 kg (123 lbs) and 54.7 kg (120.5 lbs), respectively, and with the container insert (Drawing EMF-306,176) packed into container #920 as for normal pellet shipment. The gross weight of the container was 277.1 kg (611 lbs). The container was subjected to a free fall of 9 m (30 ft) in a flat horizontal orientation followed by two drops of 1 m (40 in) onto a 15 mm (6 in) diameter 1524 mm (60 in) tall pin welded to a steel plate. Figure 2.21.1 shows the container subsequent to the 9 m drop photographed from the lid end. There is some minor distortion of the ring closure and the lid. Figures 2.21.2 and 2.21.3 are other views of the minor lid distortion. In Figure 2.21.3, the flattening of the impact side of the container is shown. The container was oriented prior to the drop so that the weight of the suitcases was directed through the short side angle iron of the container insert to the impact point of the outer drum; i.e., the impact point was at 45° to the lower right on Section "A-A" of Drawing EMF-306,175. Figure 2.21.4 shows container #920 viewed from the lower end subsequent to the 9 m flat horizontal drop. Figure 2.21.5 is a closer view of the bottom of container #920 and Figure 2.21.6 is a view of the impact side from the bottom of the container.

Figure 2.21.7 shows container #920 suspended at an angle 1 m (40 in) over the top of the 15 mm diameter pin prior to the drop onto the underside of the locking lug of the closure ring. Guy lines were utilized to prevent swinging and contact in the drop was directly on the locking lug. Figure 2.21.8 is a close-up of the lug subsequent to the impact. There is essentially no damage to the lug or the locking ring. The container was then rotated approximately 90° and a second 1 m drop onto the pin with impact on the underside of the closure ring was performed. Figure 2.21.9 shows the drop of the container just prior to impact and Figure 2.21.10 is a

close-up of the impact area. There was some minor deformation of the closure ring, but the lid remained in place.

Figure 2.21.11 shows the top of container #920 with the lid and the bagged vermiculite removed showing the distortion of Part 6 of Drawing EMF-306,175. Figure 2.21.12 is an overhead view of the standing container with the top portion of the drum removed to show the deformation of the top support hardware on the inner container. Figure 2.21.13 is a side view of the inner container of #920 showing the deformation resulting from the insert and the loaded suitcases. Figure 2.21.14 is a close-up of the lower end of the inner container and Figure 2.21.15 is a close-up of the upper end. Although there was some distortion of the inner container, there were no tears, open seam welds, or penetrations. Through handling in removing the loaded inner container from the drum and placing on the ground for display, some of the support spring welds broke and the springs came loose.

In Figure 2.21.16, the lid of the inner container has been removed to show the end of the insert and one of the pellet boxes. Figure 2.21.17 shows an end view of the insert and pellet boxes after removal from the inner container. A line drawn from the angle iron in the lower left hand corner to the upper right hand corner represented vertical in the 9 m drop with impact occurring on the upper right hand corner. The angle iron was bent around the corner of the pellet box from the force of impact. Figure 2.21.18 is another view of the minor damage to the insert and pellet box. Figure 2.21.19 is a full-length view of the insert and the pellet boxes. The insert and the boxes are effective in maintaining the geometry of the payload.

Container #921 was packed with two pellet suitcases containing lead and steel pieces totaling 55.3 kg (122 lb) and 55.6 kg (122.5 lb) and an insert as for normal pellet shipping. The gross weight of the container was 278 kg (613 lb). This container was subjected to a 9 m (30 ft) drop onto the lid edge opposite the locking lug of the closure ring. The center of gravity of the container was located over the point of impact as the container was suspended 9 m over the unyielding surface and remained so oriented through the drop until impact, after which the container toppled over to fall on the side of the container. Figures 2.22.1, 2.22.2, 2.22.3 and 2.22.4 are various views of the top end of the container showing the deformation resulting from the 9 m drop. Figures 2.22.5 and 2.22.6 are views from the bottom end of the container showing the minor deformation from the toppling action.

Subsequent to the 9 m drop onto the edge of the lid for container #921, the container was subjected to two 1 m drops onto the 15 mm diameter pin. In the first of these drops, the container was oriented at about 45° to the vertical orientation of the 1524 mm (60 in) tall pin so that impact would occur on the underside of the locking lug. Figure 2.22.7 shows container #921 in free fall just prior to impact on the pin. Impact was on the underside of the locking lug, then on the lower end of the container which toppled against the pin and remained leaning against the pin as shown in Figure 2.22.8. The container was pulled from the leaning position and allowed to fall to the unyielding surface. There was no visible damage to the locking lug or locking ring and the lid remained in place.

Container #921 was then subjected to a second 1 m drop in a vertical orientation approximately onto the center of the lid. Figure 2.22.9 shows the container at impact on the pin from which position the container toppled to the unyielding surface. Figures 2.22.10, 2.22.11 and 2.22.12 are views from three angles of the distortion resulting from the

combination of drops. Figure 2.22.13 is a view of the upper end of container #921 with the lid removed to show the distortion of the upper structure of the outer drum. The impact point in the 9 m drop is to the lower right. Figure 2.22.14 is a view of container #921 with the upper portion of the drum removed to show the distortion of the band affixed to the upper flange of the inner container. Figure 2.22.15 is an overhead view of this deformation. Figure 2.22.16 is an overall view of the inner container removed from the outer drum. Figure 2.22.17 is a view of the lid end of the inner container and Figure 2.22.18 is a view of the bottom end. Some of the support springs were broken loose in the handling subsequent to removal of the loaded inner container from the outer drum, but there were no visible breaks, tears or other openings resulting from the drop series.

The nearly vertical orientation of container #921 in the 9 m drop resulted in damage to the closure mechanisms of the pellet boxes. Since the bases of the pellet boxes extend 19 mm (0.75 in) beyond the pellet box at each end, the bases contact while the inertia of the loaded boxes results in displacement of the boxes, causing shearing of some of the closure mechanisms. This effect is shown in Figures 2.22.19 through 2.22.22. Figure 2.22.19 is a view from the upper end showing the displacement of the upper box relative to the base. Figure 2.22.20 is a view from the side at the upper end. Figure 2.22.21 is a side view of the boxes showing the displacement of the upper box onto the base of the lower box and Figure 2.22.22 is a view from the side at the bottom end. The boxes are constrained from opening by the frame insert; however, the shearing of the closure mechanisms causes some gapping between the base and the box. The gap is too small for whole pellets to escape from the box, but these results prompted additional testing which is described later.

Container #931 was loaded to simulate the shipment of powder. Four polyethylene 10 liter bottles were loaded with lead pieces and sand to obtain an approximately evenly distributed loading of 118.4 kg (216 lb). The four bottles were loaded into a shipping container insert as shown in Drawing EMF-306,176. The gross weight of the shipping container was 275 kg (606 lb). This container was subjected to a 9 m (30 ft) drop followed by three 1 m (40 in) drops onto the 15 mm diameter pin. For the 9 m drop, the container was oriented at an angle of about 15° to the horizontal by slinging the container so that the lid end was approximately 457 mm (18 in) higher than the bottom end. In this orientation, the initial impact was on the bottom and then the top end of the container slapped to the unyielding surface, whereupon the whole container bounced into the air before coming to rest on the steel plate. Figure 2.23.1 shows container #931 in free fall prior to impact on the unyielding surface. Figures 2.23.2, 2.23.3 and 2.23.4 are views of the lid end deformation resulting from this 9 m drop. Figure 2.23.5 is a view of the deformation of the bottom end of the container.

Three 1 m drops onto a 15 mm diameter pin in three orientations were performed. Figure 2.23.6 shows the container in free fall with impact on the underside of the locking lug. Figure 2.23.7 shows impact on the underside of the locking ring near the area of maximum deformation of the lid. Figure 2.23.8 shows container #931 just prior to impact onto the pin in a vertical orientation. Figures 2.23.9 and 2.23.10 are two views of the cumulative deformation of the 9 m and three 1 m drops on container #931. Although there is deformation, the lid remained in place and there was no leakage of vermiculite insulation from the container. Figures 2.23.11 and 2.23.12 are two views of the upper end of the container with the lid and bagged vermiculite removed to show the location of the inner container and the deformation of the upper structure. The inner container was removed from the outer drum to reveal that the

upper flange on the powder canister had breached the inner container wall as shown in Figure 2.23.13, whereas the powder canister showed no evidence of damage as shown in Figure 2.23.14, which is a view from the upper end of the canister. For powder shipments, the powder canister (Drawing EMF-306,176) will act as the structural member to maintain moderator control i.e., prevent the in-leakage of water, as well as maintain geometry control. The cross sectional area at the maximum tolerance diametral inside dimension, 244.5 mm (9-5/8 in), yields 469.4 cm^2 (72.76 in^2) which is less than the 507 cm^2 (78.6 in^2) allowed by the criticality analysis in Section 6. Tests have been performed to show that the powder canister with the lid bolts torqued to a minimum of 2.5 kgfm (18 ftlbs) as in ANF-250-PDR, Section 7 prevents the in-leakage of water at a submersion depth of 0.9 m (3 ft).

The testing to show the prevention of in-leakage of water consisted of the following: The shipping container insert from container #931 was submerged in the test tank utilized for immersion testing of the containers. Due to the length of the shipping container insert, the head of water to the flange of the insert was about three feet with the test vessel full of water. However, the lid of the test tank was bolted in-place and an additional three feet of head was established with a three foot open standpipe. The insert was left overnight (about 16 hours) under the six foot head and then removed from the vessel. On opening the insert, it was free of in-leakage of water.

Since this test provided only a single data point, two additional inserts were tested. Because there was no evidence of physical damage to the insert as a result of the drop testing of container #931, two additional inserts, without being subjected to drops, were each loaded with two of the powder bottles or about 125 pounds total for each - an amount calculated to be sufficient to submerge the inserts in the test tank. The two inserts were closed per the procedure (Section 7) and submerged in the test tank under about six feet total head at the flanges. The inserts remained in the test tank overnight and were examined on August 3, 1988. Neither showed any in-leakage of water.

Container #952 was loaded with simulated pellet weight in pellet boxes as for normal shipment of pellets. The gross weight of the loaded container was 277 kg (611 lb). The container was oriented vertically for a 9 m drop onto the bottom of the container. The purpose of the test was to show that the inner container of the ANF-250 has sufficient strength to contain the payload for a drop in this orientation. The container was dropped from 9 m onto the unyielding surface and remained standing on its bottom. Deformation of the outer drum was principally confined to the lowest corrugation ring which was crushed to a flange shape and the bottom of the drum which showed the impact of the six support springs and the inner container. These effects are shown in Figures 2.24.1 and 2.24.2. The upper end of the drum was undamaged as shown in Figure 2.24.3. The deformation of the bottom of the inner container resulting from the impact is shown in Figure 2.24.4. Although deformed, the bottom of the inner container showed no tears, parted metal, or broken welds.

The pellet boxes showed a displacement relative to the bases similar to that described for container #921 and a similar shearing of some of the closure mechanisms. These effects are shown in Figures 2.24.5 through 2.24.8. Figure 2.24.5 is a full length view of the two pellet boxes. A view of the upper end relative to the impact point is shown in Figure 2.24.6 which shows the displacement of the upper box relative to the base and the shorn closure mechanisms. The bent angle iron on the insert frame is the result of a prior flat horizontal 9 m

drop in container #920. Figure 2.24.7 shows the end of the lower box relative to the impact point and Figure 2.24.8 shows that the upper box is displaced onto the base of the lower box.

To determine whether the displacement of the boxes relative to the bases could be alleviated by a relatively simple alteration of the packing procedure and to obtain additional data for the case of pellet packaging in the slap drop orientation, two additional containers were subjected to hypothetical accident drop and immersion conditions. Solid aluminum blocks 31.8 mm x 102 mm x 19 mm thick (1-1/4 x 4 x 3/4 in) were taped to the ends of four pellet boxes to compensate for the overhang of the bases. These boxes were loaded with the pellet simulation weights utilized in previous testing and packed into shipping containers #924 and #925, which had been modified to strengthen the upper portion of the container as discussed previously. The total weights of the containers were 275 kg (606 lb) and 276 kg (608 lb), respectively.

Container #925 was slung so that the lid end was approximately 457 mm (18 in) higher than the bottom end. This orientation provided an angle of about 15° to horizontal. The container was raised so that the bottom end was 9 m above an unyielding plate and released for a 9 m free fall. Impact occurred on the bottom end and the lid and slapped down to the steel plate acting as the unyielding surface. Figure 2.25.1 shows container #925 just after impact and Figure 2.25.2 shows a top view of the resulting distortion at the lid end. Figure 2.25.3 is a view along the impact side of the container from the bottom and Figure 2.25.4 is a view of the bottom end. There is some distortion of the metal of the drum and lid, but no visible tears or parted metal and no vermiculite leaked from the container. Subsequent to the 9 m drop, container #925 was subjected to a series of 1 m drops onto a 15 mm diameter pin. In the first of these drops, impact was on the underside of the lid ring locking lug. The effect of this drop is shown in Figure 2.25.5. A minor amount of local displacement of the locking ring is evident. This displacement viewed from the lid end is shown in Figure 2.25.6. The container was rotated to obtain impact on the locking ring next to the area of maximum distortion from the 9 m drop, and a second 1 m drop was performed. A close-up view of the impact area is shown in Figure 2.25.7. Essentially no additional deformation resulted from this drop. The container was then subjected to a third 1 m drop onto the center of the lid. The container at impact is shown in Figure 2.25.8. Figure 2.25.9 is a lid and view of container #92S subsequent to these accumulated drops.

Following the series of drops, the locking lug was loosened to ensure water would leak into the outer drum and the container was placed in the water immersion vessel in a vertical position with lid up and a head of 0.9 m (3 ft) was established with an open standpipe. The container remained in the immersion vessel about 20 hours and was removed. On subsequent opening, it was determined that water had penetrated the inner container of the ANF-250. In the 9 m slap drop, the container was oriented so that the center of gravity was over one of the short side angle irons of the insert (Drawing EMF-306,176). The distortion of the ANF-250 inner container is shown in full length view in Figure 2.25.10 and closer views of the upper and lower ends are shown in Figures 2.25.11 and 2.25.12, respectively. Closer examination of the inner container revealed a small hole near the bottom as shown in Figure 2.25.13, which enabled water to leak into the inner container. The pellet boxes were undamaged as shown in Figure 2.25.14.

Container #924 was slung in a vertical orientation and subjected to a 9 m drop onto the bottom of the container. The container came to rest standing on its bottom. The lower corrugating ring on the outer drum was flattened to a sharp flange-like configuration. This deformation is shown in Figure 2.26.1 and duplicates other data from drops in this orientation. Figure 2.26.2 is a view from the bottom of the container showing the imprint of the inner container and slight deformations from the inner container support springs. Due to lack of damage to the upper portions of the container, and only limited deformation near the bottom, no 1 m drops onto the 15 mm diameter pin were performed. The locking lug on the lid of the container was loosened and the outer drum was punctured with a chisel in several places at top and bottom of the container to ensure in-leakage of water into the drum. The container was placed in the immersion vessel under 0.9 m (3 ft) head of water and remained there approximately 94 hours. Opening the container revealed that water had leaked into the inner container. The pellet boxes and insert were removed from the container. The aluminum blocks were effective in reducing the displacement of the boxes relative to the bases, but with the concentration of forces on the corners of the boxes, some deformation of the boxes and damage to the closure clips occurred. Figure 2.26.3 shows the upper end of the upper box with respect to the drop orientation. Minor displacement and deformation is shown. Figure 2.26.4 shows the upper end of the lower box and the deformation at the box corner and the damaged closure device near the end. Figure 2.26.5 shows the lower end of the lower box; again, some metal deformation at the corner is apparent and the metal is deformed at the lowest closure device on the side. In conjunction with the insert to hold the boxes, the boxes demonstrate that the geometry of the pellet payload is maintained.

Figure 2.26.6 is a view of the bottom of the inner container. The imprint of the pellet box with the aluminum blocks, the base of the pellet box, and the handle tab resulting from the impact are clearly visible. A careful visual examination, and filling the inner container with water, were not successful in identifying the source of water in-leakage to the inner container. Water in-leakage may have occurred in the gasket area.

2.5.8 Summary of Testing

An extensive series of testing of the ANF-250 package, both prior to and subsequent to a modification to strengthen the upper end of the container have shown:

1. The ANF-250 container provides a safe and reliable packaging for all normal conditions of transport. Conditioned upon the statements below, the ANF-250 container also provides a safe and reliable packaging for hypothetical accident conditions.

2. The ANF-250 container, unmodified to provide strengthening of the upper end, provides sufficient resistance to the effects of thermal testing of the hypothetical accident conditions to assure that the contents are not spread and remain securely packaged. Since the modification to strengthen the container does not significantly affect the heat transfer to the inner container, this applies as well to the modified container.

3. If sufficient care is exercised in the design of payload packaging, the inner container of the ANF-250 container is of adequate strength to contain the payload and prevent the in-leakage of water in the accident condition. This requires that the payload packaging

avoid stress concentrators such as sharp edges which can breach the 16 gauge shell of the inner container.

4. The ANF powder canister of Drawing EMF-306,176 will provide a reliable additional containment and prevent the in-leakage of water to the payload in the case of powder shipments. This canister is stronger than the ANF-250 inner container (14 gauge versus 16 gauge wall thickness and smaller diameter).

5. The ANF pellet shipping suitcases (Drawing EMF-304,306) in conjunction with the container insert (Drawing EMF-306,176) are effective in maintaining the geometry of the pellet payload, although in-leakage of water may not be prevented by the ANF-250 inner container in all accident conditions. In Section 6, it is shown that this is sufficient to prevent a criticality accident.

2.6 *Appendix*

2.6.1 Tables

2.6.2 Figures

Table 2.1 Regulation Requirements for Packaging for Fissile Material Transport

	10CFR71[1]	Reference IAEA 1973[2]	IAEA 1985[3]
General Standards			
Smallest overall dimension not less than 10 cm	43(a)	210	525
Seal or other means to show that package has not been opened by unauthorized person	43(b)	211	526
Containment system closed by positive fastening device	43(c)	216	530
Compatible materials	43(d)	219	512
Relief valve protection	43(3)	222	535
No loss or dispersal of contents under normal conditions of transport	43(f)	225(a)	537(a)
Surface temperature limitations	43(g)	43(h)	515
No continuous venting	43(h)		515
Lifting and Tie-Down Standards	Not applicable to ANF-250 package		
External Radiation Standards	47	526-546	462-475
General Requirements for All Fissile Material Packages			
Normal Conditions of Transport			
Contents would be subcritical	55(d)(1)	602	562
Geometric form of contents would not be substantially altered	55(d)(2)	615(c)	563(c)
No leakage of water into the containment system	55(d)(3)	615(b)	563(b)
No more than 5% reduction in effective volume of packaging	55(d)(4)(i)	615(a)	563(a)
<5% reduction in spacing	55(d)(4)(ii)	615(a)	563(a)
No hole in drum large enough to pass 10 cm cube	55(d)(4)(iii)	615(a)	563(a)
Hypothetical Accident Conditions			
Single package subcritical (1% damaged)	55(e)	618	566

1 10 CFR §71 regulations as of January 1, 1986.

2 IAEA Regulations for the Safe Transport of Radioactive Materials 1973 Revised Edition (As Amended).

3 IAEA Regulations for the Safe Transport of Radioactive Materials 1985 Edition with Supplement 1986.

	10CFR71[1]	Reference IAEA 1973[2]	IAEA 1985[3]
Specific Standards for Fissile Class II Package			
Five time allowable subcritical-undamaged	59(a)(1)	619(a)	567(a)
Twice allowable subcritical-damaged	59(a)(2)	619(b)	567(b)

Table 2.2 Applicable IAEA Standards in Addition to or Different From 10 CFR §71

Standard	Reference	
	IAEA 1973	IAEA 1985
General Requirements		
Package designed to be easily handled and properly secured on conveyance during transport	201	505
For gross weight >50 kg, designed to enable safe handling by mechanical means	203	505
Designed to avoid, as far as practicable, collection and retention of water	206	509
External surfaces easily decontaminated	207	508
Additional Requirements for Type A Packages[1]		
As far as practicable, external surfaces free from protruding features	212	508
Design shall consider storage and transport for temperature range - 40°C to 70°C[2]	213	528
Welds in accordance with national or international standards or with standards acceptable to competent authority	214	529
Capable of withstanding effects of acceleration and vibration arising during normal transport	215	511
Containment system securely closed by positive fastening device independent of any other part of the package	218	532
Containment shall retain radioactive contents under reduction of ambient pressure to 0.25 kg/cm2	221	534

[1] Based upon IAEA 1973 - The requirements may be classified differently in IAEA 1985.

[2] Temperature range is a condition of evaluation in 10 CFR §71.71(c)(1)-38°C and §71(c)(2)-40°C.

Table 2.3 Results of Inner Container Testing
for Internal Pressure of 172 kPa (25 psig)

Container Number	Initial Pressure psig	Pressure Psig (After)			
		15 min.	30 Min.	45 Min.	60 Min.
35	25	24.5	24.5	24.5	24.5
18	25	25	25	25	25
27	25	25	25	25	25
14	25	25	25	24.75	24.75
42	25	25	25	25	25

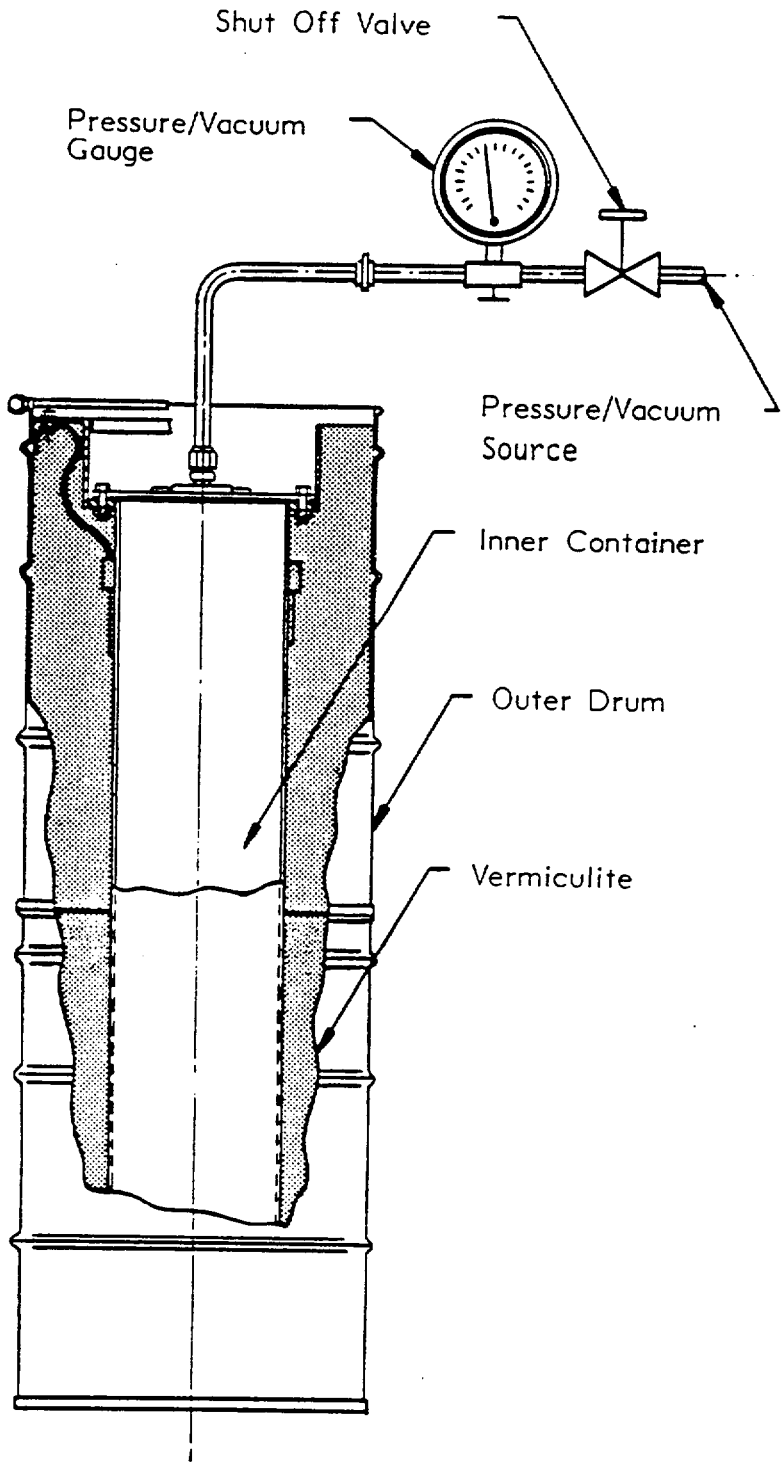

Figure 2.1

Reduced and Increased Internal Pressure Tests
10 CFR 71.71 (c) (3) & (4)

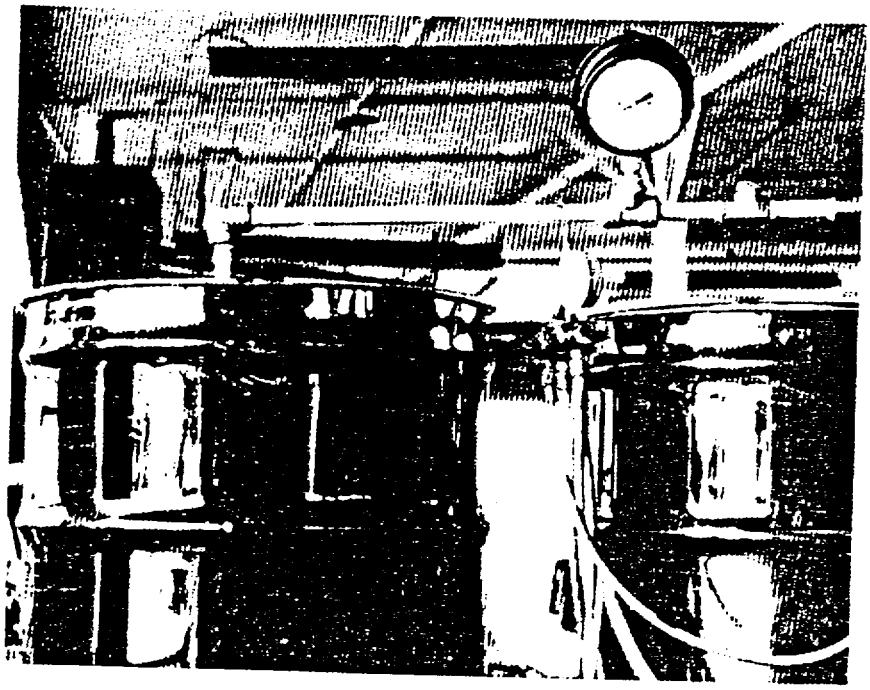

Figure 2.2.1 Differential Pressure Tests

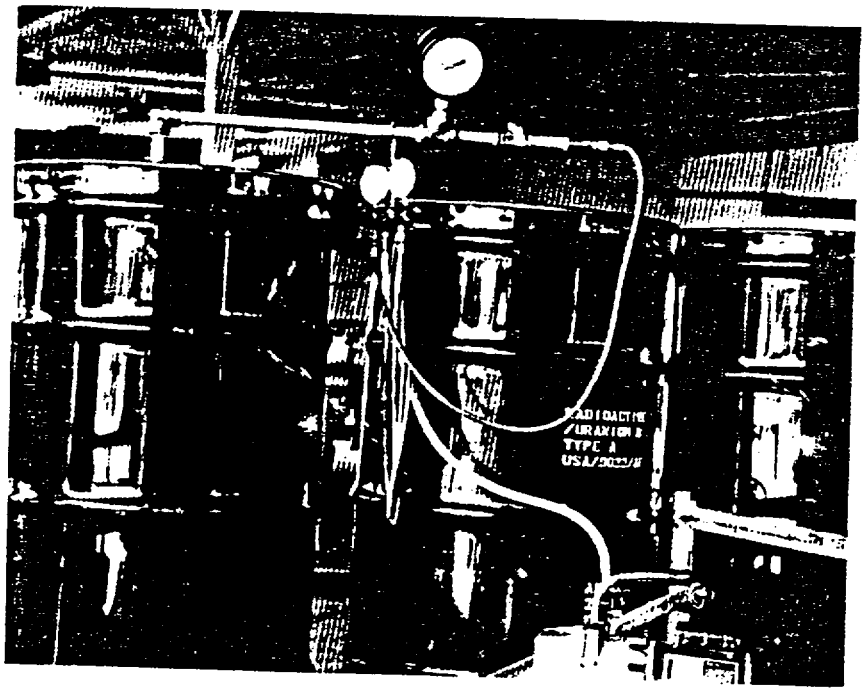

Figure 2.2.2 Differential Pressure Tests

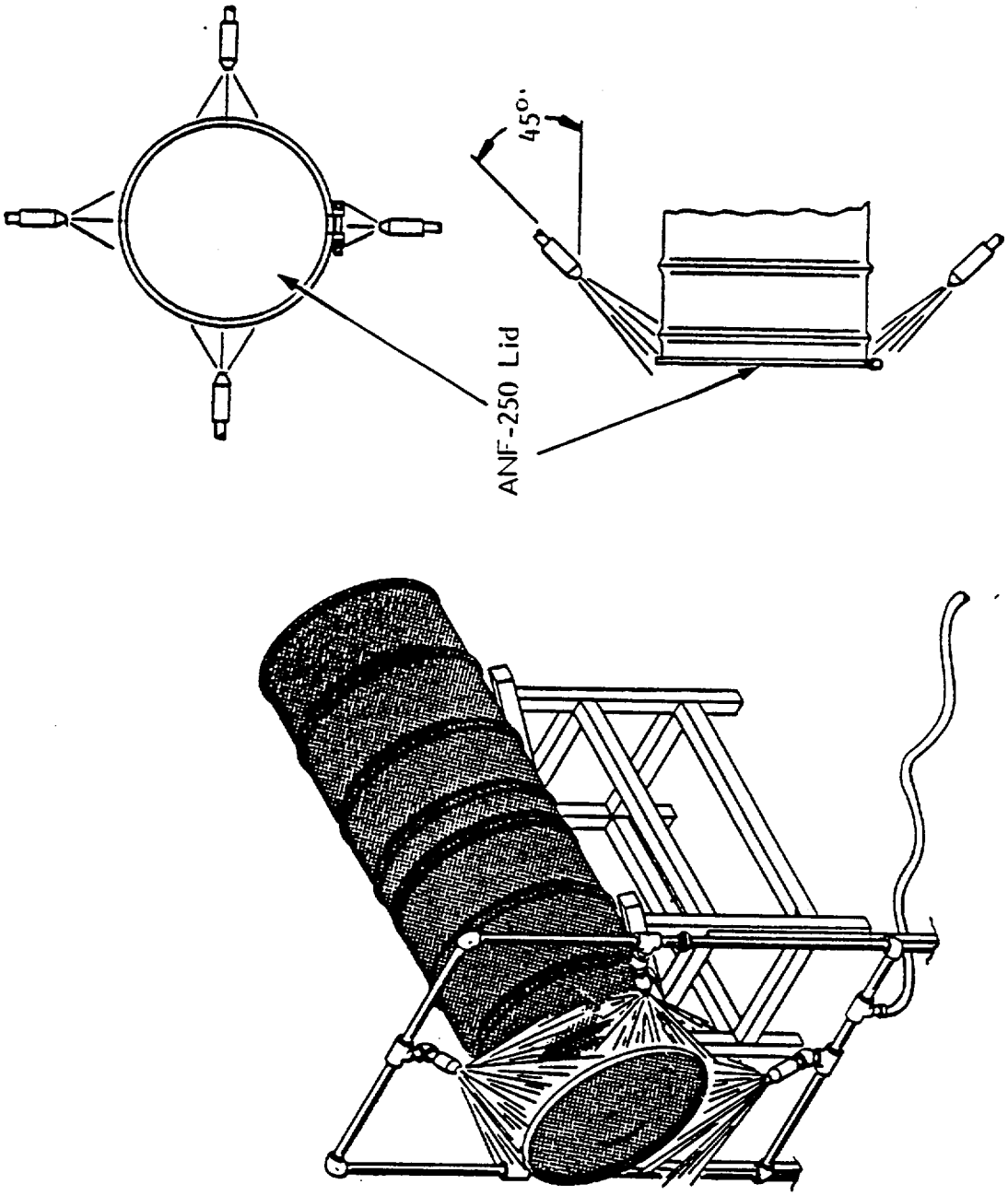

Figure 2.3
Water Spray Test
10 CFR 71.71 (c)(6)

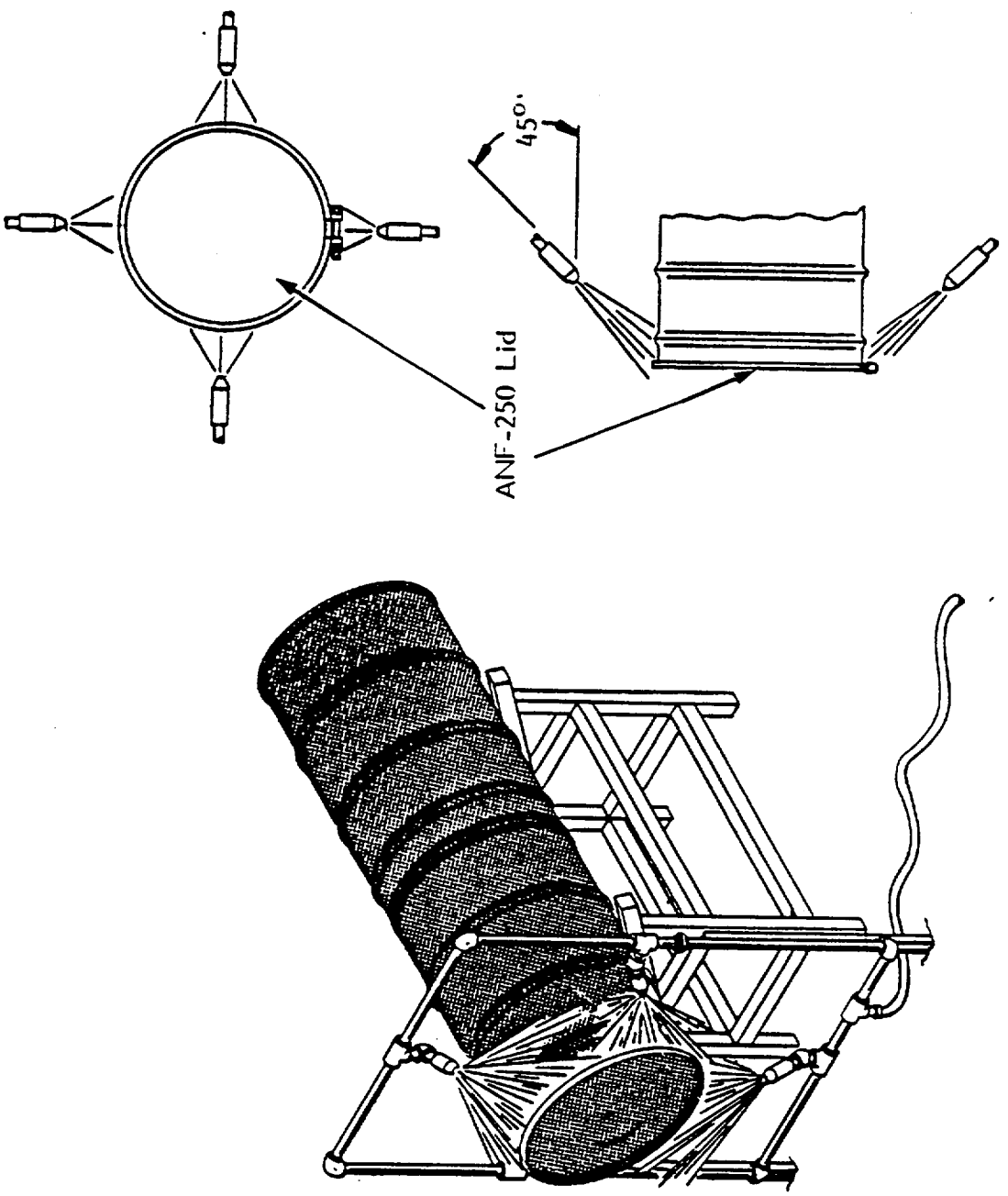

Figure 2.3
Water Spray Test
10 CFR 71.71 (6)

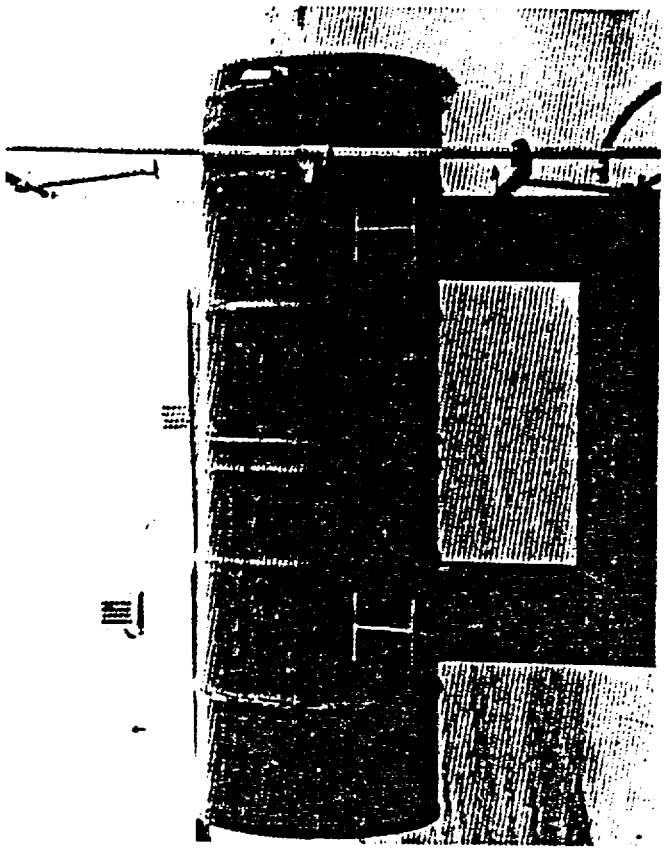

Figure 2.4.2 Water Spray Test

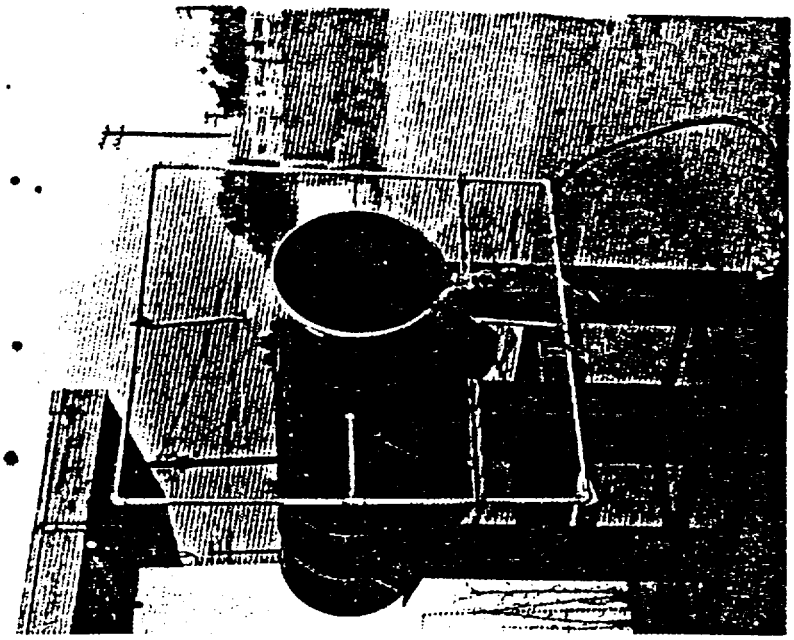

Figure 2.4.1 Water Spray Test

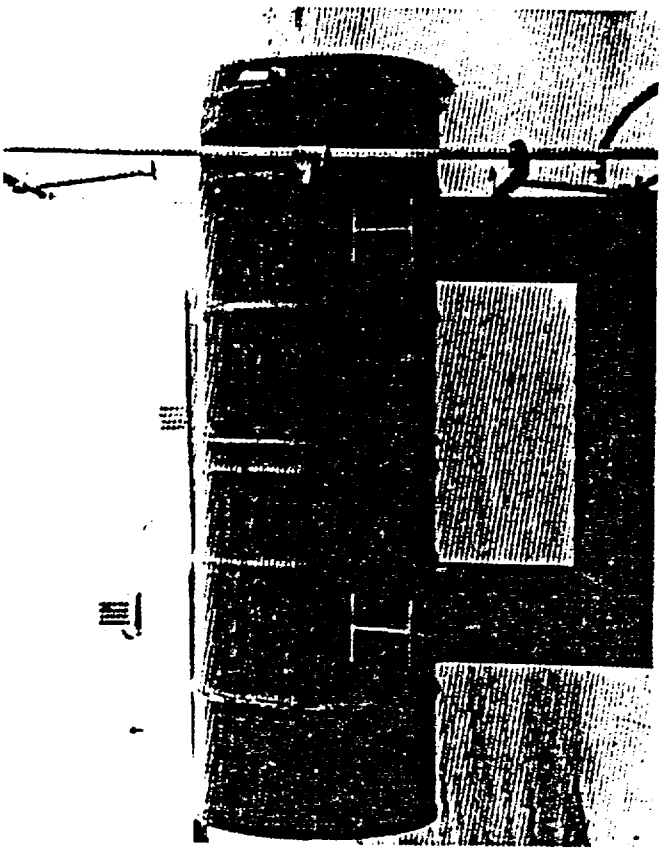

Figure 2.4.2 Water Spray Test

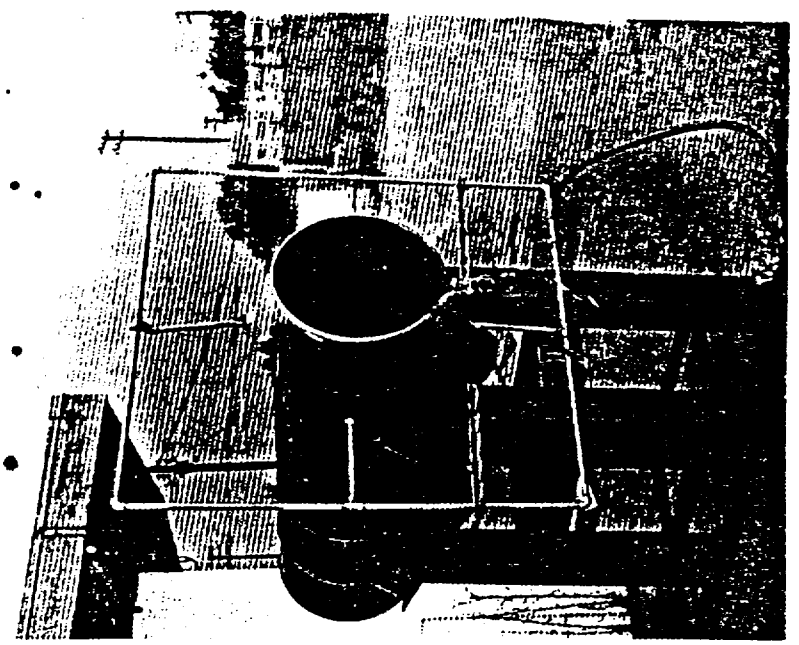

Figure 2.4.1 Water Spray Test

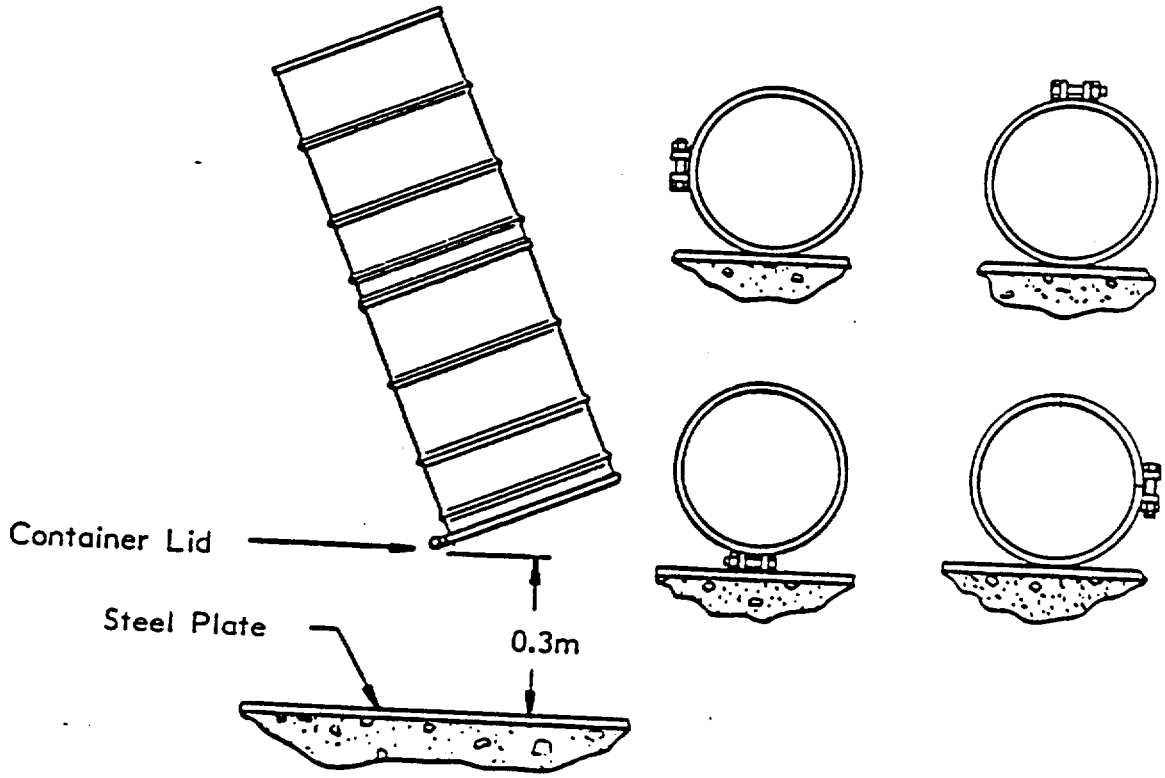

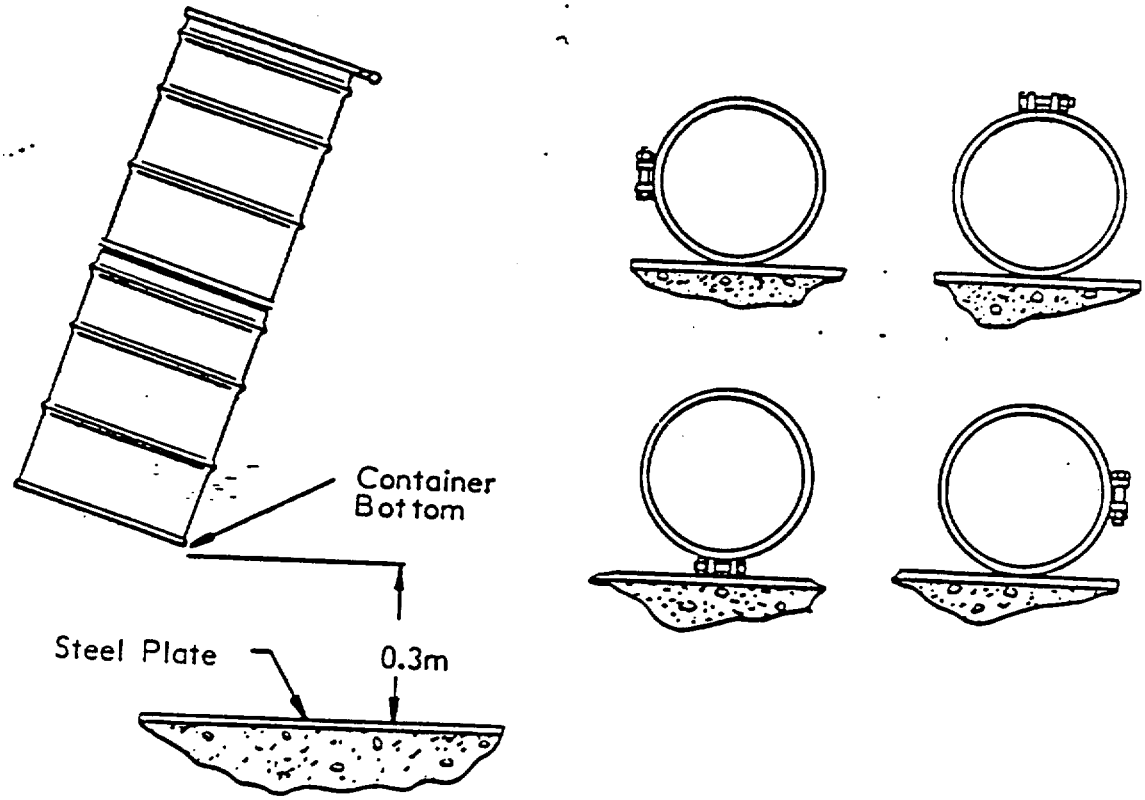

Figure 2.5.1
0.3m (1 ft.) Drop Tests
10 CFR 71.71 (c) (7)

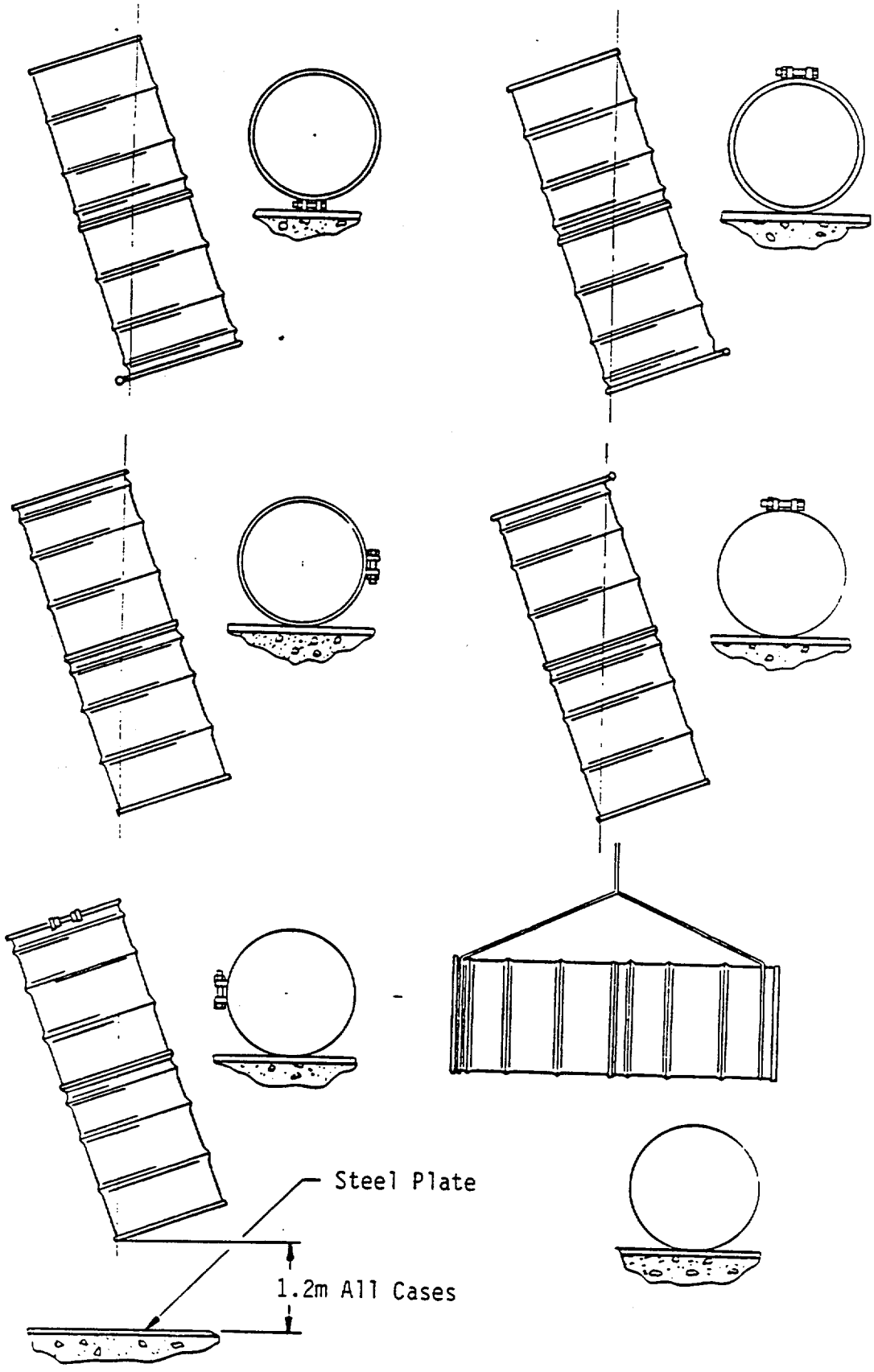

Fig. 2.5.2 1.2m (4 ft.) Drop Tests 10 CFR 71.71(c)(7)

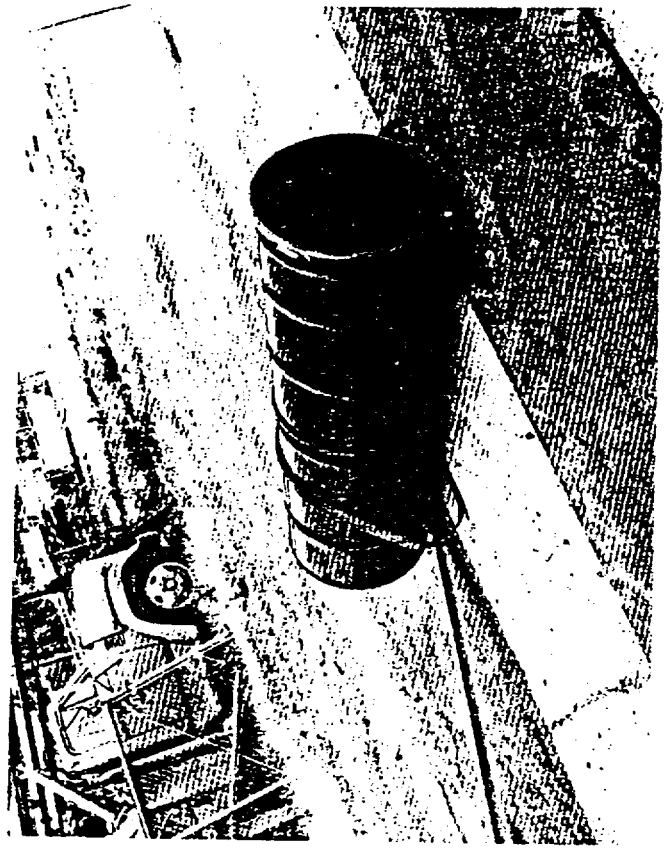

Figure 2.6.2 Container #18 After Initial 0.3m (1 ft.) Free Drop

Figure 2.6.1 Initial 0.3m (1 ft.) Free Drop Test Container #18

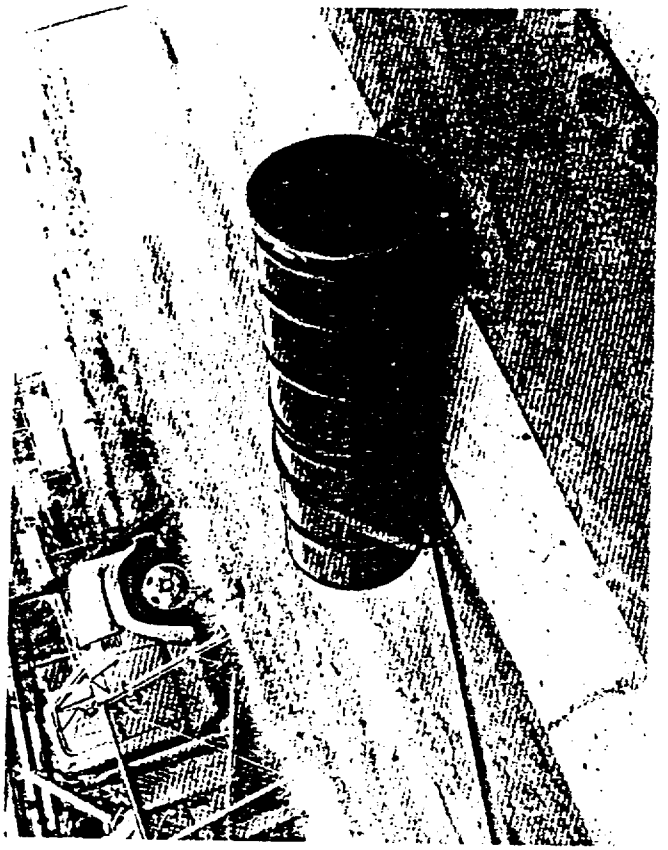

Figure 2.6.2 Container #18 After Initial 0.3m (1 ft.) Free Drop

Figure 2.6.1 Initial 0.3m (1 ft.) Free Drop Test Container #18

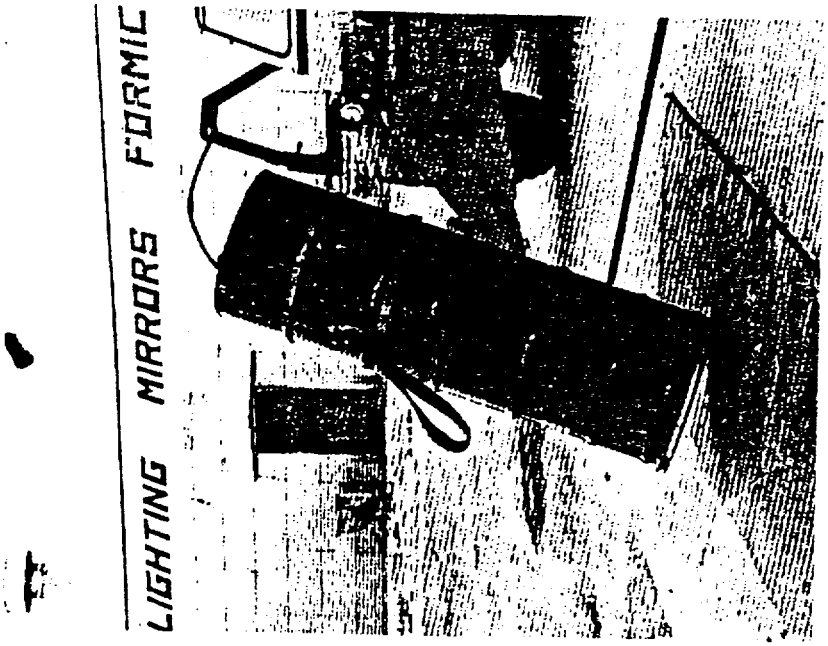

Figure 2.6.4 Third 0.3m (1 ft.) Free Drop Container #18

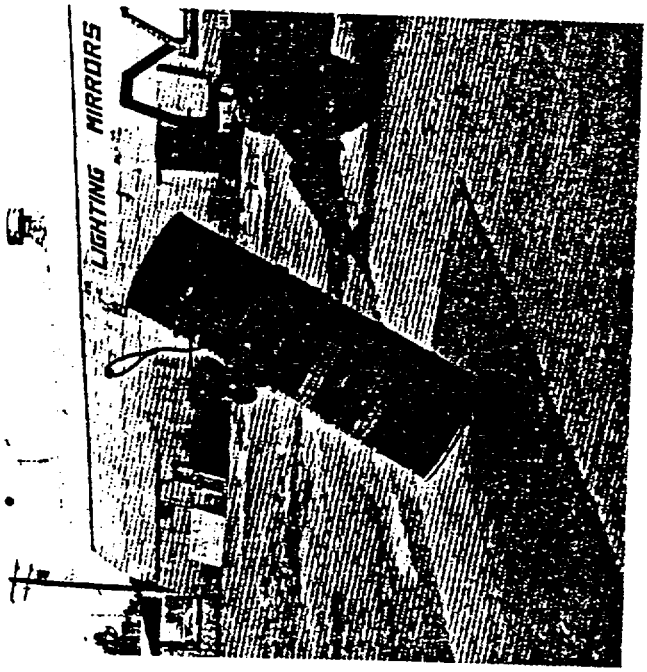

Figure 2.6.3 Second 0.3m (1 ft.) Free Drop Container #18

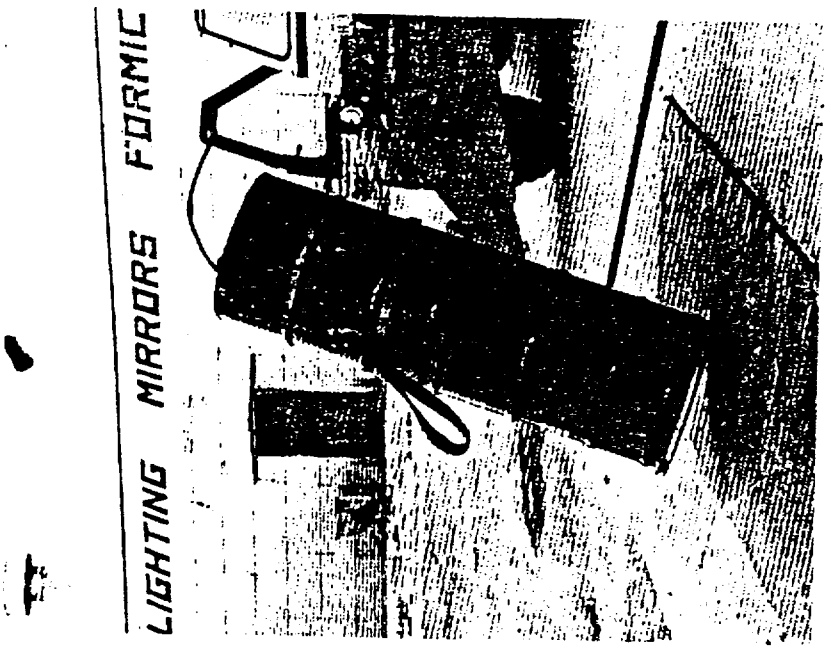

Figure 2.6.4 Third 0.3m (1 ft.) Free Drop Container #18

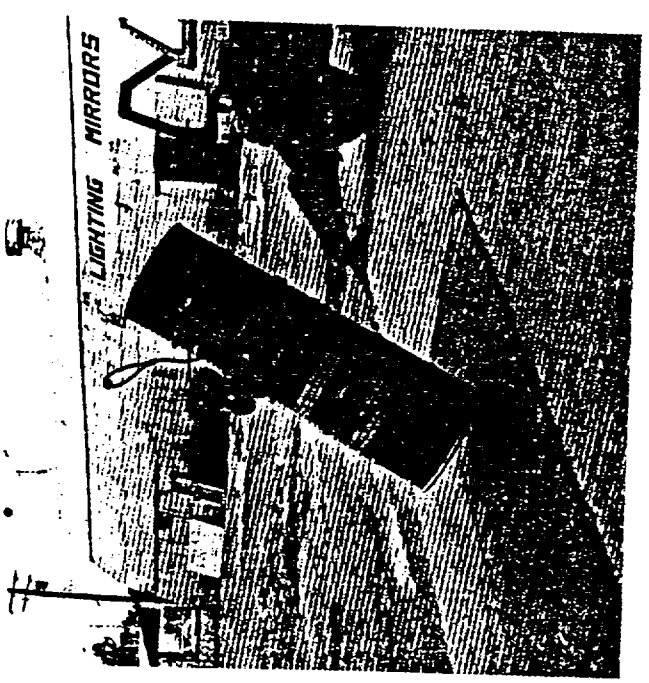

Figure 2.6.3 Second 0.3m (1 ft.) Free Drop Container #18

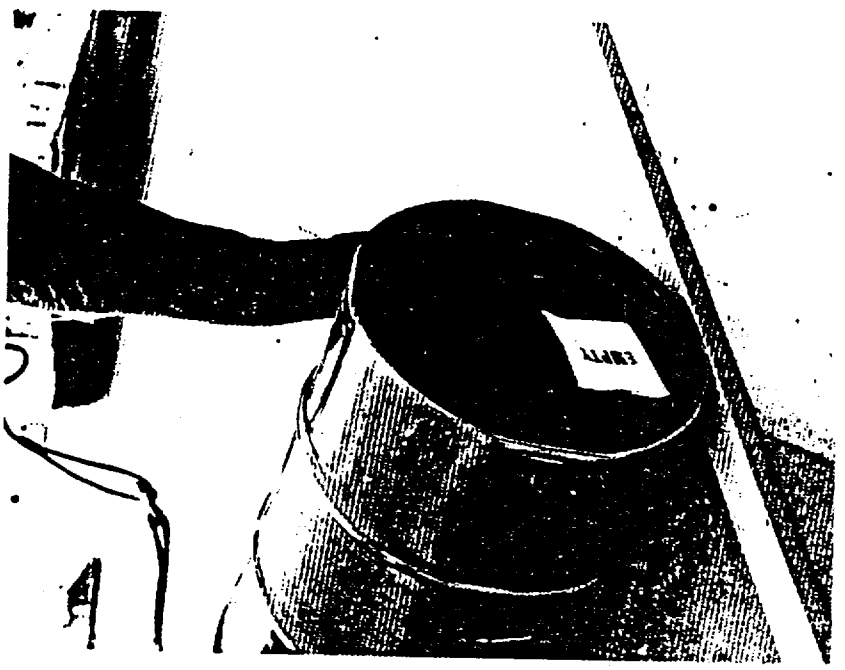

Figure 2.6.6 Cumulative Effect on Bottom of Four 0.3m Free Drops on Upper Rim Container #18

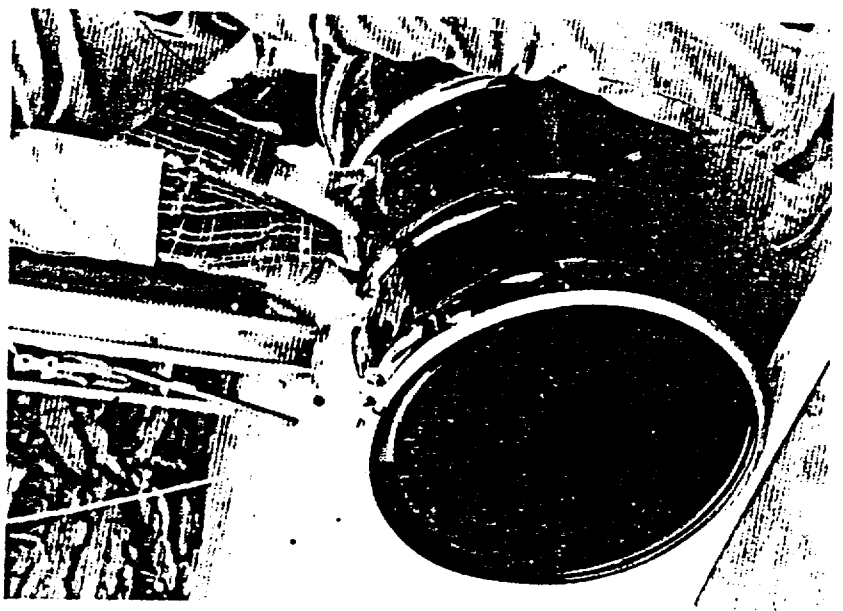

Figure 2.6.5 Cumulative Effect of Four 0.3m Free Drops on Upper Rim Container #18

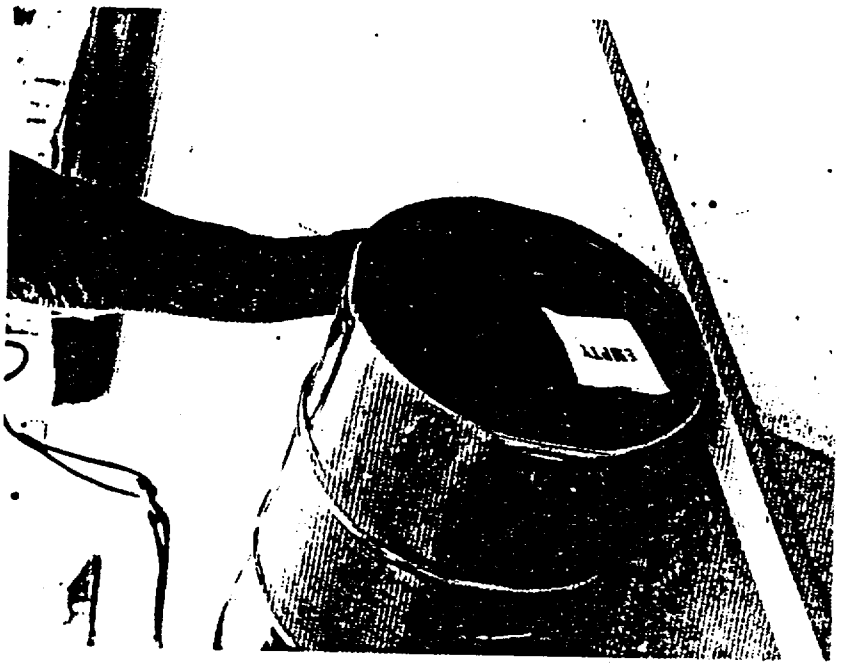

Figure 2.6.6 Cumulative Effect on Bottom of Four 0.3m Free Drops on Upper Rim Container #18

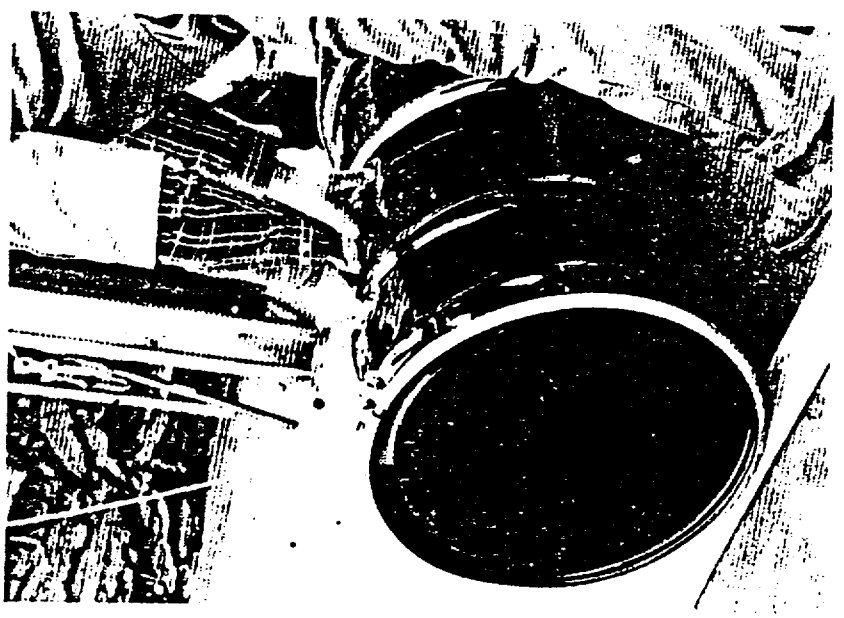

Figure 2.6.5 Cumulative Effect of Four 0.3m Free Drops on Upper Rim Container #18

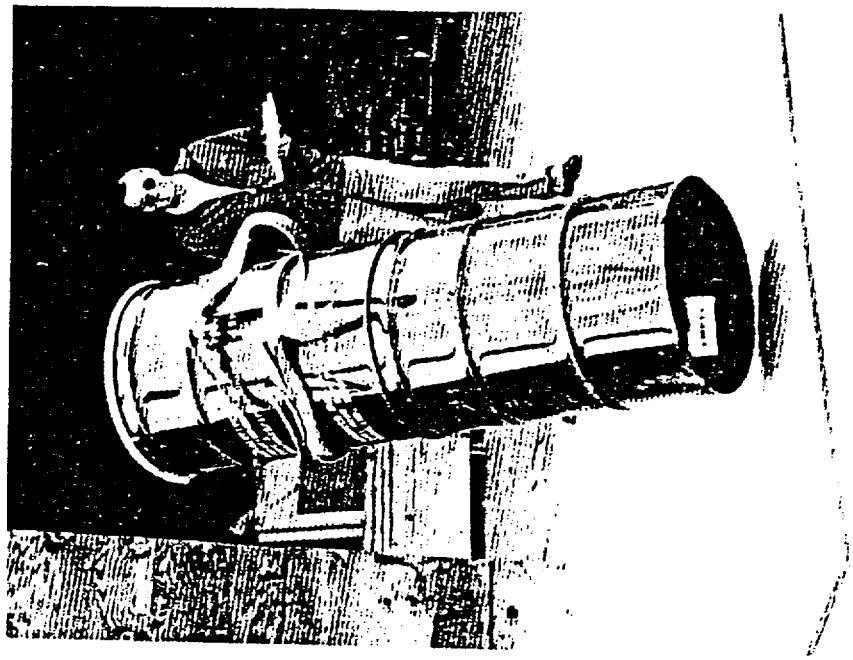

Figure 2.6.8 0.3m Free Drop Tests Container
#18 Bottom Rim

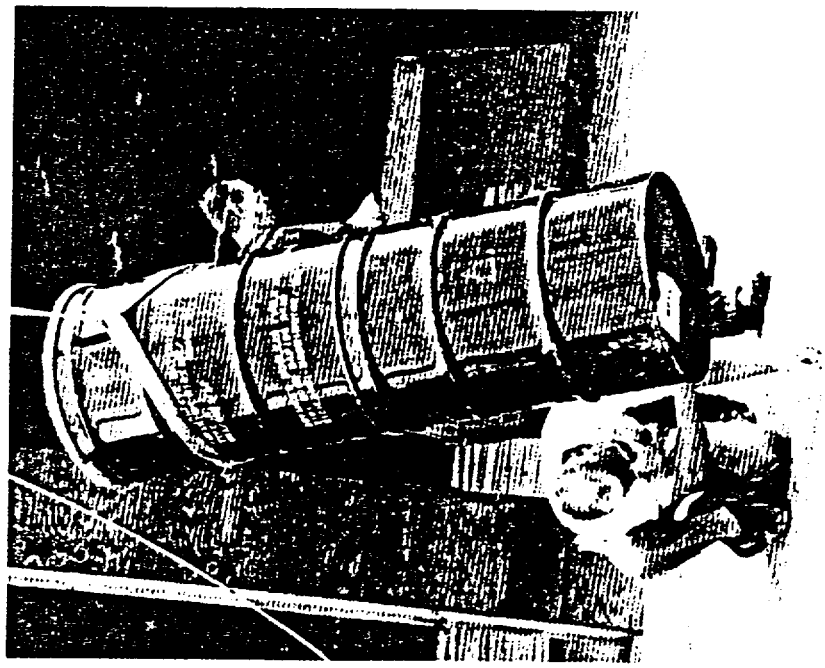

Figure 2.6.7 0.3m Free Drop Tests Container
#18 Bottom Rim

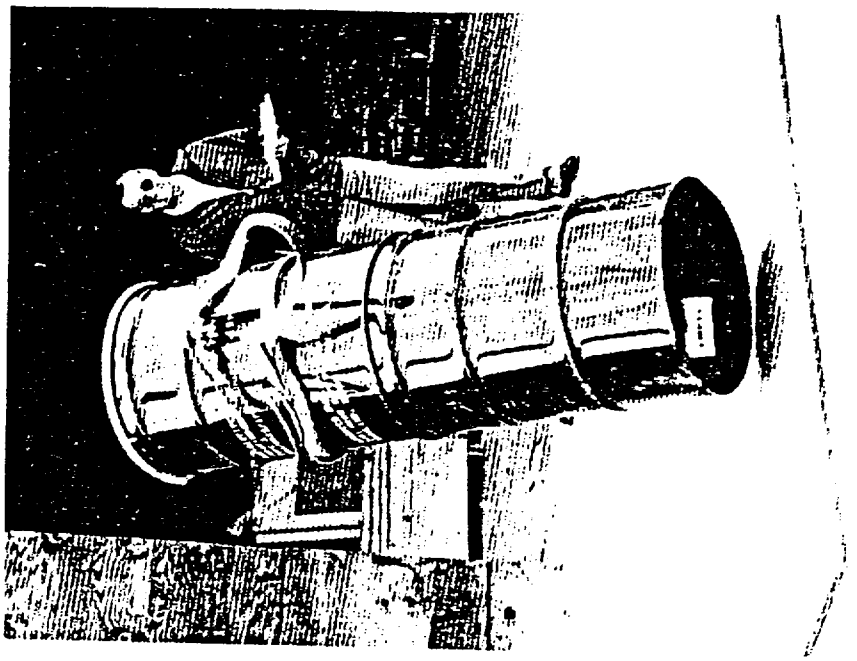

Figure 2.6.8 0.3m Free Drop Tests Container
#18 Bottom Rim

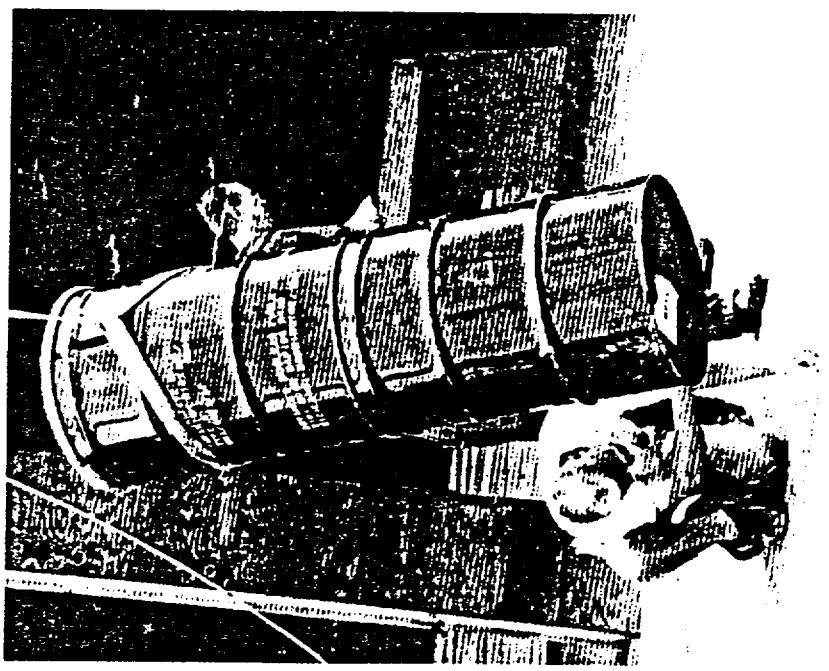

Figure 2.6.7 0.3m Free Drop Tests Container
#18 Bottom Rim

Figure 2.6.10 Container #18 Lower End After Completion of 0.3m Drops

Figure 2.6.9 Container #18 After Completion of the 0.3m Drops

Figure 2.6.10 Container #18 Lower End After Completion of 0.3m Drops

Figure 2.6.9 Container #18 After Completion of the 0.3m Drops

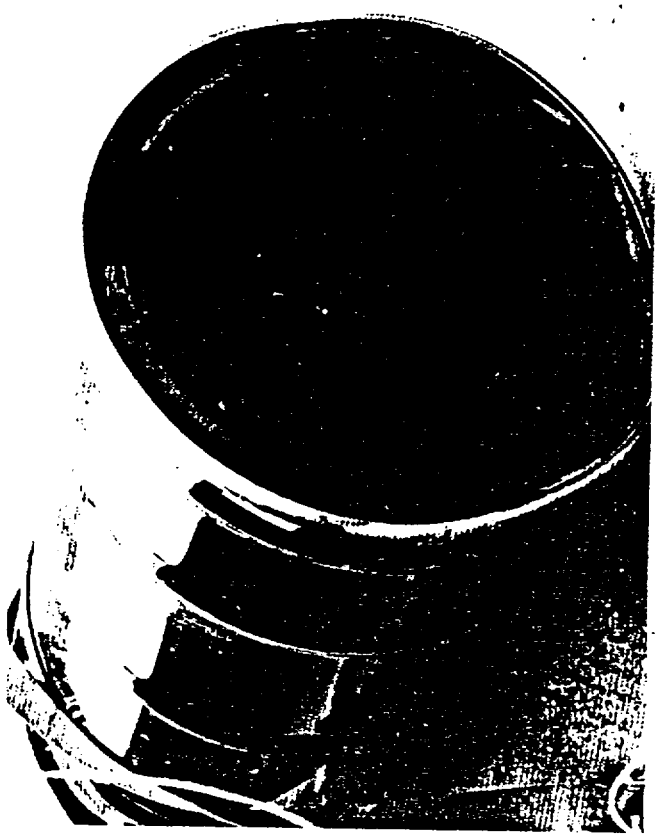

Figure 2.7.2 Upper Rim Deformation from Initial 1.2m Free Drop - Container #18

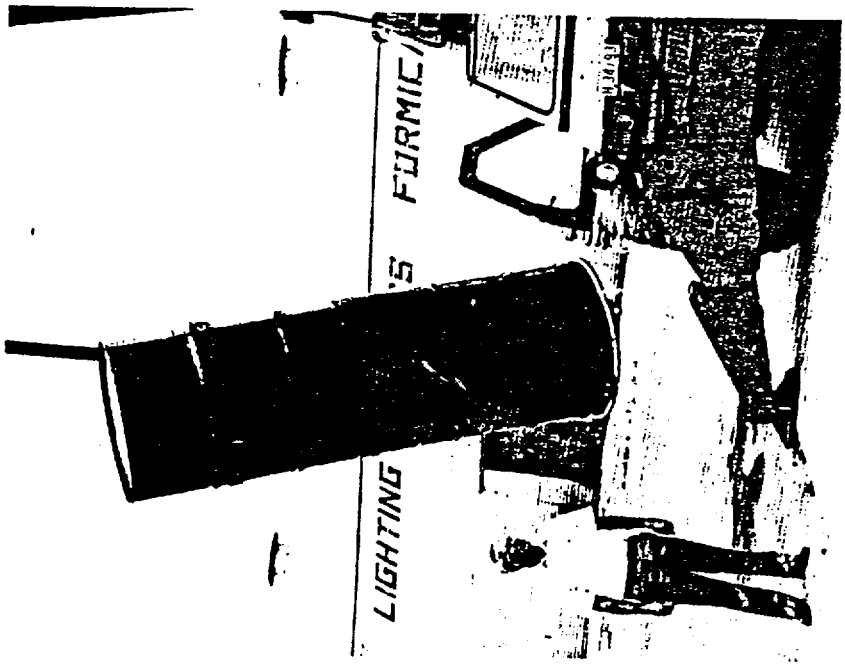

Figure 2.7.1 Container #18 Suspended for Initial 1.2m Free Drop

Figure 2.7.2 Upper Rim Deformation from Initial 1.2m Free Drop - Container #18

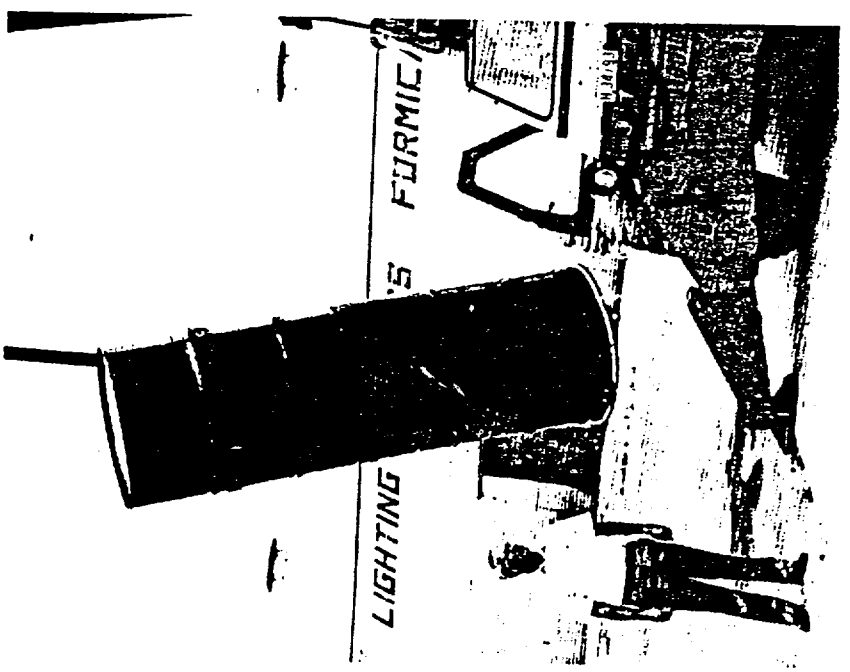

Figure 2.7.1 Container #18 Suspended for Initial 1.2m Free Drop

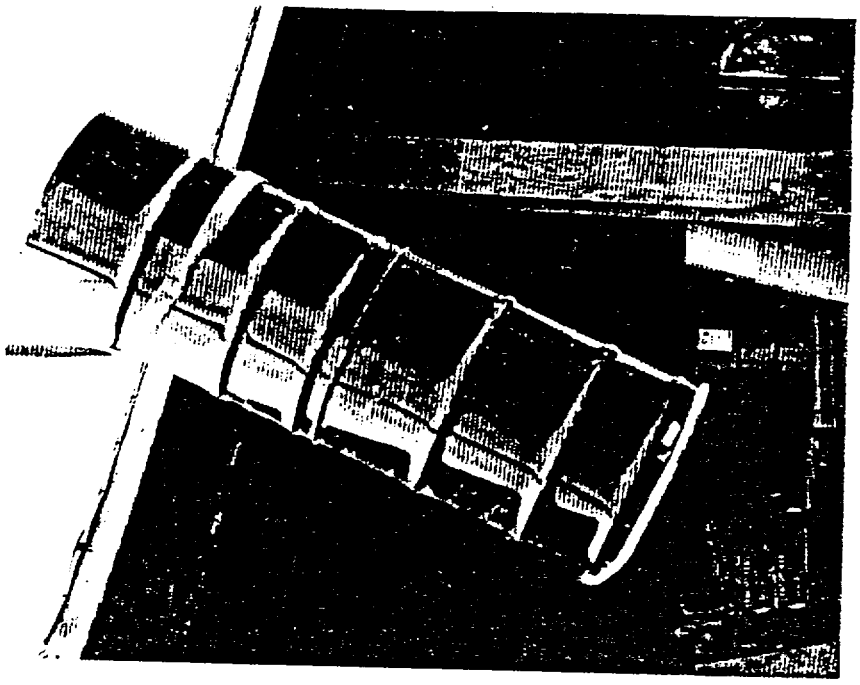

Figure 2.7.4 Container #18 Suspended for Second 1.2m Drop

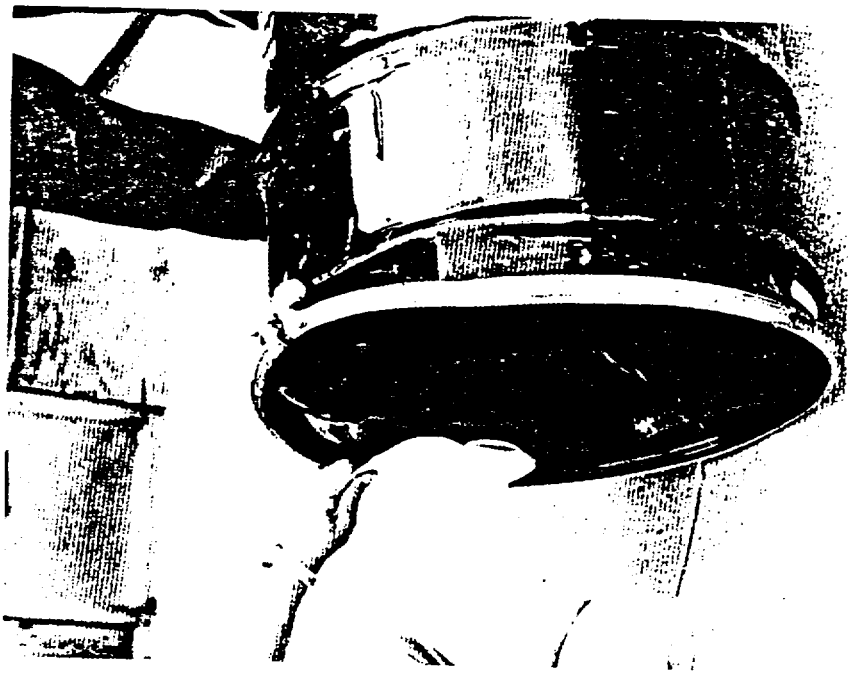

Figure 2.7.3 Container #18 Showing Deformation After Initial 1.2m Drop

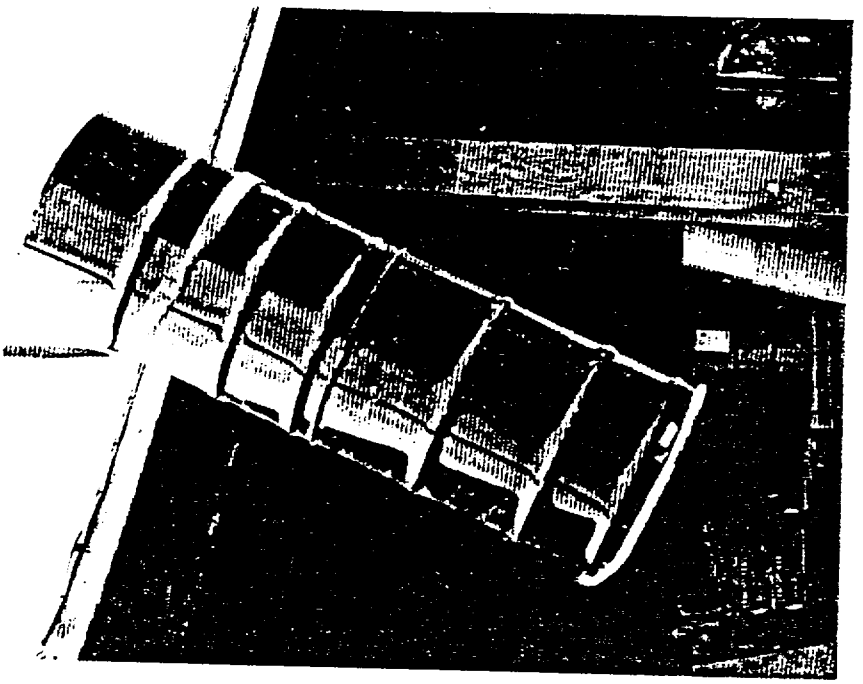

Figure 2.7.4 Container #18 Suspended for Second 1.2m Drop

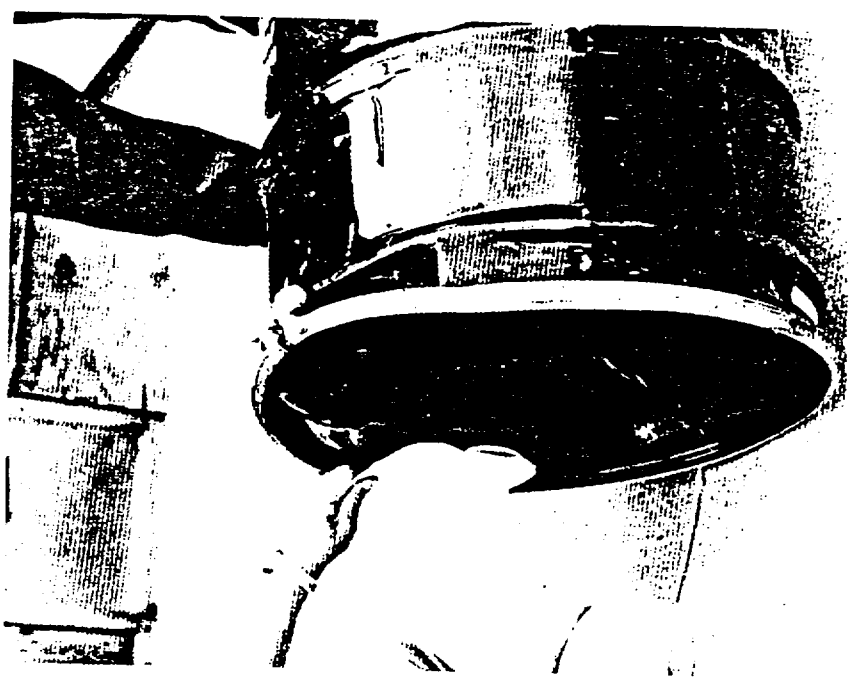

Figure 2.7.3 Container #18 Showing Deformation After Initial 1.2m Drop

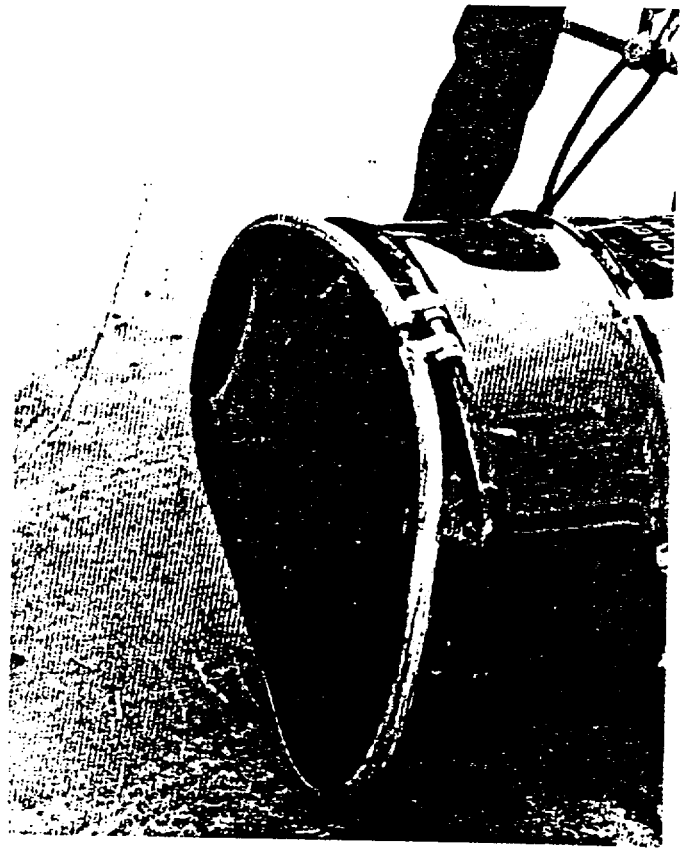

Figure 2.7.5 Container #18 Upper End After Completion of six 1.2m Drops

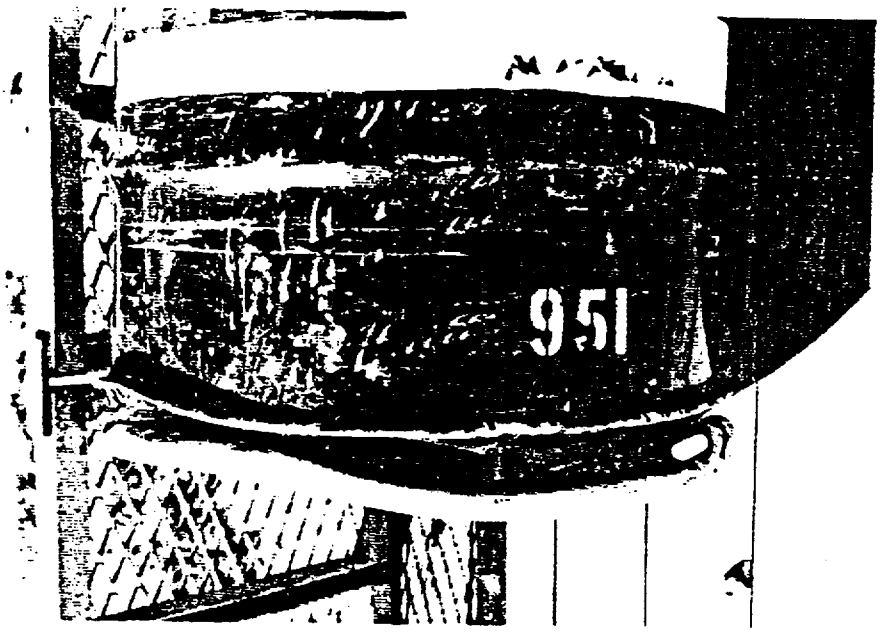

Fig. 2.7.7 Container #951 Alternate View Showing Cumulative Effect of 14 Drops of Normal Conditions of Transport

Fig. 2.7.6 Container #951 Subsequent to Series of 14 Drops of Normal Conditions of Transport

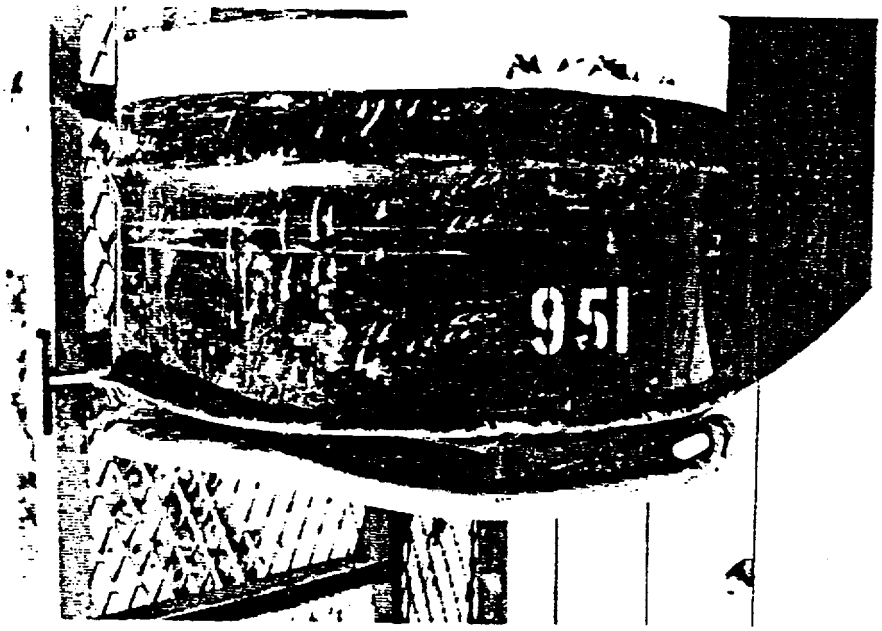

Fig. 2.7.7 Container #951 Alternate View Showing Cumulative Effect of 14 Drops of Normal Conditions of Transport

Fig. 2.7.6 Container #951 Subsequent to Series of 14 Drops of Normal Conditions of Transport

Figure 2.8.2 Compression Test - Longitudional View

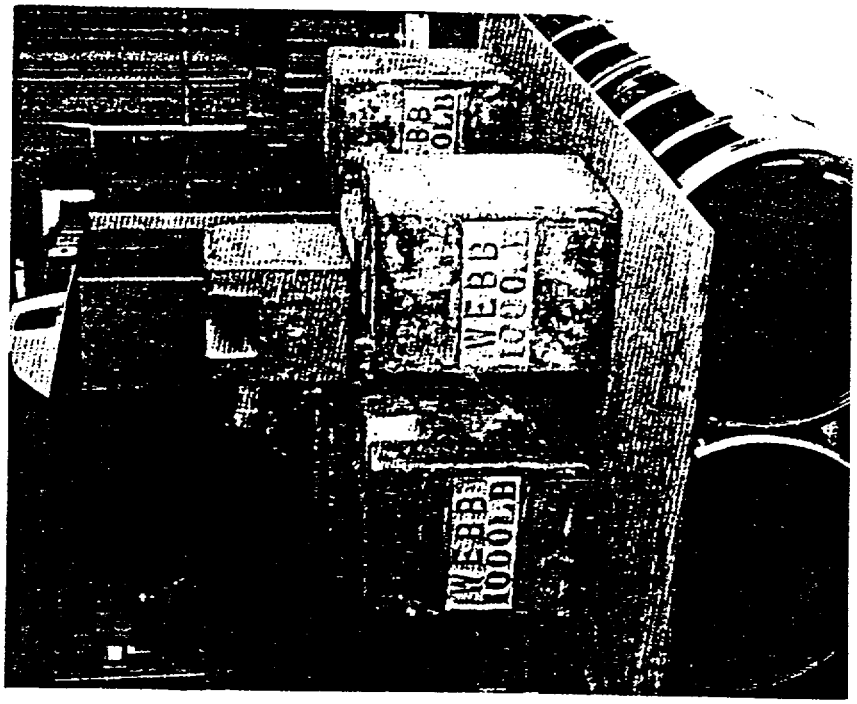

Figure 2.8.1 Compression Test

Figure 2.8.2 Compression Test - Longitudional View

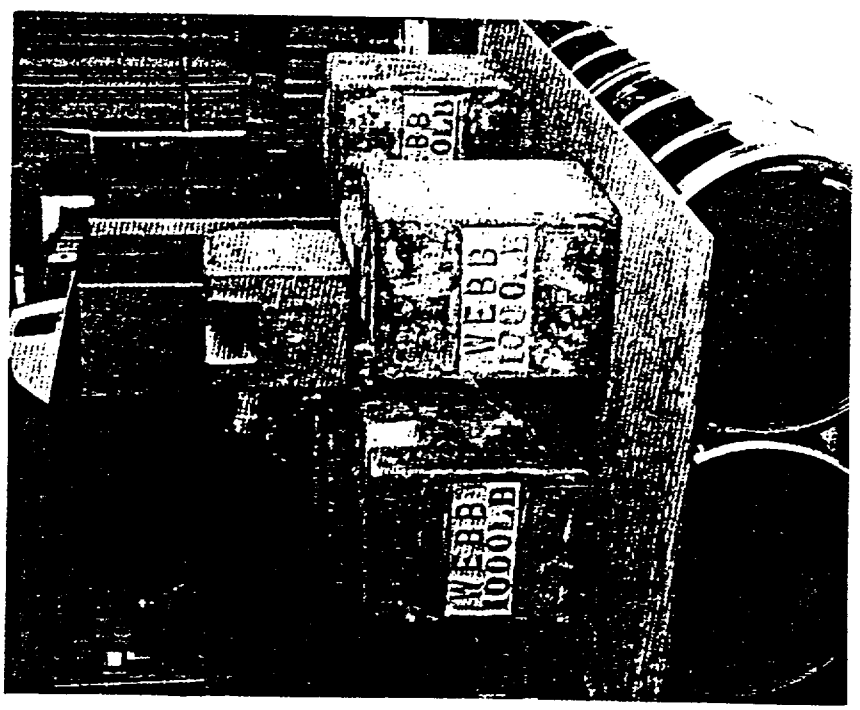

Figure 2.8.1 Compression Test

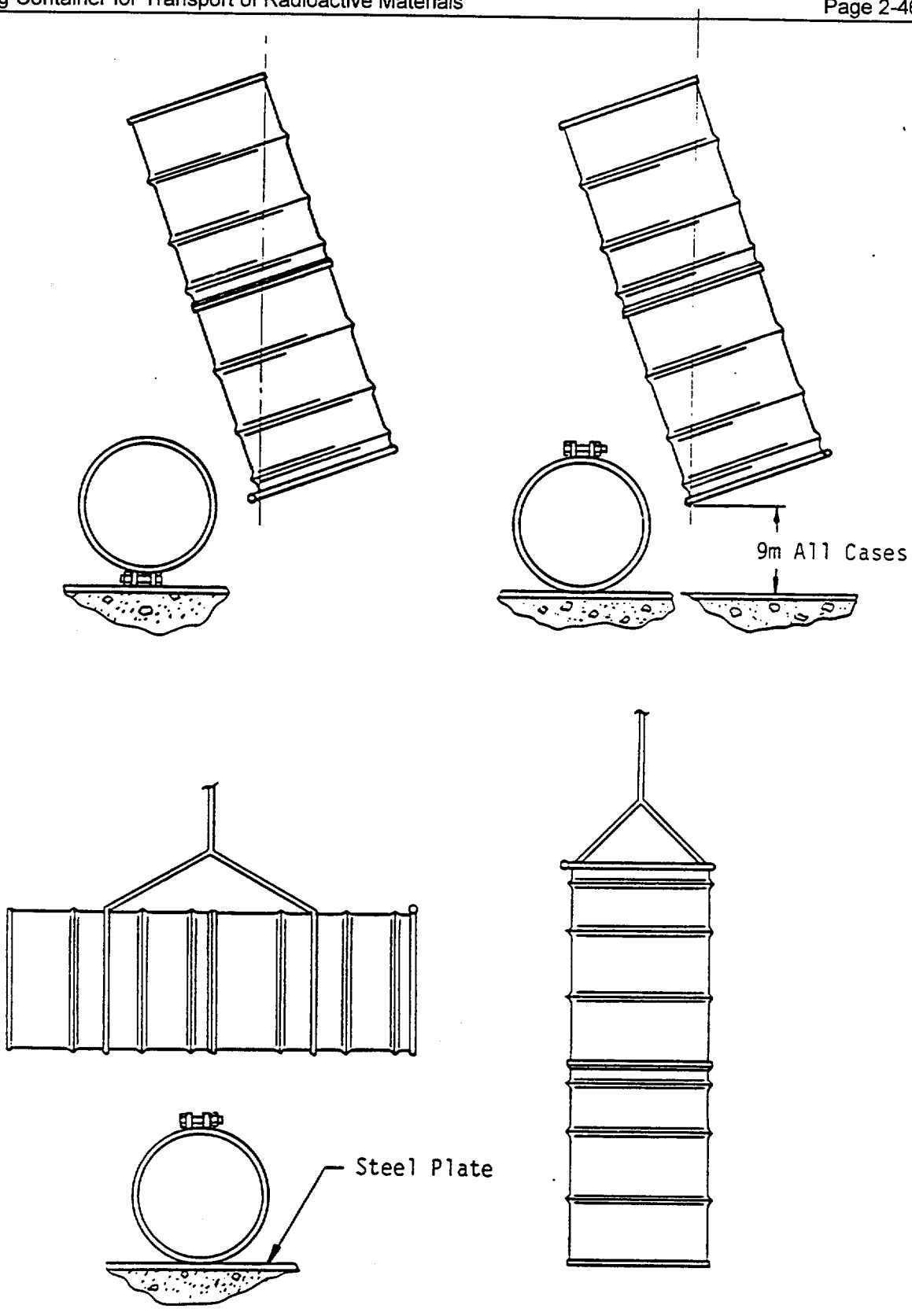

Fig. 2.9 9m (30 ft) Drop Test Orientations 10 CFR 71.73(c)(1)

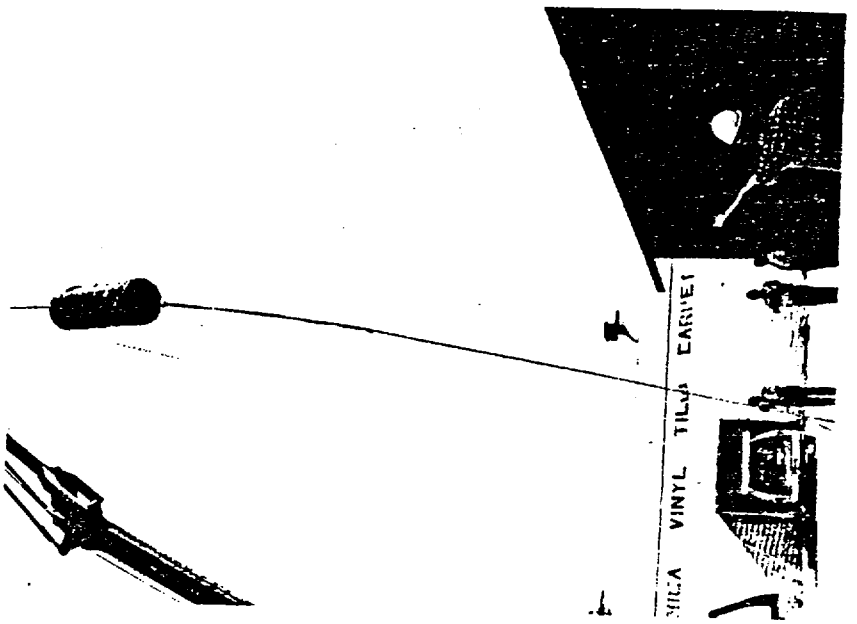

Figure 2.10.2 Container #57 Prior to 9m Drop

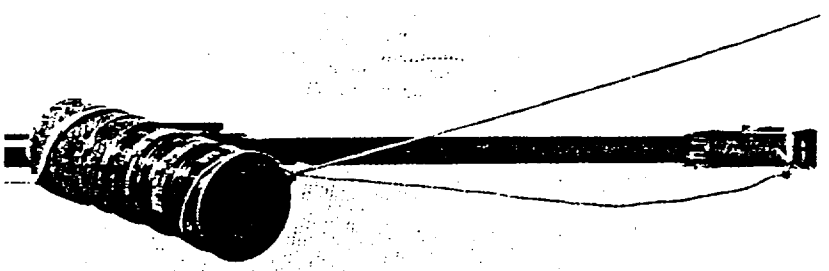

Figure 2.10.1 Container #57 Suspended for 9m Drop

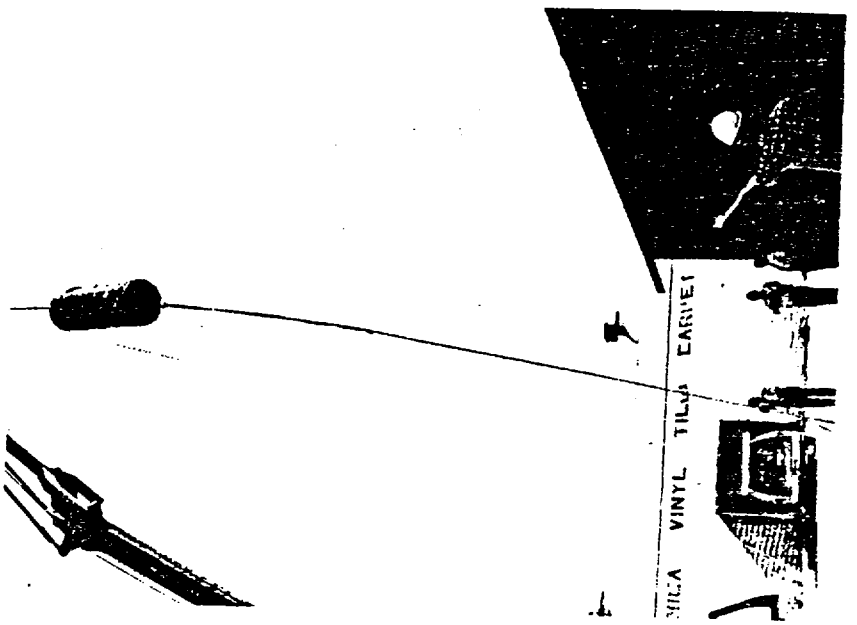

Figure 2.10.2 Container #57 Prior to 9m Drop

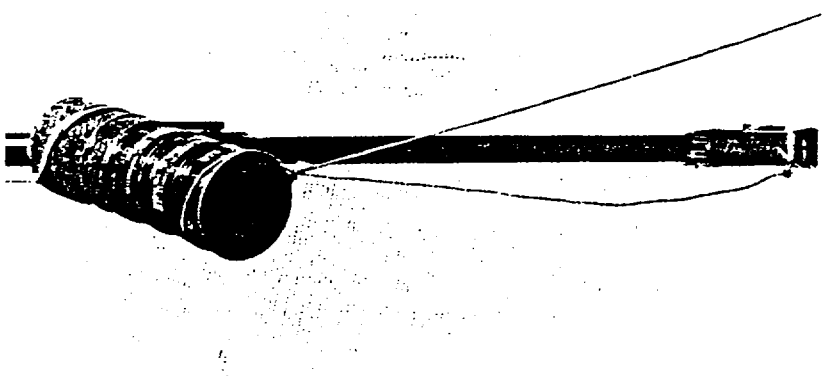

Figure 2.10.1 Container #57 Suspended for 9m Drop

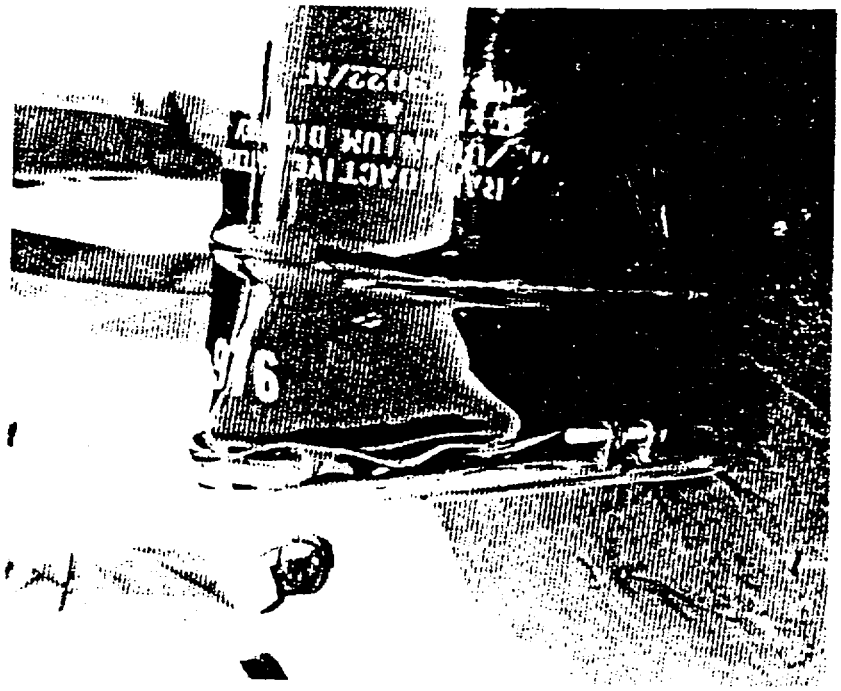

Figure 2.10.4 Container #57 Deformation from 9m Drop onto Ring Locking Lug

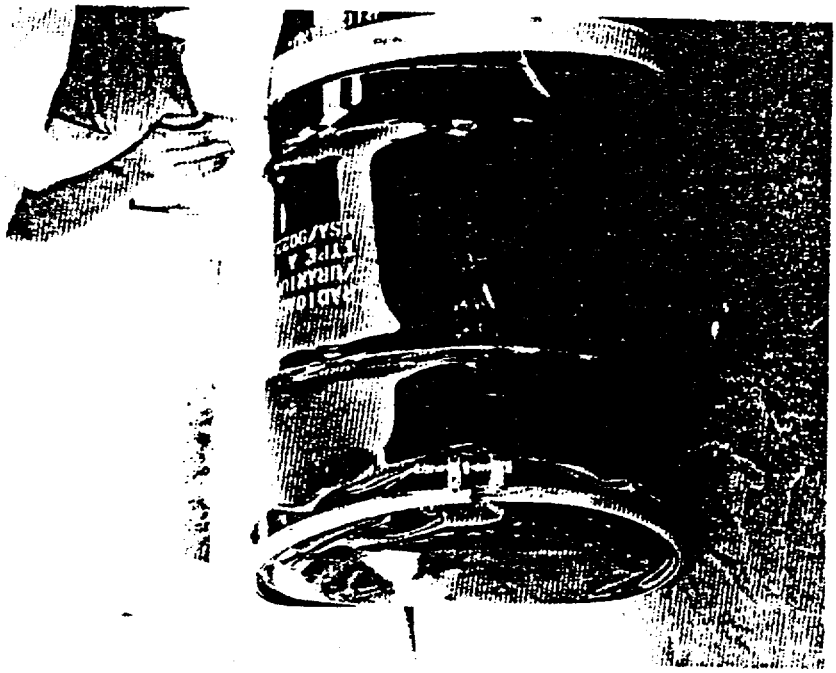

Figure 2.10.3 Container #57 Deformation from 9m Drop onto Ring Locking Lug

Figure 2.10.4 Container #57 Deformation from 9m Drop onto Ring Locking Lug

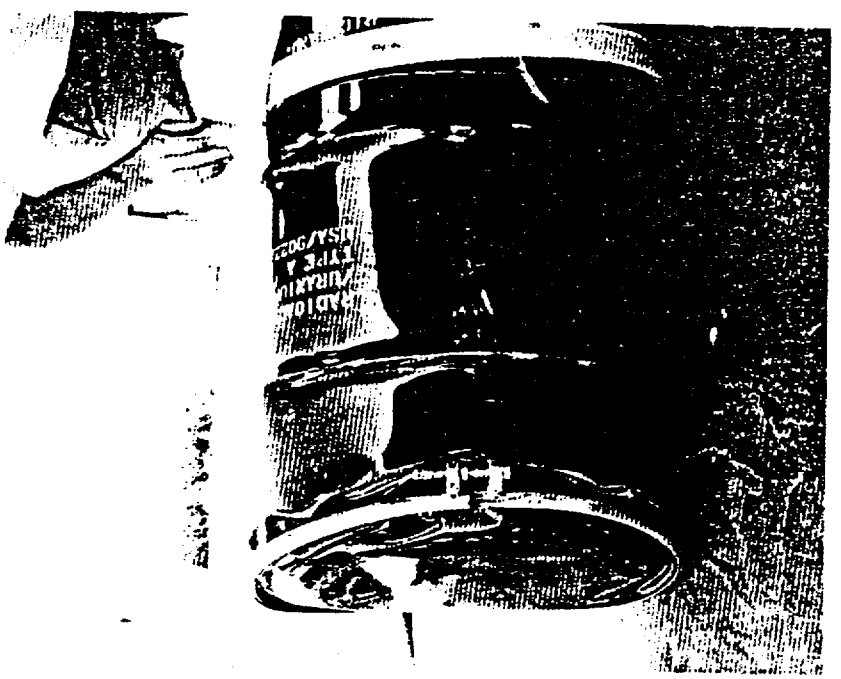

Figure 2.10.3 Container #57 Deformation from 9m Drop onto Ring Locking Lug

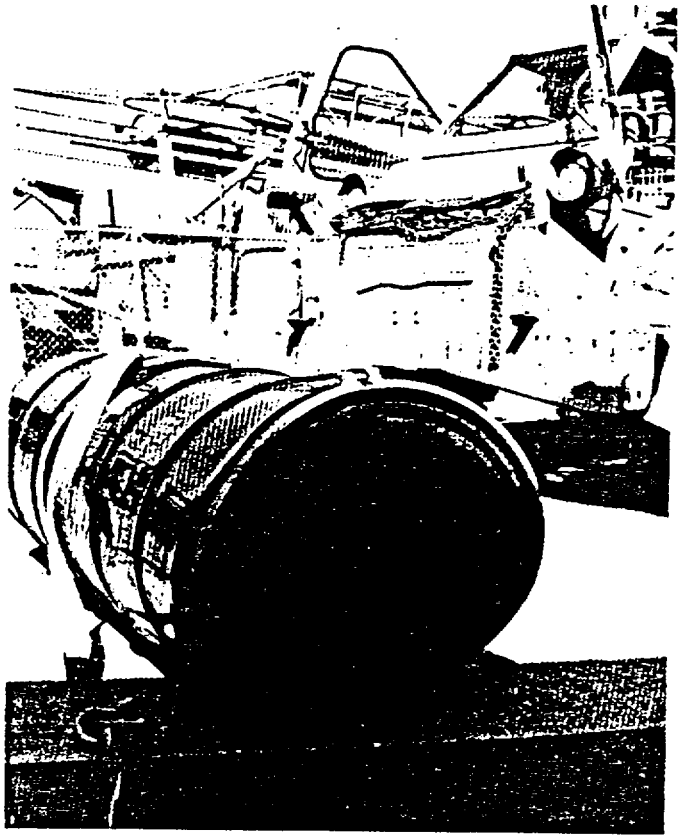

Figure 2.10.5 Container #57 Deformation from 9m Drop onto Ring Locking Lug

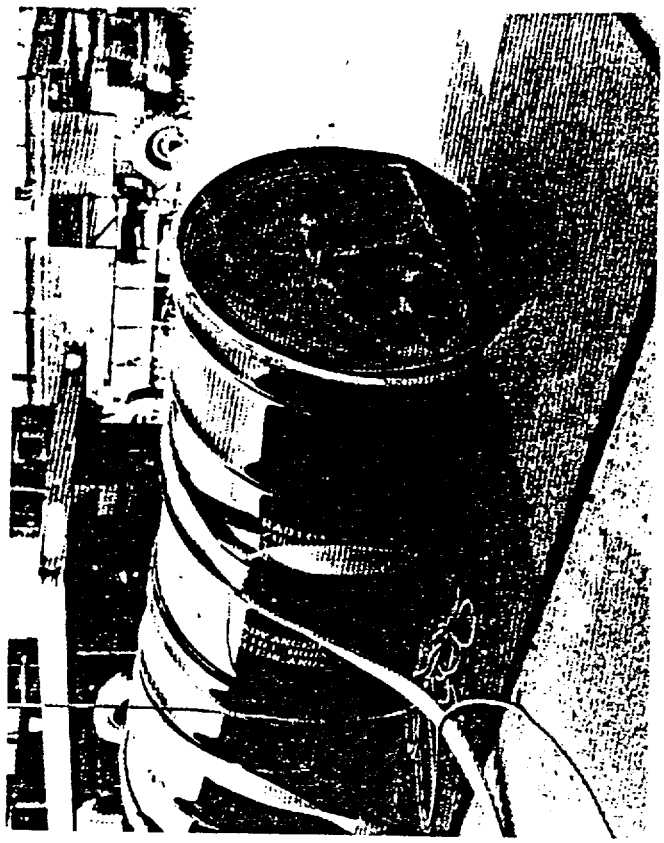

Figure 2.11.2 Container #14 Following Impact of 9m Drop

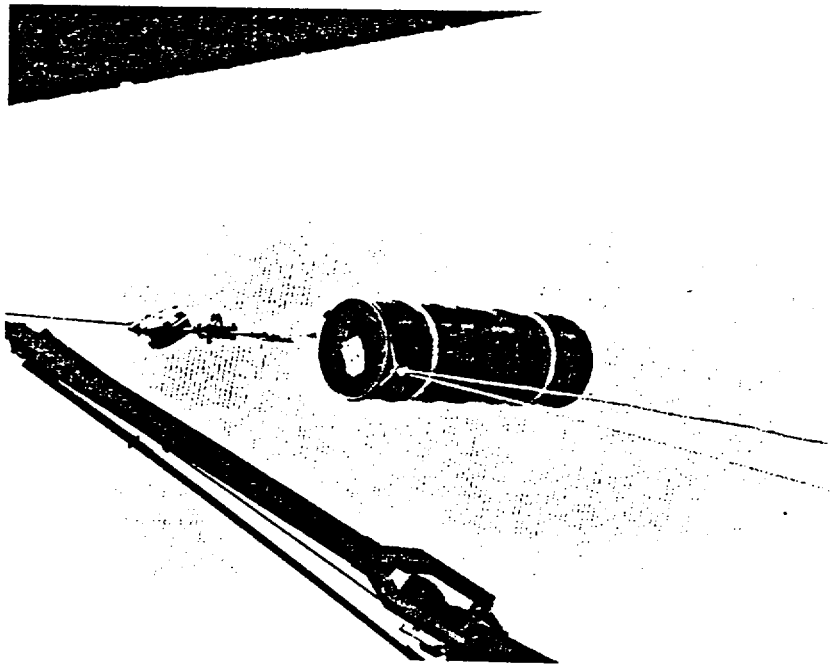

Figure 2.11.1 Container #14 Suspended for 9m Drop

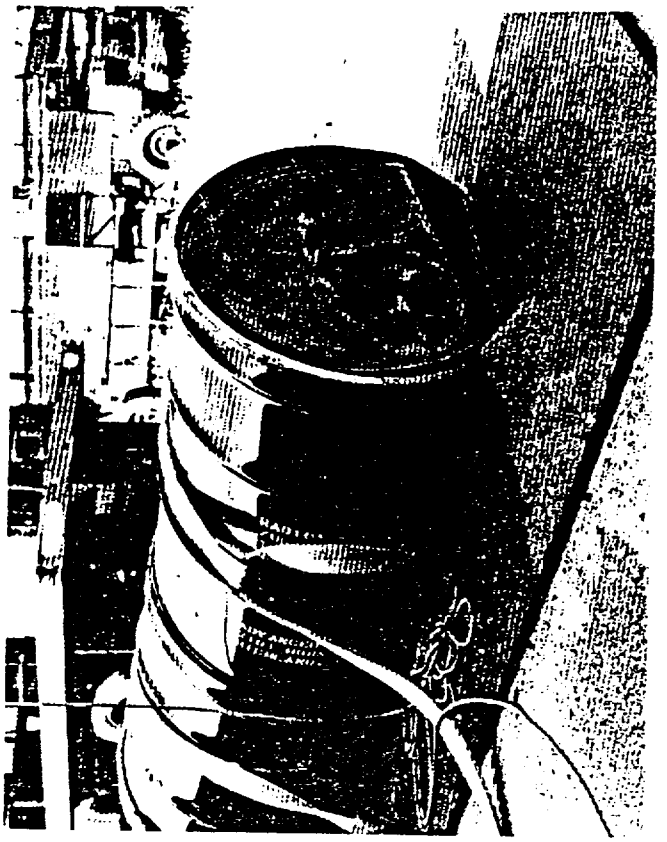

Figure 2.11.2 Container #14 Following Impact of 9m Drop

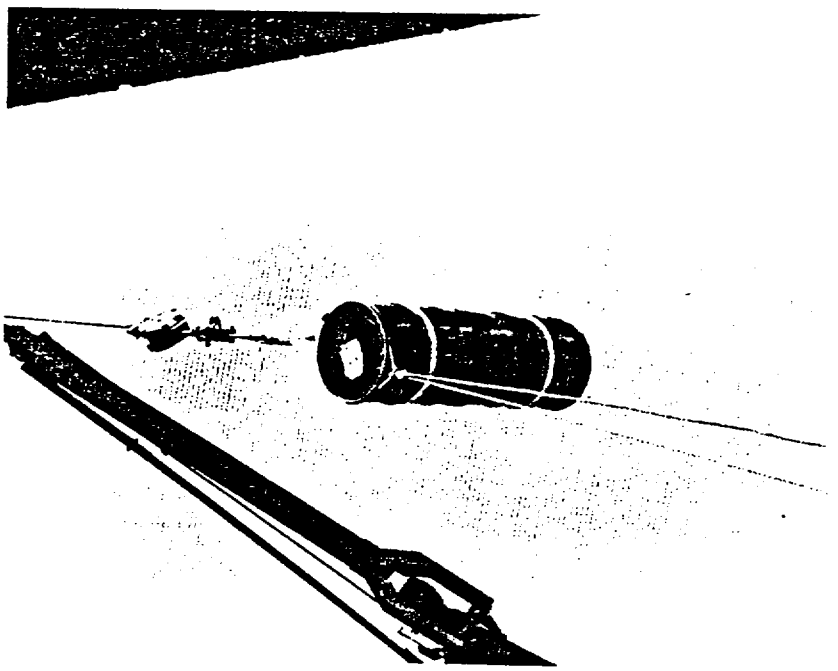

Figure 2.11.1 Container #14 Suspended for 9m Drop

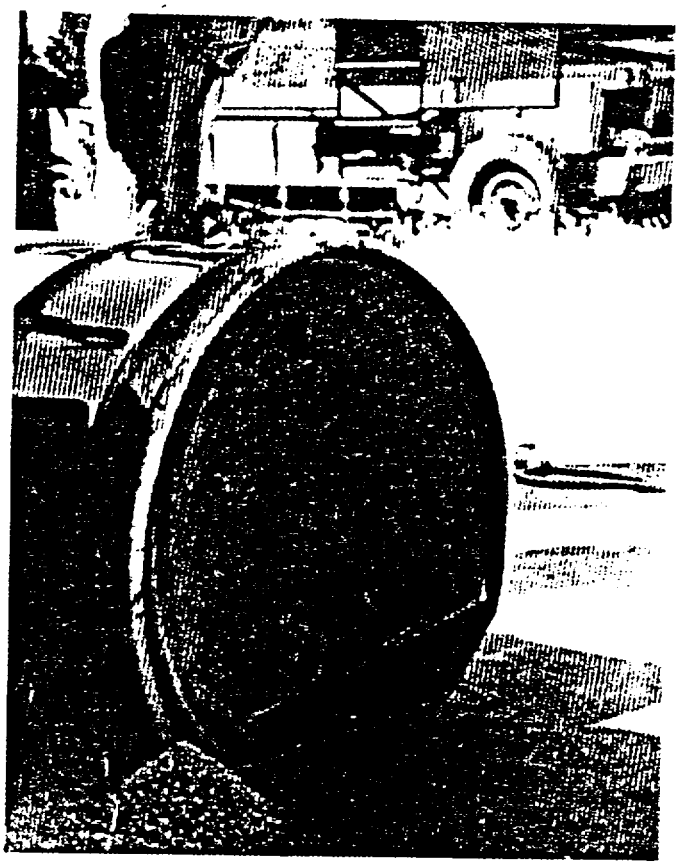

Figure 2.11.3 Container #14 Deformation from 9m Drop

Figure 2.12.2 Container #42 Deformation Resulting from 9m Drop

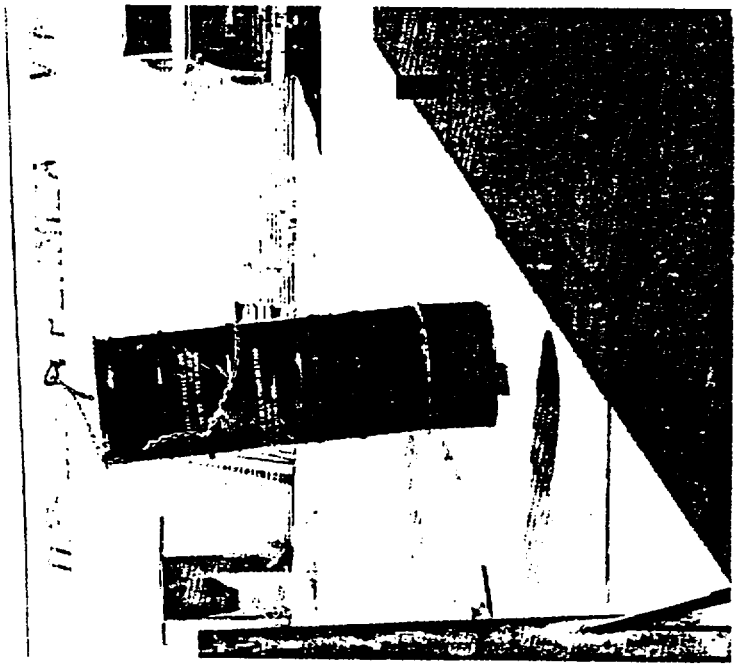

Figure 2.12.1 Container #42 Bounced from Impact Plate After 9m Drop

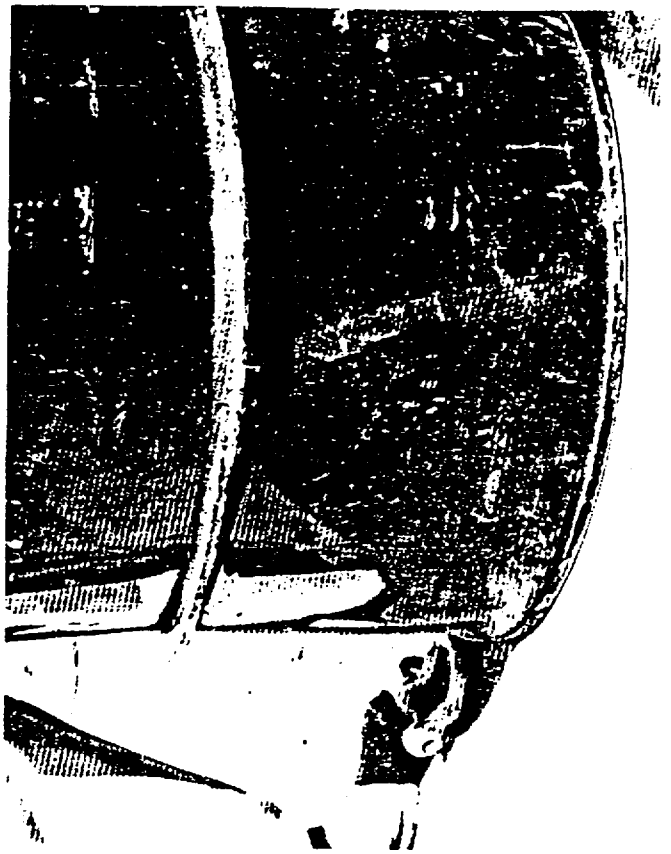

Figure 2.12.2 Container #42 Deformation Resulting from 9m Drop

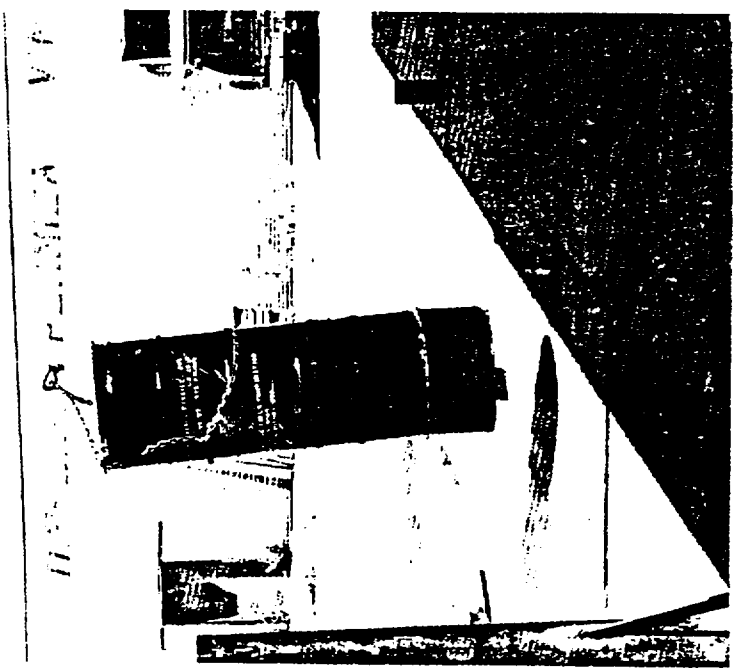

Figure 2.12.1 Container #42 Bounced from Impact Plate After 9m Drop

Figure 2.12.3 Container #42 Raised to show Imprint from Inner Container on Container Bottom

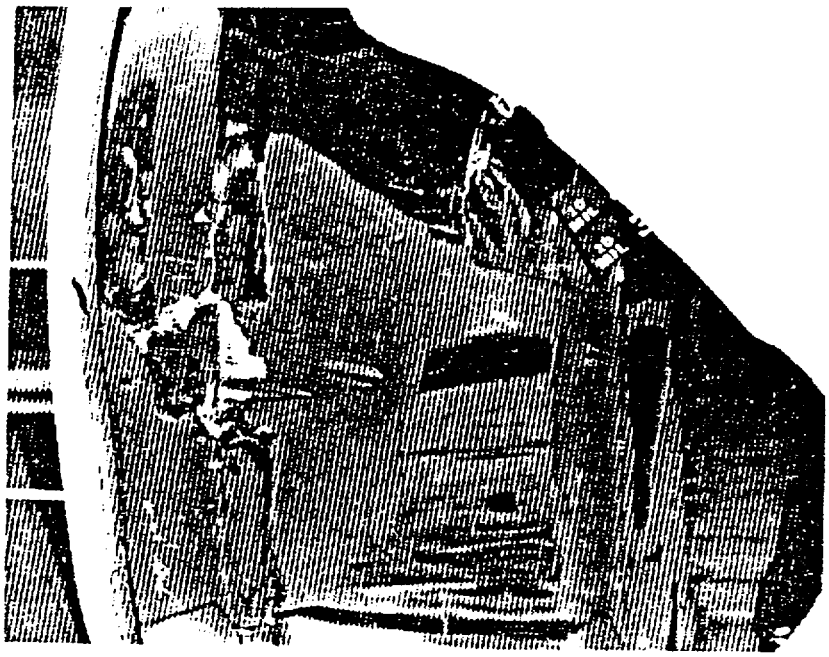

Figure 2.13.2 Damage from 1m Drop onto Penetration Test Bar

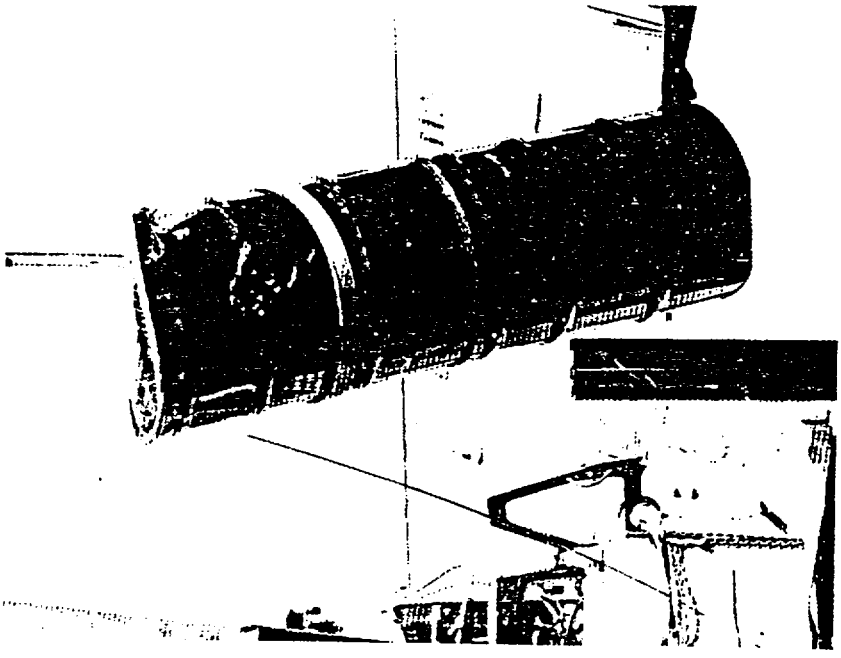

Figure 2.13.1 Container #57 Suspended Over Penetration Test Bar

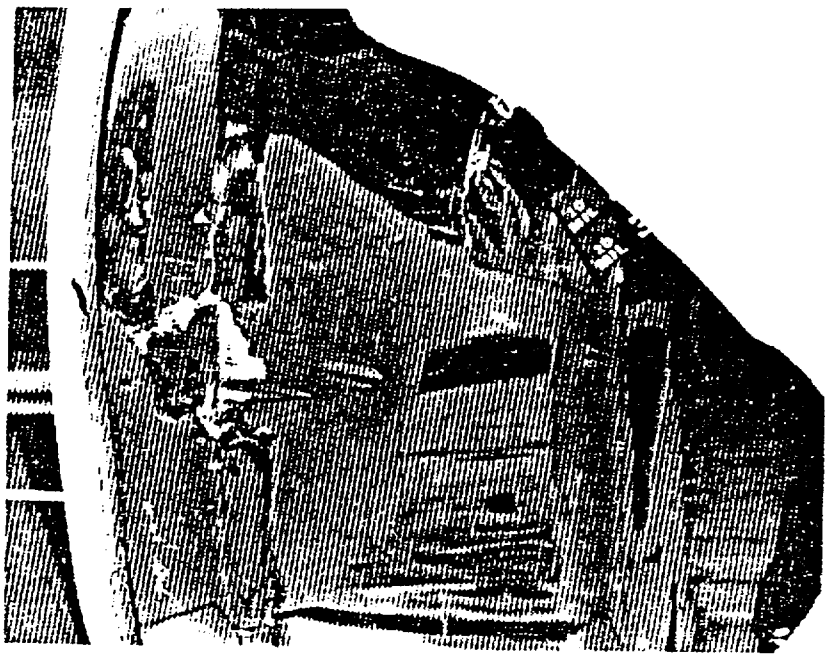

Figure 2.13.2 Damage from 1m Drop onto Penetration Test Bar

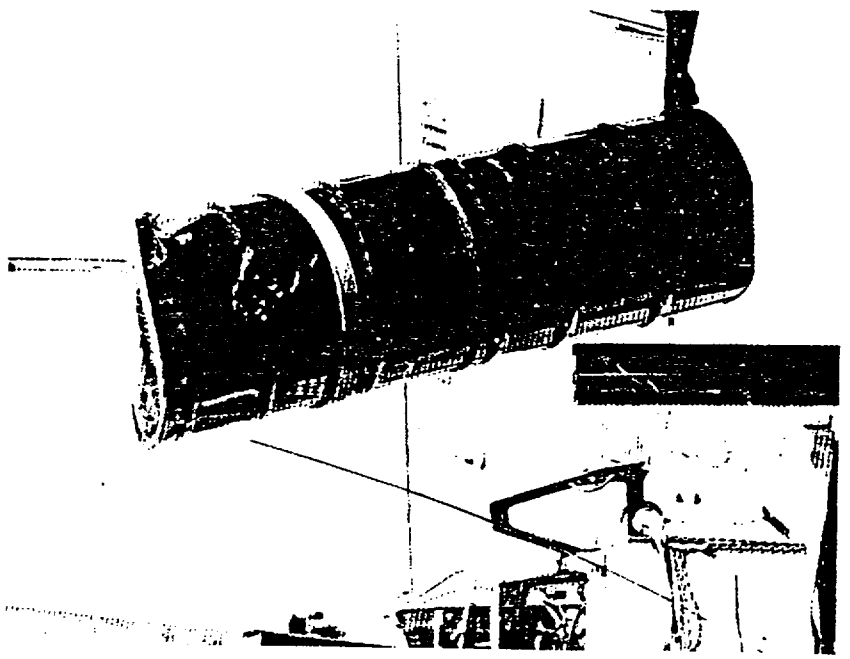

Figure 2.13.1 Container #57 Suspended Over Penetration Test Bar

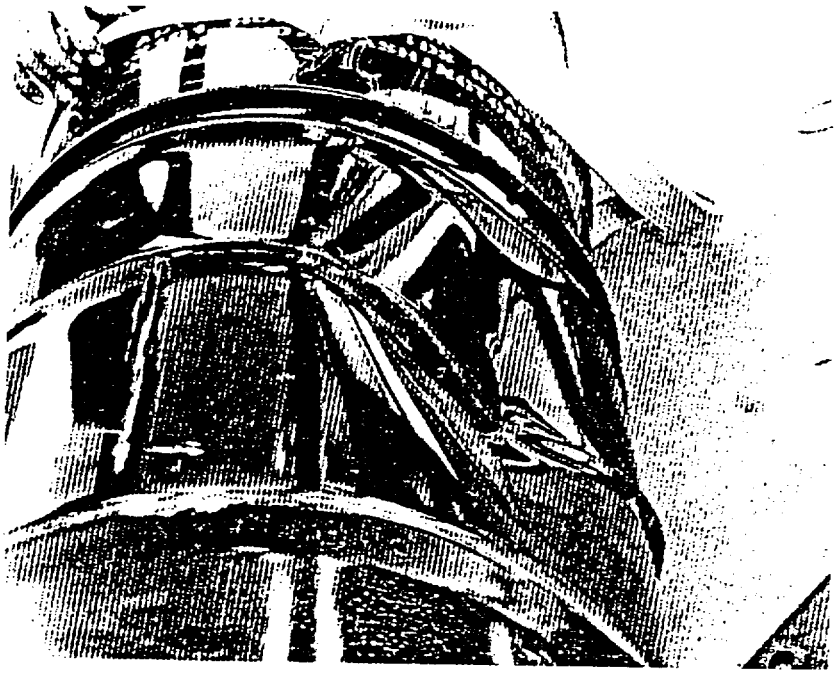

Figure 2.13.4 Deformation Resulting from Puncture Drop on Side of Container #57

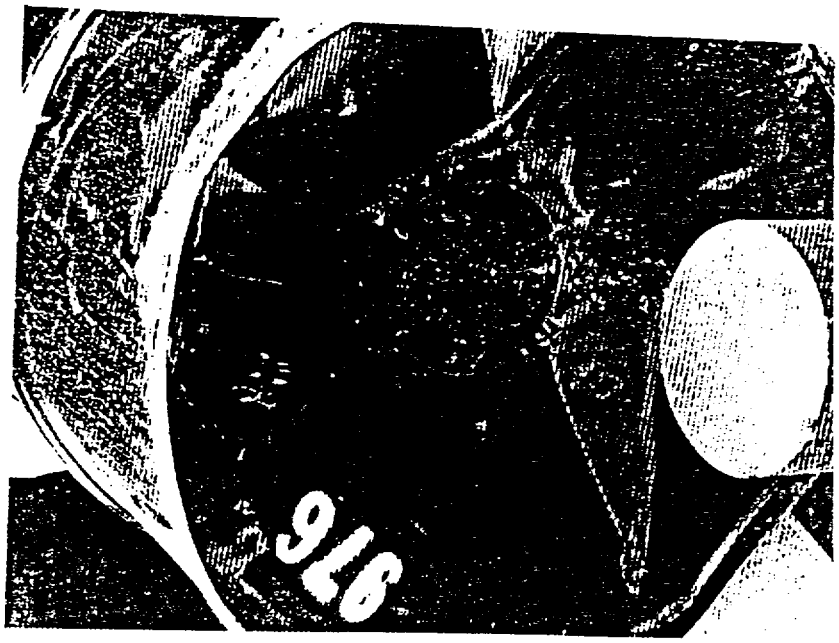

Figure 2.13.3 Deformation Resulting from Puncture Drop on Bottom of Container #57

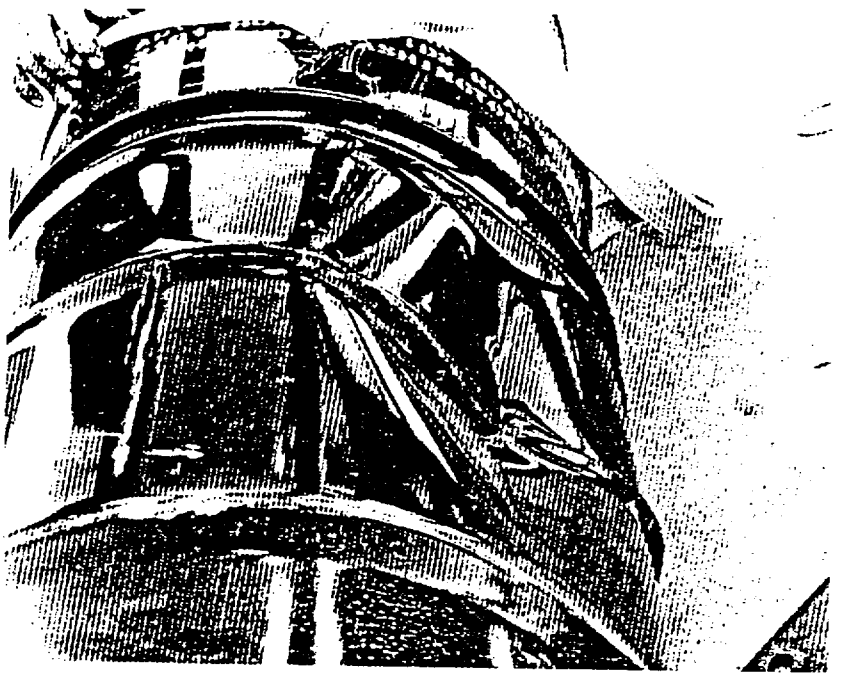

Figure 2.13.4 Deformation Resulting from Puncture Drop on Side of Container #57

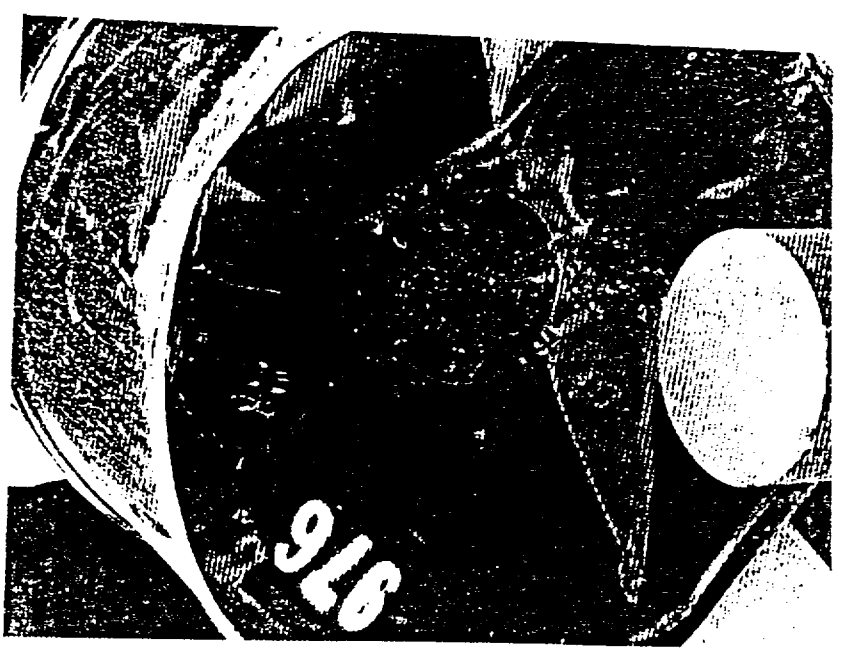

Figure 2.13.3 Deformation Resulting from Puncture Drop on Bottom of Container #57

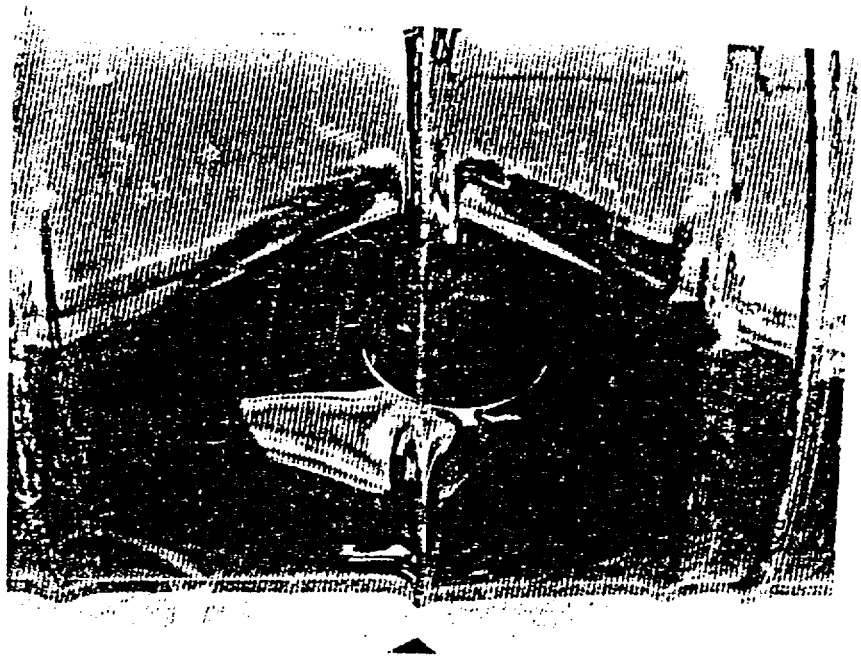

Figure 2.13.5 Deformation Resulting from Puncture Drop on Side - Container #57

Figure 2.14.2 Deformation from Oblique Strike of Figure 2.14.1 Container #35

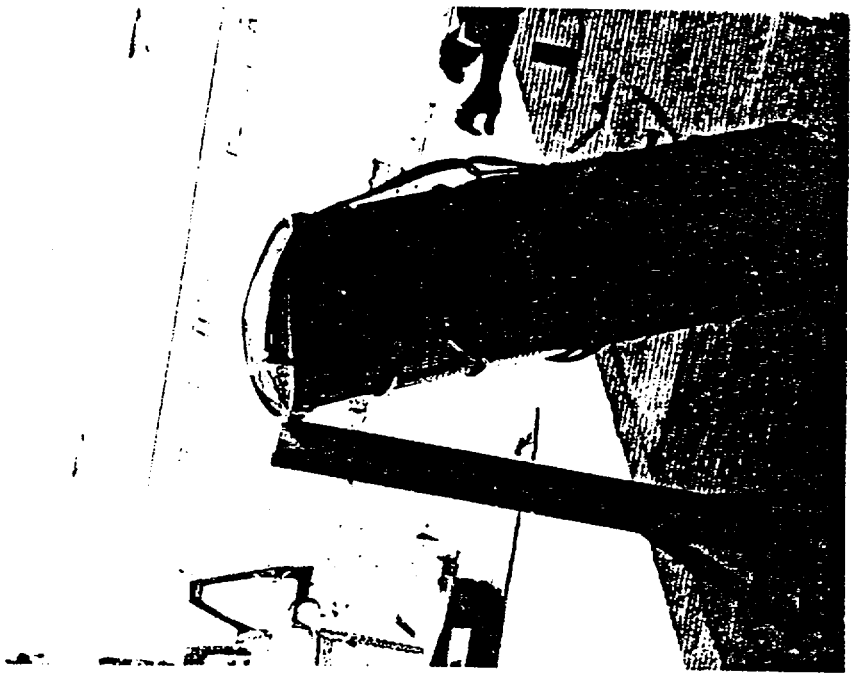

Figure 2.14.1 Oblique Drop on Lid Edge Container #35

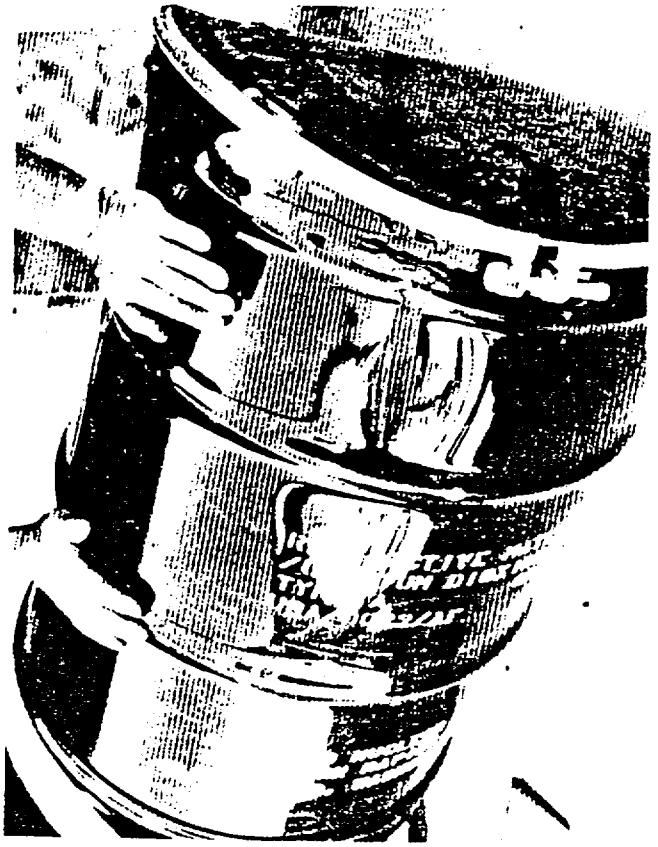

Figure 2.14.2 Deformation from Oblique Strike of Figure 2.14.1 Container #35

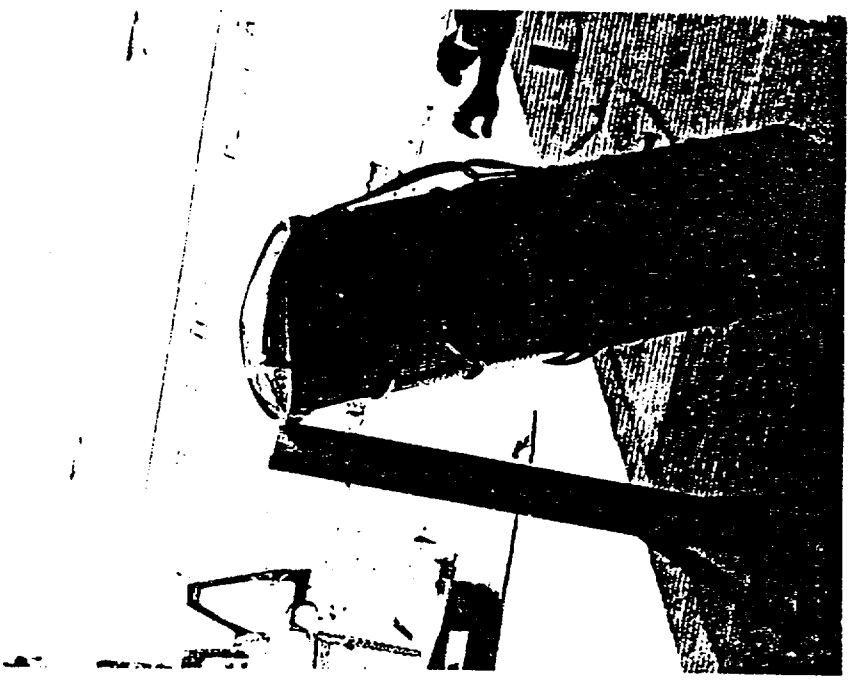

Figure 2.14.1 Oblique Drop on Lid Edge Container #35

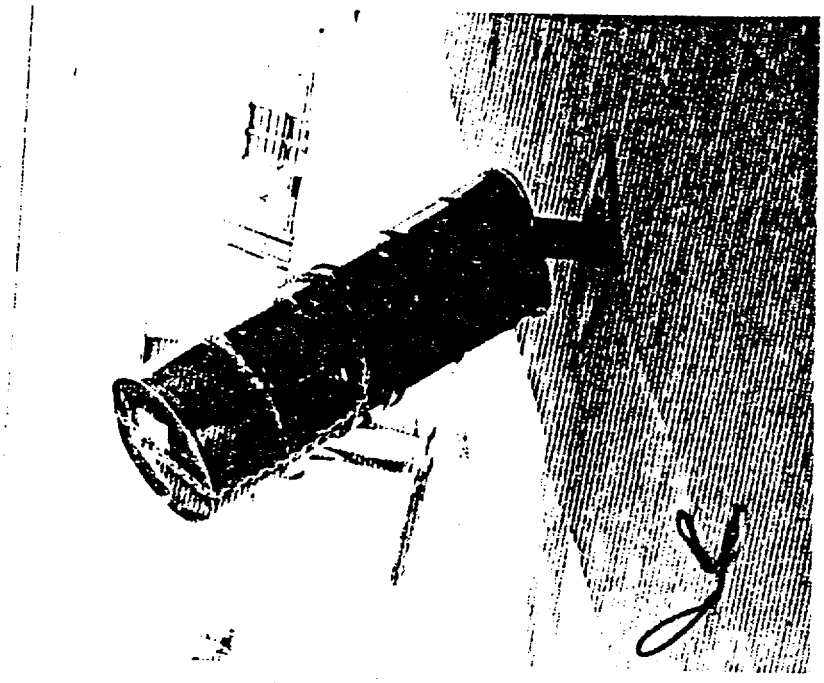

Figure 2.14.4 Impact on Container #35 Bottom

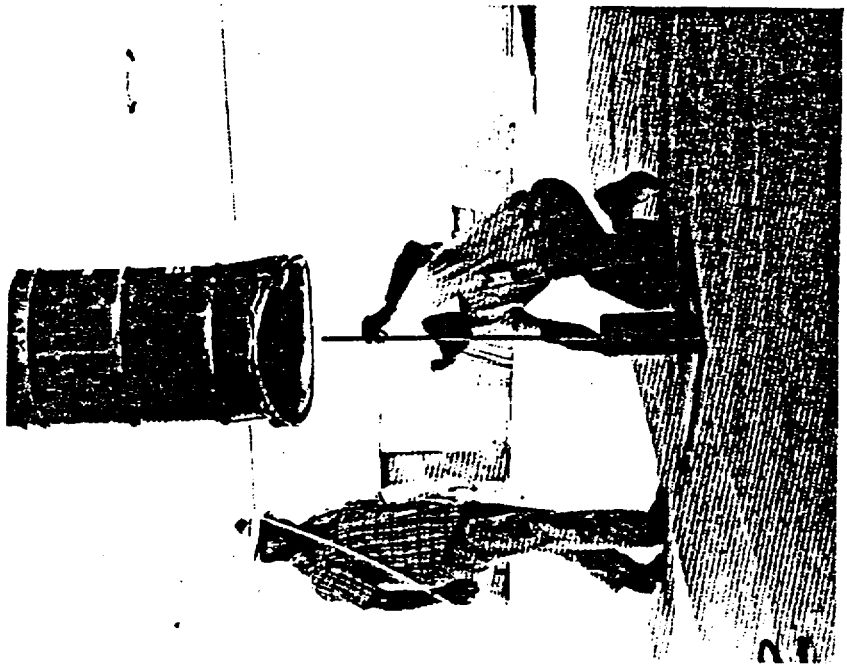

Figure 2.14.3 Preparations for Puncture Drop on Container #35 Bottom

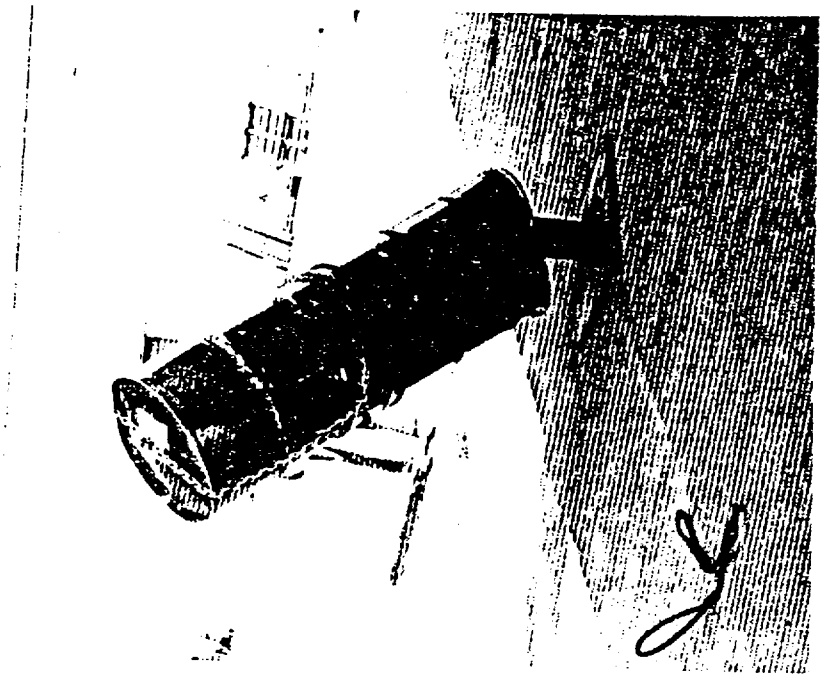

Figure 2.14.4 Impact on Container #35 Bottom

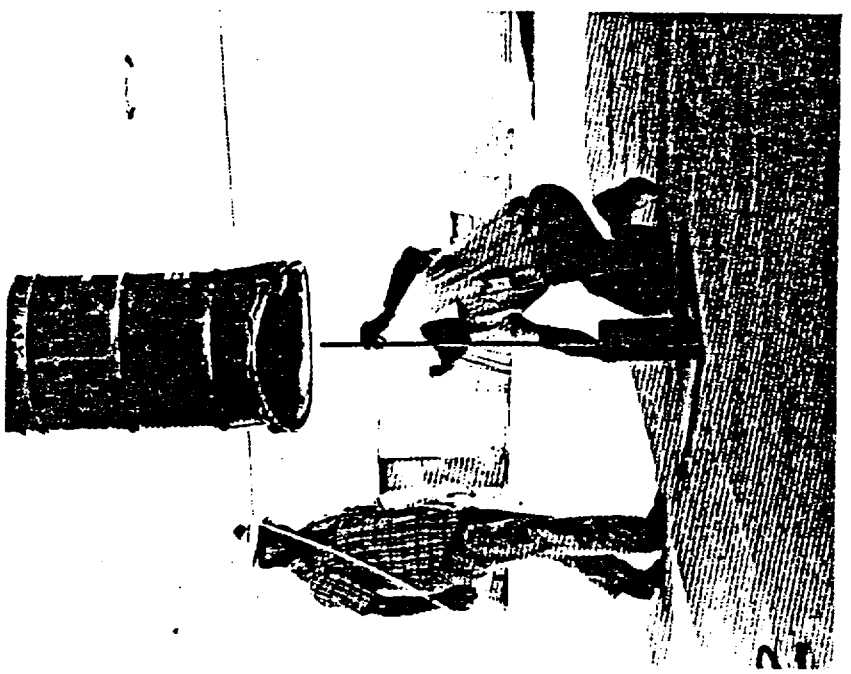

Figure 2.14.3 Preparations for Puncture Drop on Container #35 Bottom

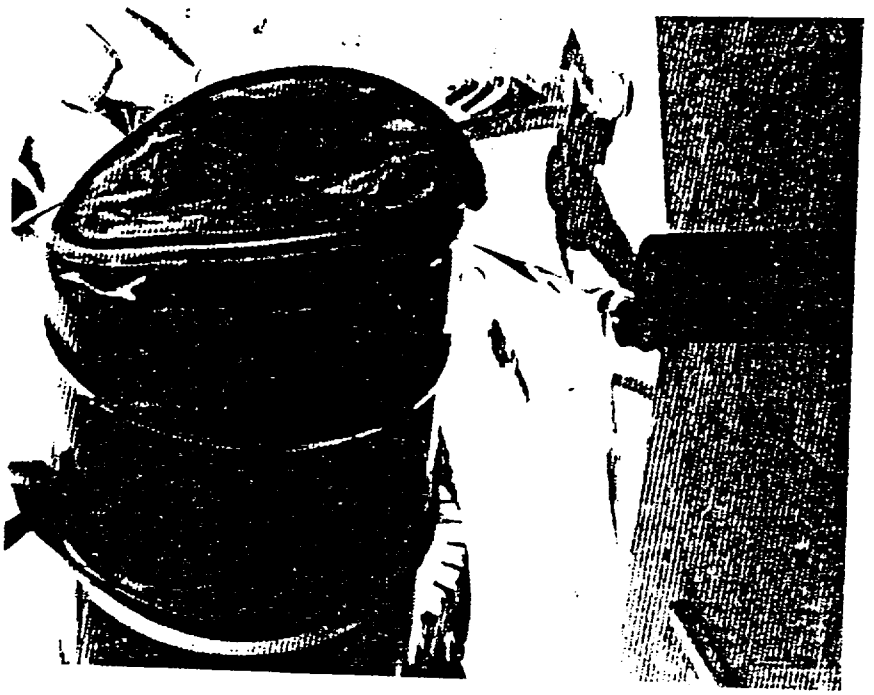

Figure 2.14.6 Container #35 Just Prior To Impact of Horizontal Puncture Drop

Figure 2.14.5 Deformation from Puncture Drop on Bottom of container #35

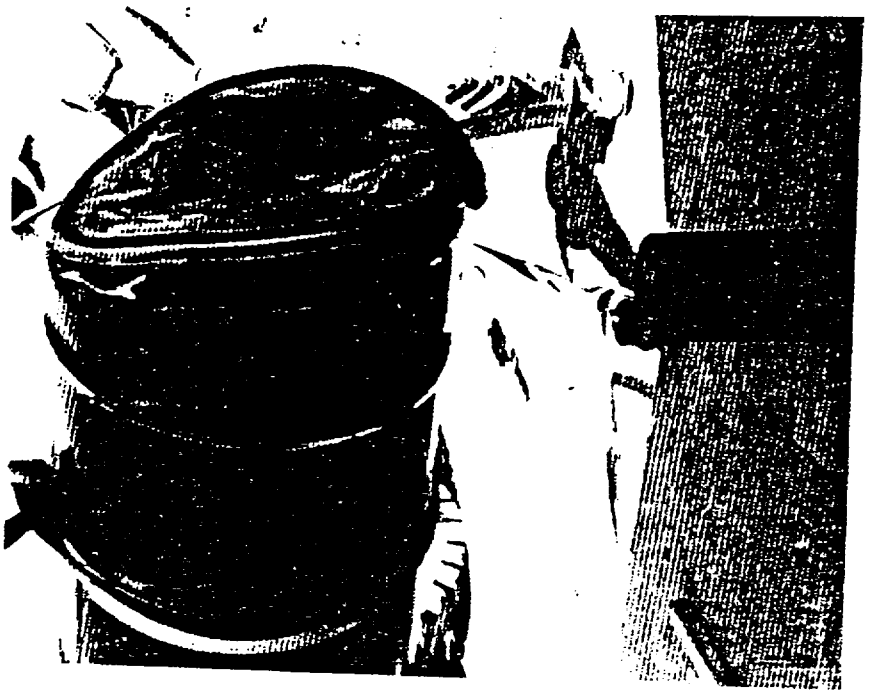

Figure 2.14.6 Container #35 Just Prior To Impact of Horizontal Puncture Drop

Figure 2.14.5 Deformation from Puncture Drop on Bottom of container #35

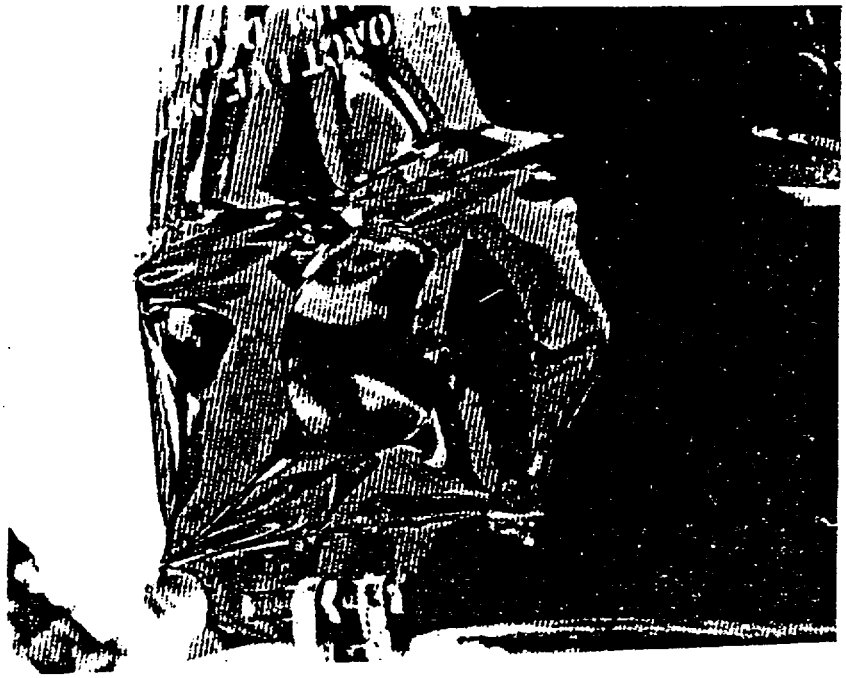

Figure 2.14.8 Deformation from Puncture Drop Shown in Figure 2.14.7

Figure 2.14.7 Container #35 After Impact of Puncture Drop on Side

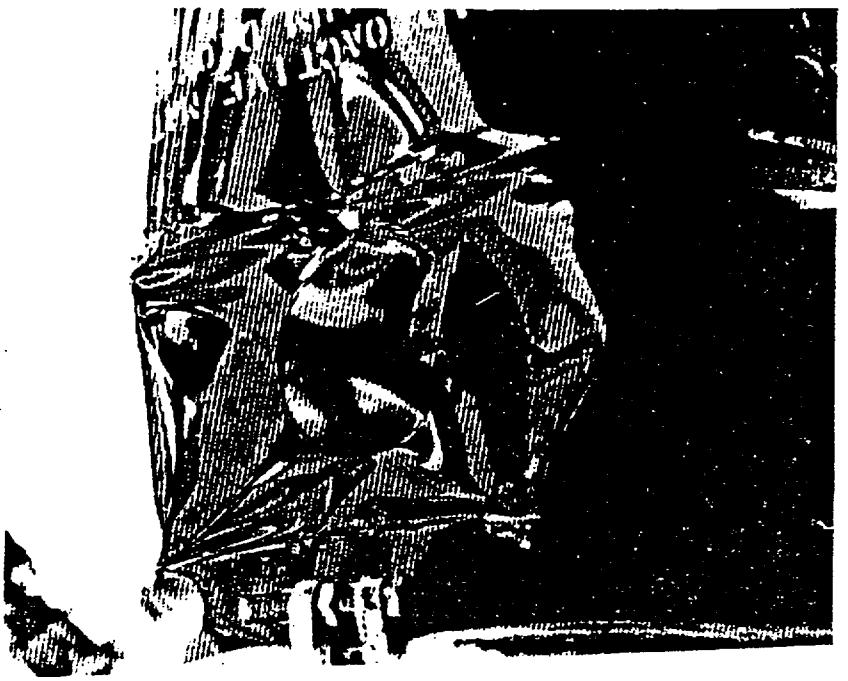

Figure 2.14.8 Deformation from Puncture Drop Shown in Figure 2.14.7

Figure 2.14.7 Container #35 After Impact of Puncture Drop on Side

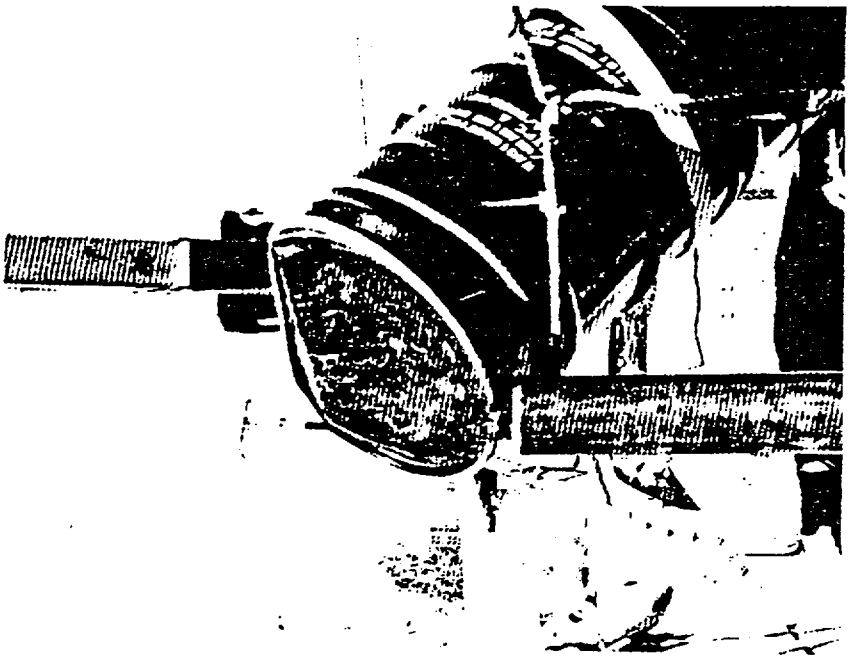

Figure 2.15.1 Container #14 About to Impact on Edge Of Lid

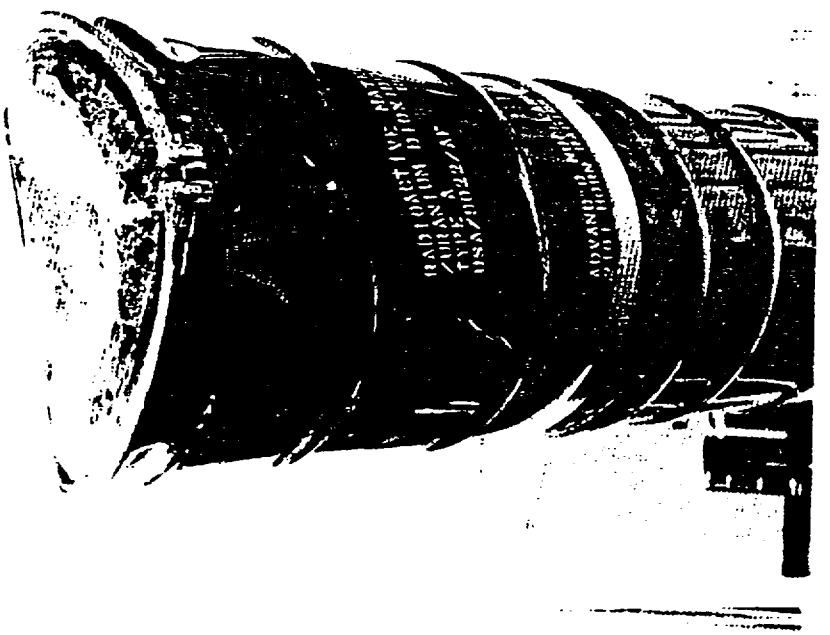

Figure 2.14.9 Another View of Deformation from Puncture Drops on Lid and Side of Container #35

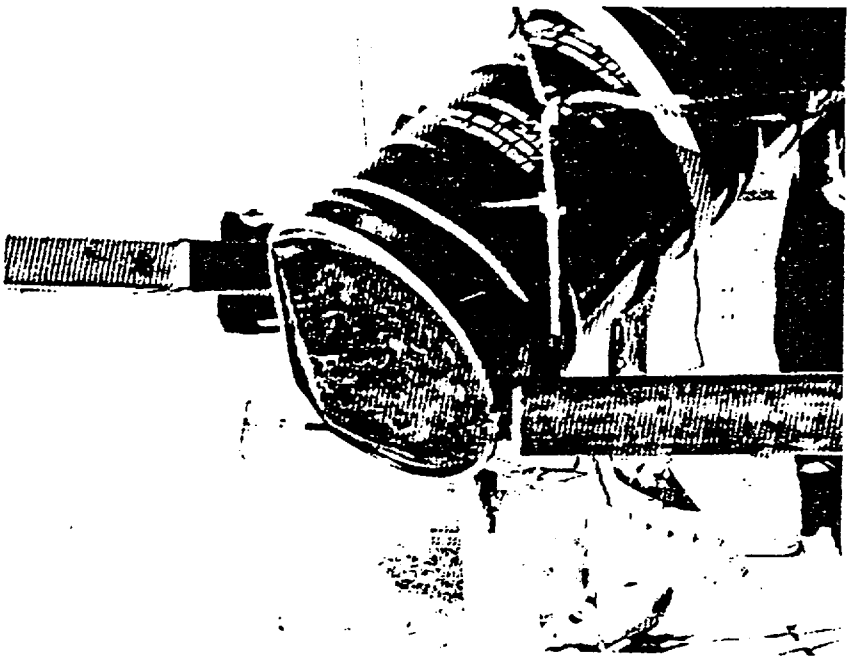

Figure 2.15.1 Container #14 About to Impact on Edge Of Lid

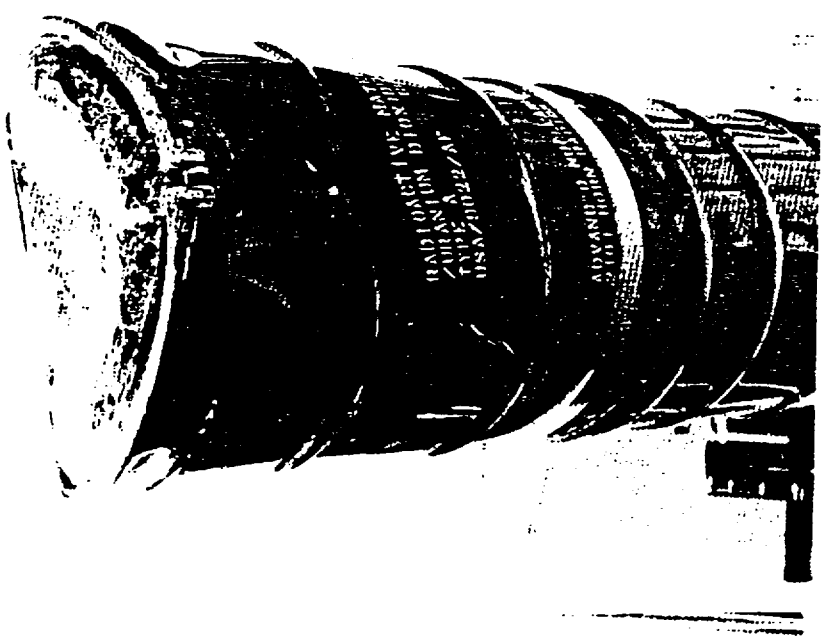

Figure 2.14.9 Another View of Deformation from Puncture Drops on Lid and Side of Container #35

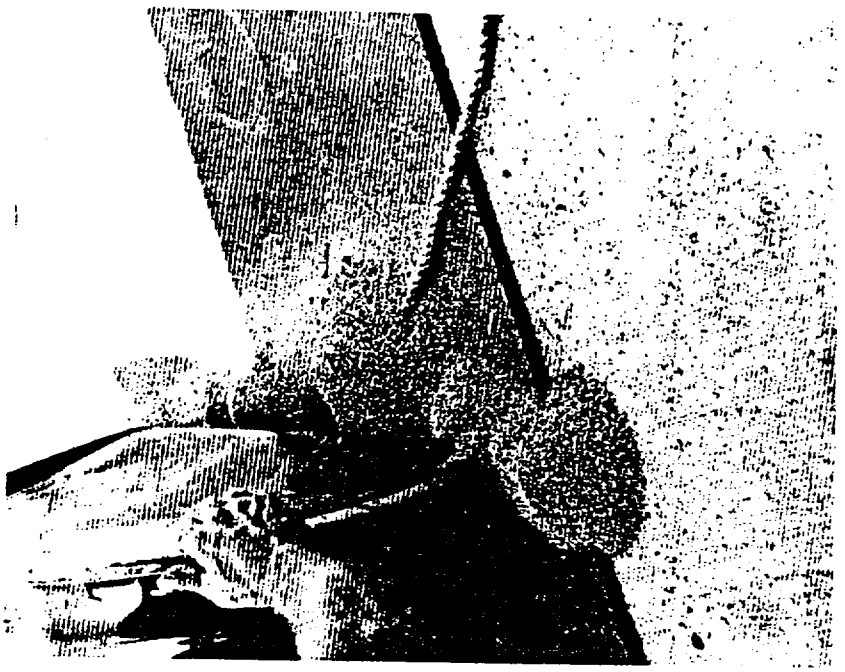

Figure 2.15.3 Vermiculite Leakage from Lid of Container #14 After Toppling from Puncture Test

Figure 2.15.2 Damage From Oblique Strike on Locking Lug of Container #14

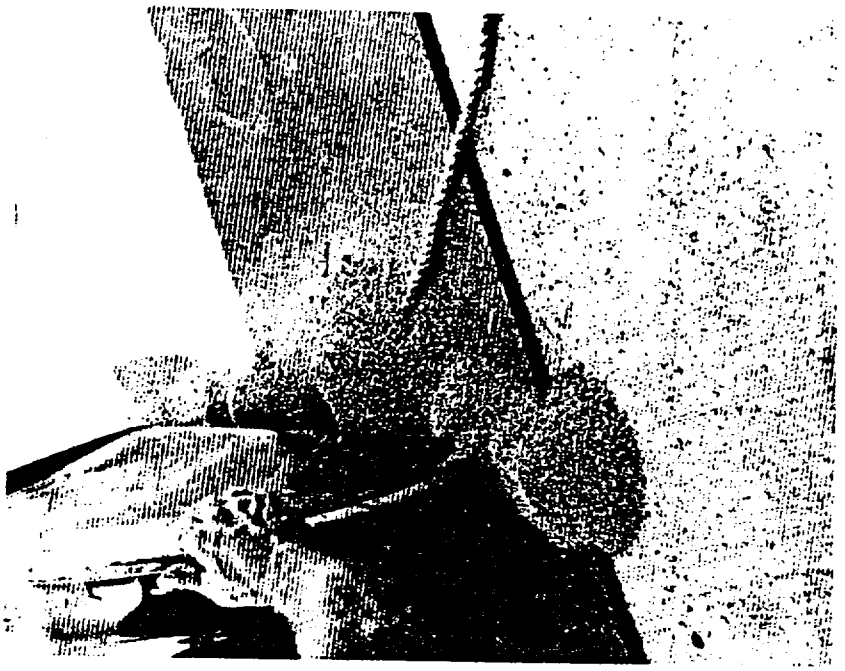

Figure 2.15.3 Vermiculite Leakage from Lid of Container #14 After Toppling from Puncture Test

Figure 2.15.2 Damage From Oblique Strike on Locking Lug of Container #14

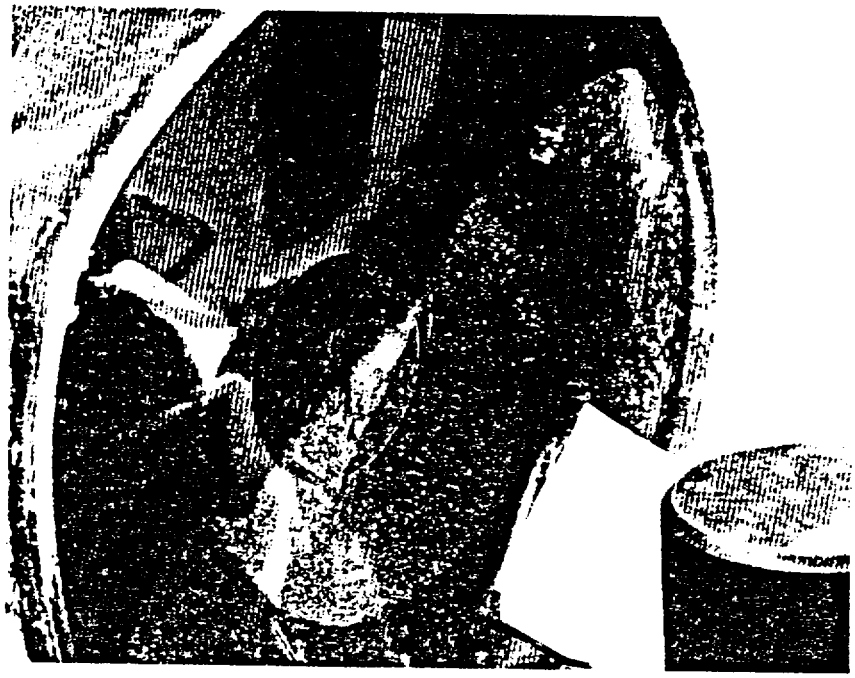

Figure 2.16.1 Deformation from Puncture Drop on Bottom of Container #42

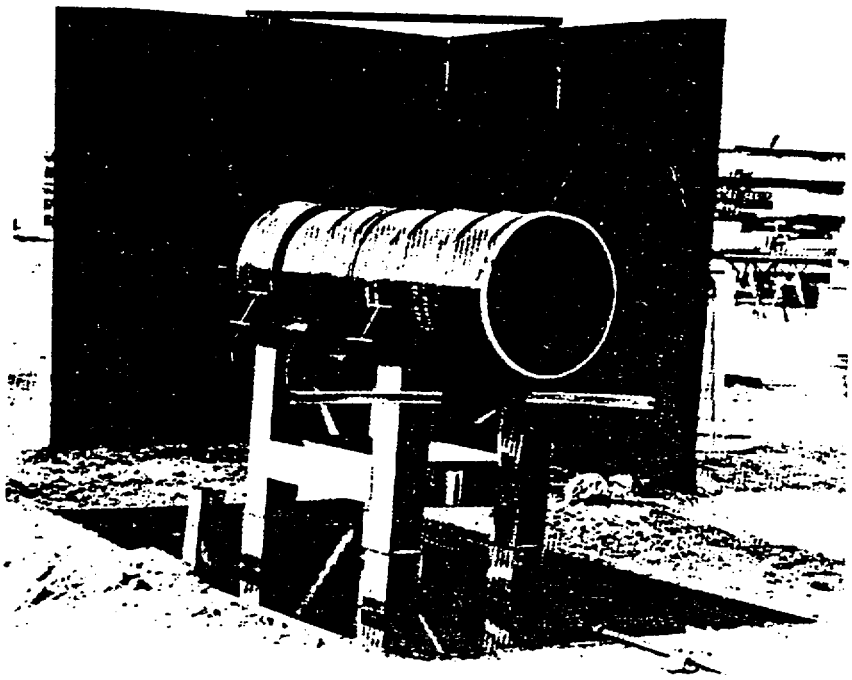

Figure 2.17.1 Test Set Up for Thermal Tests

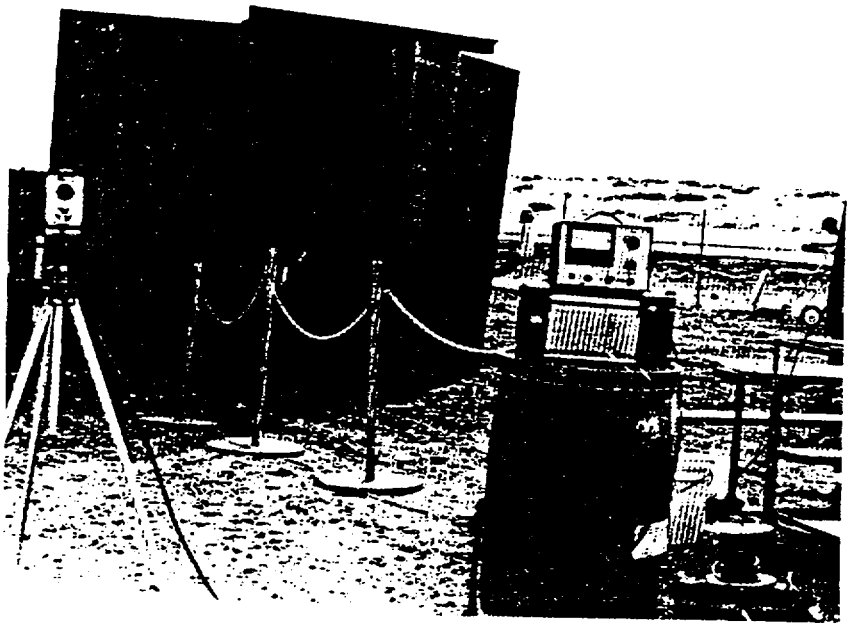

Figure 2.17.2 Pyrometer Set Up for Thermal Tests

Figure 2.18.1 Container #57 Thermal Test

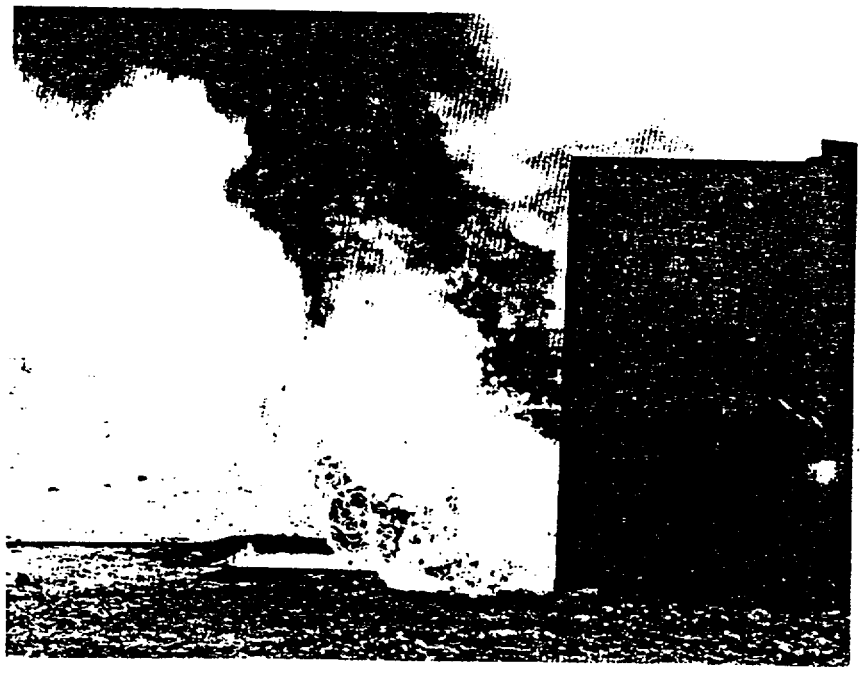

Figure 2.18.2 Container #57 Thermal Test

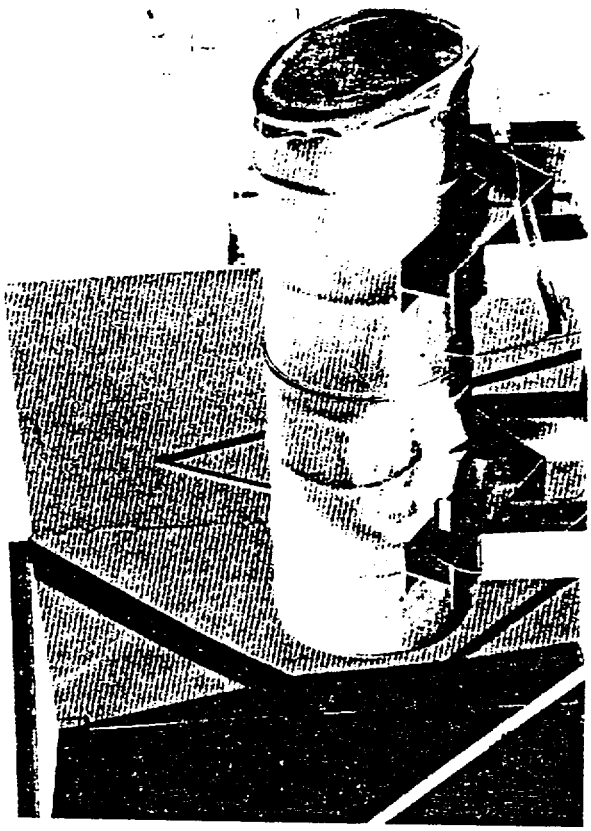

Figure 2.18.4 Container #57 After Thermal Test

Figure 2.18.3 Container #57 Thermal Test

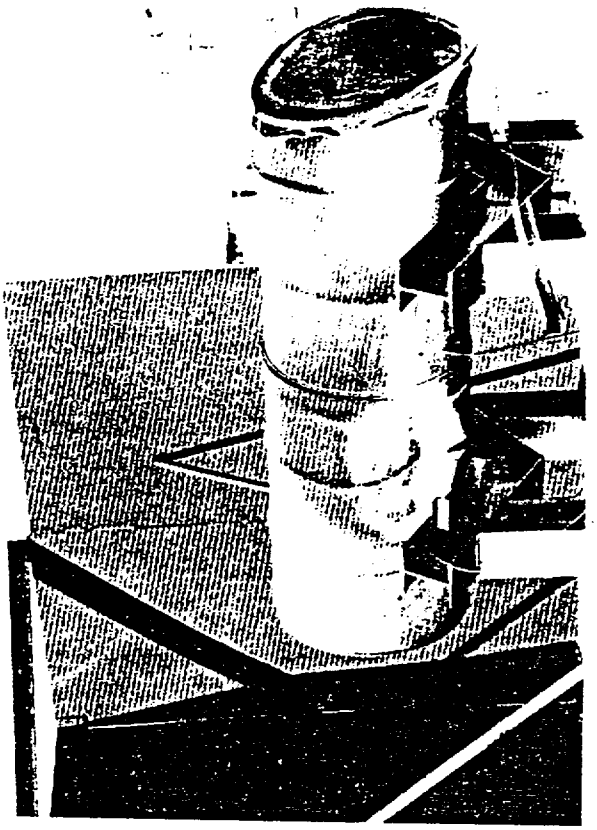

Figure 2.18.4 Container #57 After Thermal Test

Figure 2.18.3 Container #57 Thermal Test

Figure 2.18.6 Container #42 Thermal Test

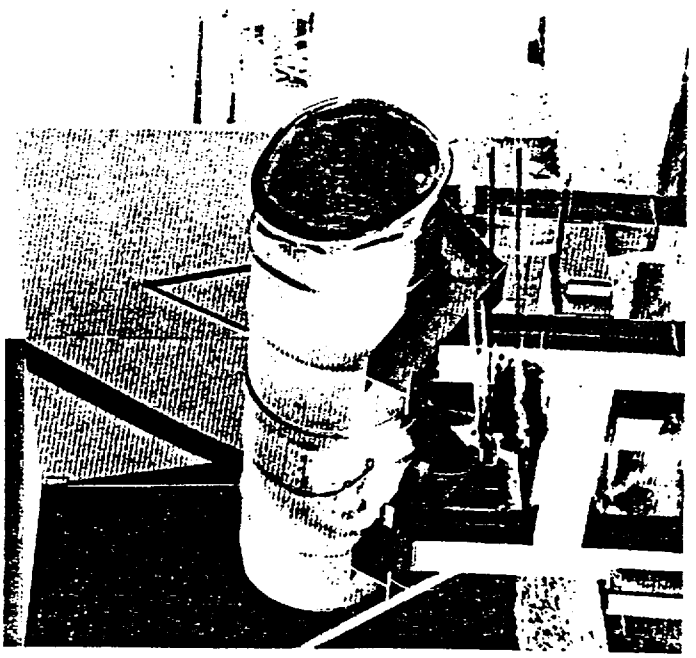

Figure 2.18.5 Container #57 After Thermal Test

Figure 2.18.6 Container #42 Thermal Test

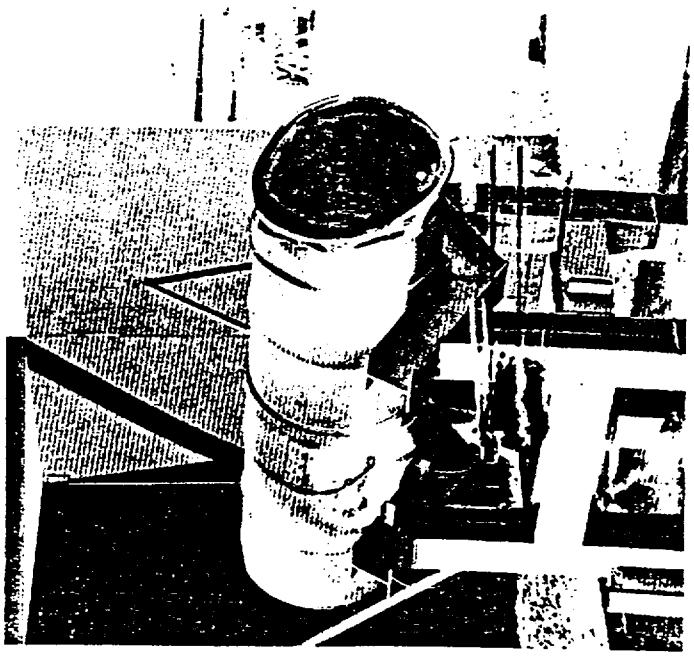

Figure 2.18.5 Container #57 After Thermal Test

Figure 2.18.7 Container #42 Test

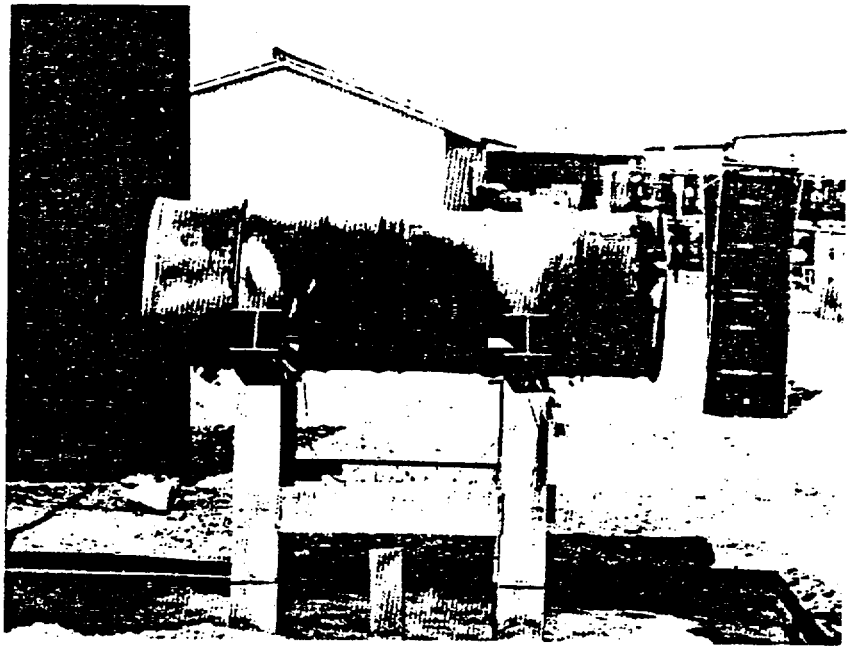

Figure 2.18.8 **Container** #42 Subsequent to Thermal Test

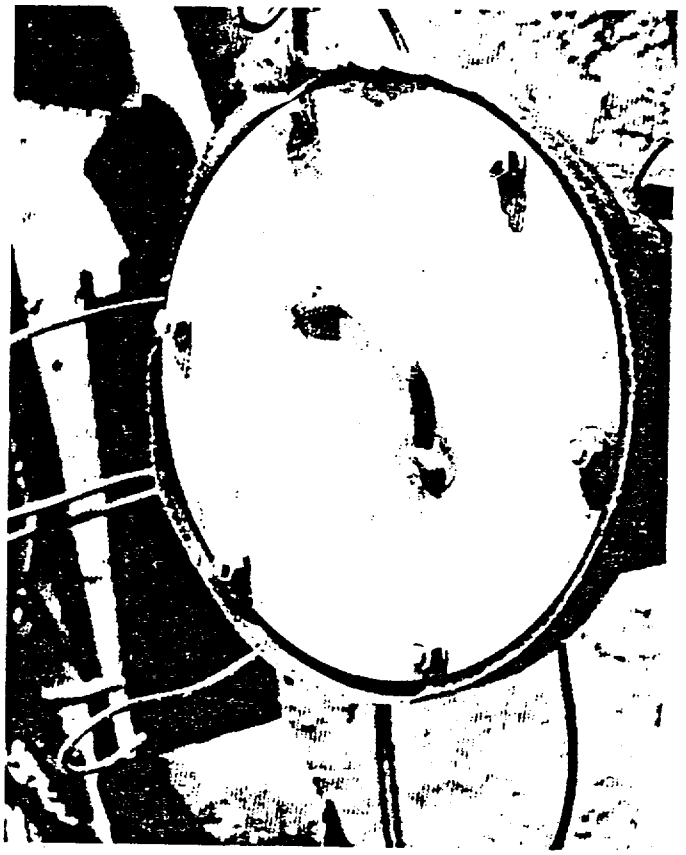

Figure 2.19.2 Container #57 Inner Container After Immersion Test

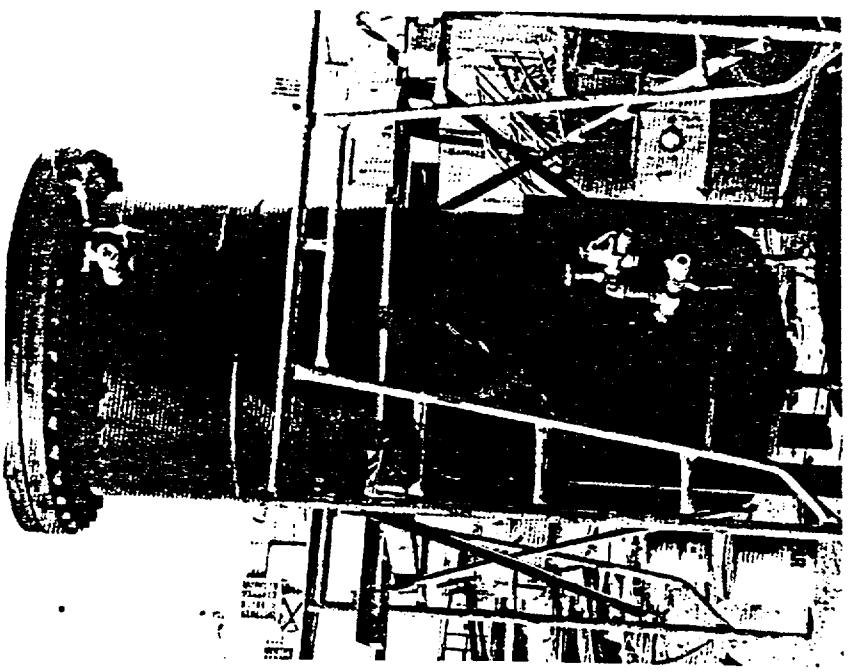

Figure 2.19.1 Immersion Chamber

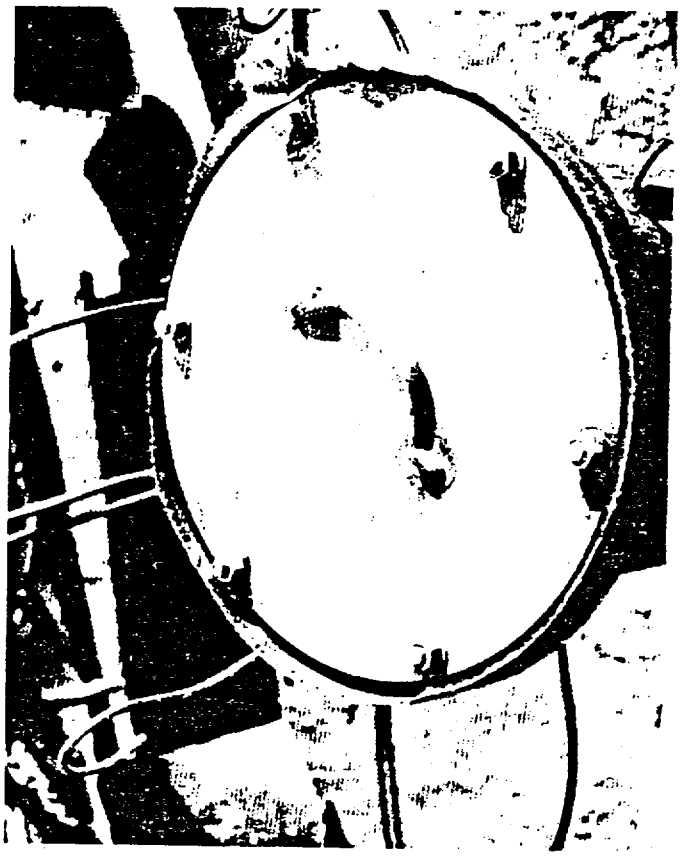

Figure 2.19.2 Container #57 Inner Container After Immersion Test

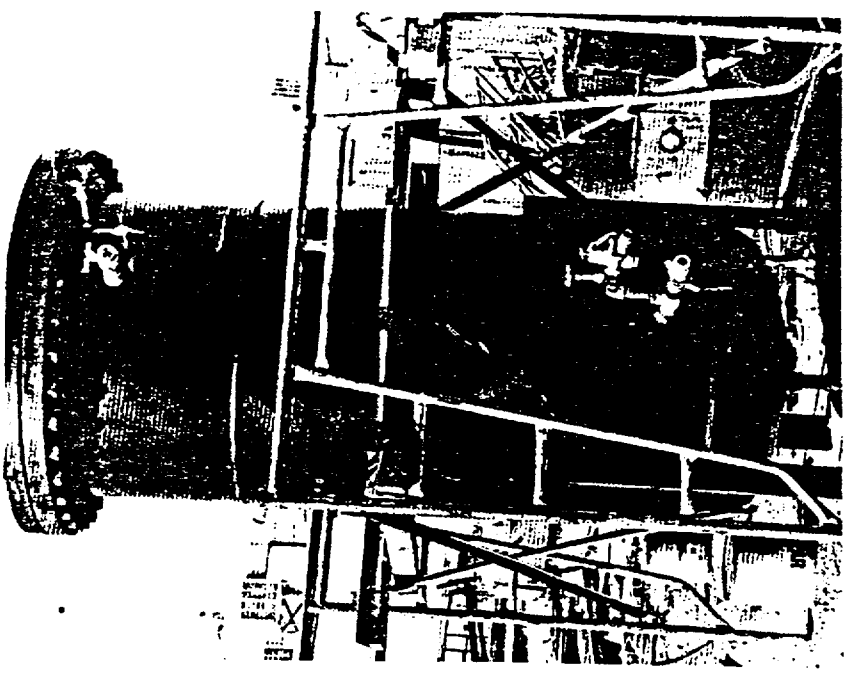

Figure 2.19.1 Immersion Chamber

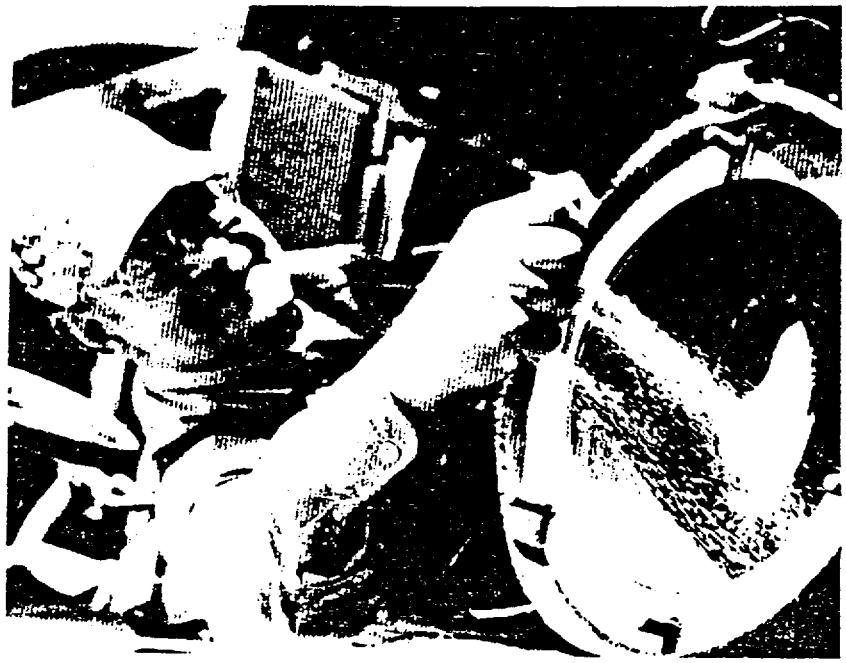

Figure 2.19.4 Laborer Demonstrating Dryness of Sand in Interior of Container #57

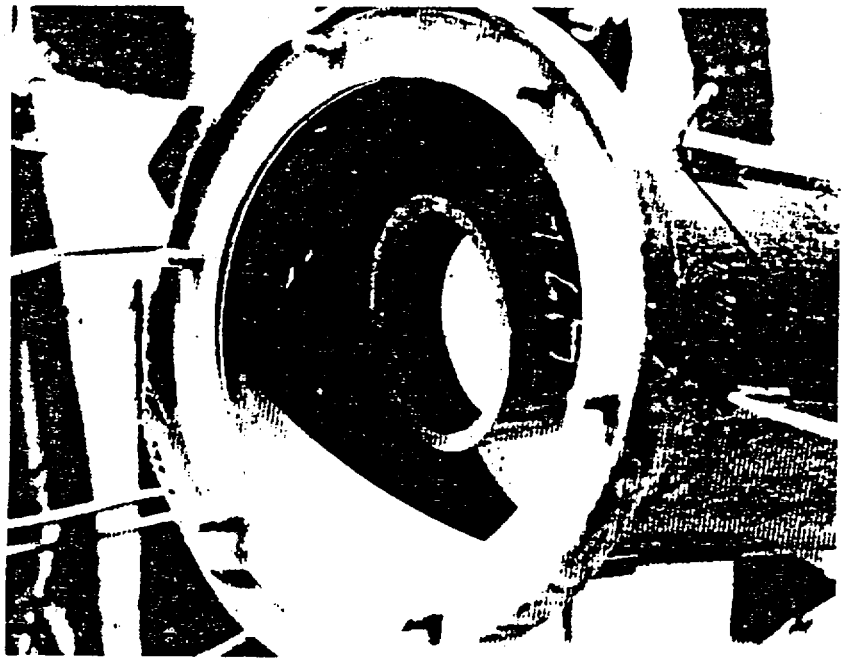

Figure 2.19.3 Dry Interior Of Container #57 on Completion of the Hypothetical Accident Tests

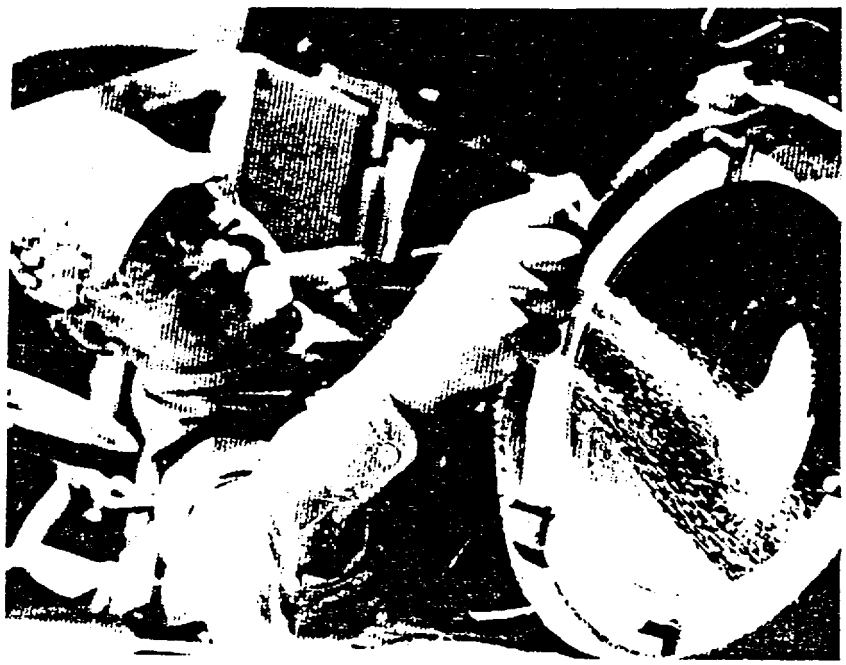

Figure 2.19.4 Laborer Demonstrating Dryness of Sand in Interior of Container #57

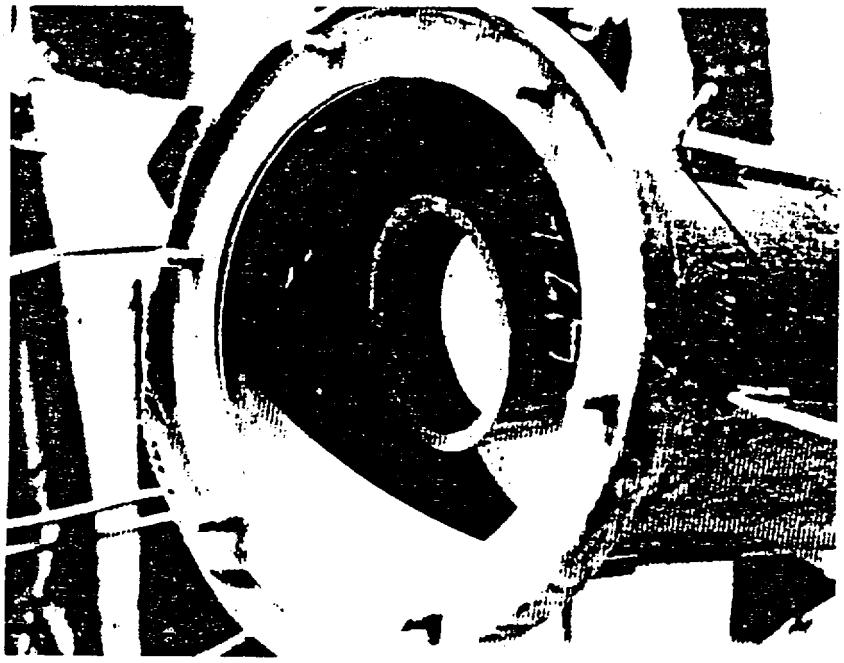

Figure 2.19.3 Dry Interior Of Container #57 on Completion of the Hypothetical Accident Tests

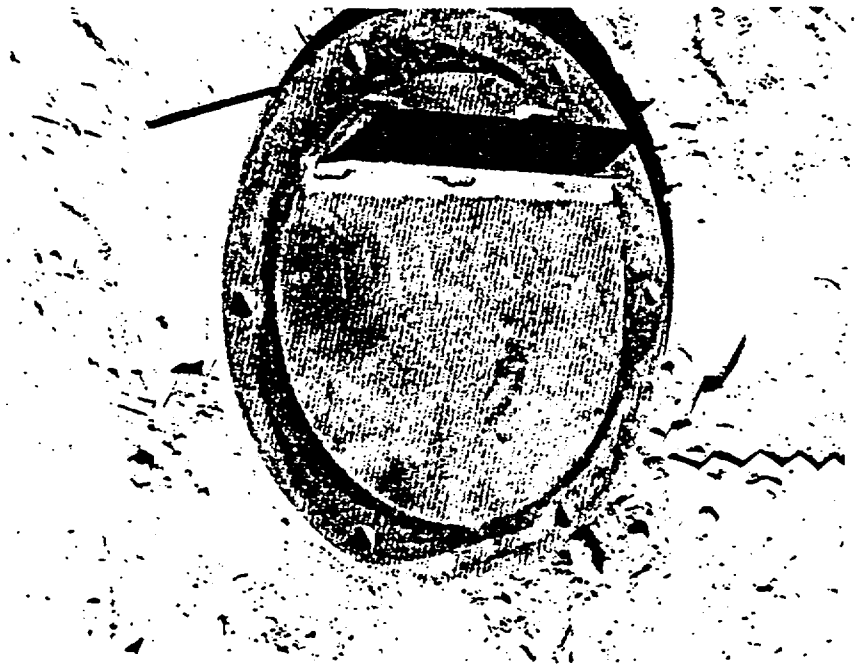

Figure 2.19.6 Temperature Indicators on Inside of Inner Container Lid of Container #57

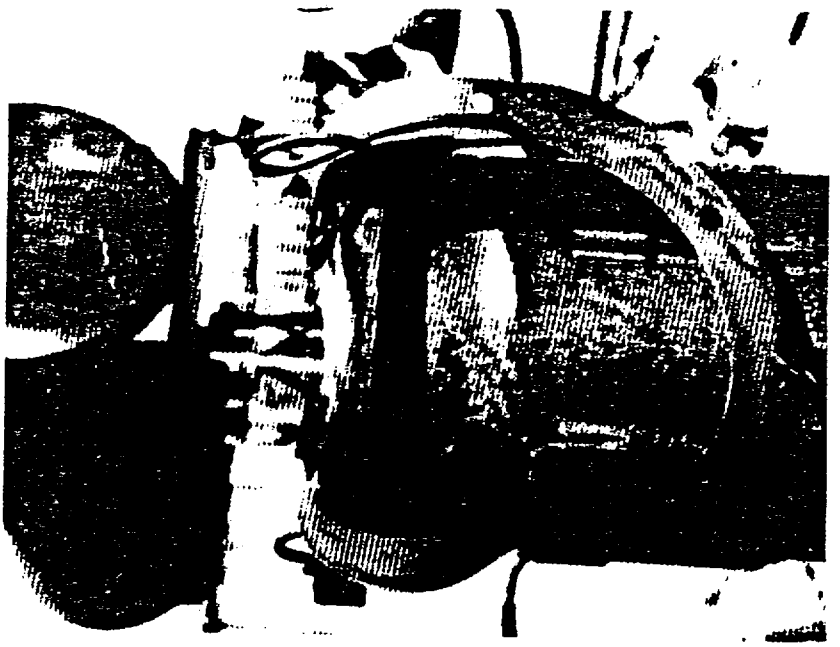

Figure 2.19.5 Undamaged Gasket Material Container #57

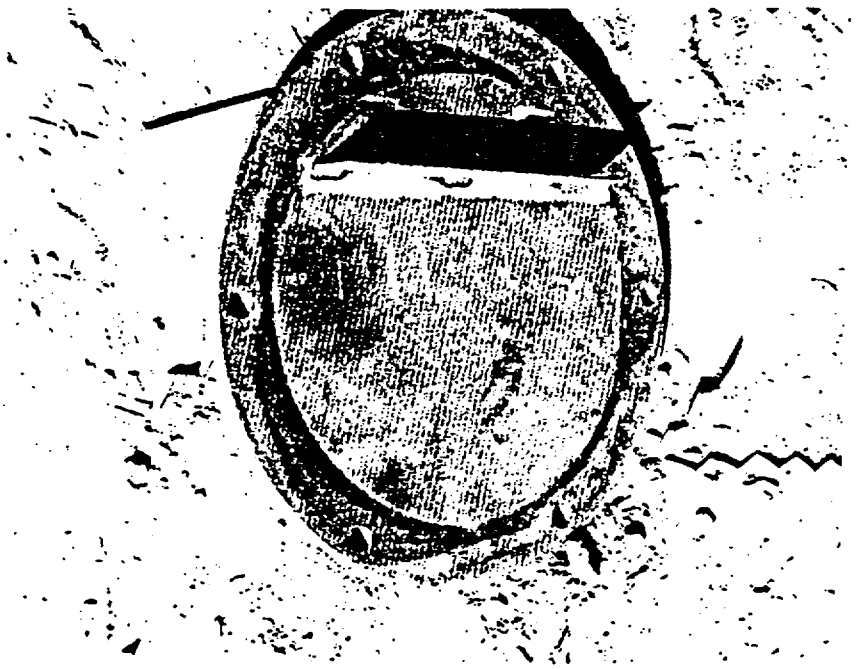

Figure 2.19.6 Temperature Indicators on Inside of Inner Container Lid of Container #57

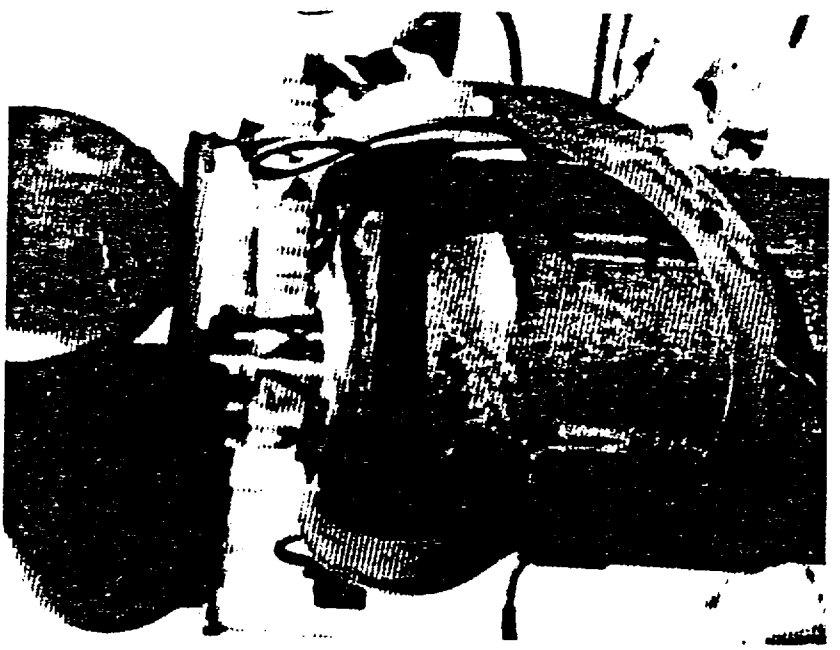

Figure 2.19.5 Undamaged Gasket Material Container #57

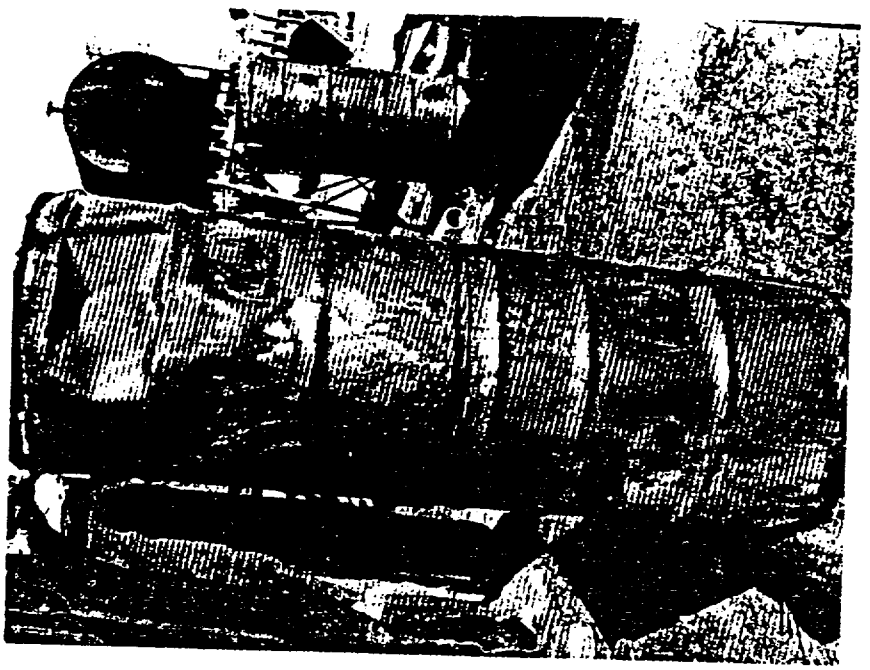

Figure 2.19.8 Container #35 Prior to Opening Subsequent to the Immersion Test

Figure 2.19.7 Dry Interior of Container #42 After Hypothetical Accident Tests

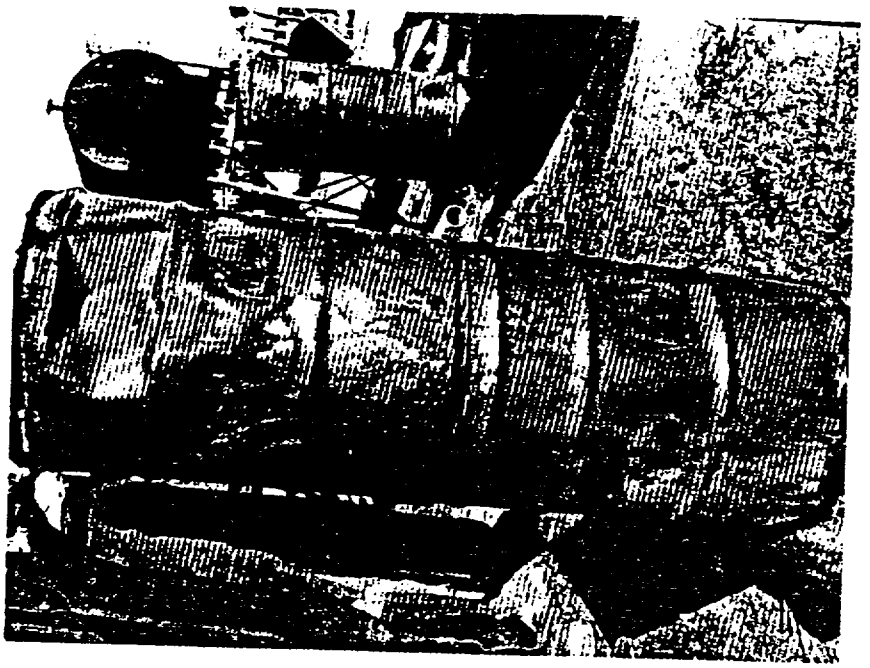

Figure 2.19.8 Container #35 Prior to Opening Subsequent to the Immersion Test

Figure 2.19.7 Dry Interior of Container #42 After Hypothetical Accident Tests

Figure 2.19.10 Temperature Indicators on Inside of Inner Container Lid - Container #35

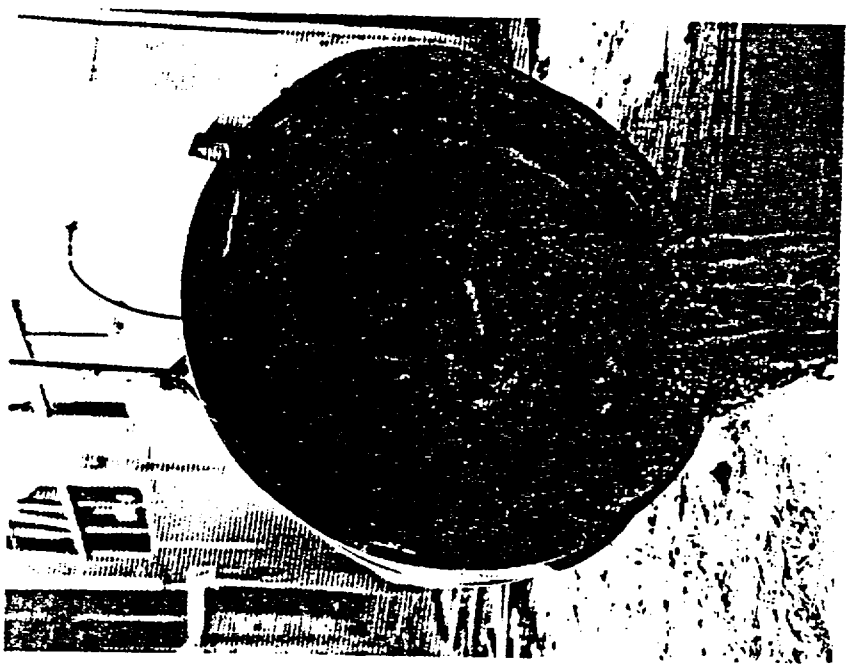

Figure 2.19.9 Water/Vermiculite Mixture Pouring from Outer Drum Container #35

Figure 2.19.10 Temperature Indicators on Inside of Inner Container Lid - Container #35

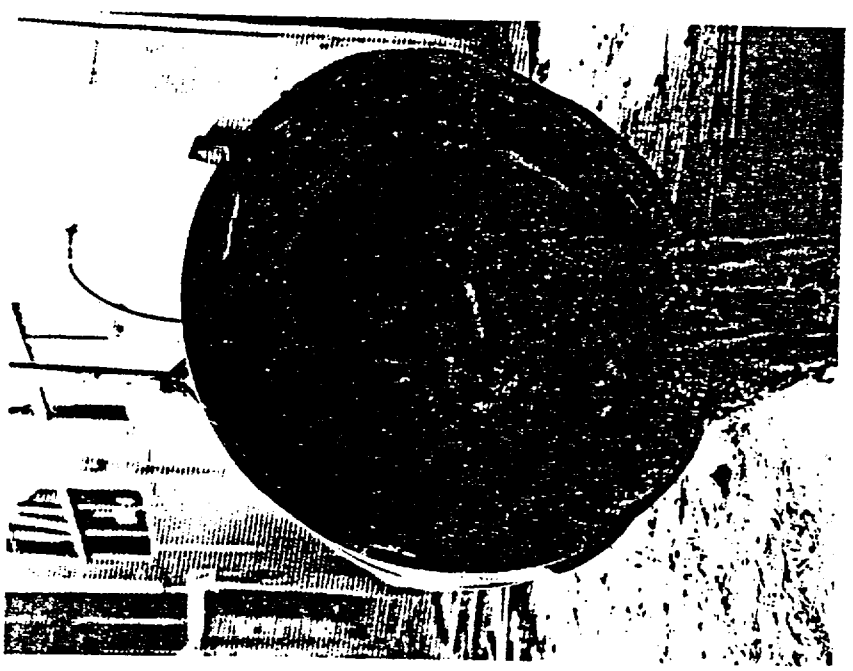

Figure 2.19.9 Water/Vermiculite Mixture Pouring from Outer Drum Container #35

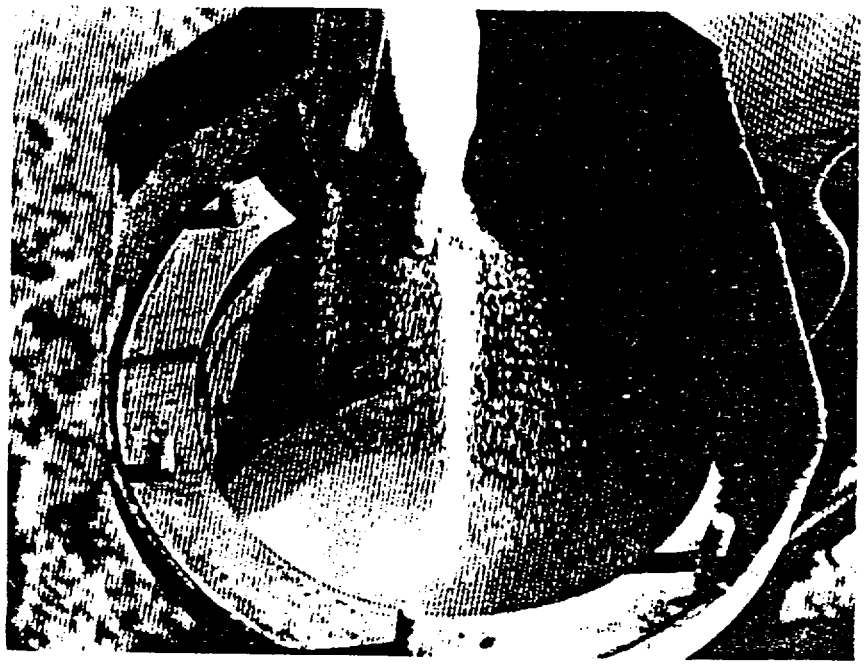

Figure 2.19.11 Dry Interior of Container #35

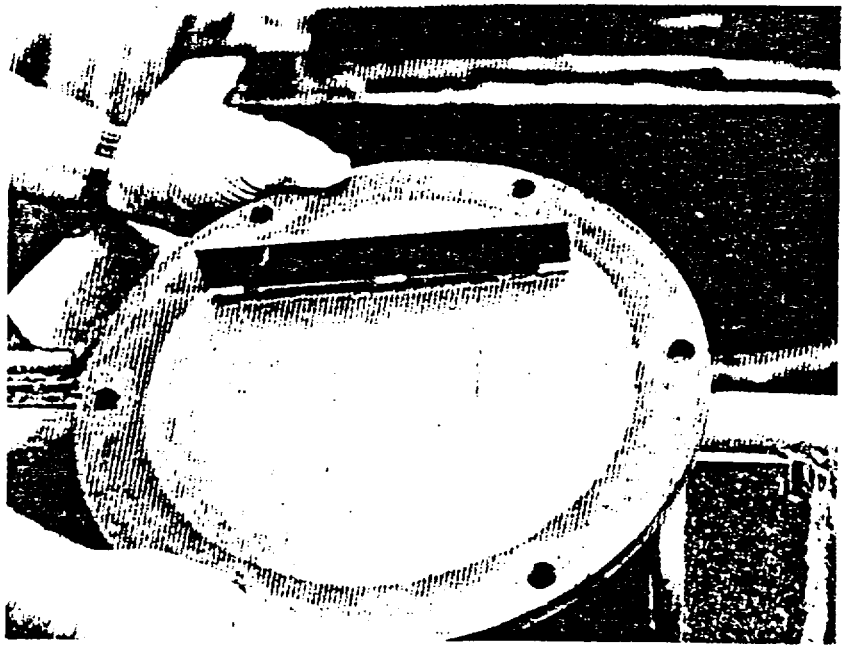

Figure 2.19.12 Inside of Inner Lid Container #14

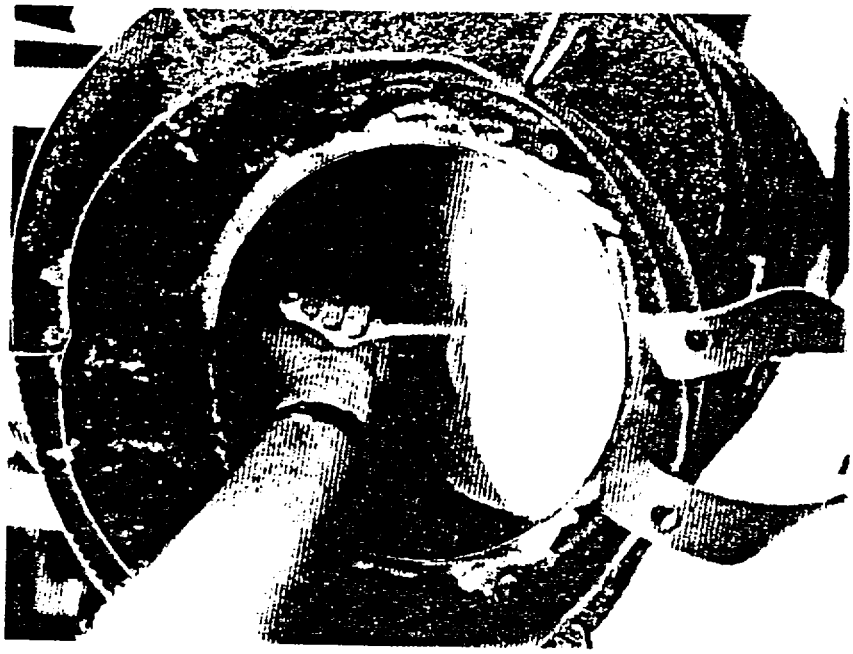

Figure 2.19.14 Dry Interior Container #14

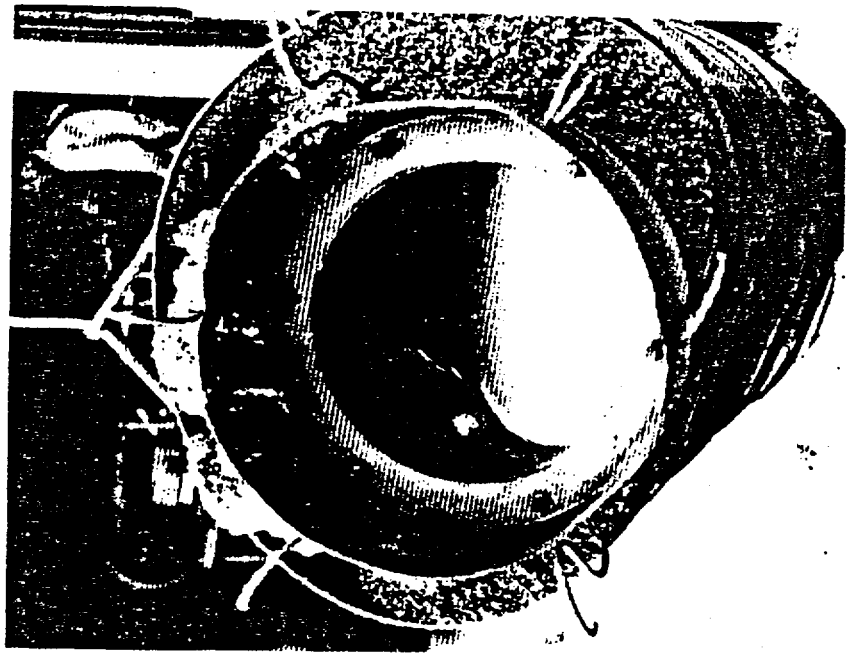

Figure 2.19.13 Dry Interior Container #14

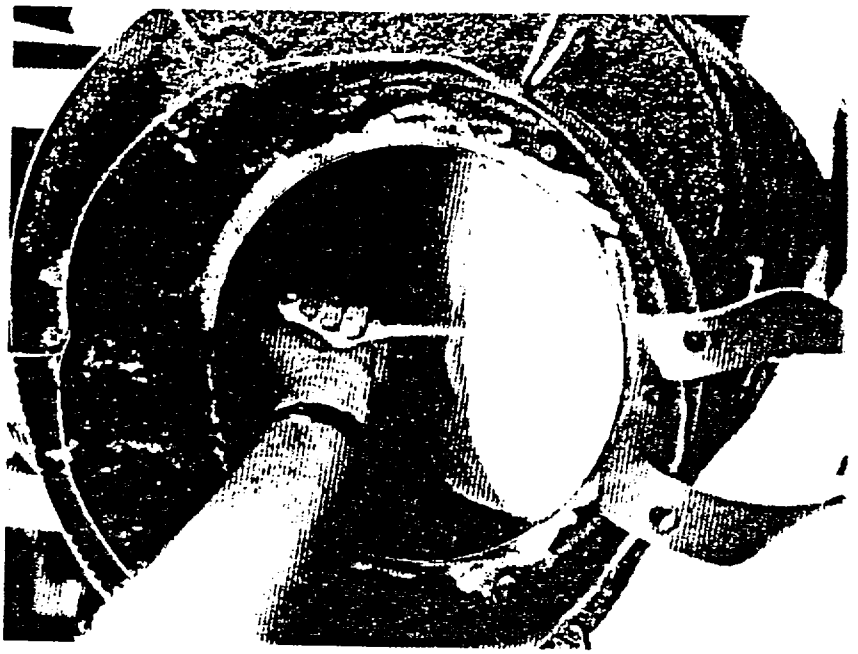

Figure 2.19.14 Dry Interior Container #14

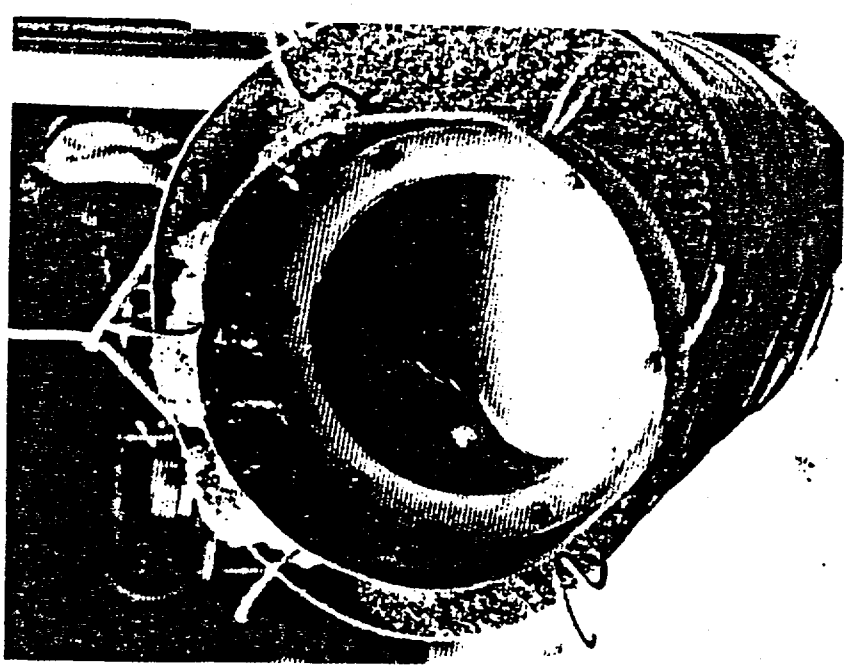

Figure 2.19.13 Dry Interior Container #14

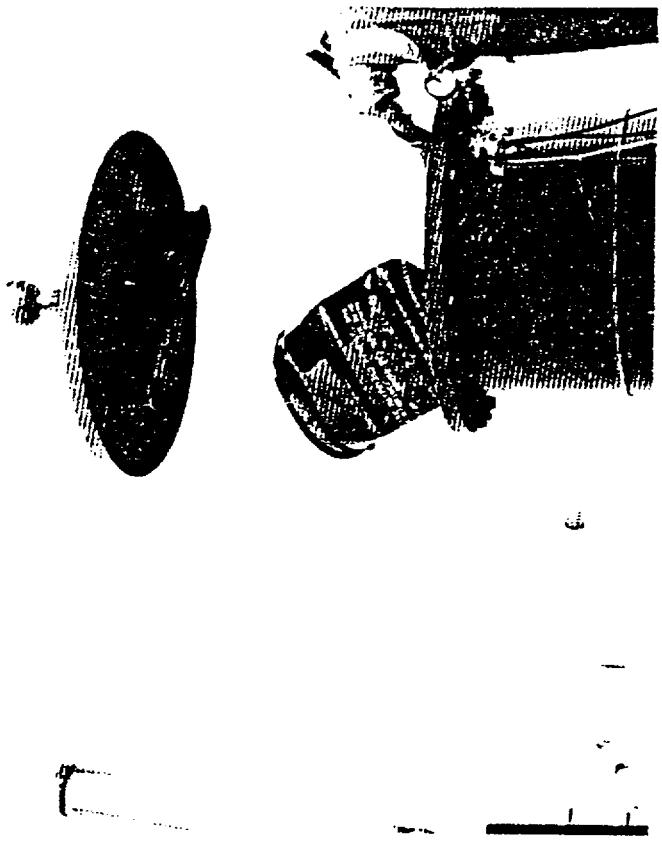

Figure 2.20.1 Removal of the Container Following Simulated 15m Immersion Test

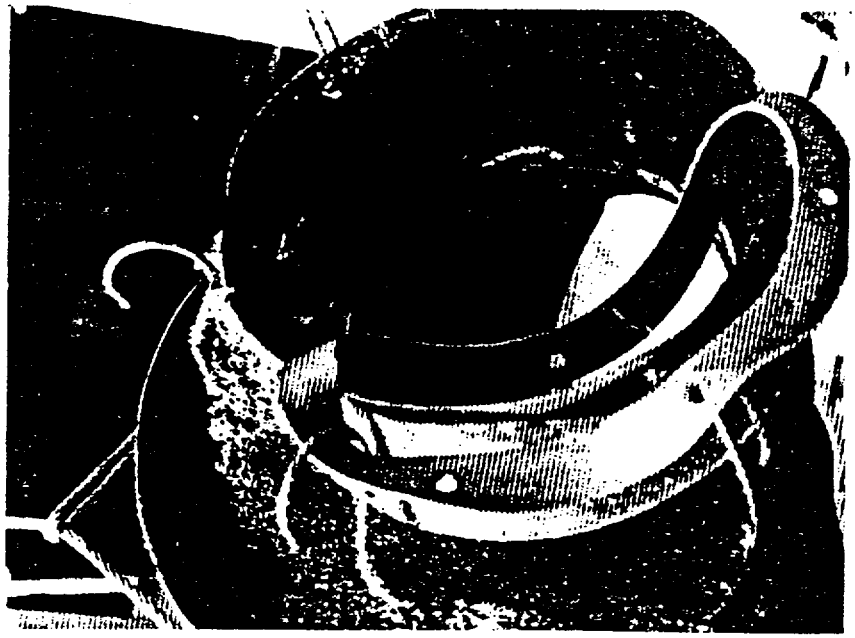

Figure 2.19.15 Dry Interior and Undamaged Gasket Container #14

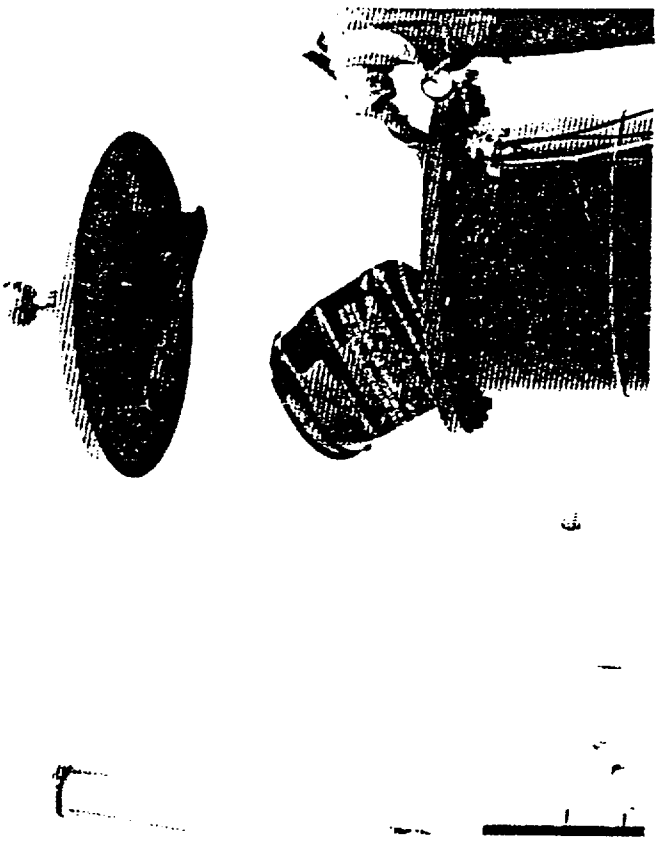

Figure 2.20.1 Removal of the Container Following Simulated 15m Immersion Test

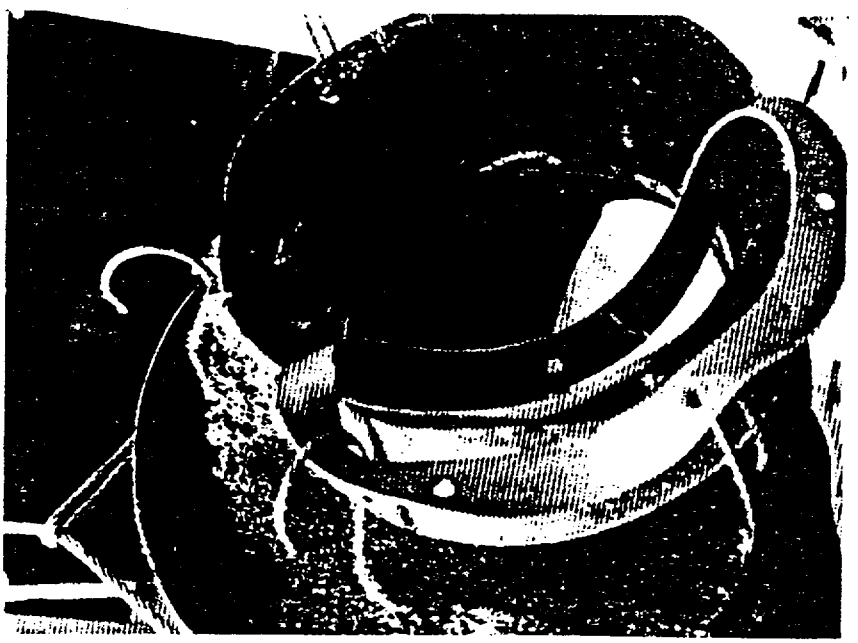

Figure 2.19.15 Dry Interior and Undamaged Gasket Container #14

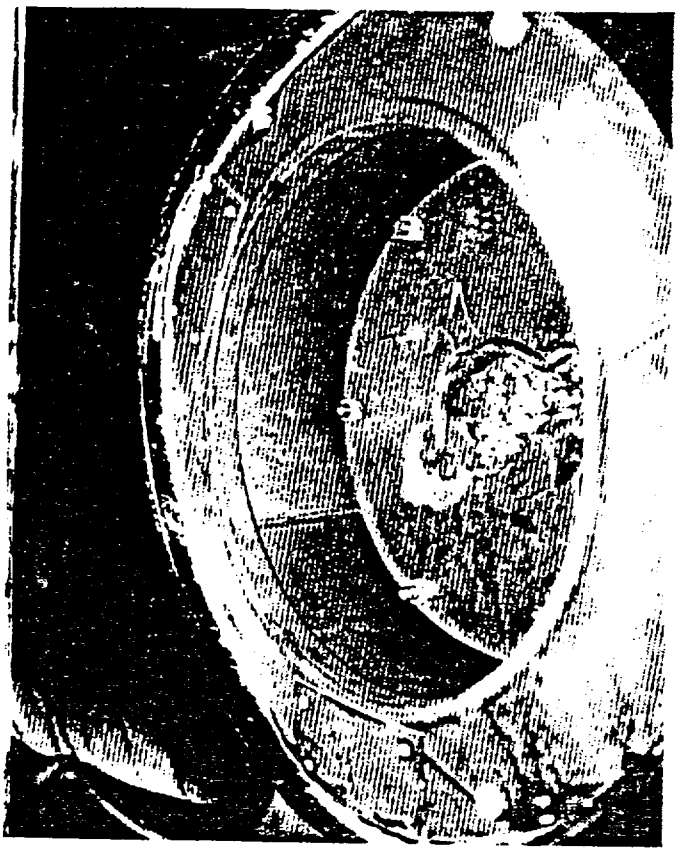

Figure 2.20.3 Interior of Container Following 15m simulated Immersion Test

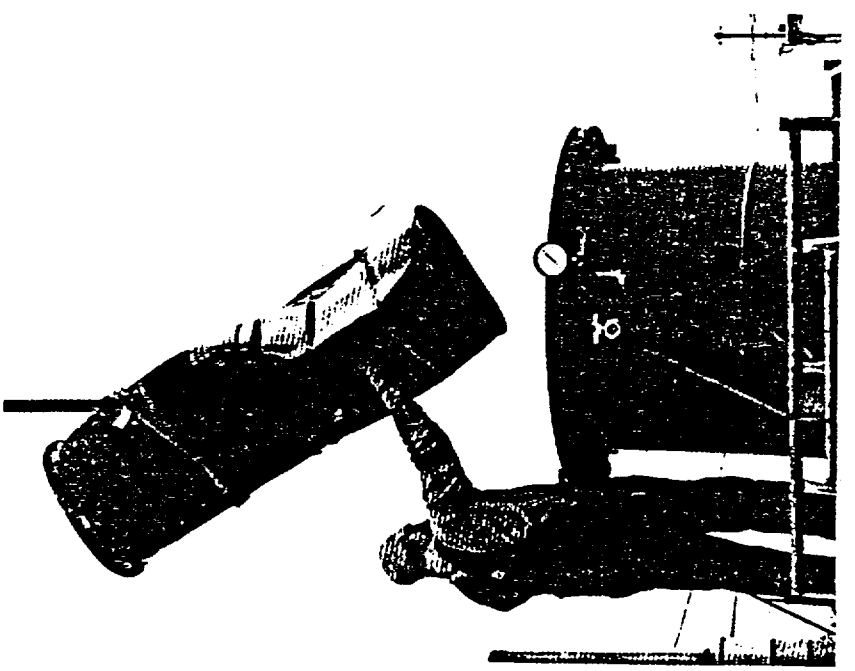

Figure 2.20.2 Removal of Container Following Simulated 15m Immersion Test

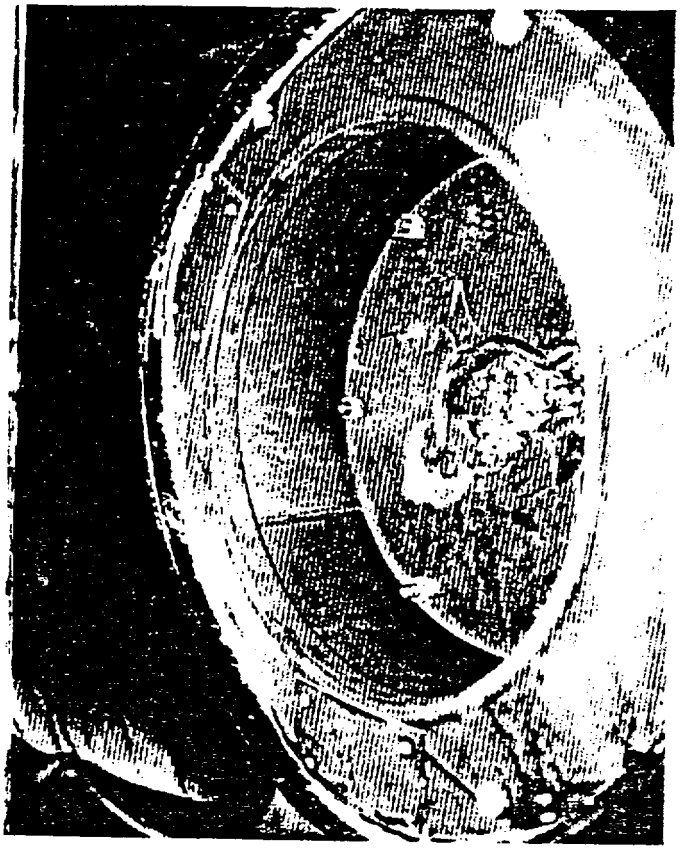

Figure 2.20.3 Interior of Container Following 15m simulated Immersion Test

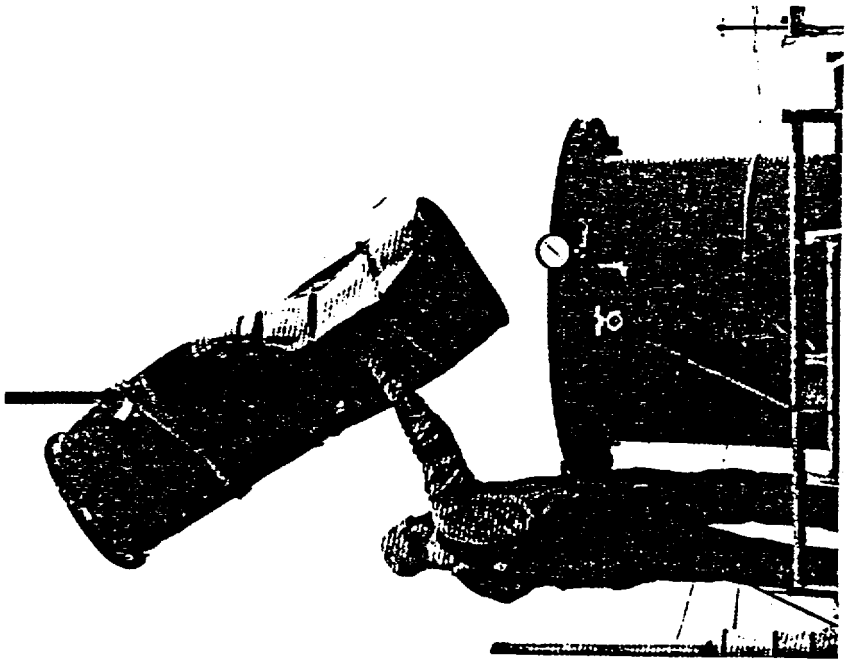

Figure 2.20.2 Removal of Container Following Simulated 15m Immersion Test

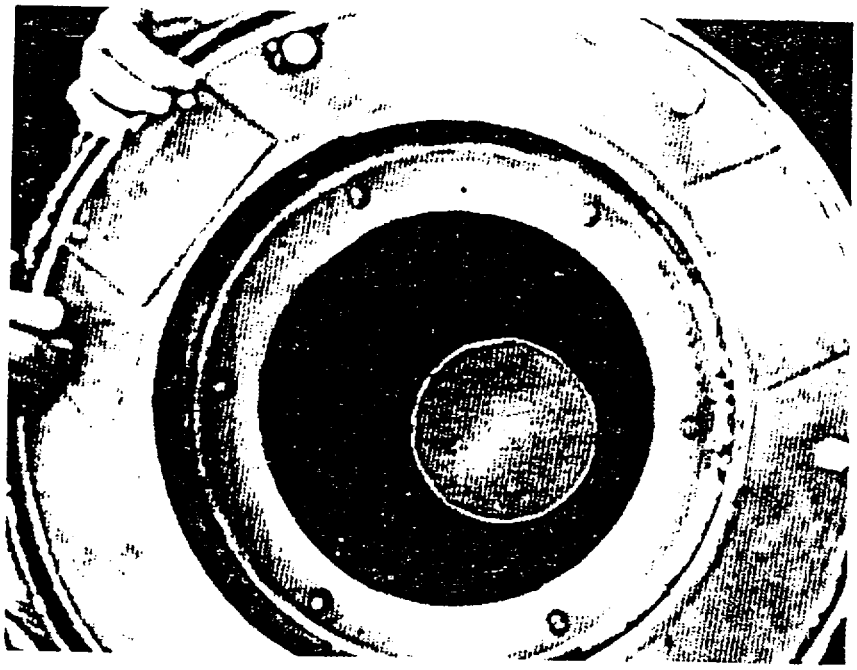

Figure 2.20.4 Dry Interior of Inner Container
Following Simulated 15m Immersion Test

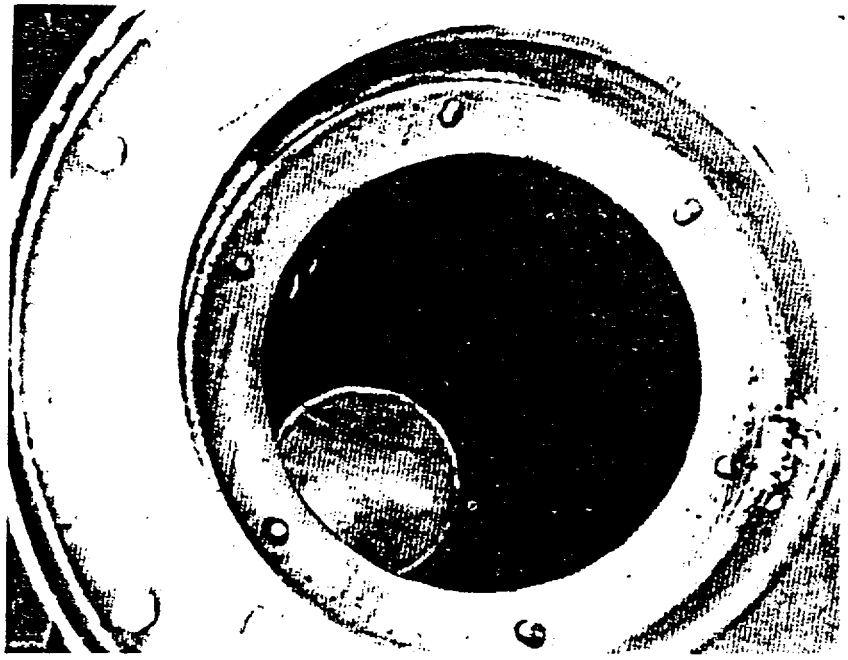

Figure 2.20.5 Dry Interior of Inner Container
Following Simulated 15m Immersion Test

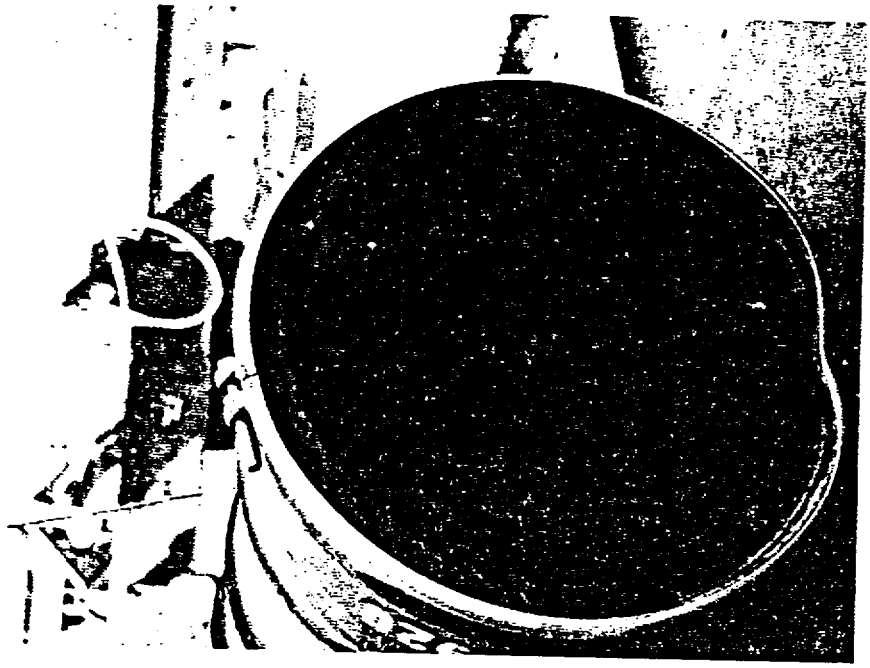

Fig. 2.21.2 Container #920 Lid End Deformation From 9m Drop

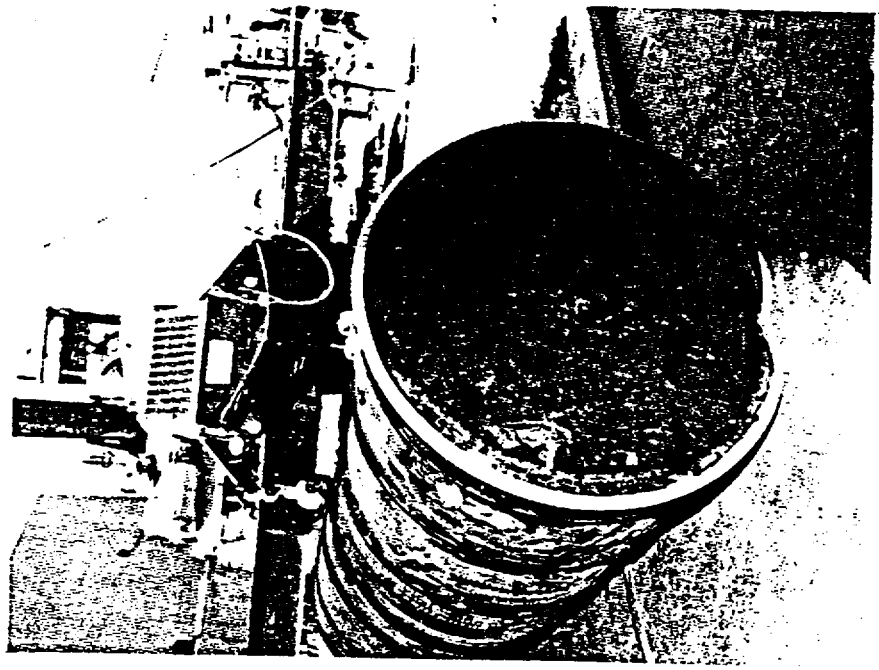

Fig. 2.21.1 Container #920 View From Lid End of Deformation From 9m Drop

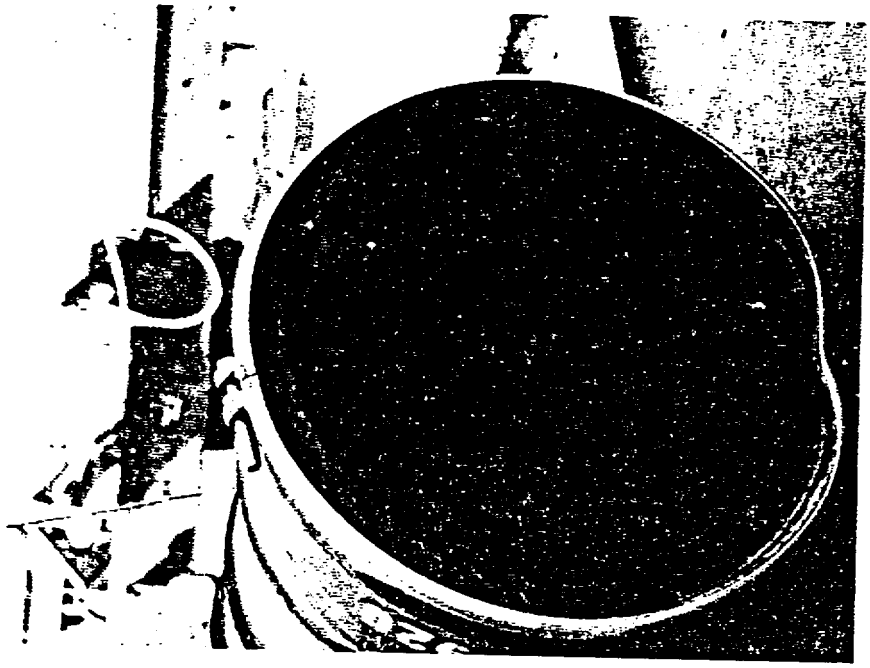

Fig. 2.21.2 Container #920 Lid End Deformation From 9m Drop

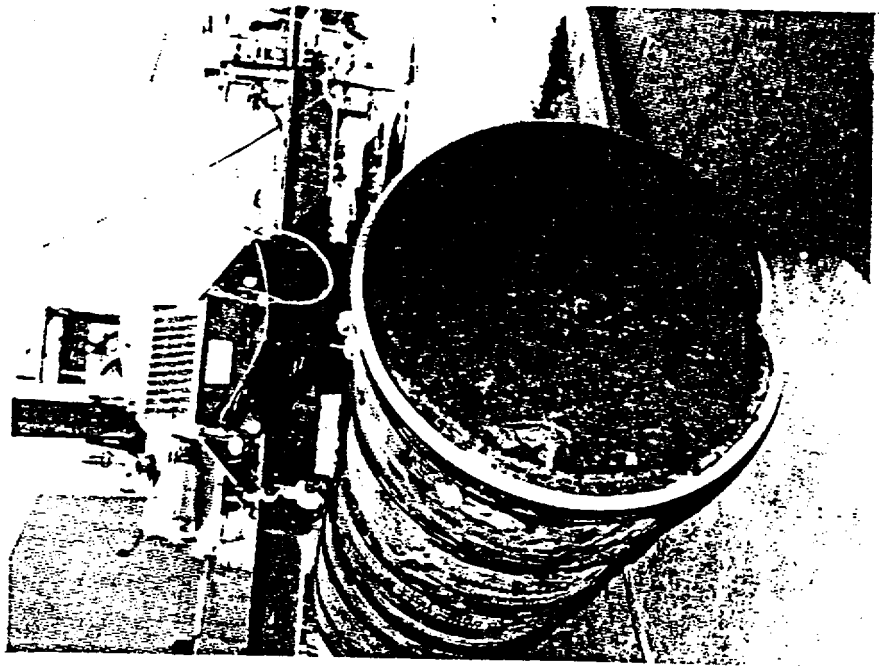

Fig. 2.21.1 Container #920 View From Lid End of Deformation From 9m Drop

Fig. 2.21.4 Container #920
View From Bottom End of
Container After 9m Drop

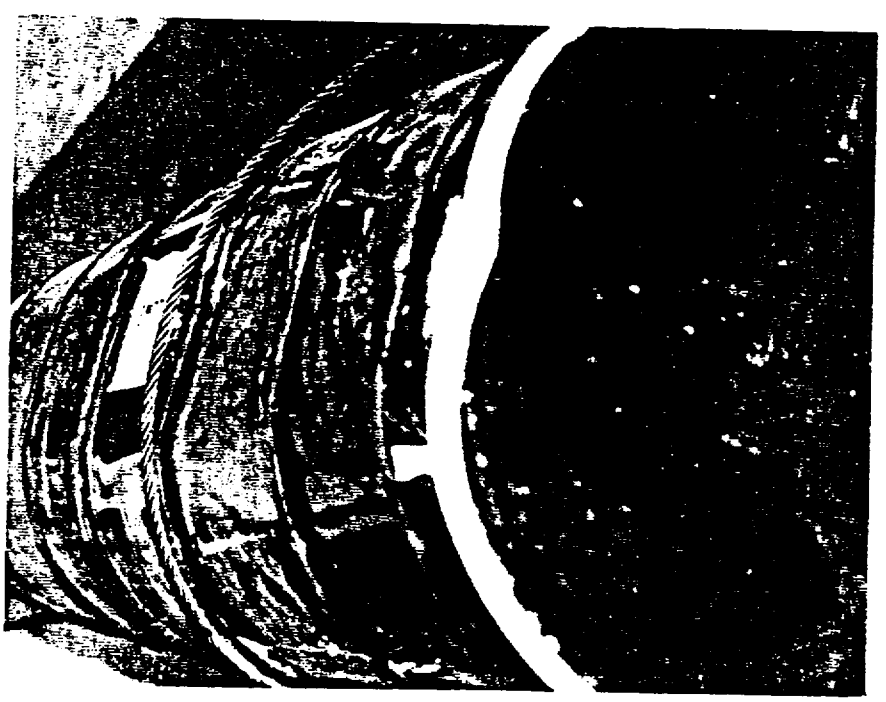

Fig. 2.21.3 Container #920
Showing Impact Side From Lid End
After 9m Drop

Fig. 2.21.4 Container #920
View From Bottom End of
Container After 9m Drop

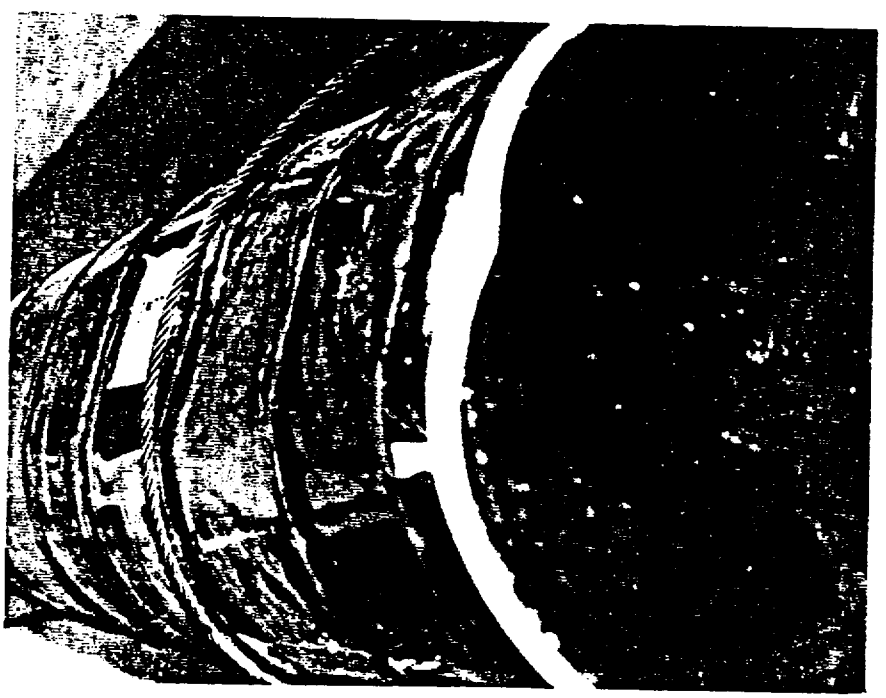

Fig. 2.21.3 Container #920
Showing Impact Side From Lid End
After 9m Drop

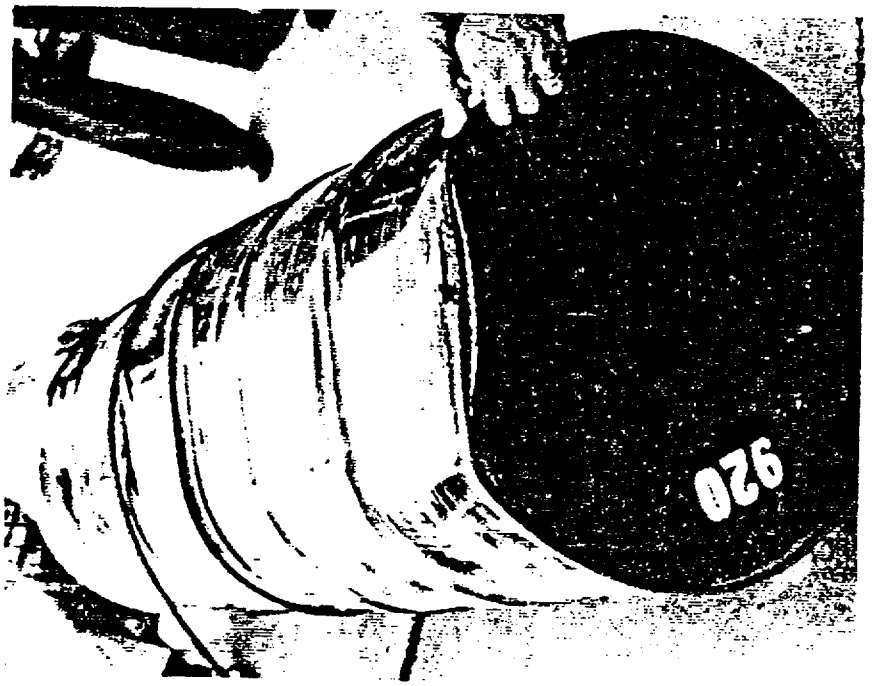

Fig. 2.21.6 Container #920
Impact Side Viewed From Bottom
End

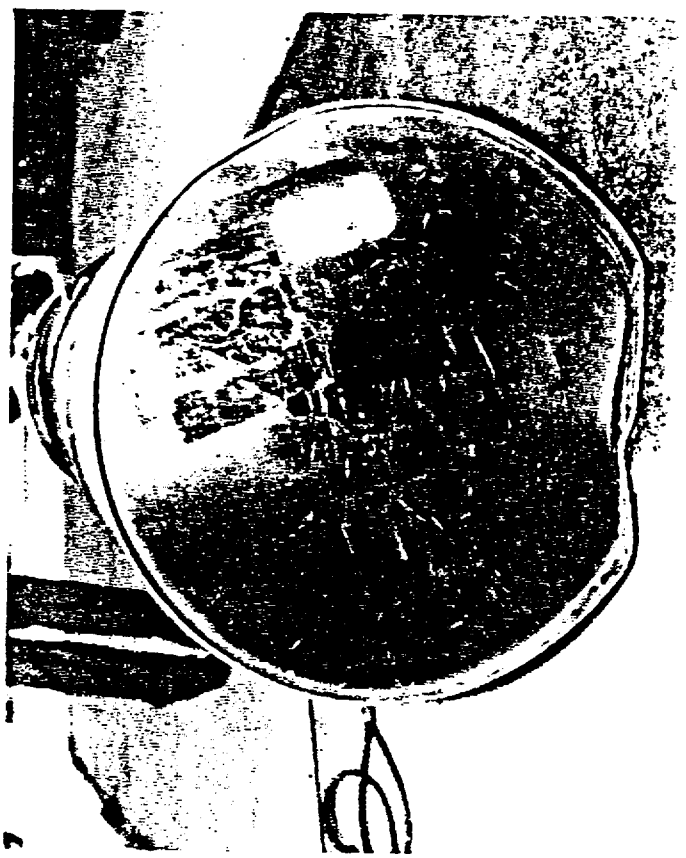

Fig. 2.21.5 Container #920
Bottom Deformation from 9m Drop

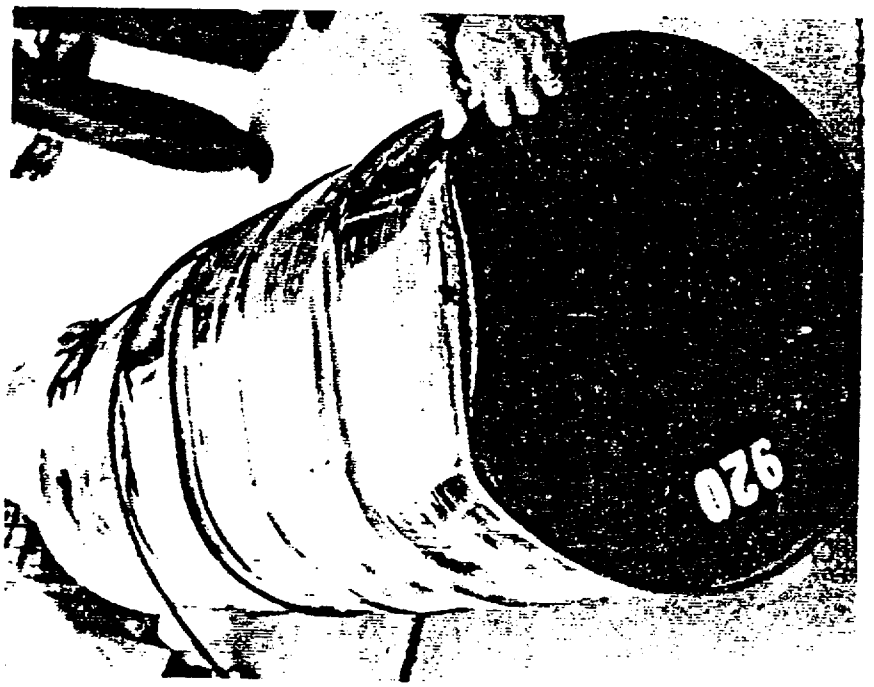

Fig. 2.21.6 Container #920
Impact Side Viewed From Bottom
End

Fig. 2.21.5 Container #920
Bottom Deformation from 9m Drop

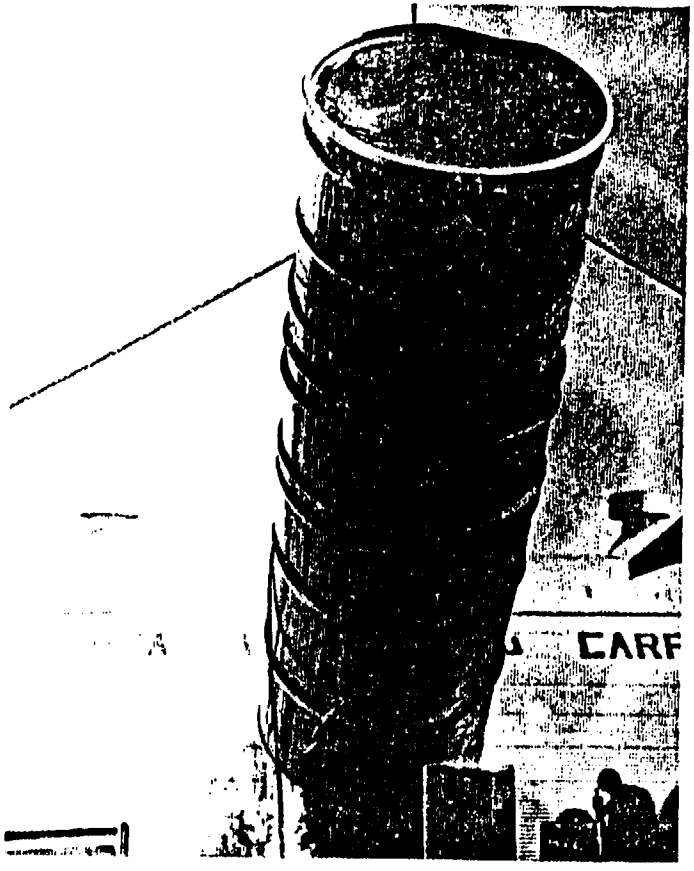

Fig. 2.21.7 Container #920 Suspended Above 15mm Diameter Pin Prior to 1m Drop on Locking Lug

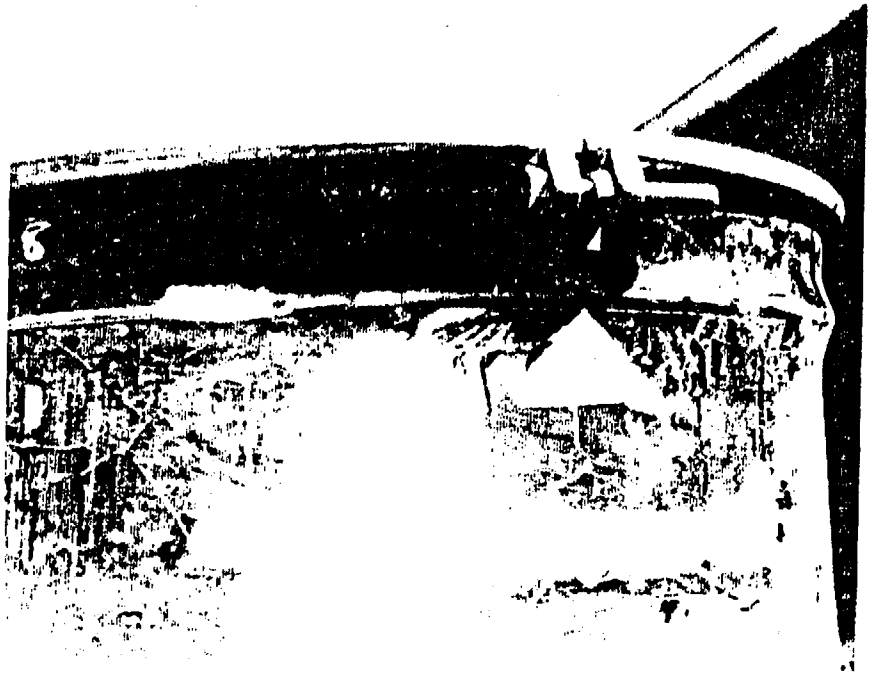

Fig. 2.21.8 Container #920 Showing Locking Lug Subsequent to 1m Drop on 15mm Diameter Pin

Fig. 2.21.8 Container #920 Showing Locking Lug Subsequent to 1m Drop on 15mm Diameter Pin

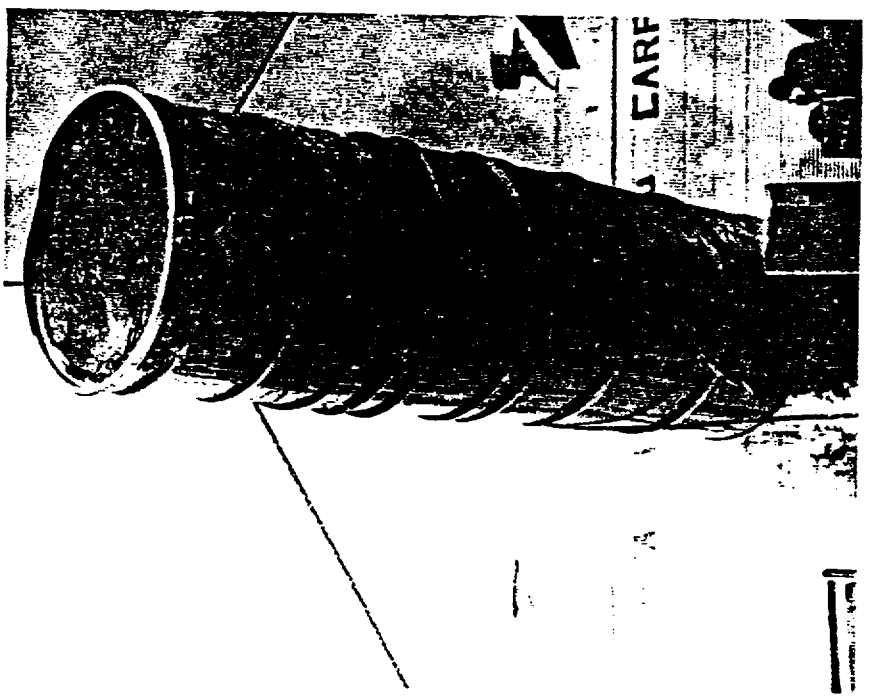

Fig. 2.21.7 Container #920 Suspended Above 15mm Diameter Pin Prior to 1m Drop on Locking Lug

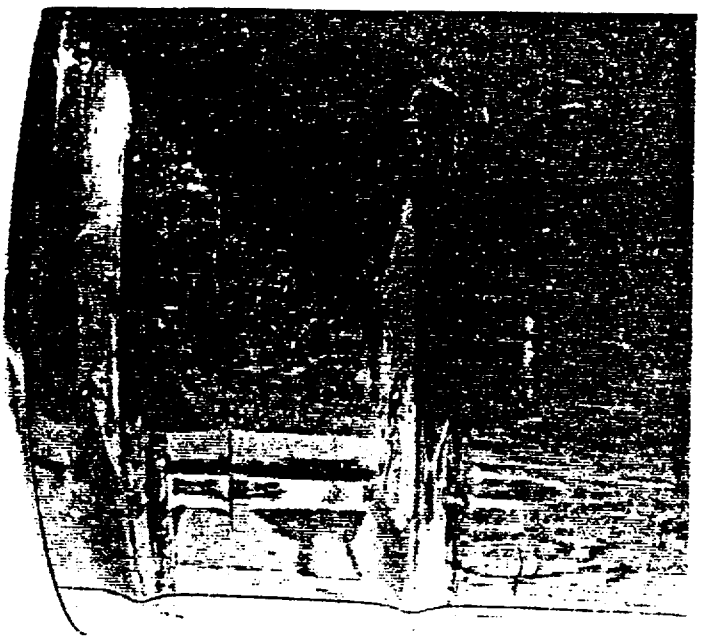

Fig. 2.21.10 Container #920
Showing Impact Area on Locking
Ring After Second 1m Drop

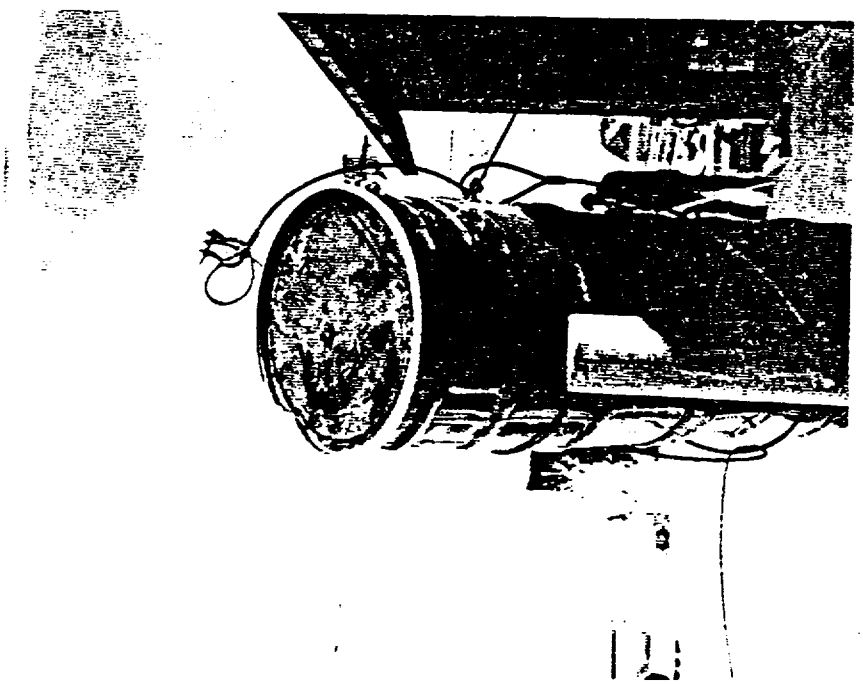

Fig. 2.21.9 Container #920
Just Prior to Impact on 15mm
Diameter Pin in Second 1m Drop

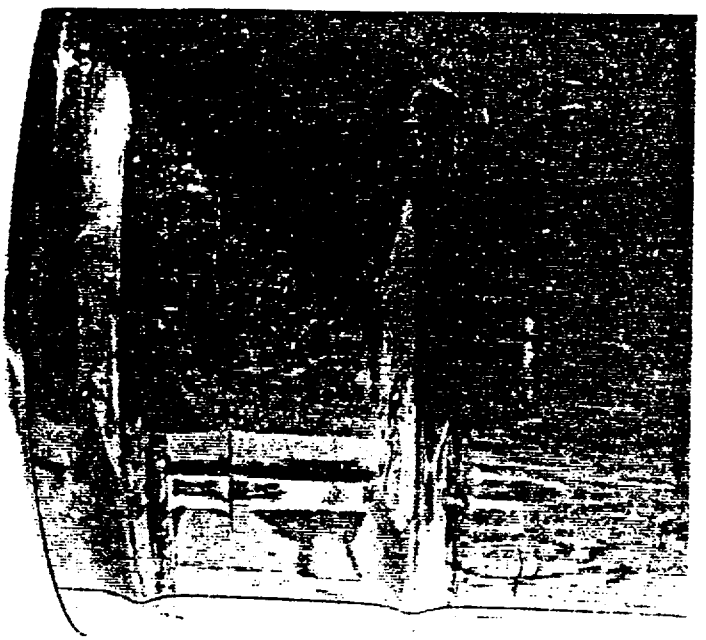

Fig. 2.21.10 Container #920
Showing Impact Area on Locking
Ring After Second 1m Drop

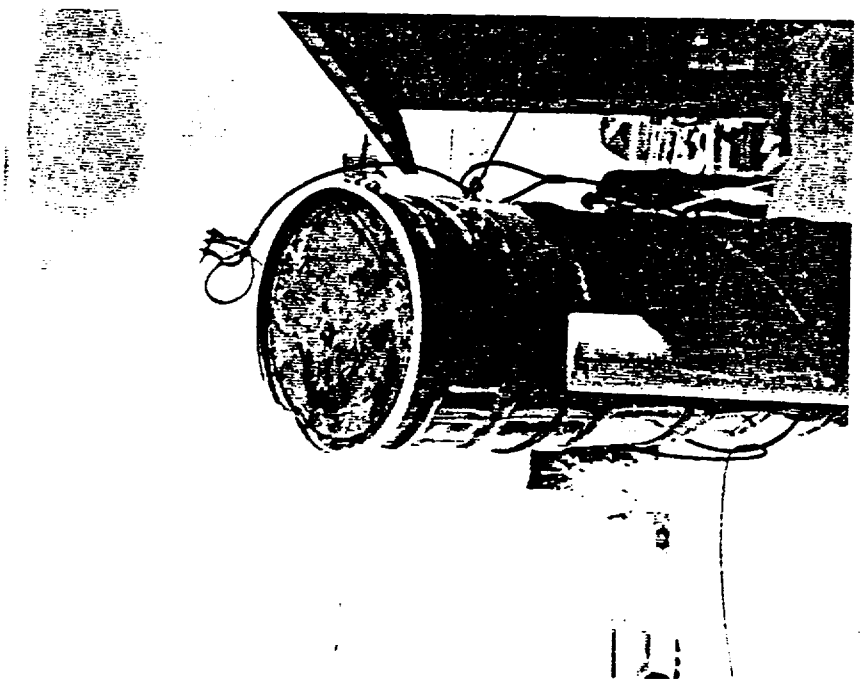

Fig. 2.21.9 Container #920
Just Prior to Impact on 15mm
Diameter Pin in Second 1m Drop

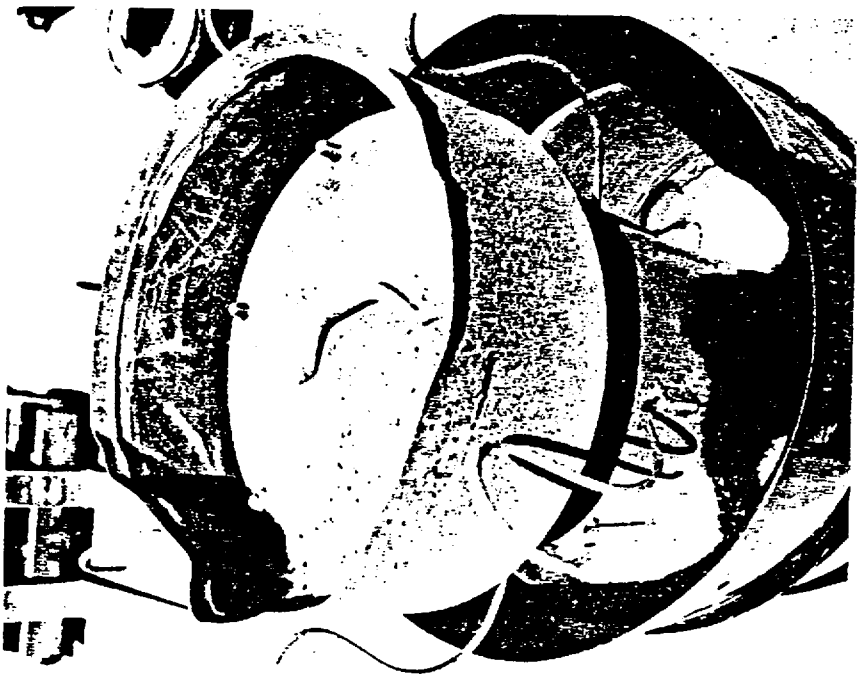

Fig. 2.21.12 Container #920 With Top Portion to Show Deformation of Part 7 of the Upper Support Hardware

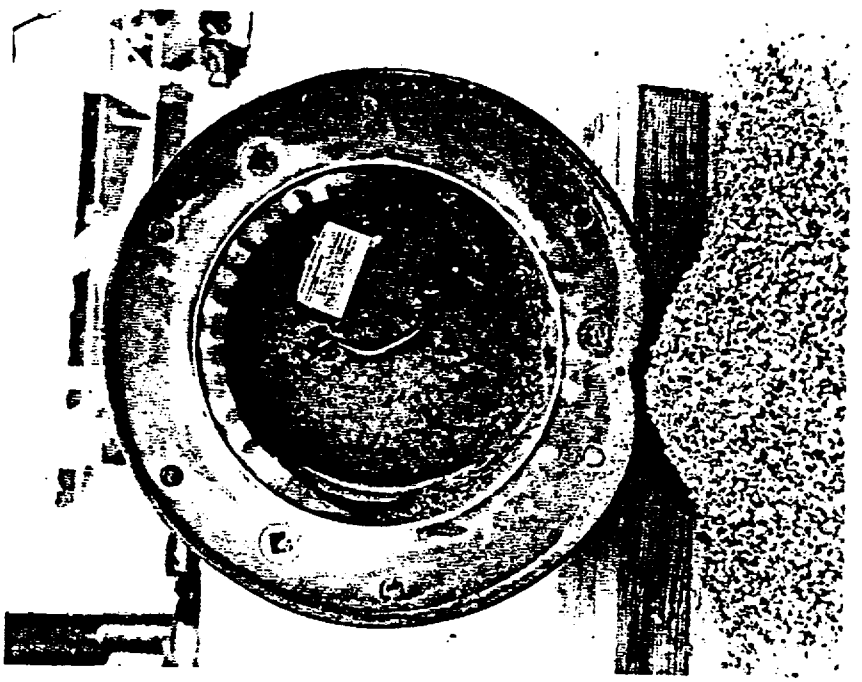

Fig. 2.21.11 Container #920 With Lid Removed Showing Deformation of Part 6 as a Result of 9m and 1m Drops

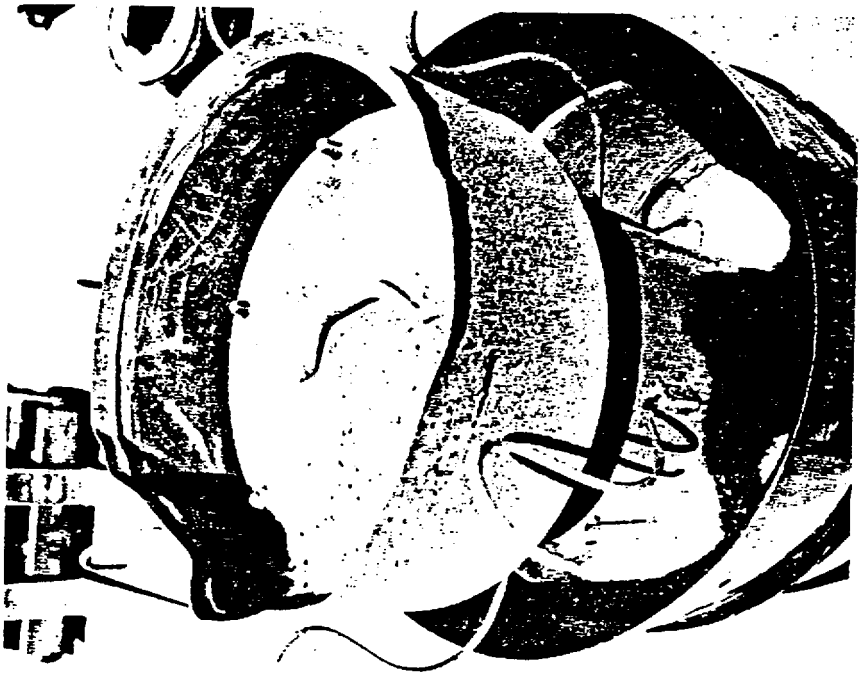

Fig. 2.21.12 Container #920 With Top Portion to Show Deformation of Part 7 of the Upper Support Hardware

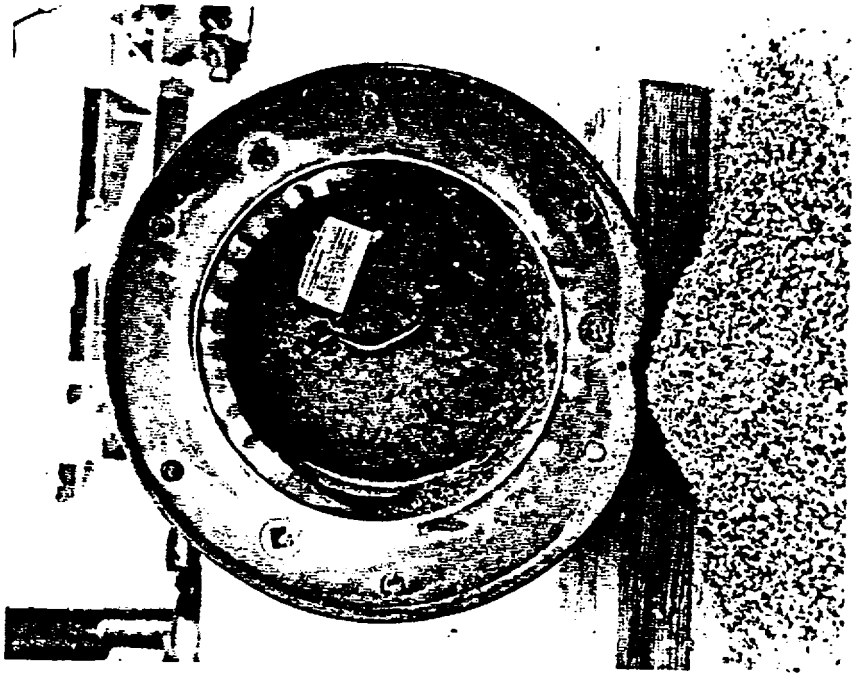

Fig. 2.21.11 Container #920 With Lid Removed Showing Deformation of Part 6 as a Result of 9m and 1m Drops

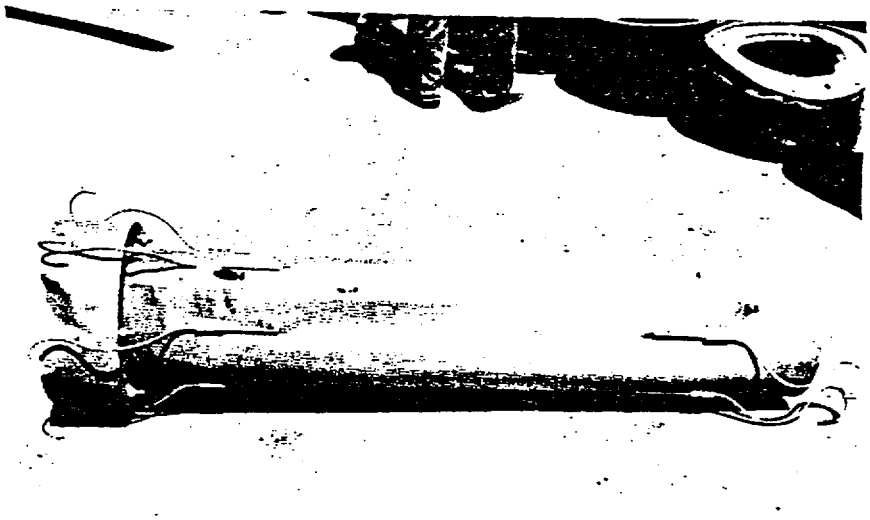

Fig. 2.21.13 Inner Container of #920 Showing Deformation Resulting from 9m and 1m Drops

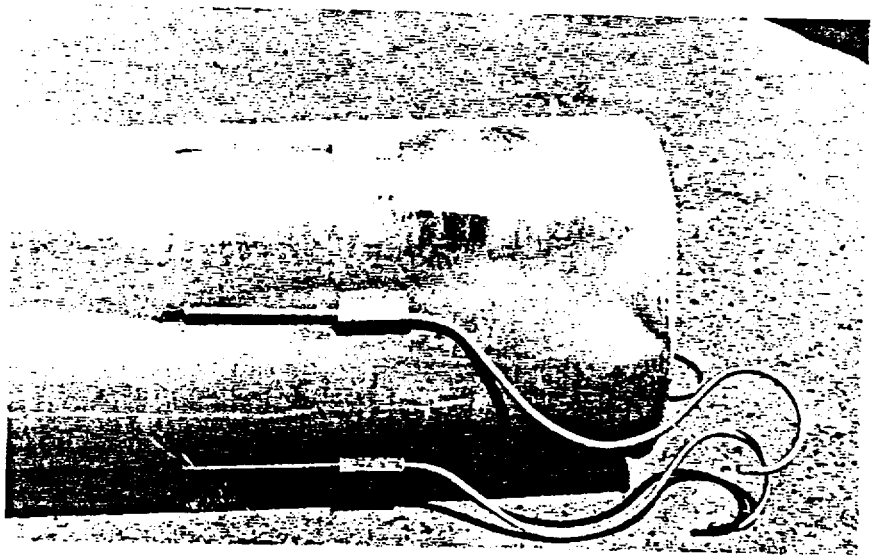

Fig. 2.21.14 Close-Up View of the Bottom End of Inner Container #920

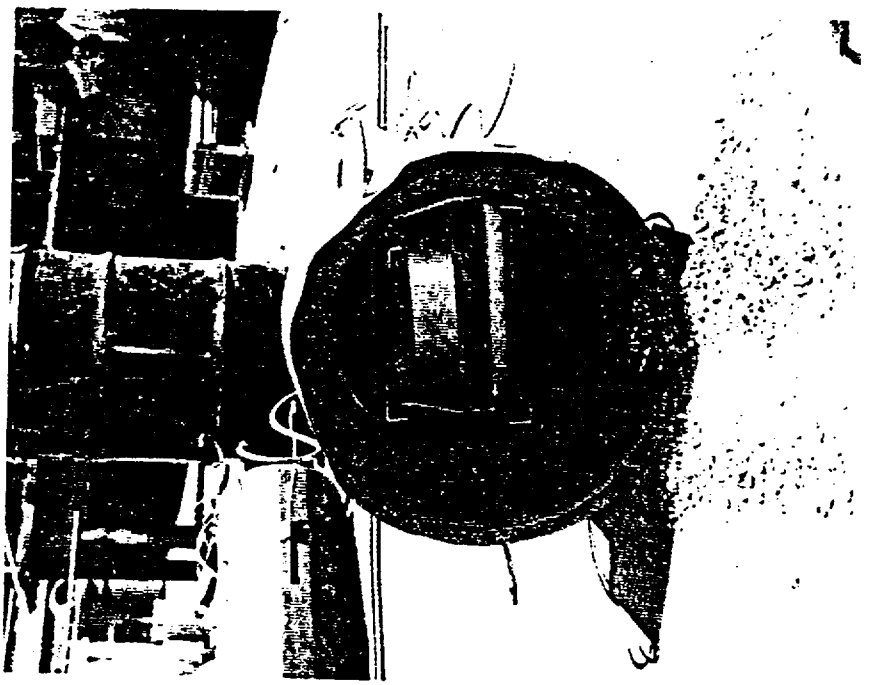

Fig. 2.21.16 End-On View of Inner Container #920 with Lid Removed to Show Insert and Pellet Box

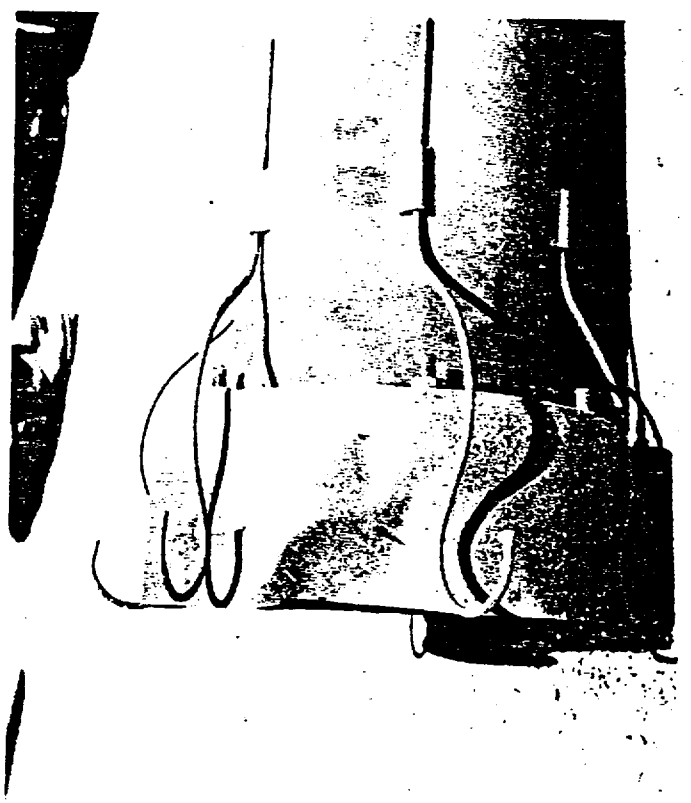

Fig. 2.21.15 Close Up of the Upper End of Inner Container #920

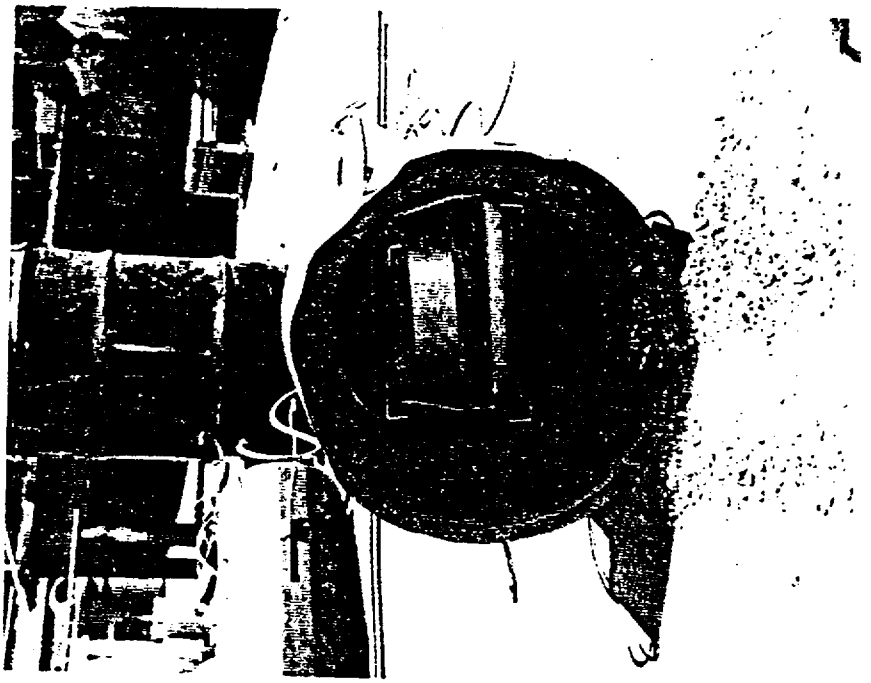

Fig. 2.21.16 End-On View of Inner Container #920 with Lid Removed to Show Insert and Pellet Box

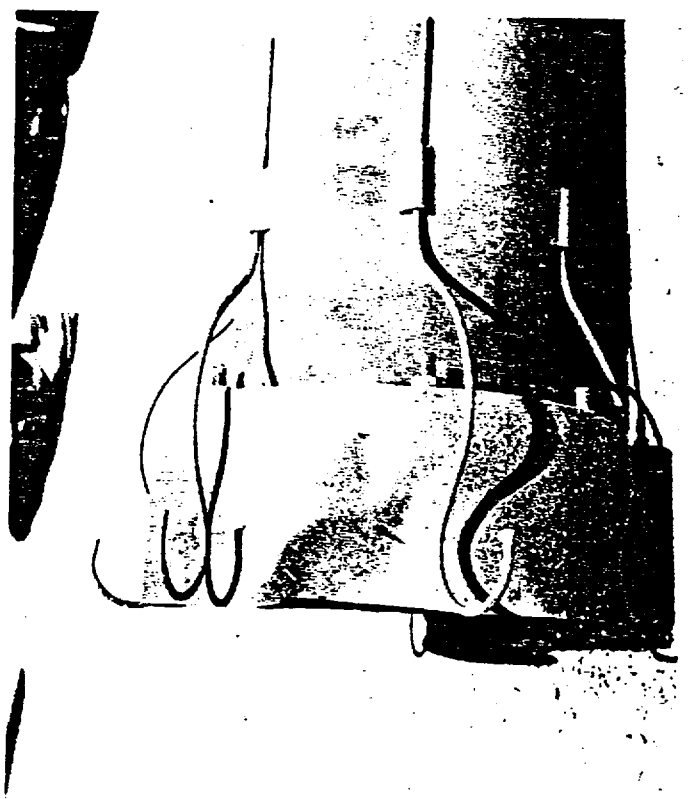

Fig. 2.21.15 Close Up of the Upper End of Inner Container #920

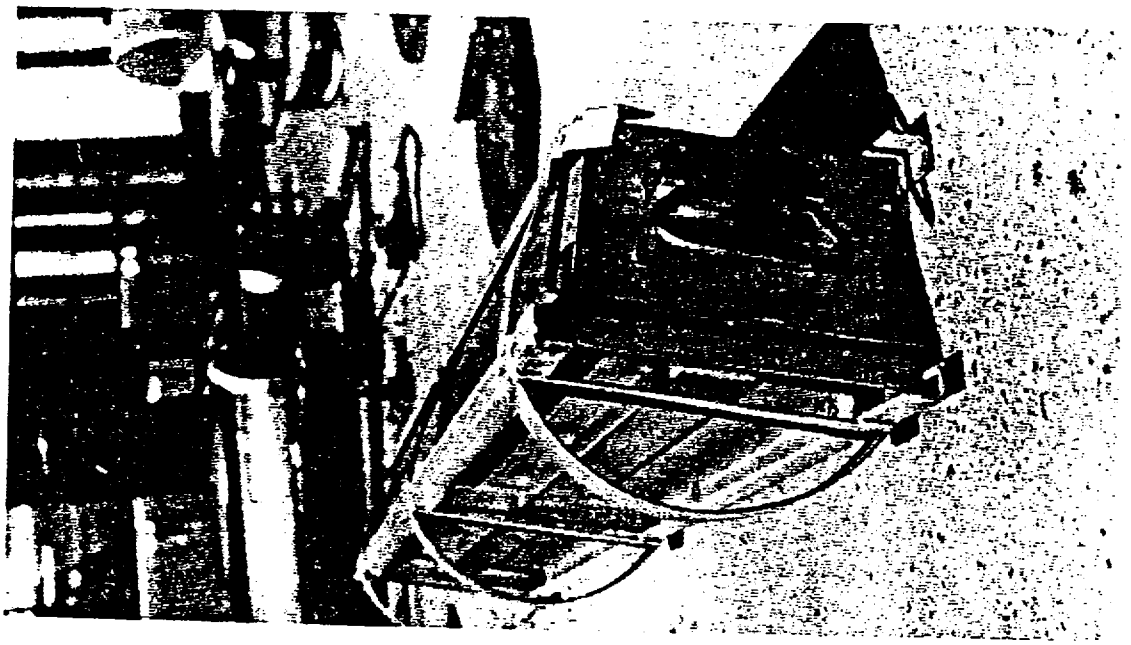

Fig. 2.21.17 End View of Insert and Pellet Box - Container #920

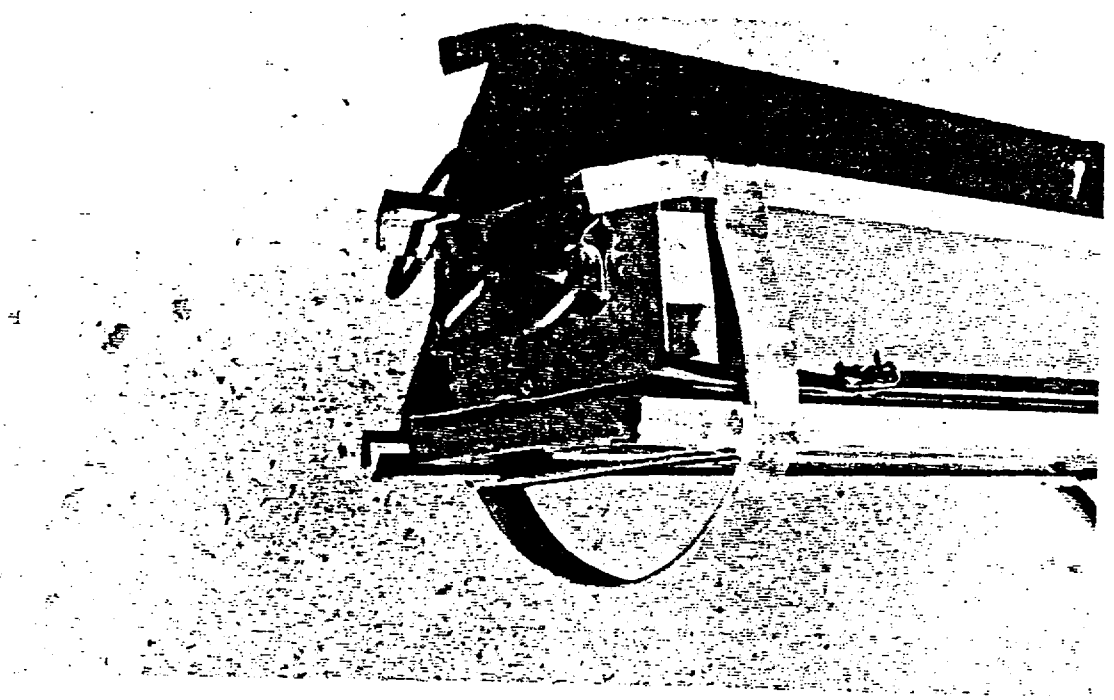

Fig. 2.21.18 Another View of Insert and Pellet Box - Container #920

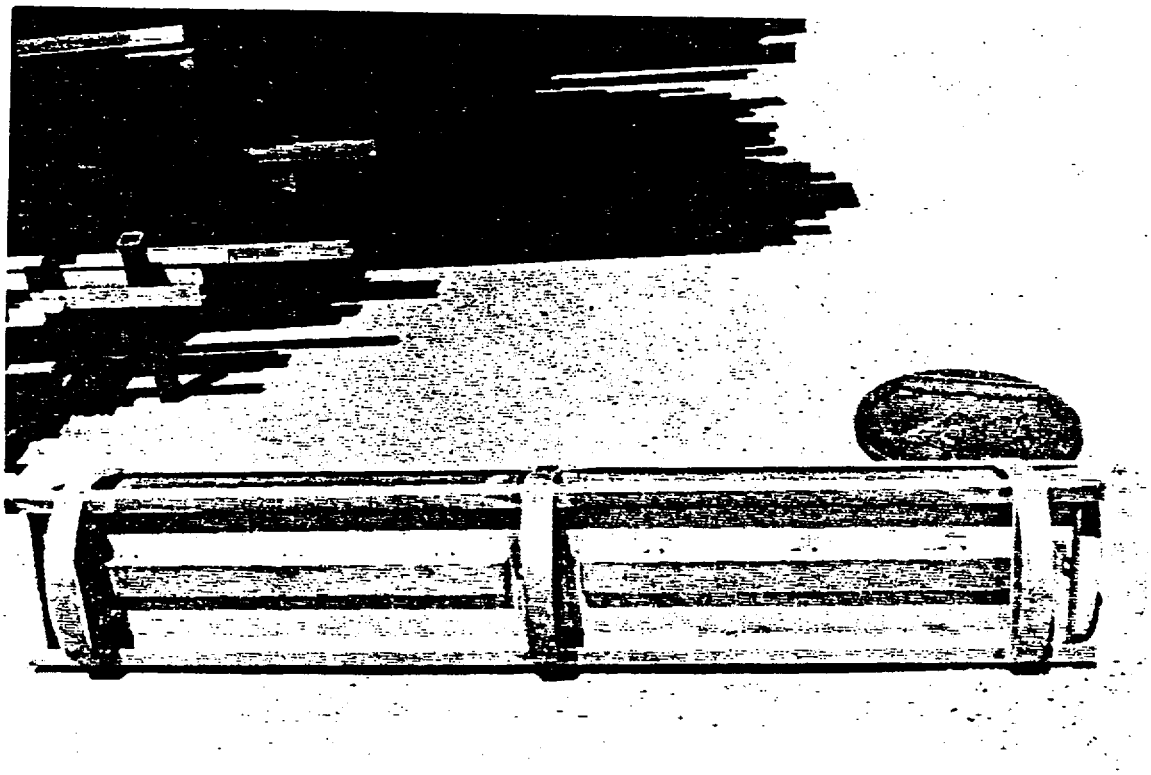

Fig. 2.21.19 Full-Length View of Insert and Pellet Boxes - Container #920

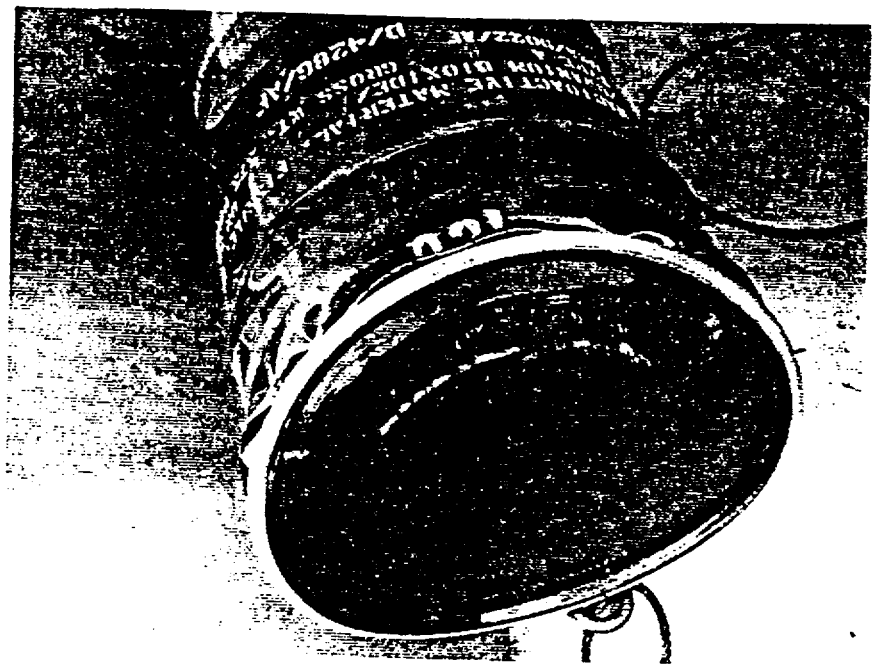

Fig. 2.22.1 Container #921 Showing Deformation from 9m Drop

Fig. 2.22.2 Container #921 Side View of Deformation from 9m Drop

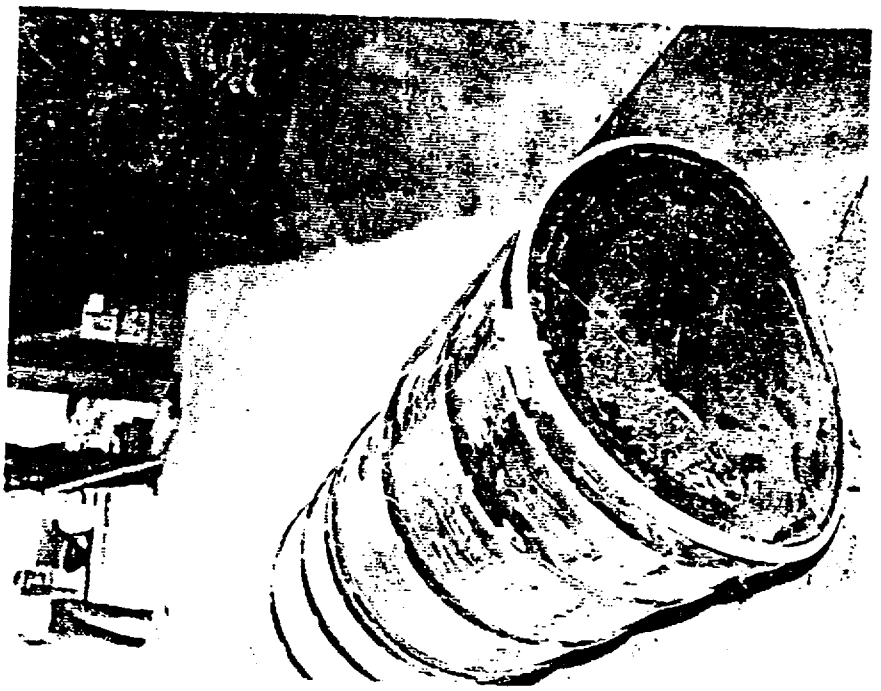

Fig. 2.22.4 Container #921
View from Top End Showing
Deformation from 9m Drop

Fig. 2.22.3 Container #921
Alternate Side View Showing
Deformation from 9m Drop

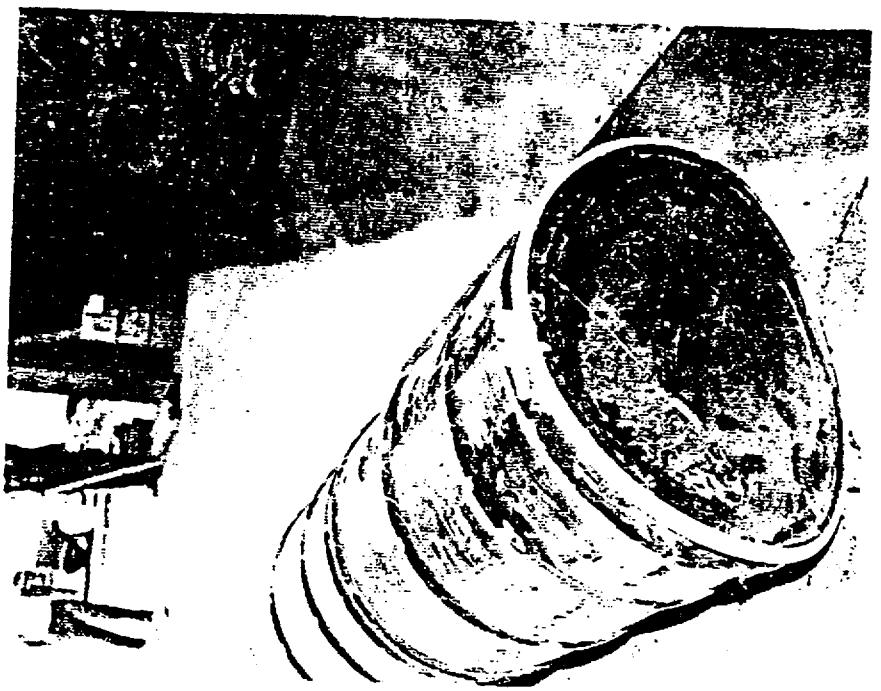

Fig. 2.22.4 Container #921
View from Top End Showing
Deformation from 9m Drop

Fig. 2.22.3 Container #921
Alternate Side View Showing
Deformation from 9m Drop

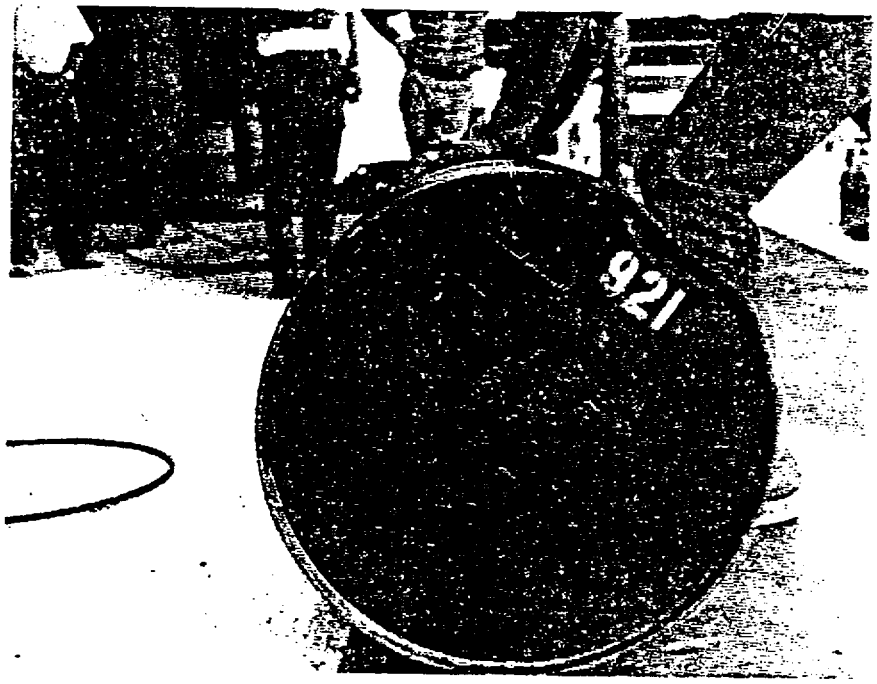

Fig. 2.22.5 Container #921 Lower End Minor Deformation Resulting from 9m Drop

Fig. 2.22.6 Container #921 Overhead View From Lower End Showing Deformation As Result of 9m Drop

Fig. 2.22.8 Container #921 Leaning Against 15mm Diameter Pin Subsequent to 1m Drop with Impact on Locking Lug

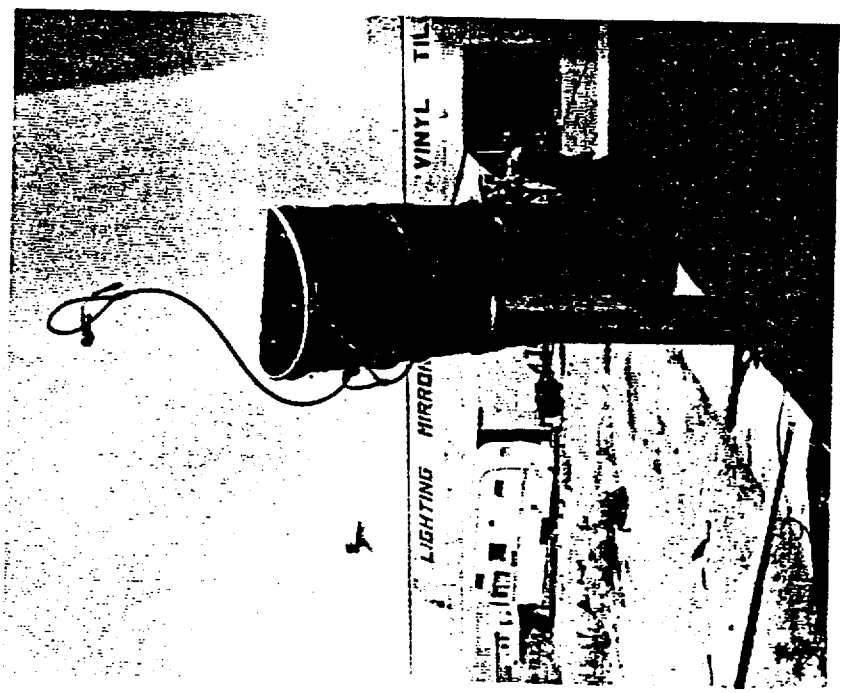

Fig. 2.22.7 Container #921 in Free Fall Onto 15mm Diameter Pin

Fig. 2.22.8 Container #921 Leaning Against 15mm Diameter Pin Subsequent to 1m Drop with Impact on Locking Lug

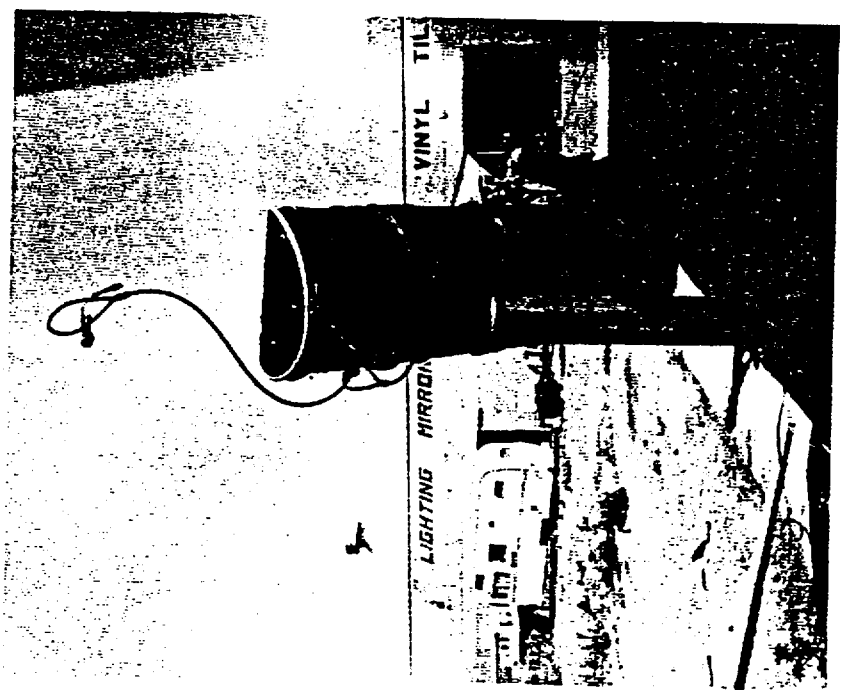

Fig. 2.22.7 Container #921 in Free Fall Onto 15mm Diameter Pin

Fig. 2.22.10 View of the Distortion of Lid End of Container #921 Subsequent to Drop Test Series

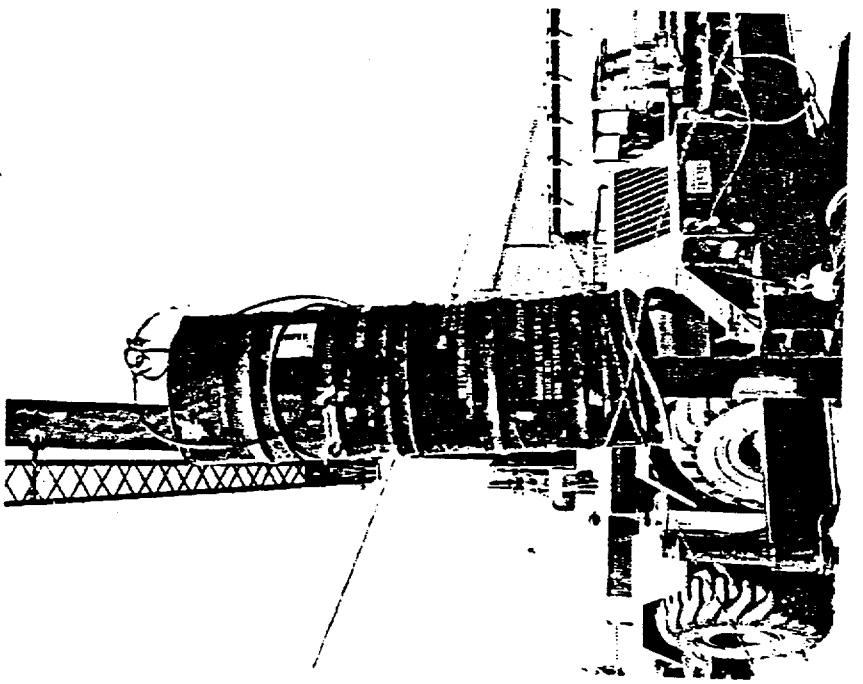

Fig. 2.22.9 Container #921 at Impact During 1m Drop Onto the Lid in Vertical Orientation

Fig. 2.22.10 View of the Distortion of Lid End of Container #921 Subsequent to Drop Test Series

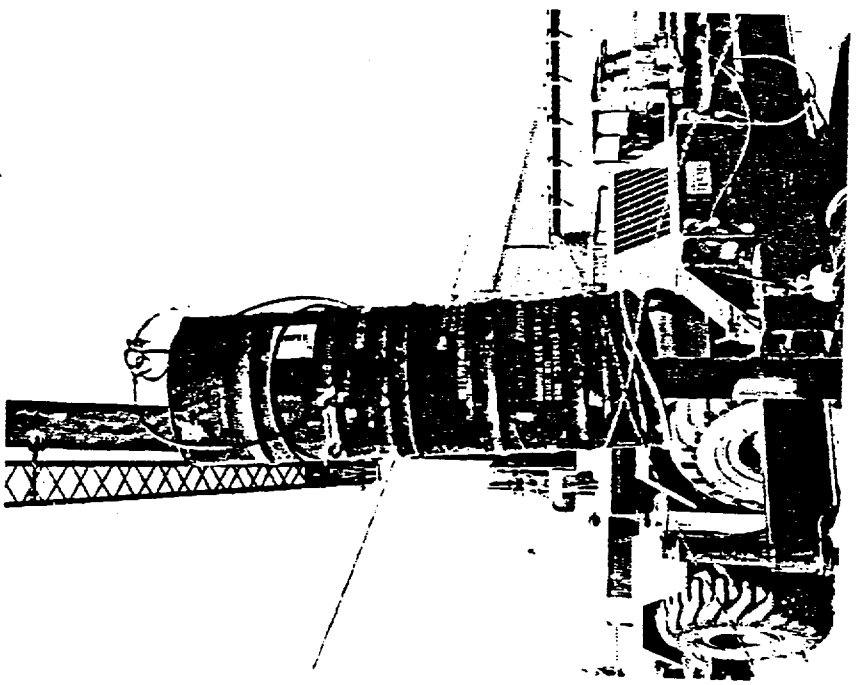

Fig. 2.22.9 Container #921 at Impact During 1m Drop Onto the Lid in Vertical Orientation

Fig. 2.22.12 Second Alternate View of Distortion of Lid End of Container #921 Subsequent to Drop Test Series

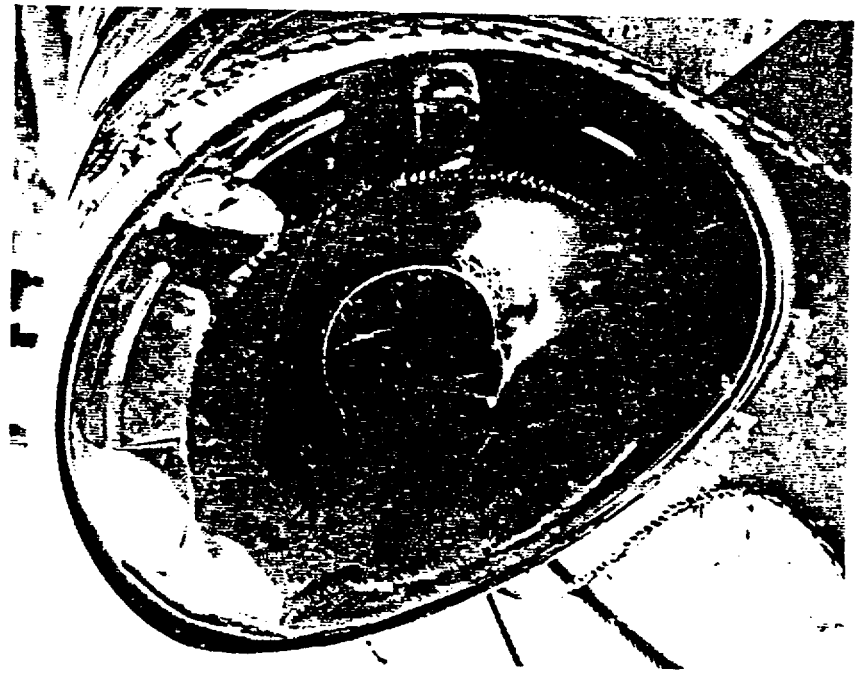

Fig. 2.22.11 Container #921 Alternate View of Distortion of Lid End of Container Subsequent to Drop Test Series

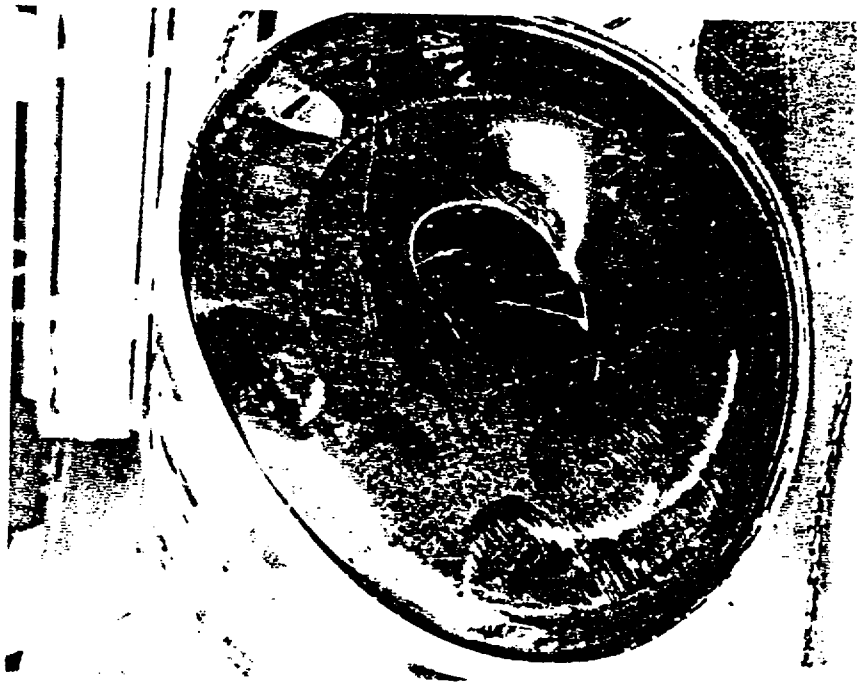

Fig. 2.22.12 Second Alternate View of Distortion of Lid End of Container #921 Subsequent to Drop Test Series

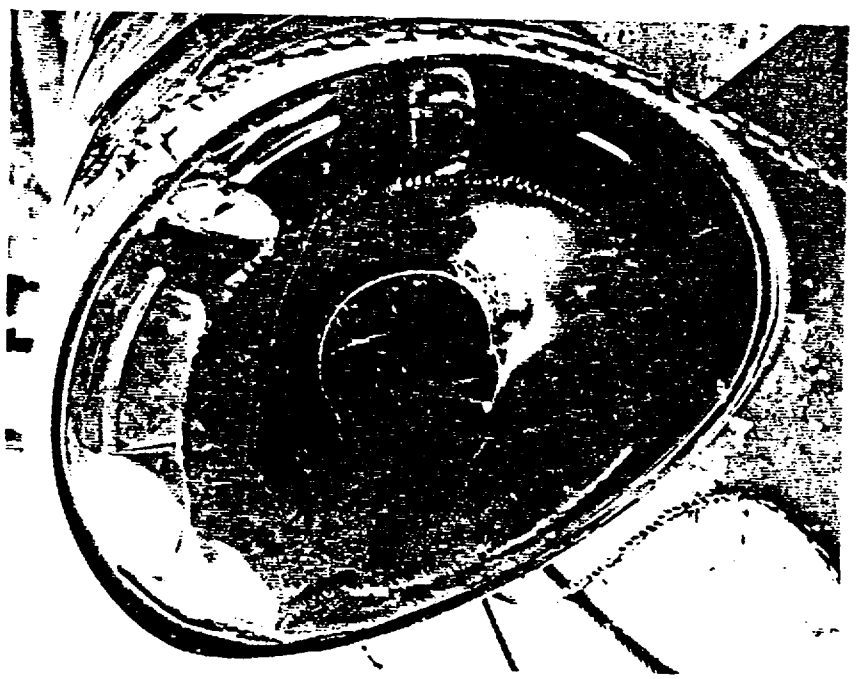

Fig. 2.22.11 Container #921 Alternate View of Distortion of Lid End of Container Subsequent to Drop Test Series

Fig. 2.22.13 Container #921 with Lid Removed to Show Deformation Resulting from Drop Series

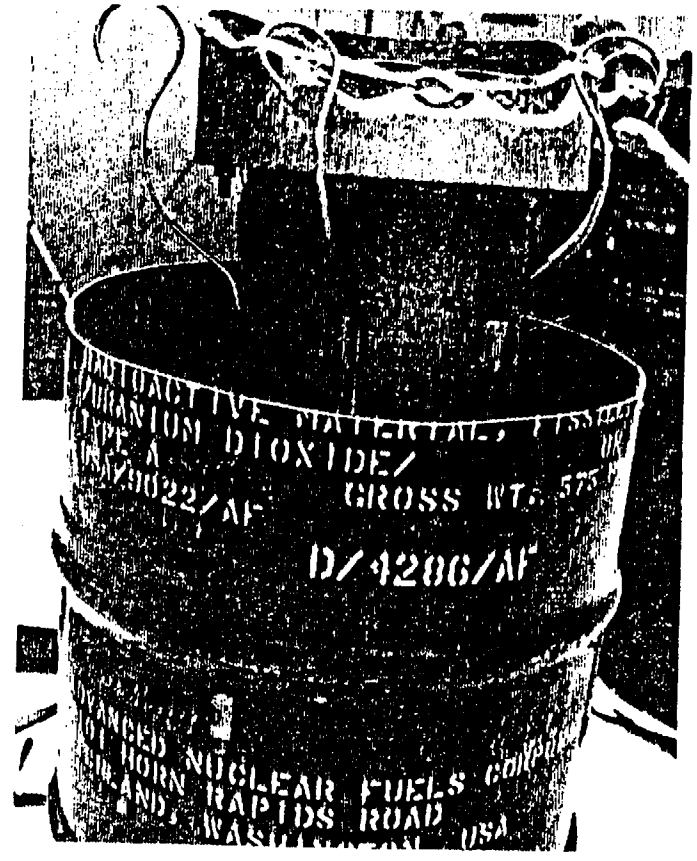

Fig. 2.22.14 Container #921 with Upper Portion Removed to Show Deformation to Upper Band of Inner Container

Fig. 2.22.13 Container #921 with Lid Removed to Show Deformation Resulting from Drop Series

Fig. 2.22.14 Container #921 with Upper Portion Removed to Show Deformation to Upper Band of Inner Container

Fig. 2.22.15 Container #921 Overhead View of Deformation on Band of Inner Container

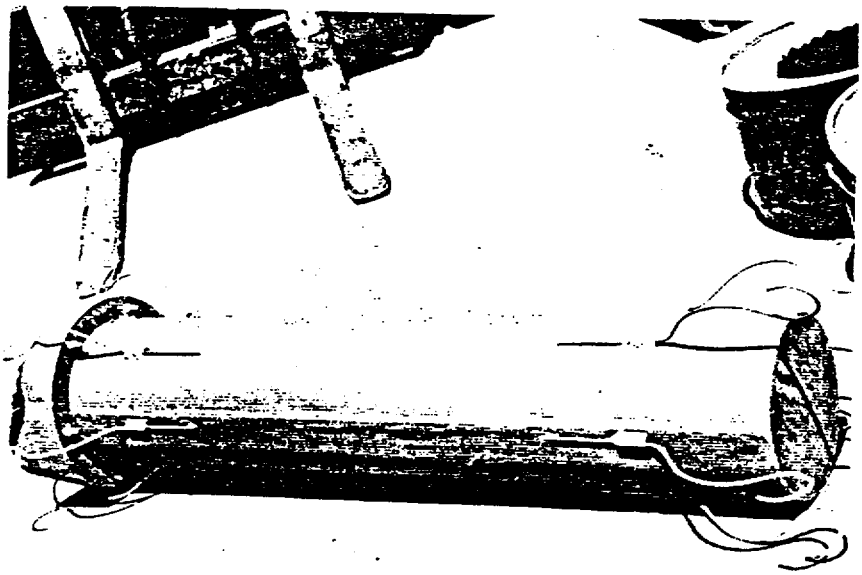

Fig. 2.22.16 Full Length View of the Inner Container from Container #921

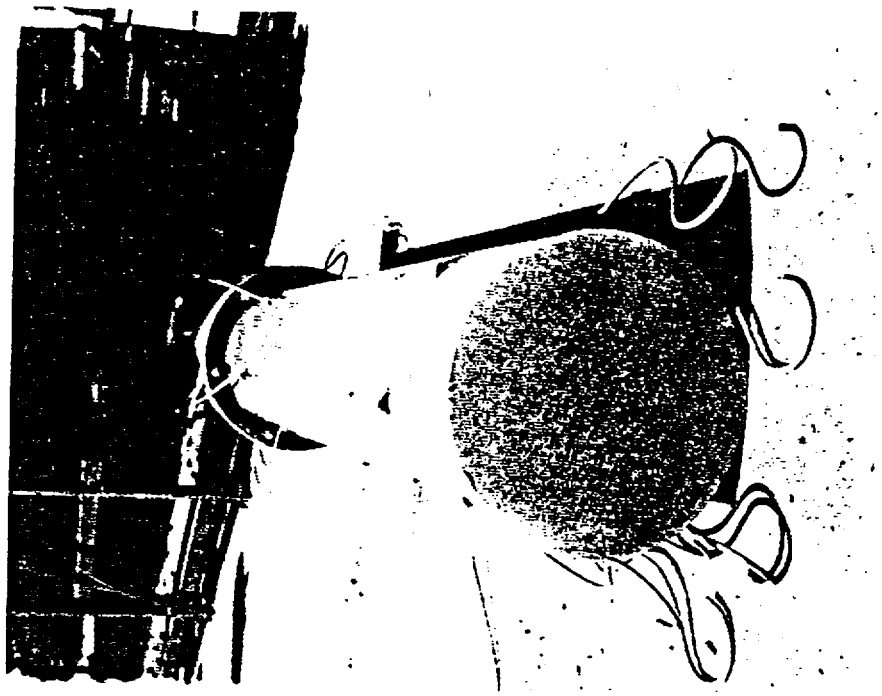

Fig. 2.22.18 Bottom End View of Inner Container of Container #921 Following Drop Series

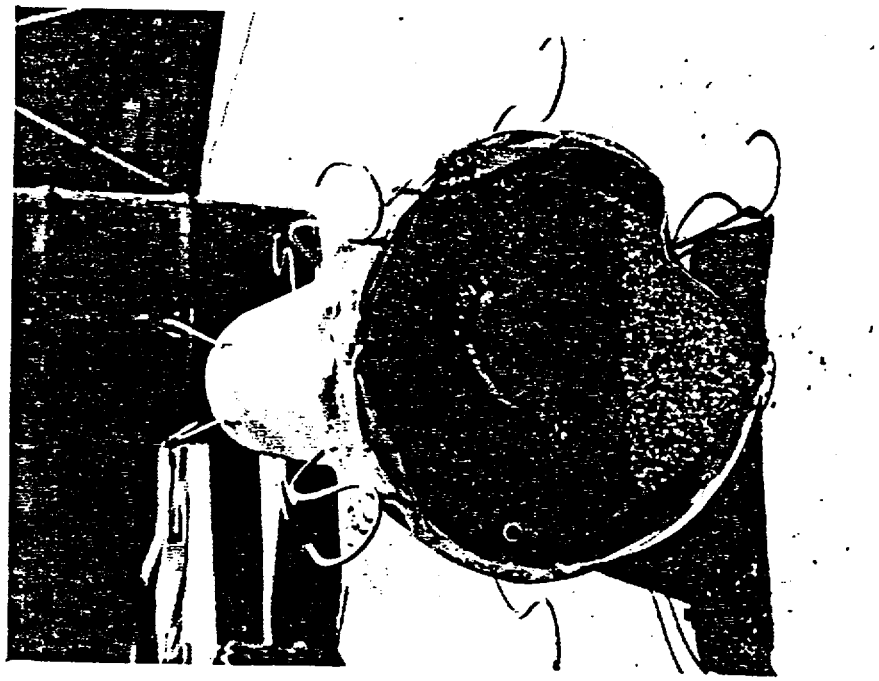

Fig. 2.22.17 Lid End View of Inner Container of Container #921 Following Drop Series

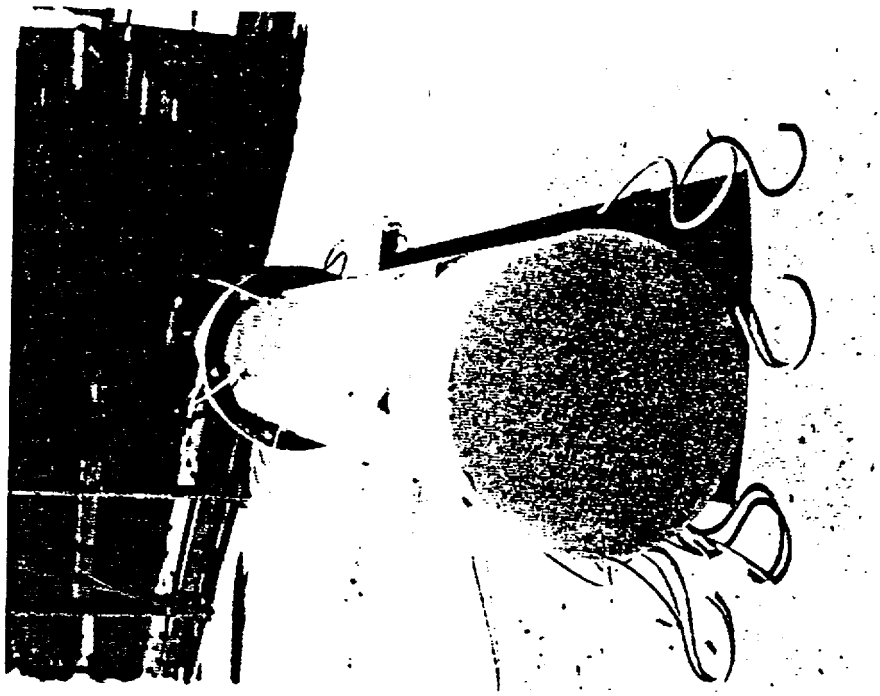

Fig. 2.22.18 Bottom End View of Inner Container of Container #921 Following Drop Series

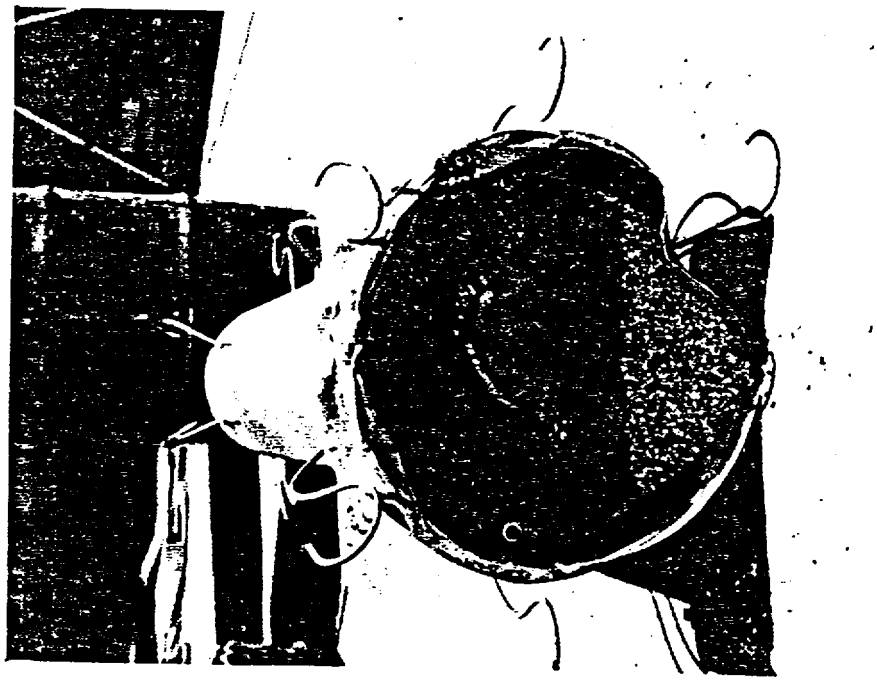

Fig. 2.22.17 Lid End View of Inner Container of Container #921 Following Drop Series

Fig. 2.22.20 Side View at Upper End of Pellet Boxes From Container #921

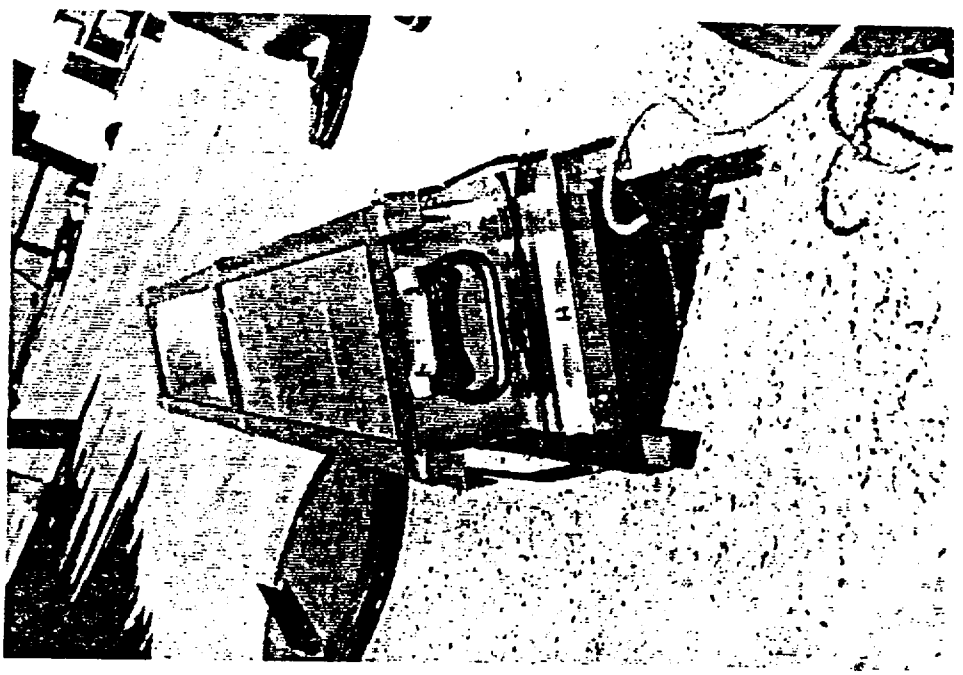

Fig. 2.22.19 Pellet Boxes From Container #921 Showing Displacement of Upper Box Relative to the Base

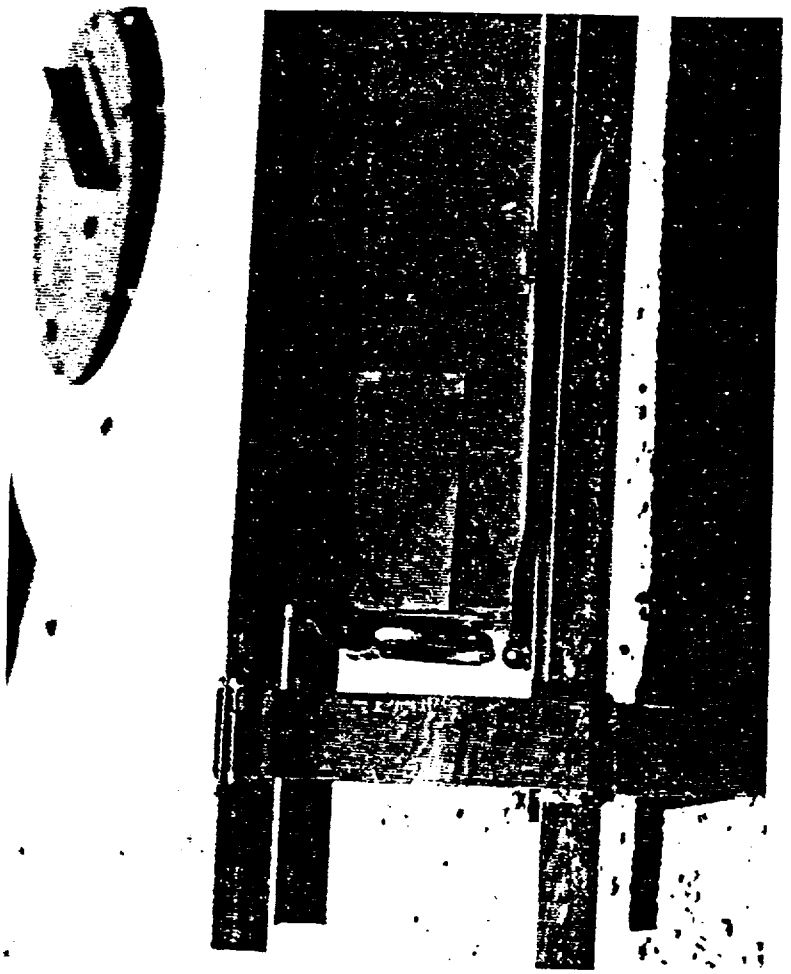

Fig. 2.22.20 Side View at Upper End of Pellet Boxes From Container #921

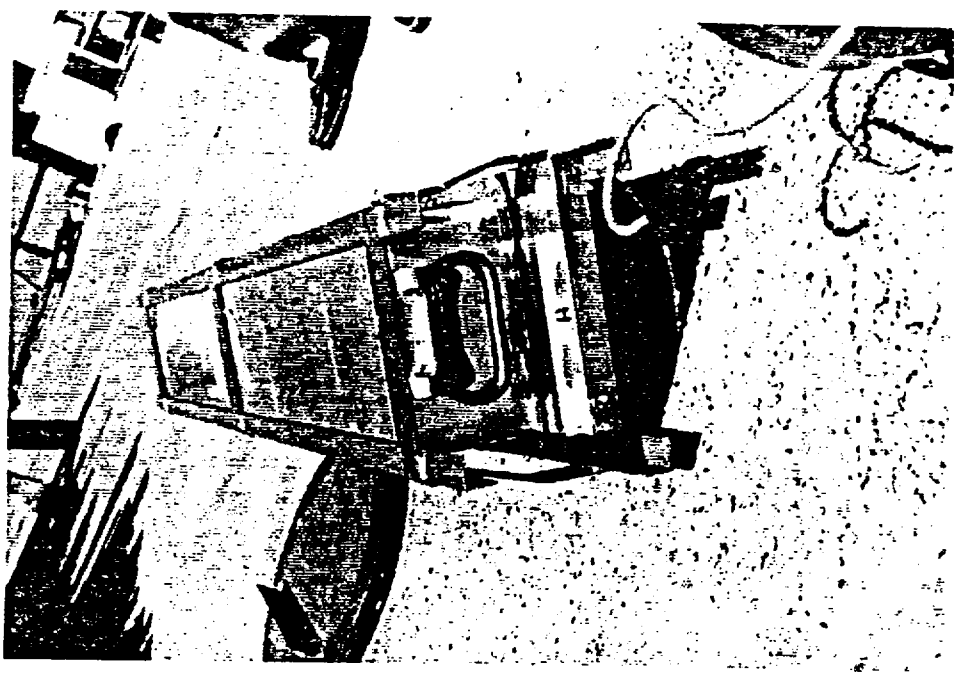

Fig. 2.22.19 Pellet Boxes From Container #921 Showing Displacement of Upper Box Relative to the Base

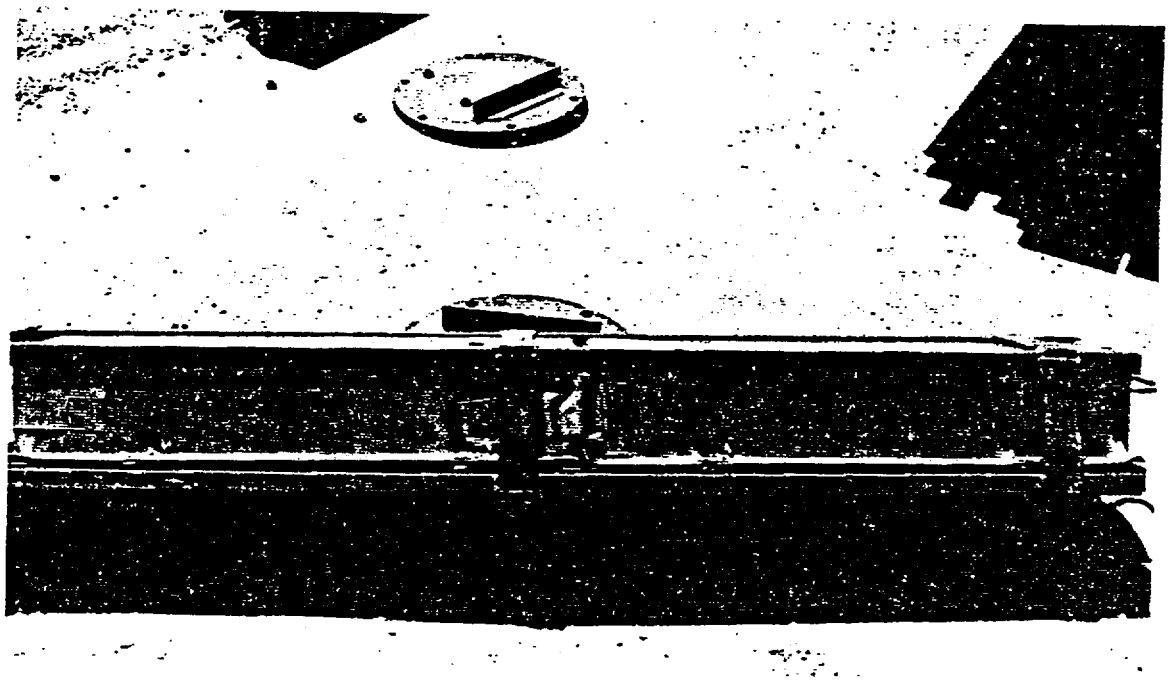

Fig. 2.22.21 Full Length View of Two Pellet Boxes From Container #921

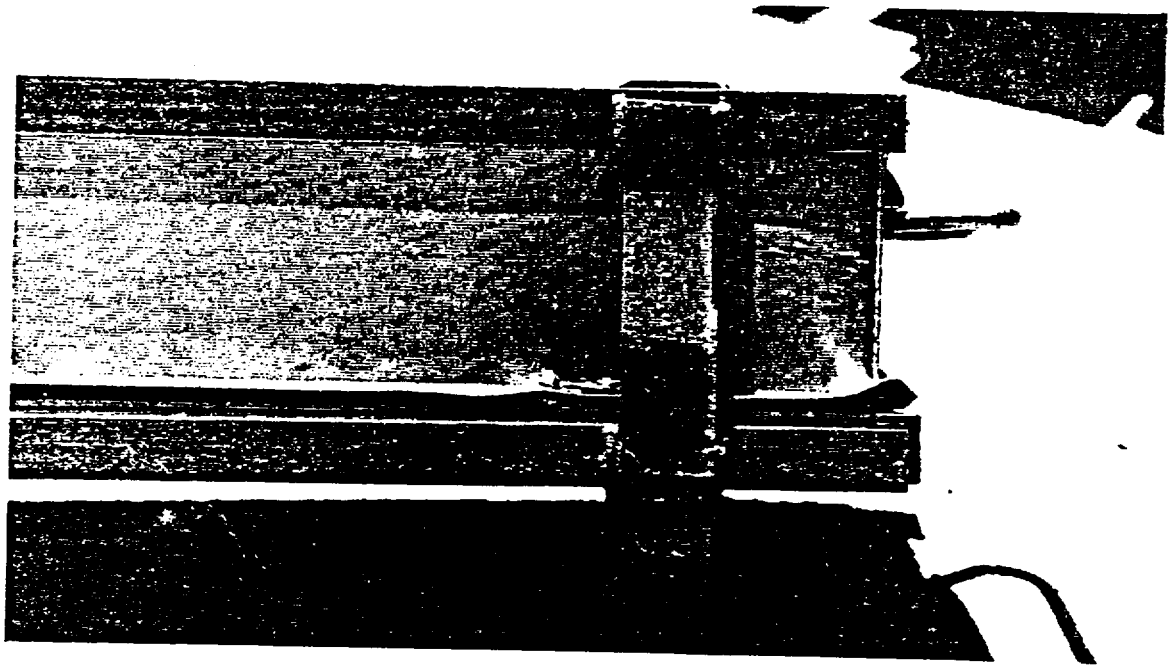

Fig. 2.22.22 Closeup View of Bottom End Pellet Box From Container #921

Fig. 2.23.2 Container #931 Lid End
Subsequent to 9m Drop

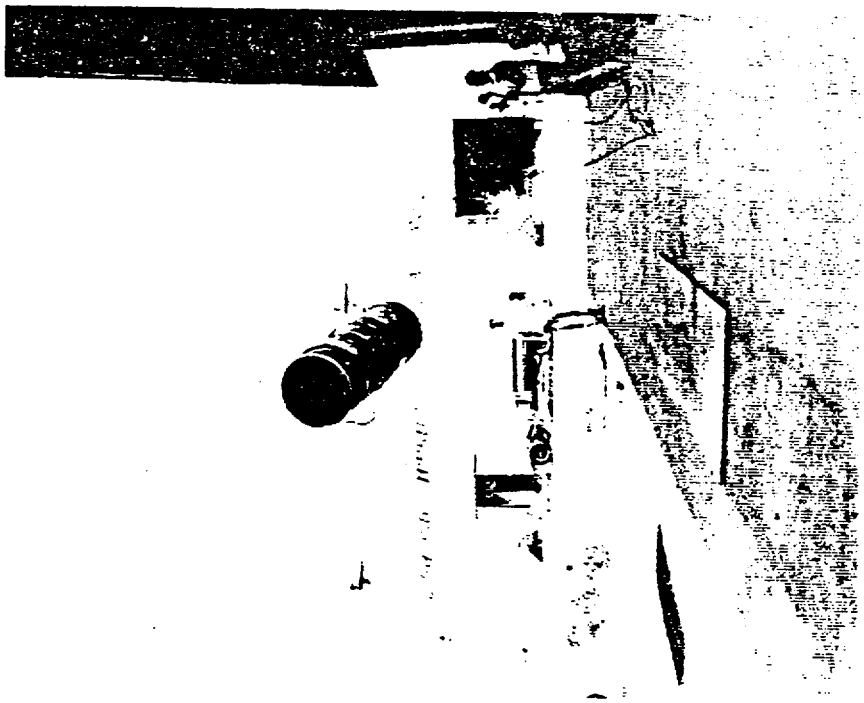

Fig. 2.23.1 Container #931 in
Free Fall of 9m Drop

Fig. 2.23.2 Container #931 Lid End
Subsequent to 9m Drop

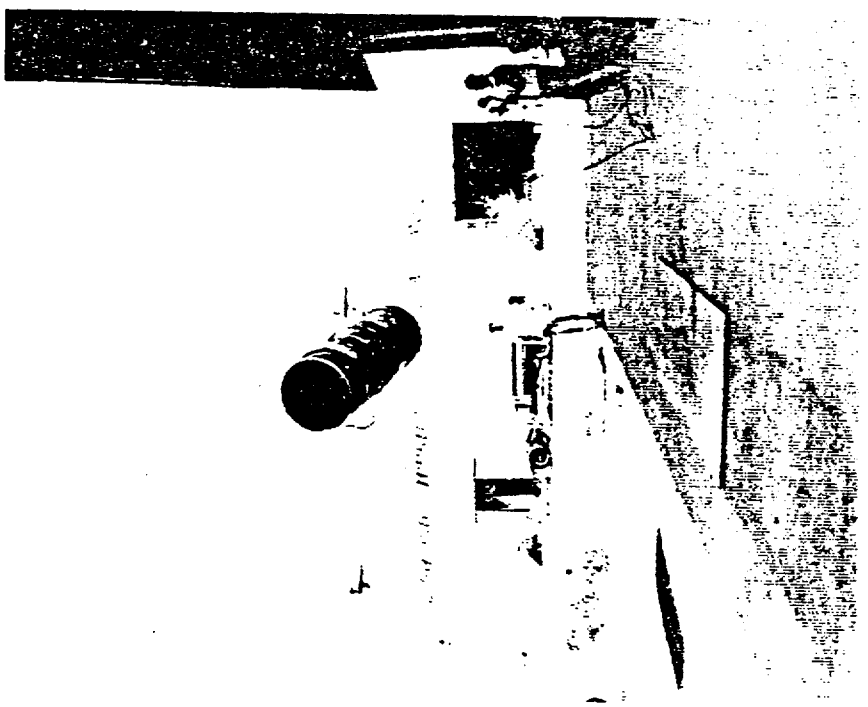

Fig. 2.23.1 Container #931 in
Free Fall of 9m Drop

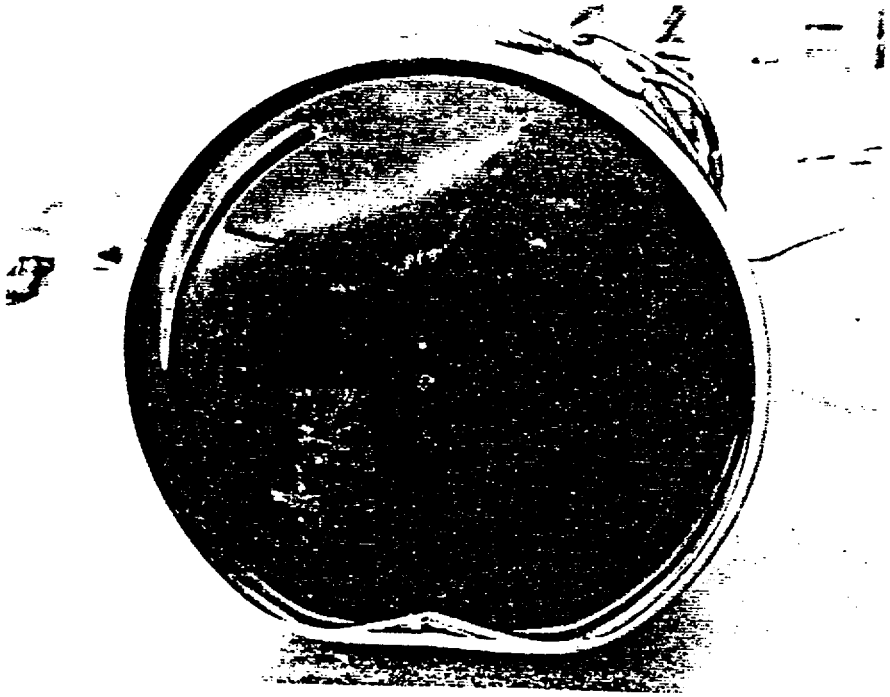

Fig. 2.23.3 Container #931 View of Lid Subsequent to 9m Drop

Fig. 2.23.4 Container #931 Closeup View of Lid Subsequent to 9m Drop

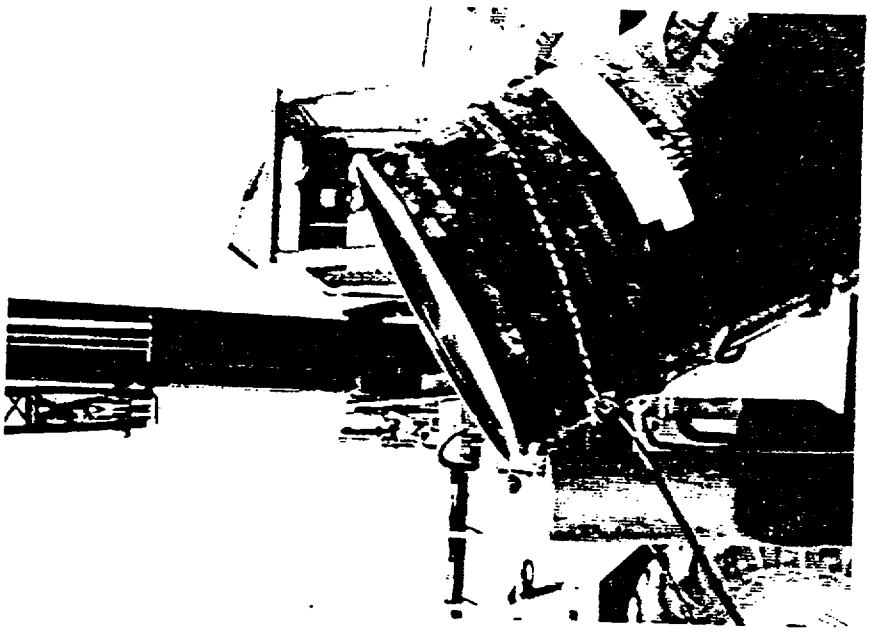

Fig. 2.23.6 Container #931 Showing Impact in First of Three 1m Drops

Fig. 2.23.5 Container #931 Bottom Deformation from 9m Drop

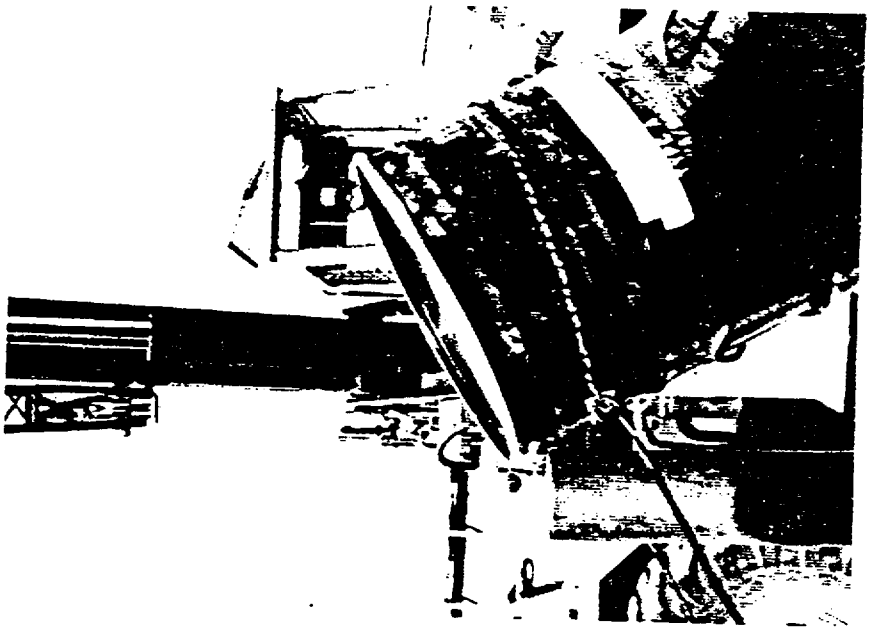

Fig. 2.23.6 Container #931 Showing Impact in First of Three 1m Drops

Fig. 2.23.5 Container #931 Bottom Deformation from 9m Drop

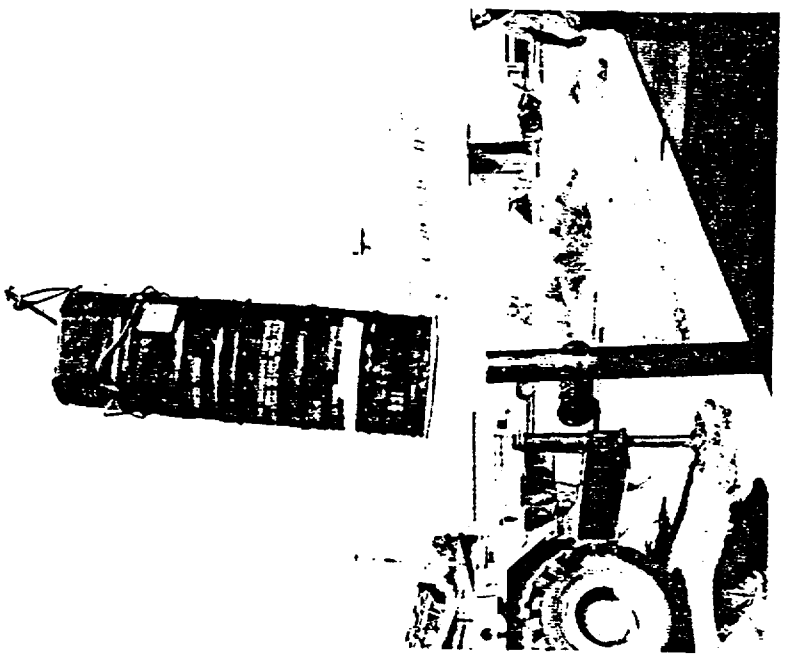

Fig. 2.23.8 Container #931 Just Prior to Impact in Third of Three 1m Drops

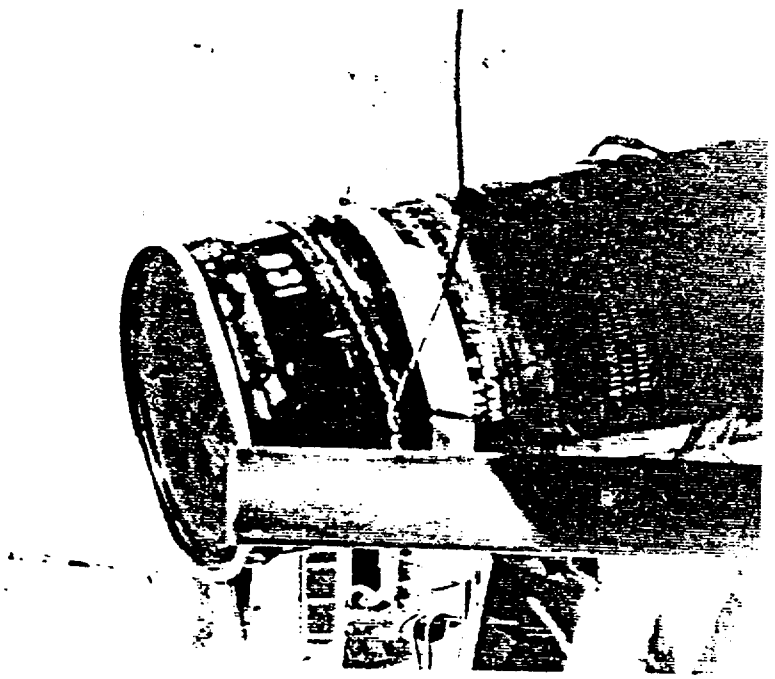

Fig. 2.23.7 Container #931 Impact in Second of Three 1m Drops

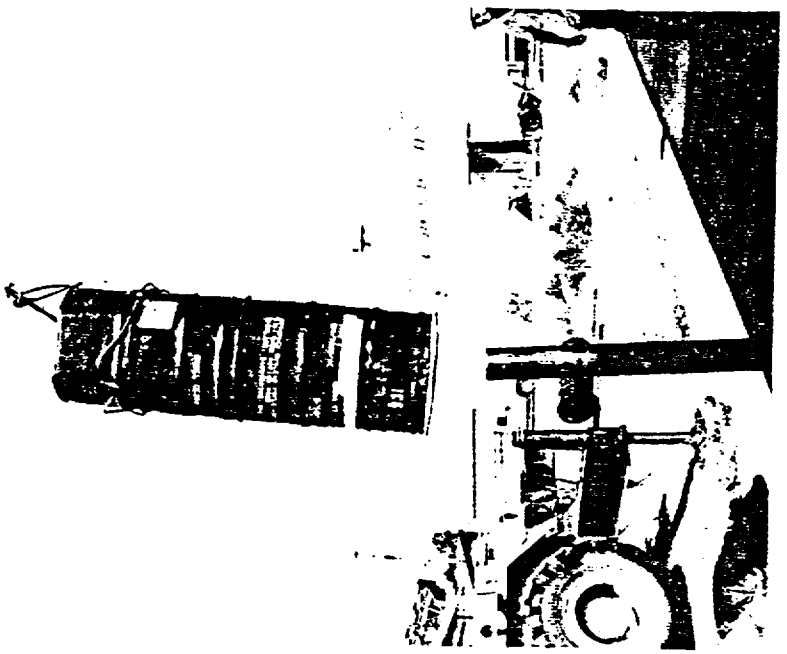

Fig. 2.23.8 Container #931 Just Prior to Impact in Third of Three 1m Drops

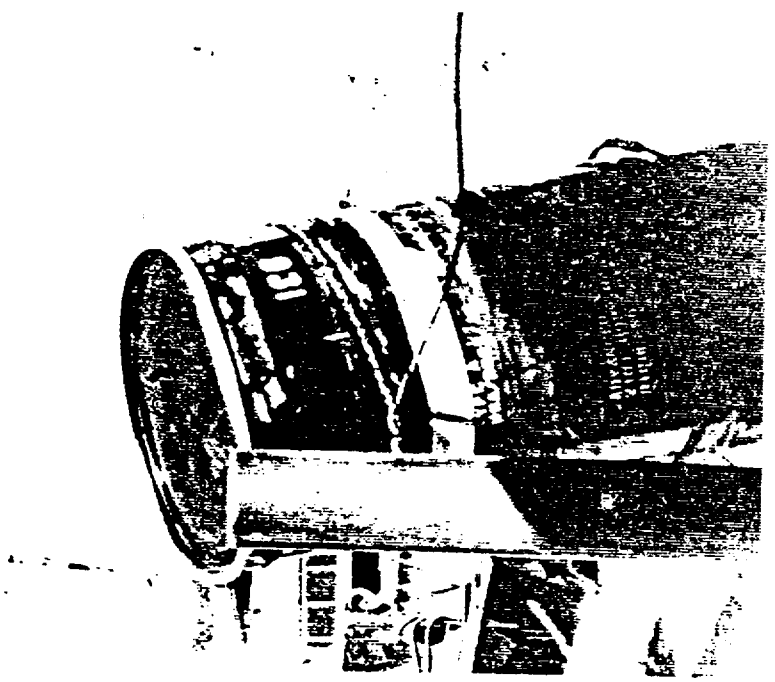

Fig. 2.23.7 Container #931 Impact in Second of Three 1m Drops

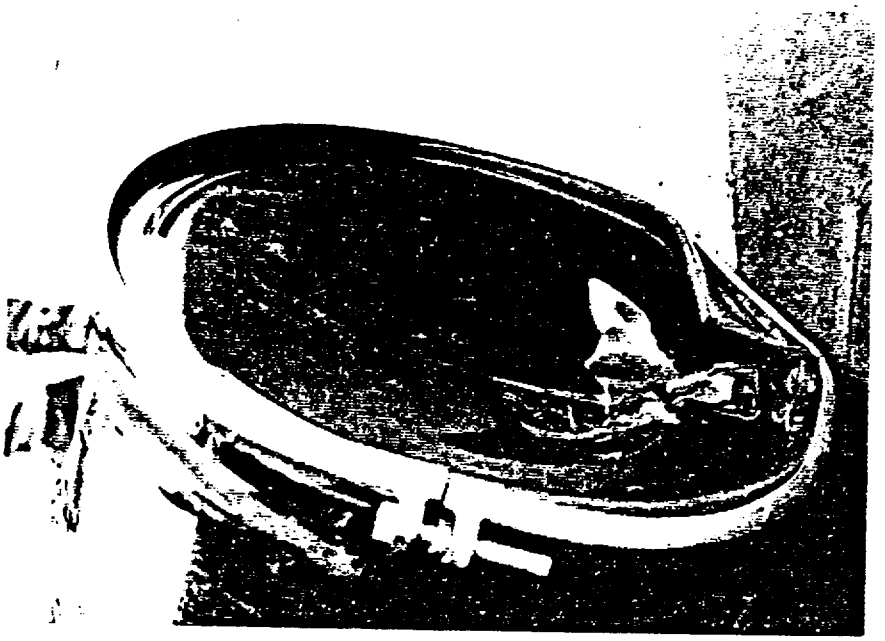

Fig. 2.23.10 Container #931
Alternate View Showing Cumulative
Effect of Drop Tests

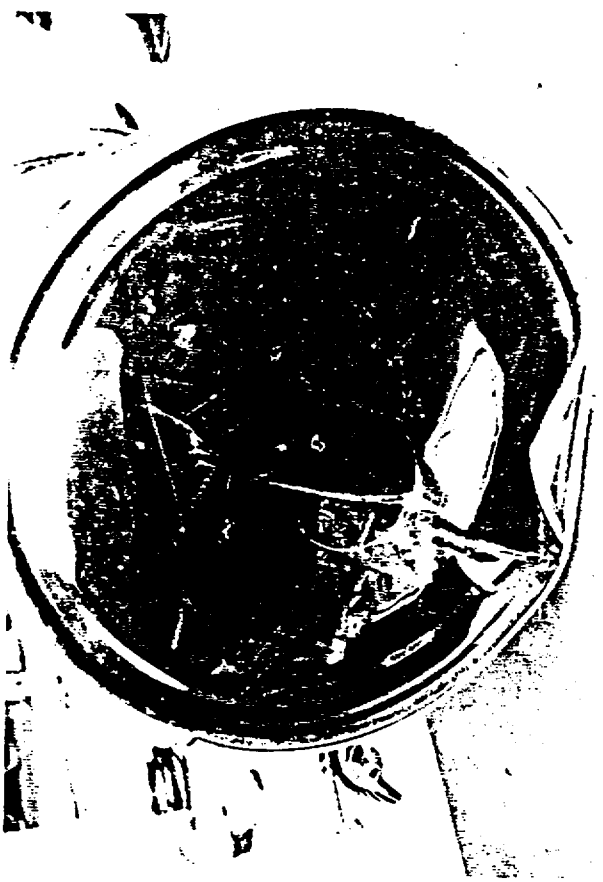

Fig. 2.23.9 Container #931
Showing Cumulative Effect of 9m
and Three 1m Drops

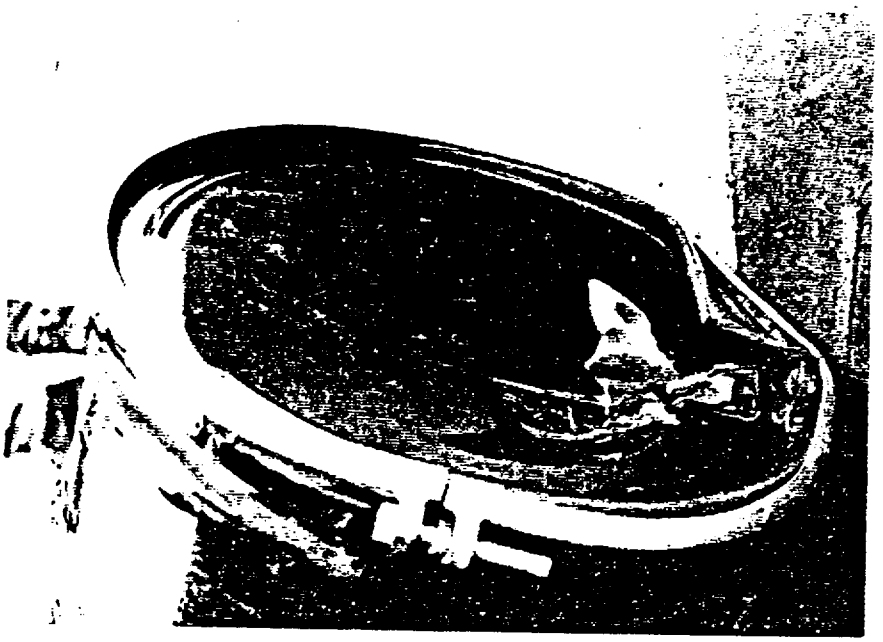

Fig. 2.23.10 Container #931
Alternate View Showing Cumulative
Effect of Drop Tests

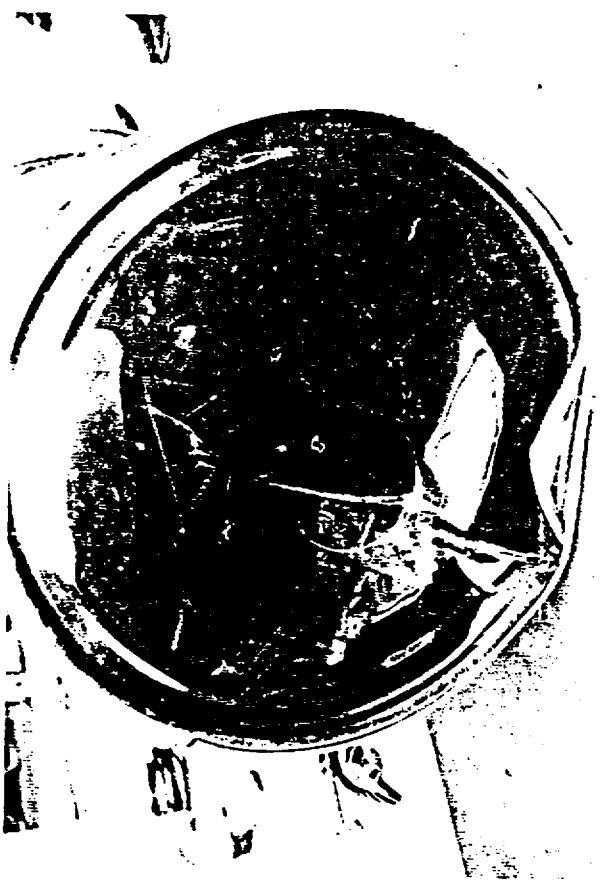

Fig. 2.23.9 Container #931
Showing Cumulative Effect of 9m
and Three 1m Drops

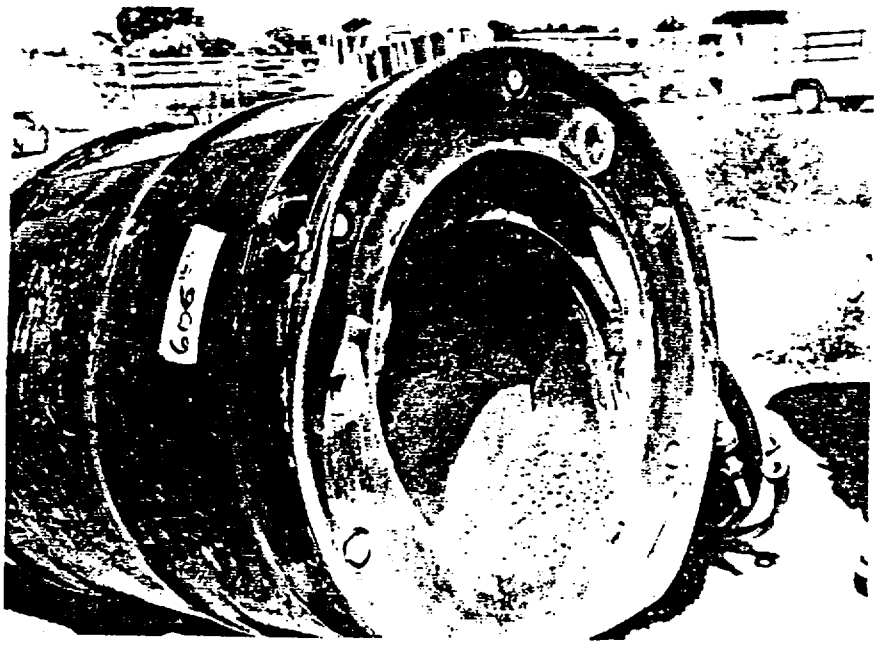

Fig. 2.23.11 Container #931 With Lid Removed to Show Deformation on Upper Structure

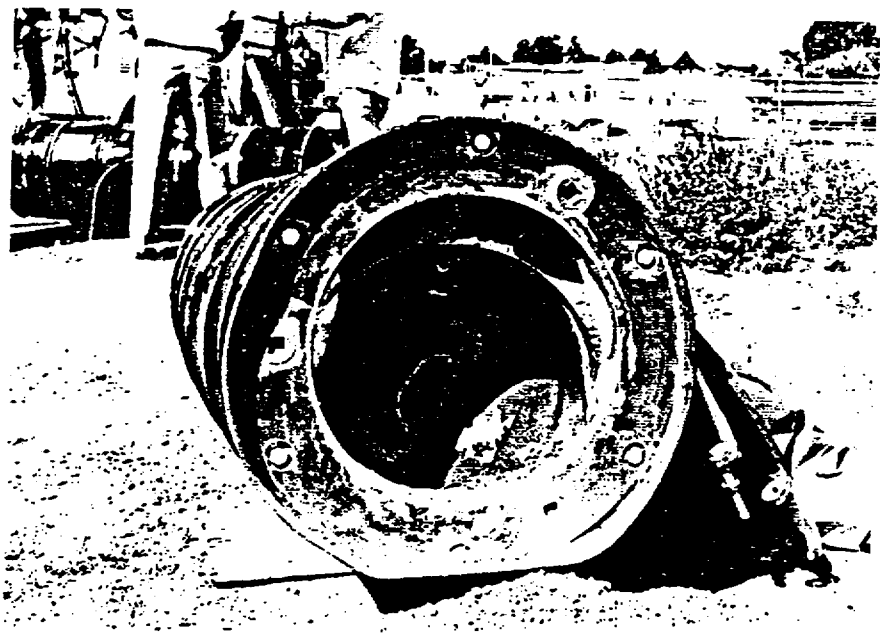

Fig. 2.23.12 Container #931 Alternate View of Deformation of Upper Structure

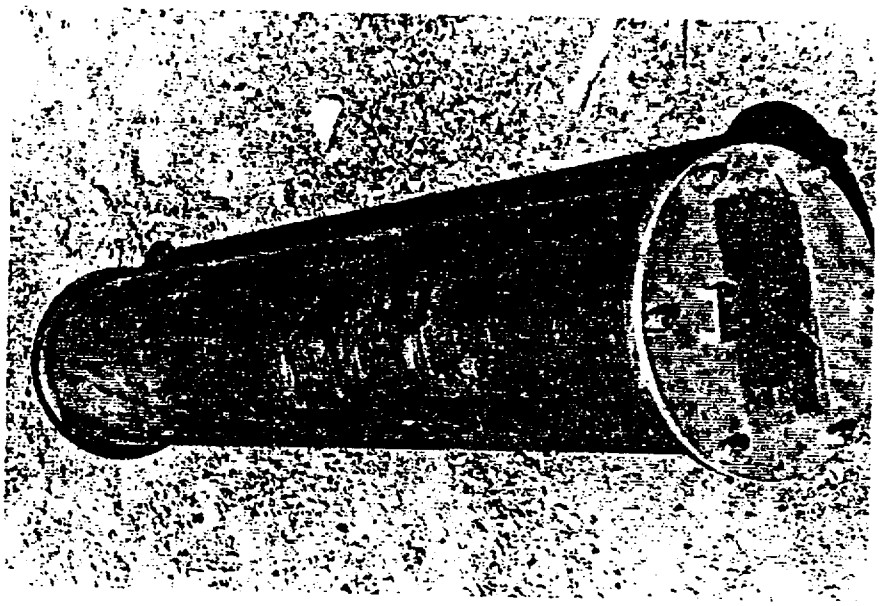

Fig. 2.23.14 Powder Canister From Container #931 View From Top End Showing No Damage

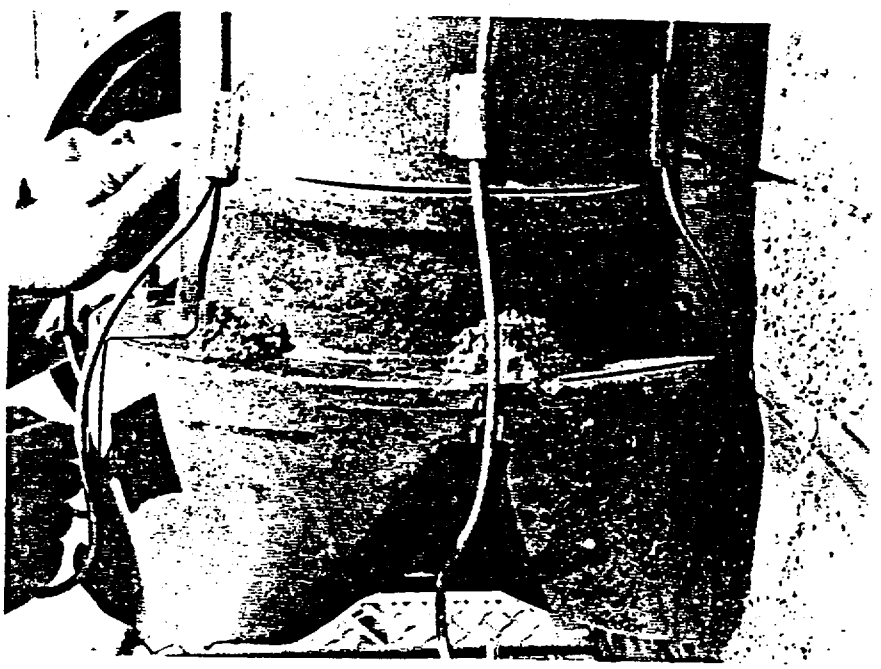

Fig. 2.23.13 Container #931 Showing Breach of Inner Container from the Loaded Powder Canister in 9m Drop

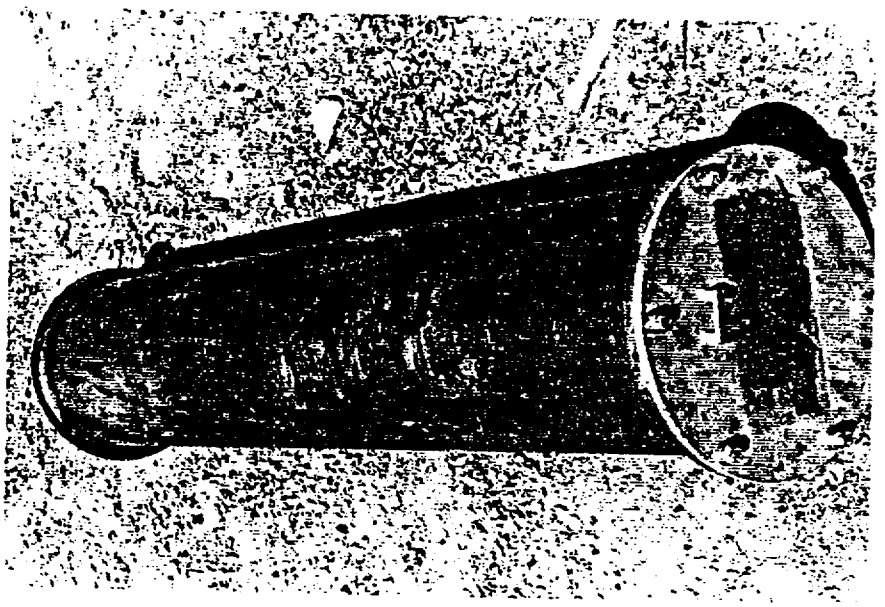

Fig. 2.23.14 Powder Canister From Container #931 View From Top End Showing No Damage

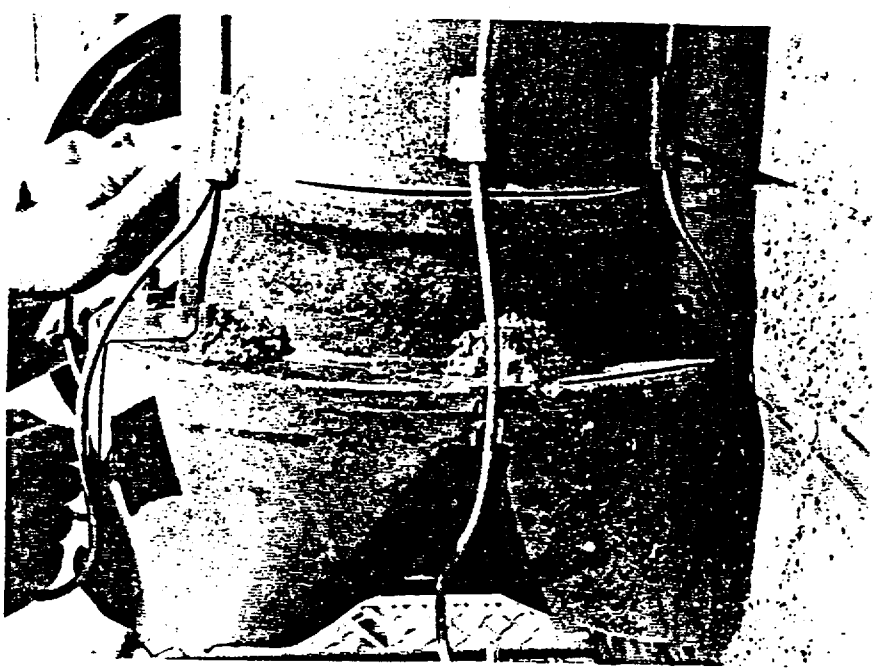

Fig. 2.23.13 Container #931 Showing Breach of Inner Container from the Loaded Powder Canister in 9m Drop

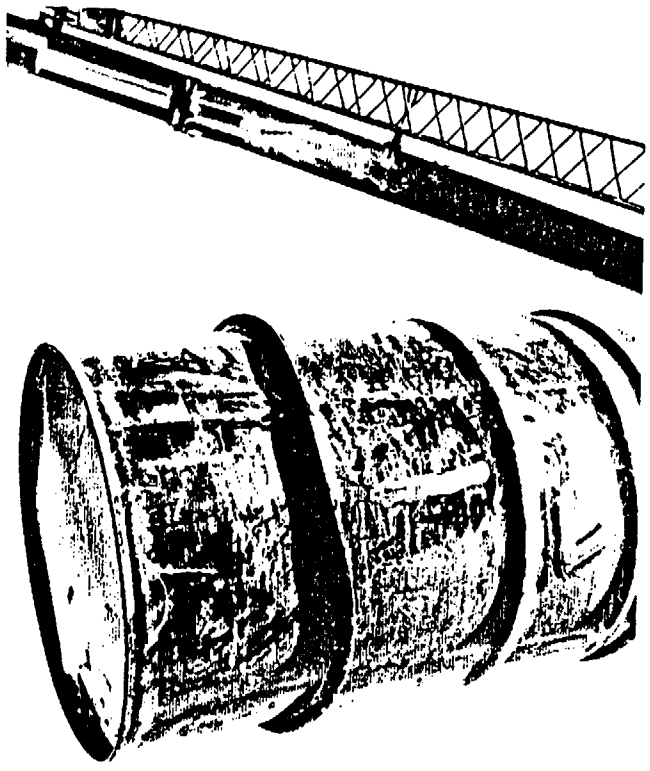

Fig. 2.24.1 Container #952 Showing Deformation to Lowest Corrugation Ring

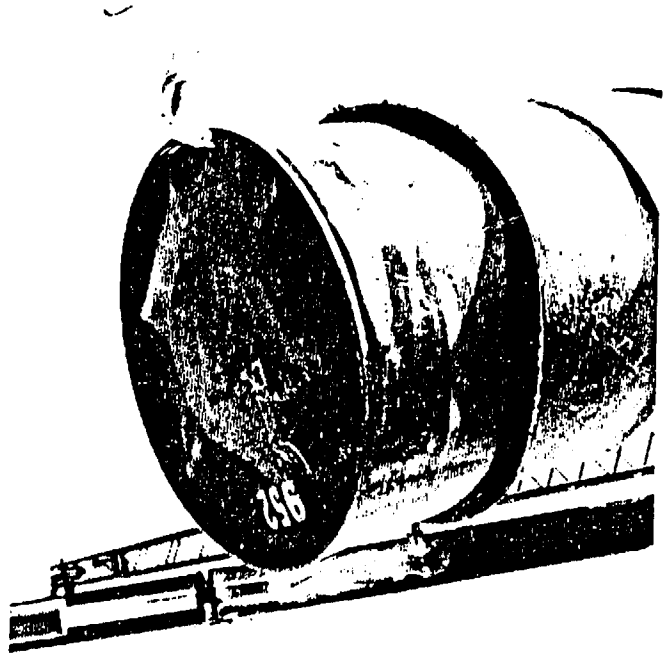

Fig. 2.24.2 Container #952 Showing Impact Effects on Bottom of the Drum

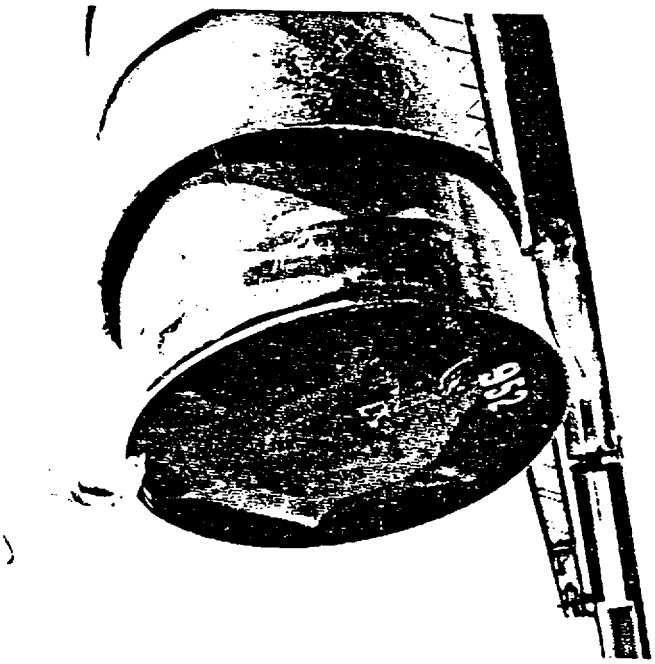

Fig. 2.24.2 Container #952 Showing Impact Effects on Bottom of the Drum

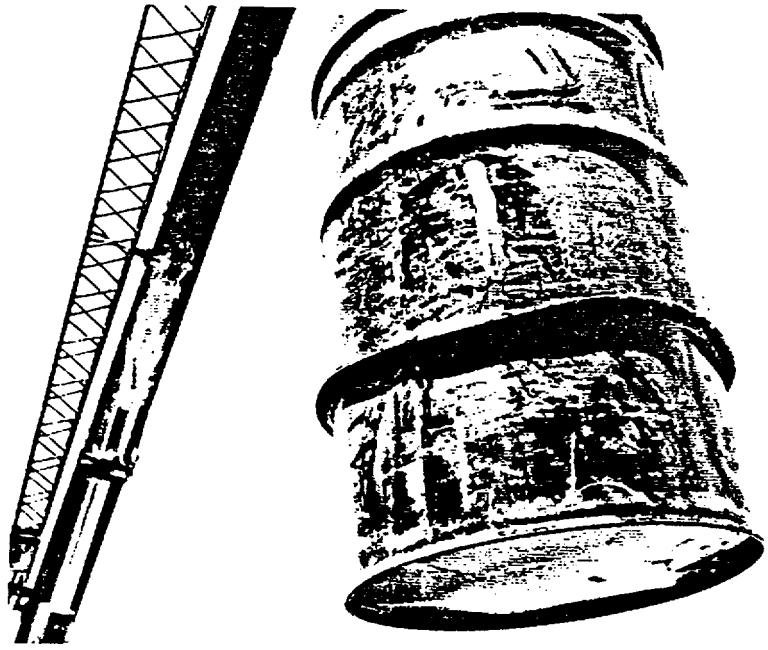

Fig. 2.24.1 Container #952 Showing Deformation to Lowest Corrugation Ring

Fig. 2.24.4 Bottom End of Inner Container of Container #952 Showing Deformation From 9m Drop

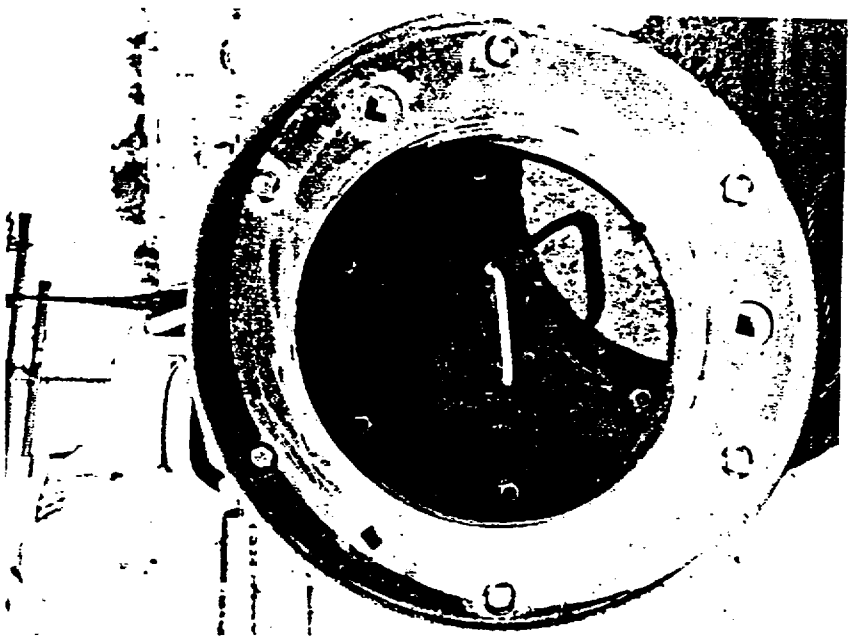

Fig. 2.24.3 Upper End of Container #952 Showing No Damage From 9m Drop on Bottom

Fig. 2.24.4 Bottom End of Inner Container of Container #952 Showing Deformation From 9m Drop

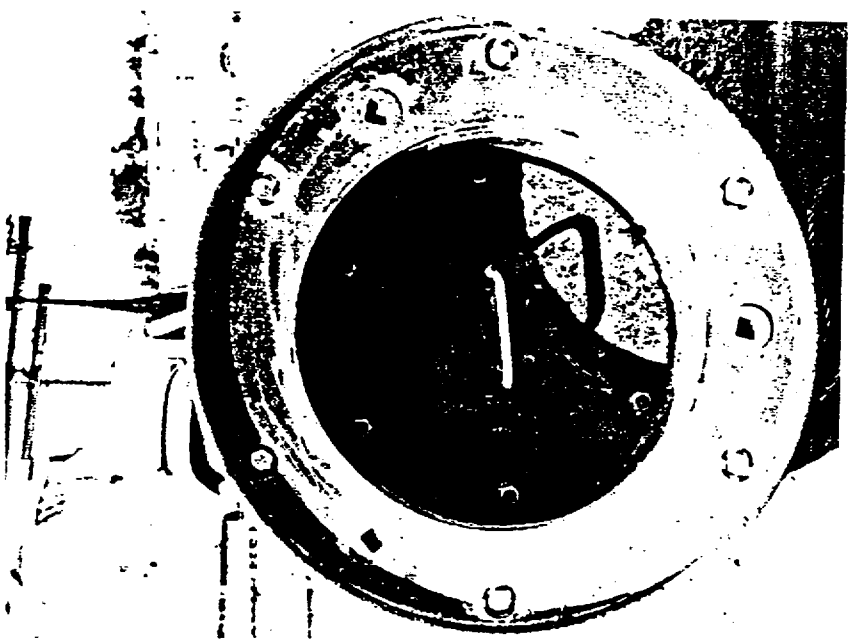

Fig. 2.24.3 Upper End of Container #952 Showing No Damage From 9m Drop on Bottom

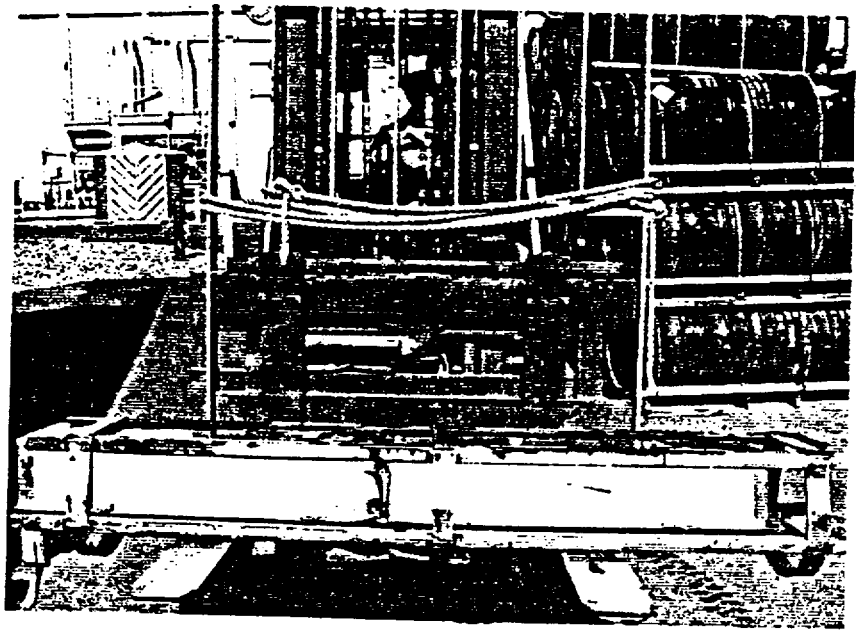

Fig. 2.24.5 Full Length View of Pellet Boxes From Container #952

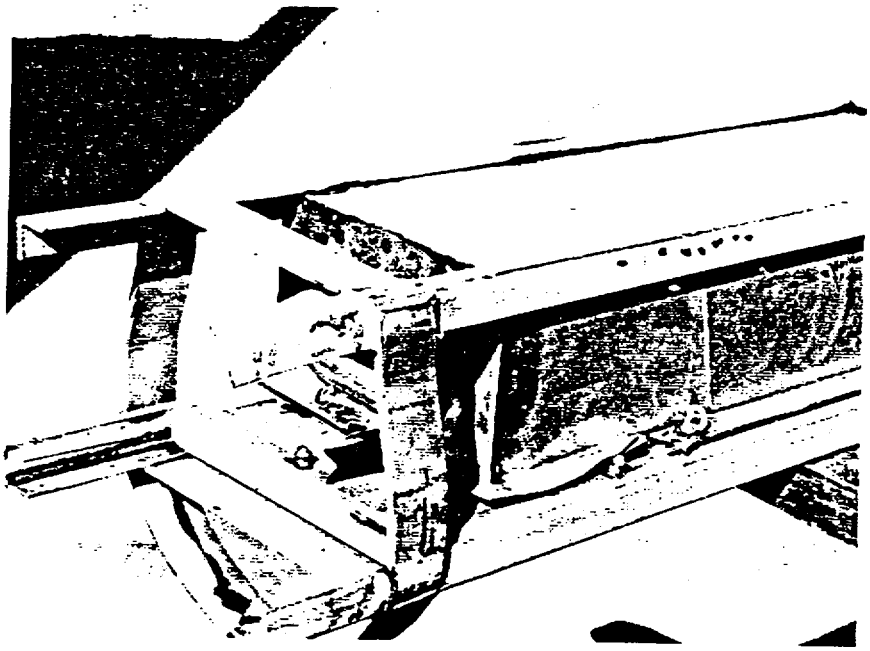

Fig. 2.24.6 View of Upper End of Pellet Box From Container #952 Showing Displacement of Box Relative to Base

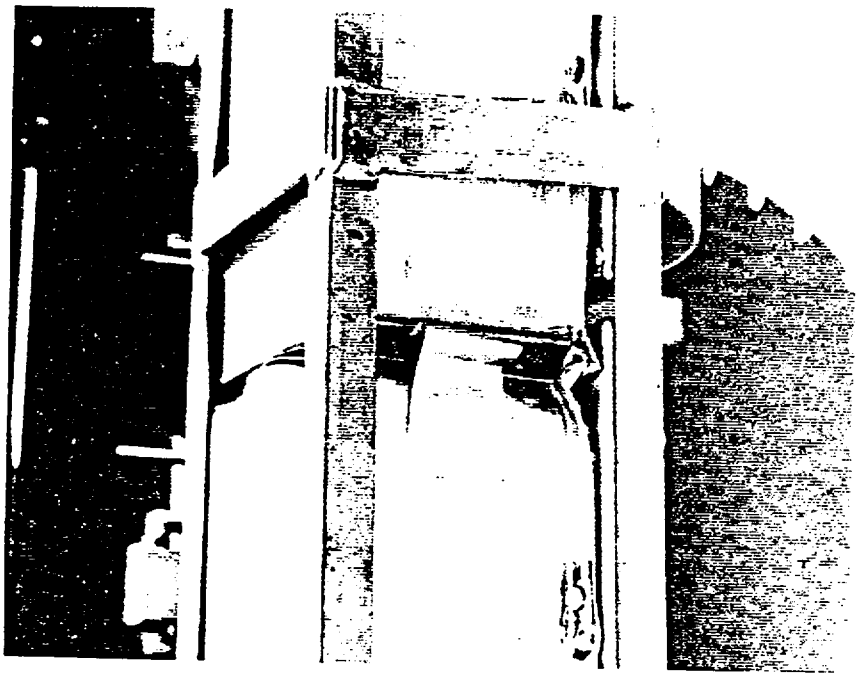

Fig. 2.24.8 View of Displacement of Upper Box onto Lower Base From Container #952

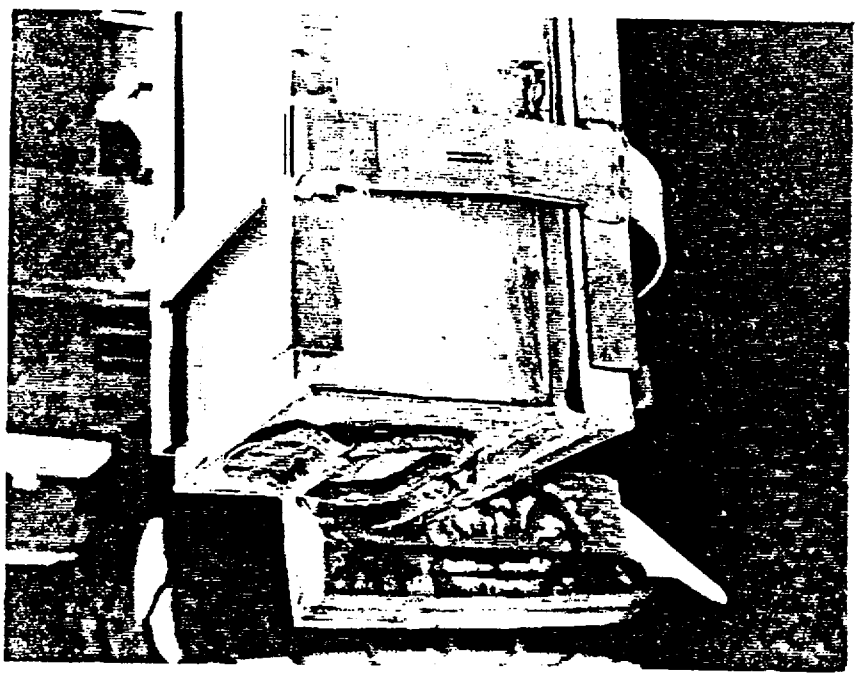

Fig. 2.24.7 View of Lower End Pellet Box From Container #952

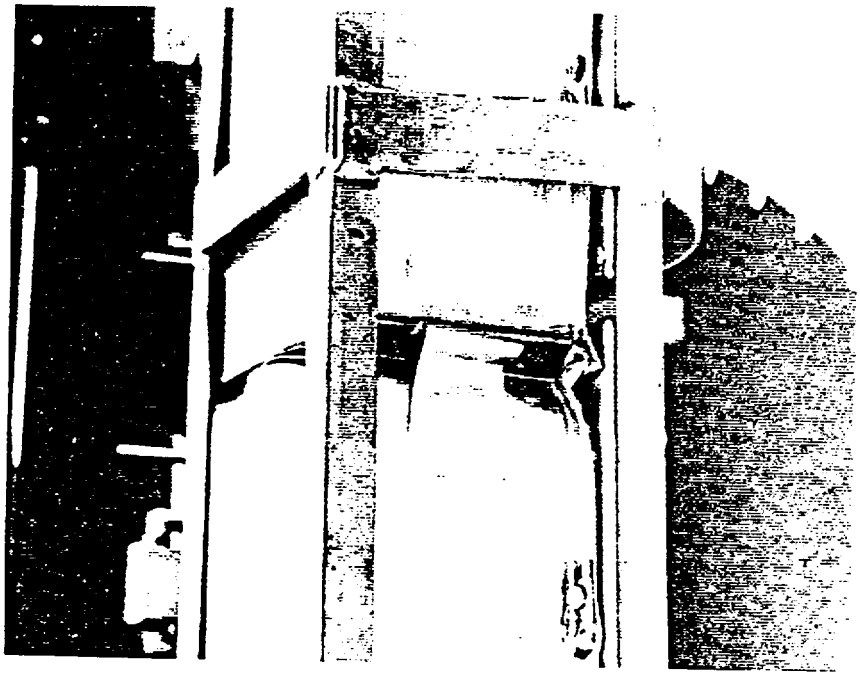

Fig. 2.24.8 View of Displacement of Upper Box onto Lower Base From Container #952

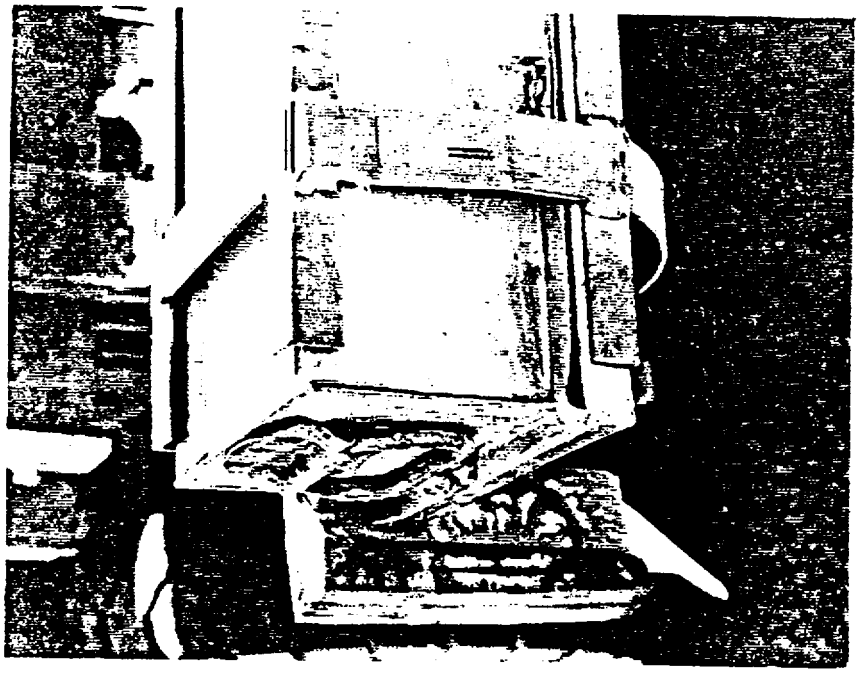

Fig. 2.24.7 View of Lower End Pellet Box From Container #952

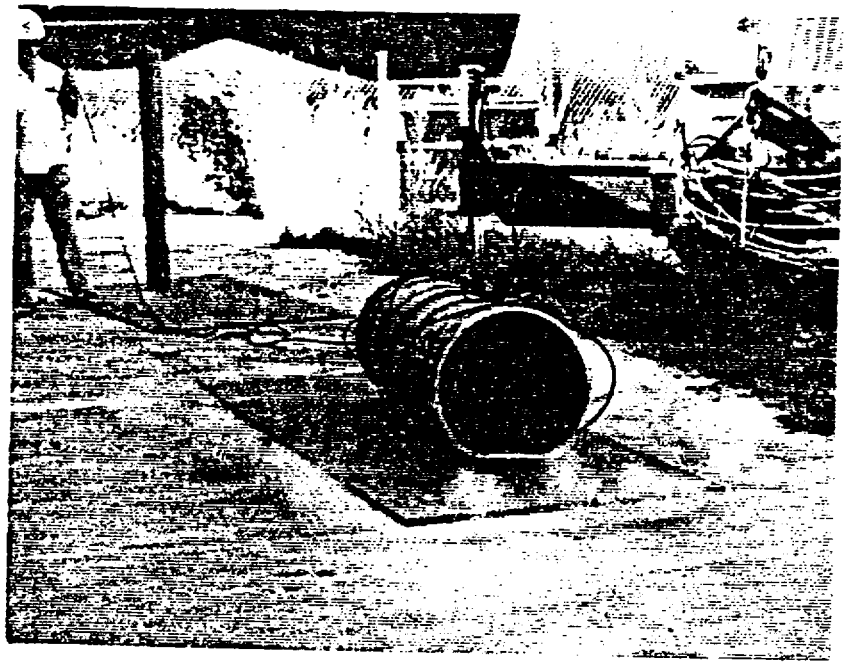

Fig. 2.25.1 Container #925 Just After Impact in 9m Slap Drop

Fig. 2.25.2 Closeup View of Lid of Container #925 Showing Distortion From 9m Drop

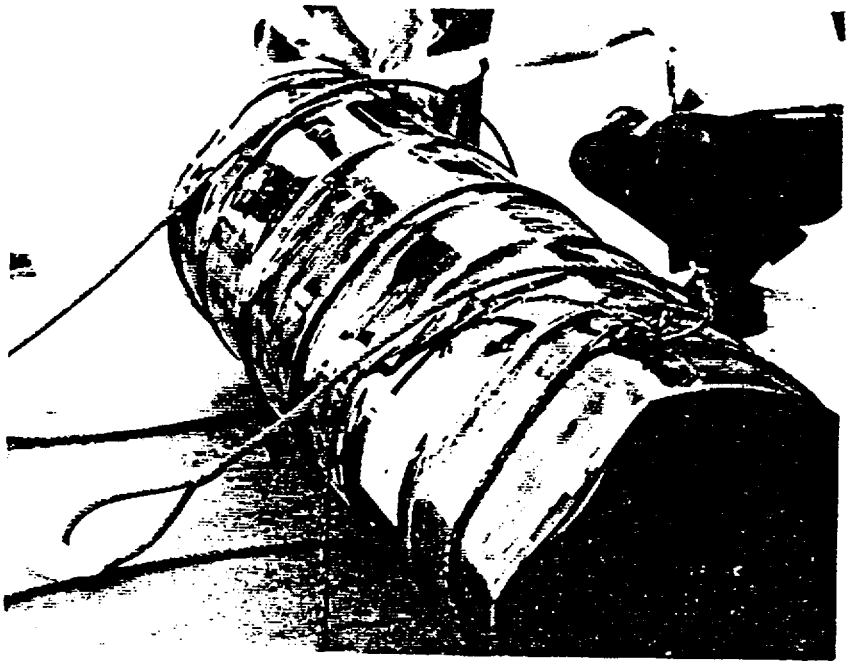

Fig. 2.25.3 View of Impact Side of Container #925 After 9m Drop

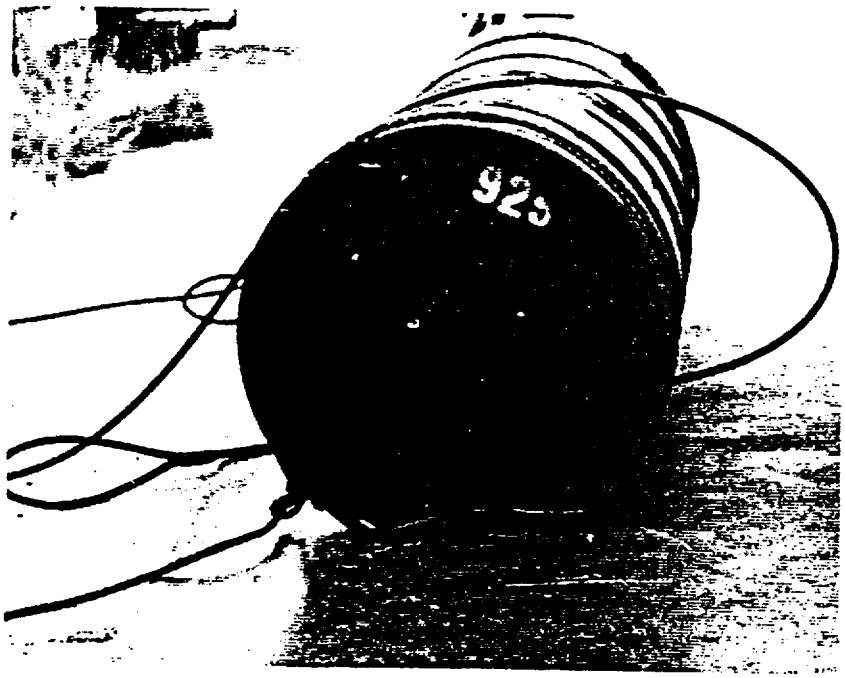

Fig. 2.25.4 View of Bottom End of Container #925 After 9m Drop

Fig. 2.25.5 View of Locking Lug After Impact on 15mm Diameter Pin from 1m

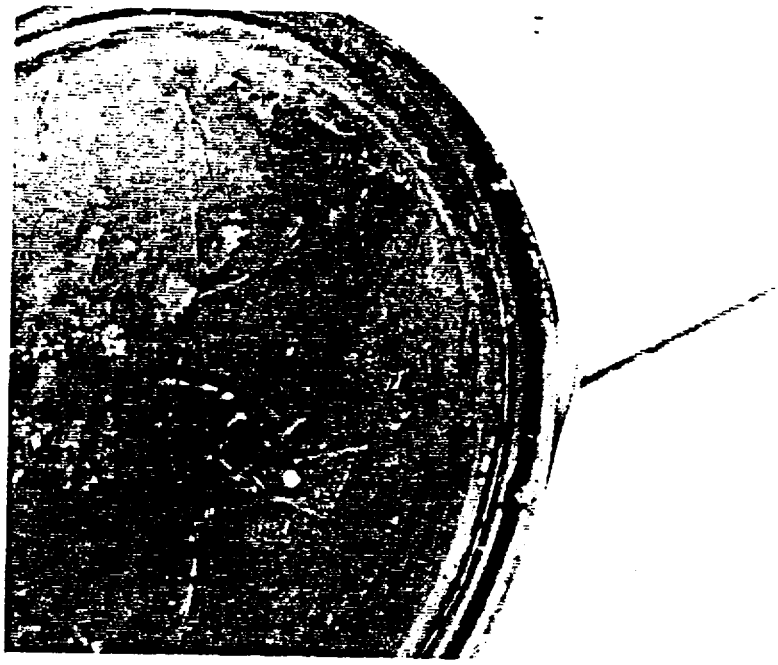

Fig. 2.25.6 View from Lid Side of Displacement of Locking Ring After Impact from 1m on Locking Lug

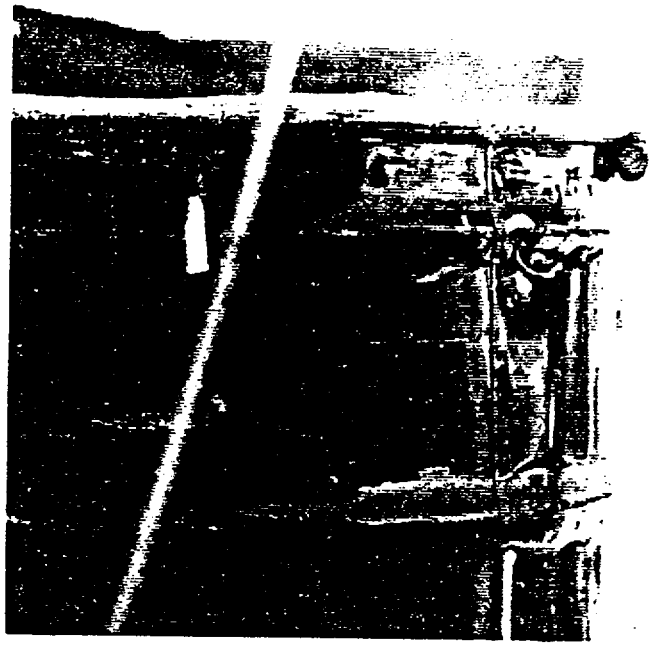

Fig. 2.25.7 View of Impact Area on Locking Ring After Second 1m Drop onto 15mm Diameter Pin

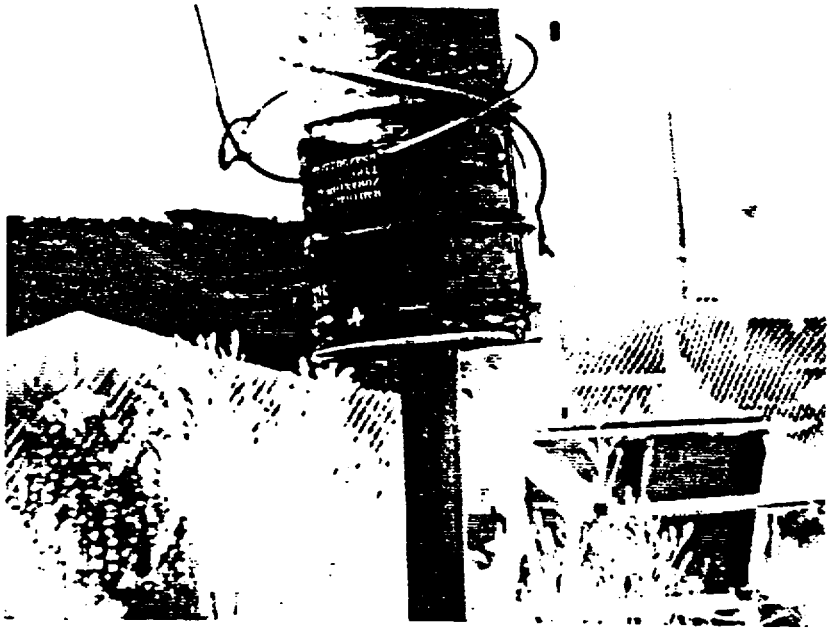

Fig. 2.25.8 Container #925 at Impact in Vertical Orientation on 15mm Diameter Pin

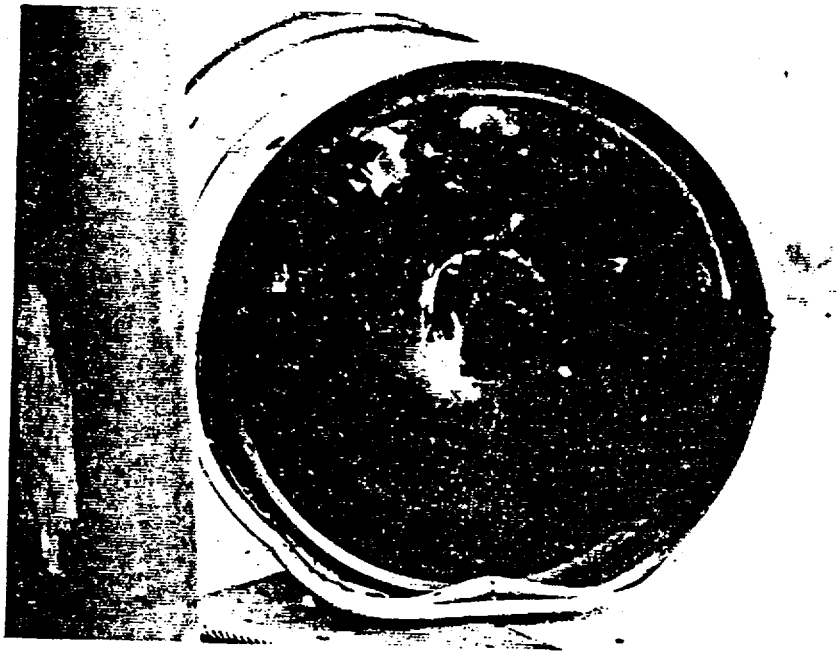

Fig. 2.25.9 View of Lid End of Container #925 Subsequent to 9m and Three 1m Drops

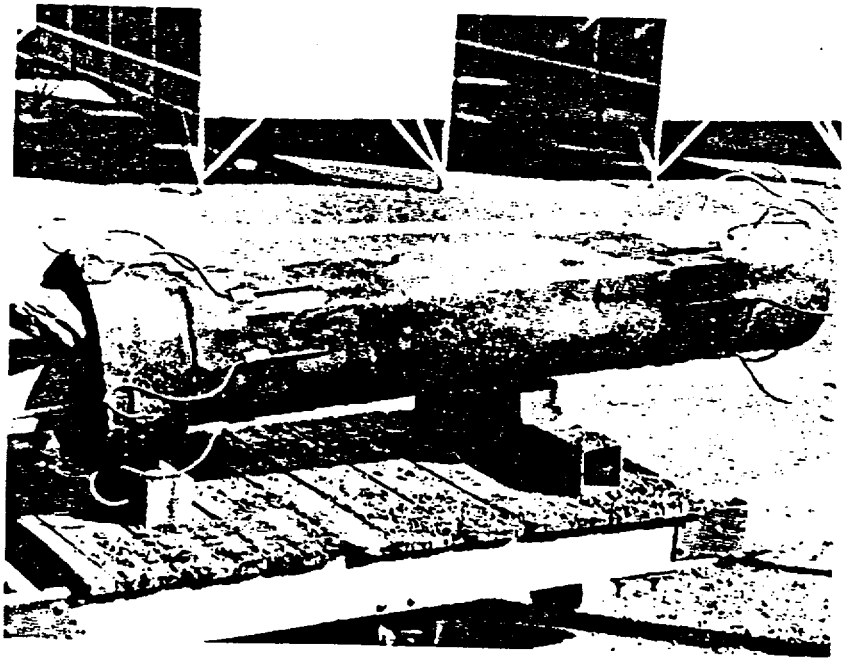

Fig. 2.25.10 Full Length View of Inner Container from Container #925 Showing Distortion Resulting From Drop Series

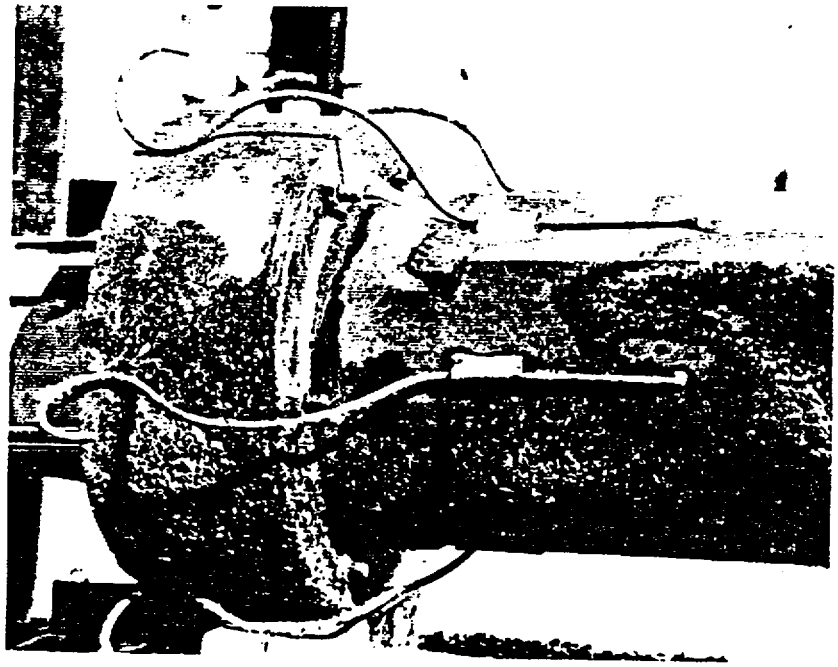

Fig. 2.25.11 Upper End of Inner Container
Showing Distortion From 9m Drop

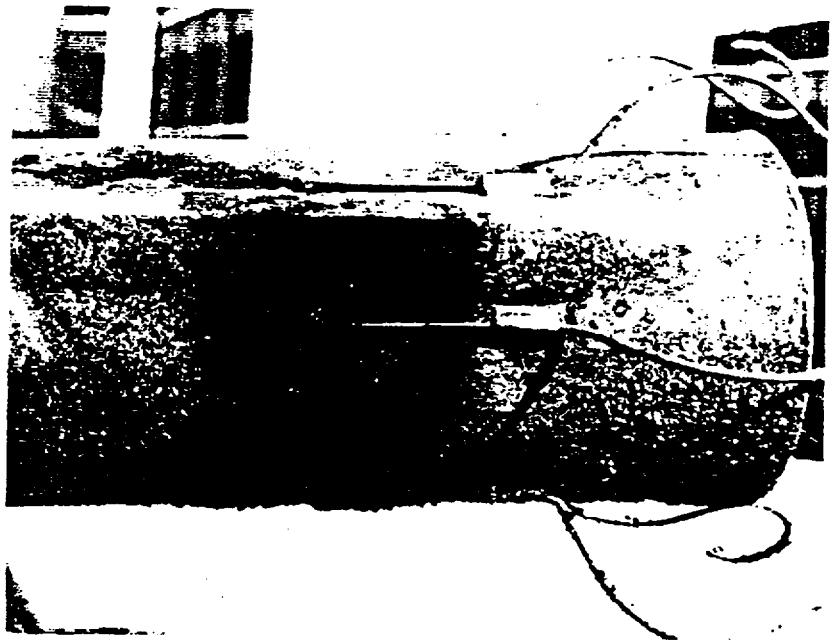

Fig. 2.25.12 Lower End of Inner Container
Showing Distortion From 9m Drop

Fig. 2.25.13 Closeup View Showing Hole in Inner Container of Container #925

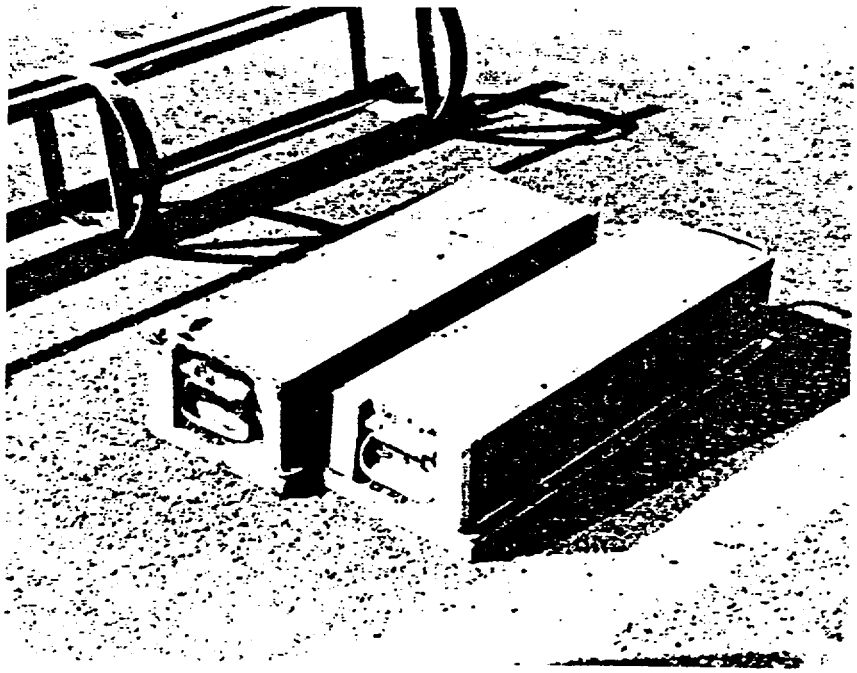

Fig. 2.25.14 Pellet Boxes From Container #925 Showing Undamaged Condition

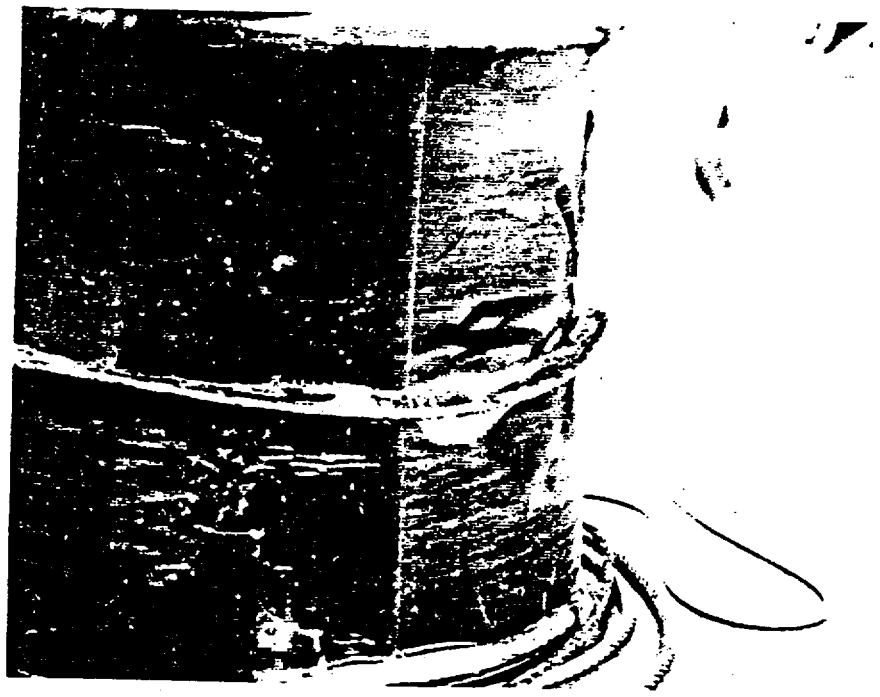

Fig. 2.26.1 Container #924 Showing Deformation From 9m Drop onto Bottom of Container

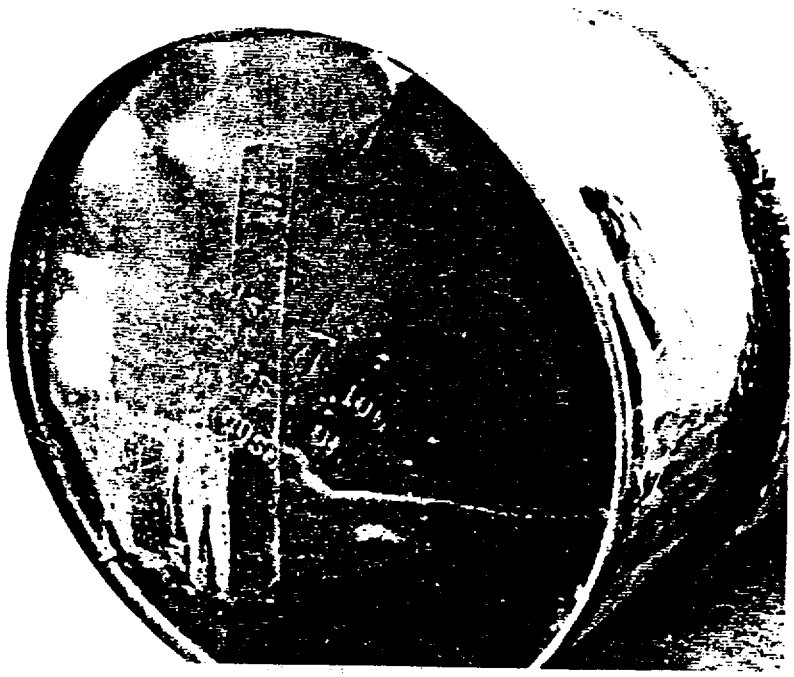

Fig. 2.26.2 View of Bottom of Container #924 Showing Deformation From 9m Drop

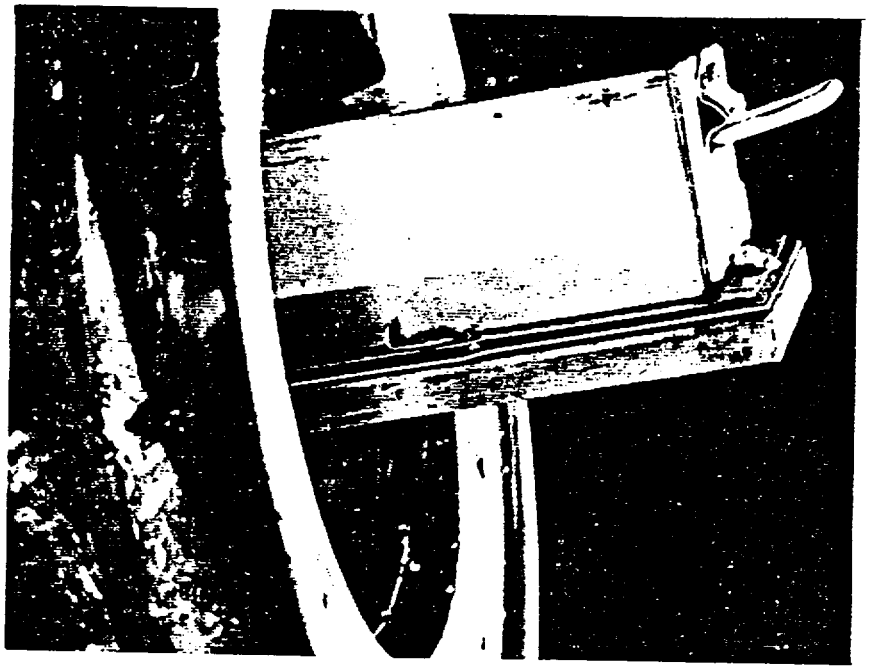

Fig. 2.26.3 View of the Upper End of the Upper Pellet Box From Container #924

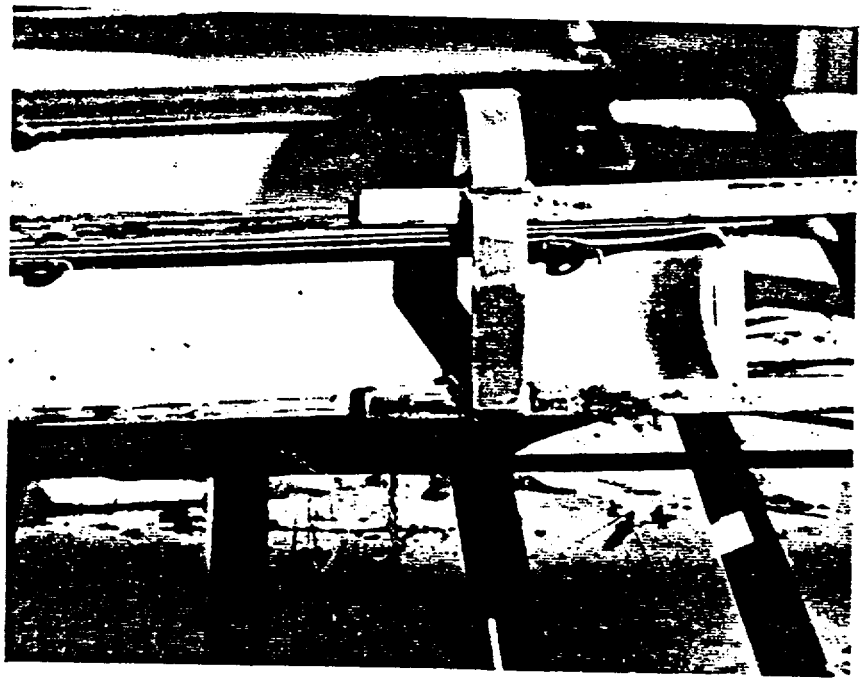

Fig. 2.26.4 View of the Upper End of the Lower Pellet Box From Container #924

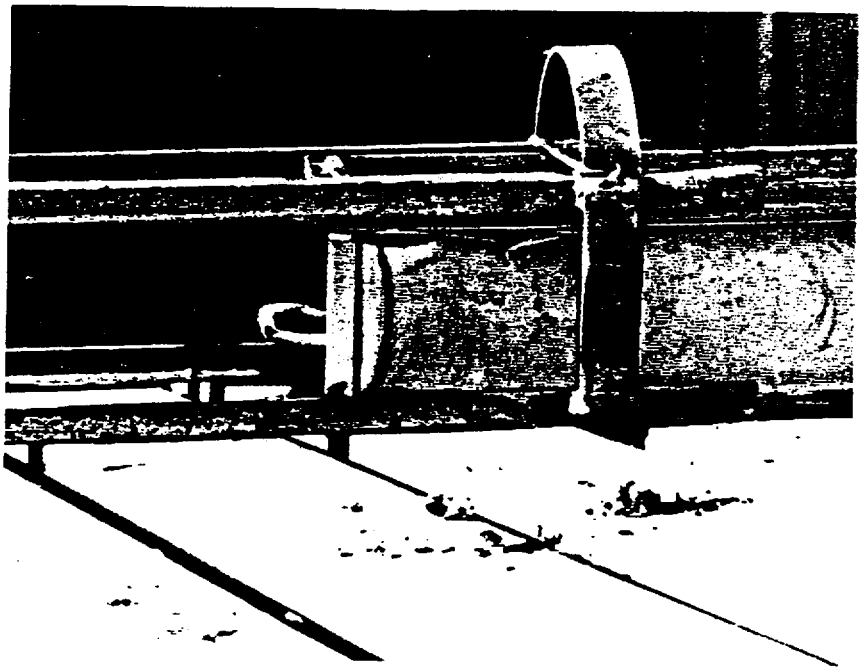

Fig. 2.26.5 View of the Lower End of Lower Pellet Box From Container #924

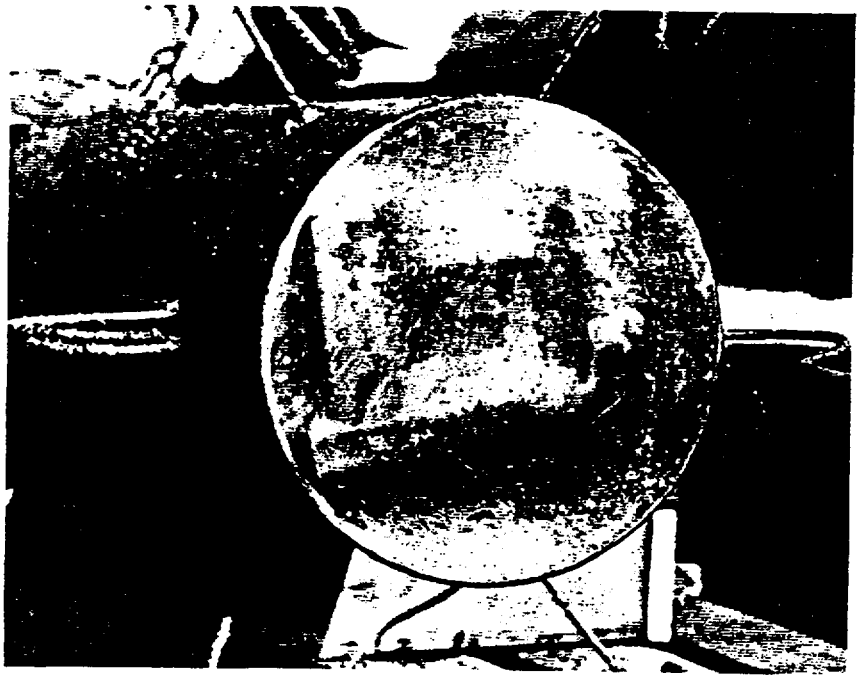

Fig. 2.26.6 View of the Bottom End of the Inner Container From Container #924

3. Thermal Evaluation

The thermal evaluation of the ANF-250 package was performed by submitting four individual packages to the Hypothetical Accident Conditions of 10 CFR 71.73. This testing and the results were discussed in Section 2 of this SAR.

4. Containment

4.1 *Containment Vessel*

Within the ANF-250 package a cylindrical inner container provides the containment boundary for the radioactive contents. The inner container has a carbon steel cylindrical shell seam welded the length of the cylinder with a 3.2 mm (0.125 inch) to 6.4 mm (0.25 inch) thick bottom plate welded to the cylindrical body. The top closure is by means of a 12.7 mm (0.5 inch) carbon steel plate bolted to an external flange welded to the cylindrical body. A seal is formed by a silicon rubber gasket 6.4 mm (0.25 inch) thick.

4.2 *Containment Penetrations*

There are no penetrations into the inner containment vessel.

4.3 *Seals and Welds*

The seal of the inner container closure is formed by a silicon rubber gasket 6.4 mm (0.25 inch) thick and 38 mm (1.5 inches) wide between the surfaces of a flange welded to the outer surface of the cylindrical body and the top closure plate. The silicon rubber seal is rated for 260°C (500°F) service and since there is no significant heat generated by the package payload, the seal is unaffected by temperatures encountered in normal conditions of transport. Also, testing described in Section 2.5.3 has shown that the silicon rubber gasket is unaffected by the temperatures attained in the Hypothetical Accident Conditions.

All welds are GTA and made with qualified and documented welding procedures by qualified welders. A copy of the welding procedures to be used are transmitted to Siemens Power Corporation for approval prior to the welding of any component. All welds are visually inspected to ensure that parent metals are well fused and that the weld (or heat affected zone) is free of cracks, craters, or burnouts.

4.4 *Closure*

The inner container closure is formed by a 12.7 mm (0.5 inch) carbon steel plate bolted to an external flange welded to the cylindrical inner container. Material specifications for the plate and the bolts and nuts are listed on Drawing EMF-306,175. Tests have shown that with a 6.4 mm (0.25 inch) thick gasket, an initial torque on the bolts of 4.2 kgfm (30 ftlbs) is sufficient to maintain an initial differential pressure of 172 kPa (25 psig).

4.5 *Requirements for Normal Conditions of Transport*

Submittal of two ANF-250 packages to the tests specified in 10 CFR 71.71 (Normal Conditions of Transport) has shown that there will be no loss or dispersal of radioactive contents, no significant increase in external radiation levels, and no substantial reduction in the effectiveness of the packaging. The inner container remained pressure tight for a range of internal pressures from 33.7 kPa (4.9 psia) to 274 kPa (39.7 psia), with the external pressure atmospheric. A fully loaded container subjected to the full series of spray, free drop and

penetration tests showed no degradation of effectiveness of the inner container and no leakage of water into either the outer or inner container. A second container submitted to the series of drop tests specified for the Normal Conditions of Transport also showed no degradation of containment.

4.6 *Containment Requirements for Hypothetical Accident Conditions*

10 CFR 71.51 is written specifically for Type B packages and would permit no release of radioactive material exceeding a total amount A_2 in one week. The A_2 value for uranium enriched to less than 20 weight percent U-235 is unlimited, and the paragraph does not apply to shipments of low enriched uranium.

5. Shielding Evaluation

The ANF-250 packages are used for the shipment of oxides of low enriched uranium ($\leq$ 5 wt% U-235) in pellet and powder form in containers which are placed inside the inner container.

The dose rate at one meter from the external surface of an ANF-250 containing low enriched uranium results in a transport index less than that derived from criticality safety considerations. Thus, shielding is not a consideration in the design and construction of the package.

6. Criticality Evaluation

Compliance with the criticality safety requirements of 10 CFR Part 71 is demonstrated.

6.1 *Introduction and Summary*

The ANF-250 package has been used for the shipment of low enriched uranium oxide pellets and powder for nearly twenty years. The allowable contents (as identified below) have been analyzed and found to meet the requirements of 10 CFR Part 71 as bounded by this section and current certification.

6.2 *Allowable Contents*

1. Dry uranium oxide powder enriched to a maximum 5.0 wt% in the ^{235}U isotope. Quantity and contents not to exceed 310 pounds and:

Maximum Enrichment (wt% ^{235}U)	Maximum Uranium Mass (kg U)	Maximum ^{235}U Mass (kg ^{235}U)
3.4	62.4	2.12
3.8	41.0	1.56
4.6	31.2	1.44
5.0	27.7	1.38

and:

Not to exceed a maximum mass of 1149 g H, considering all sources of hydrogenous material within the inner vessel. The powder must be contained according to drawings EMF-306,176, Sheets 1 and 2, revision 5. The total transport index for this content per package is 1.8.

2. Dry uranium oxide pellets enriched to a maximum 5.0 wt% in the ^{235}U isotope. Quantity and contents not to exceed 310 pounds and a maximum of 120 kg U, with the ^{235}U content not to exceed 6 kg. Not to exceed a maximum mass of 1149 g H, including a maximum mass of 600 g polyethylene, considering all sources of hydrogenous material within the inner vessel. The contents must be contained according to drawings EMF-304,306, revision 8, and EMF-306,176, Sheets 1 and 2, revision 5. The total transport index for this content per package is 0.6.

3. Uranium oxide pellets enriched to a maximum of 1.0 wt% in the ^{235}U isotope. Quantity and contents not to exceed 310 pounds and a maximum 120 kg U, with the ^{235}U content not to exceed 1.2 kg. The contents must be contained according to drawings EMF-304,306, revision 8, and EMF-306,176, Sheets 1 and 2, revision 5. The total transport index for this content per package is 0.4.

4. Uranium oxide powder enriched to a maximum of 1.0 wt% in the ^{235}U isotope. Quantity and contents not to exceed 310 pounds and a maximum 120 kg U, with the ^{235}U content not to exceed 1.2 kg. The contents must be contained according to drawings EMF-306,176, Sheets 1 and 2, revision 5. The total transport index for this content per package is 0.4.

6.3 *Analytical Methodology and Benchmarking*

6.3.1 Methodology

SPC has used various versions of the SCALE system of computer codes for criticality safety analyses for over 20 years. SPC currently uses the SCALE 4.2 version of the system of codes to do criticality safety evaluations. This system of codes has been extensively used and validated by SPC for this use. The limiting cases included in this application used SCALE 4.2. Documentation of the majority of SPC's validation efforts for this version is included in EMF-94-175, "Validation and Verification of KENO.Va." Previous versions used by SPC were validated in a similar fashion but the details are not included in this application.

6.3.2 SPC Verification of Scale 4.2 Code

The Radiation Safety Information Computational Center (RSIC) provides sample problems including inputs and outputs for test cases run on RSIC computers so users of SCALE 4.2 can check each of the modules used and ensure that they are running correctly. After the SCALE 4.2 package was installed and appeared to be functioning correctly, several of these sample programs were used on an SPC HP workstation to verify that each of the criticality safety modules was providing expected results. These test cases exercised each of the modules in the criticality safety sequence and included 25 separate KENO.Va runs. The file id information for both inputs and outputs are listed below.

1782	Dec 16 1993 07:11:05 drd-bonami
9072	Dec 16 1993 07:11:05 drd-csas
1296	Dec 16 1993 07:11:05 drd-ice
62421	Jul 8 1994 09:46:57 drd-kenova
567	Dec 16 1993 07:11:06 drd-nitawl
2349	Dec 16 1993 07:11:08 drd-xsdrn
56272	Jul 8 1994 07:29:03 dro-bonami
1489975	Jul 8 1994 08:13:27 dro-csas
60897	Jul 8 1994 07:30:34 dro-ice
2567979	Jul 8 1994 10:11:04 dro-kenova
12522	Jul 8 1994 07:31:09 dro-nitawl
17441	Jul 8 1994 07:32:30 dro-xsdrn

It is noted that the input for keno case 18 was modified slightly. The case had an input random number in hex format which was not read correctly by the code. This random number input was deleted, but the original line was retained ("commented out").

A comparison of the 25 KENO.Va test cases provided by RSIC and these same cases run on the SPC HP workstation SSL01 is given in Table 6.1 below. All cases except #21 agree within normal statistical uncertainties. No anomalies were found in the output for Case #21.

Table 6.1 Compare 25 KENO.Va RSIC Test Cases with SPC HP Workstation SSL01

Case ID	RSIC k_{eff}		SPC k_{eff}		Delta-k (RSIC minus SPC)	Pooled Std.Dev.	t (Delta-k/Pooled Sigma)
	Avg.	Std. Dev.	Avg.	Std. Dev.			
1	1.0065	0.0047	1.00608	0.00446	4.20E-04	6.48E-03	0.06
2	1.0065	0.0047	1.00608	0.00446	4.20E-04	6.48E-03	0.06
3	1.0116	0.0053	1.00540	0.00517	6.20E-03	7.40E-03	0.84
4	1.0122	0.0054	1.01067	0.00528	1.53E-03	7.55E-03	0.20
5	1.0245	0.0036	1.02225	0.00422	2.2.5E-03	5.55E-03	0.41
6	0.7496	0.0037	0.74949	0.00382	1.10E-04	5.32E-03	0.02
7	1.0055	0.0038	1.00026	0.00409	5.24E-03	5.58E-03	0.94
8	0.9491	0.0041	0.94911	0.00412	-1.00E-05	5.81E-03	-0.00
9	2.2848	0.0078	2.28484	0.00777	-4.00E-05	1.10E-02	-0.00
10	1.0065	0.0047	1.00608	0.00446	4.20E-04	6.48E-03	0.06
11	1.0065	0.0047	1.00608	0.00446	4.20E-04	6.48E-03	0.06
12	1.0094	0.0055	1.00327	0.00518	6.13E-03	7.56E-03	0.81
13	1.0030	0.0043	1.00213	0.00358	8.70E-04	5.60E-03	0.16
14	0.9976	0.0049	1.00324	0.00465	-5.64E-03	6.76E-03	-0.83
15	1.0095	0.0049	1.00087	0.00430	8.63E-03	6.52E-03	1.32
16	0.9885	0.0029	0.99212	0.00267	-3.62E-03	3.94E-03	-0.92
17	1.0101	0.0164	1.00890	0.01664	1.20E-03	2.34E-02	0.05
18	1.0146	0.0073	1.01892	0.00752	-4.32E-03	1.05E-02	-0.41
19	1.0117	0.0047	1.01518	0.00628	-3.48E-03	7.84E-03	-0.44
20	1.0001	0.0063	1.00883	0.00570	-8.73E03	8.50E-03	-1.03
21	0.9844	0.0036	1.00063	0.00316	-1.62E-02	4.79E-03	-3.39
22	1.0079	0.0048	1.00579	0.00444	2.11E-03	6.54E-03	0.32
23	1.0048	0.0046	1.00618	0.00446	-1.38E-03	6.41E-03	-0.22
24	1.0044	0.0043	1.00617	0.00412	-1.77E-03	5.96E-03	-0.30
25	1.0059	0.0043	0.99998	0.00390	5.92E-03	5.81E-03	1.02

6.3.3 SPC Benchmarking of Scale 4.2 SPC Version UJUL94A

The purpose here is to demonstrate that the codes and databases function correctly and produce "normal" results when used by SPC personnel.

All calculations indicate that the code and databases function correctly and produce "normal" results. These data are considered adequate to satisfy the "verification and validation" requirements.

6.3.4 Validation for Heterogeneous (Pellet) Calculations)

The Reference 3 experiments involve three flooded clusters of 4.31% enriched rods with variable spacings between the clusters and with various absorbers between the clusters. These benchmarks have been verified to be acceptable experiments by international experts in a cooperative effort by NEA. These benchmark experiments include moderated heterogeneous fuel regions separated by moderators and steel absorbers. They are, therefore, similar to the accident conditions evaluated in this CSE. The case numbers referenced below were taken from Reference 3. The data used for these cases include the corrections made to Reference 3 on August 14, 1979. Among these corrections was a change in the ^{235}U enrichment from 4.29 wt% to 4.31 wt%. Figure 6.1 shows the general layout of the critical mass experiments.

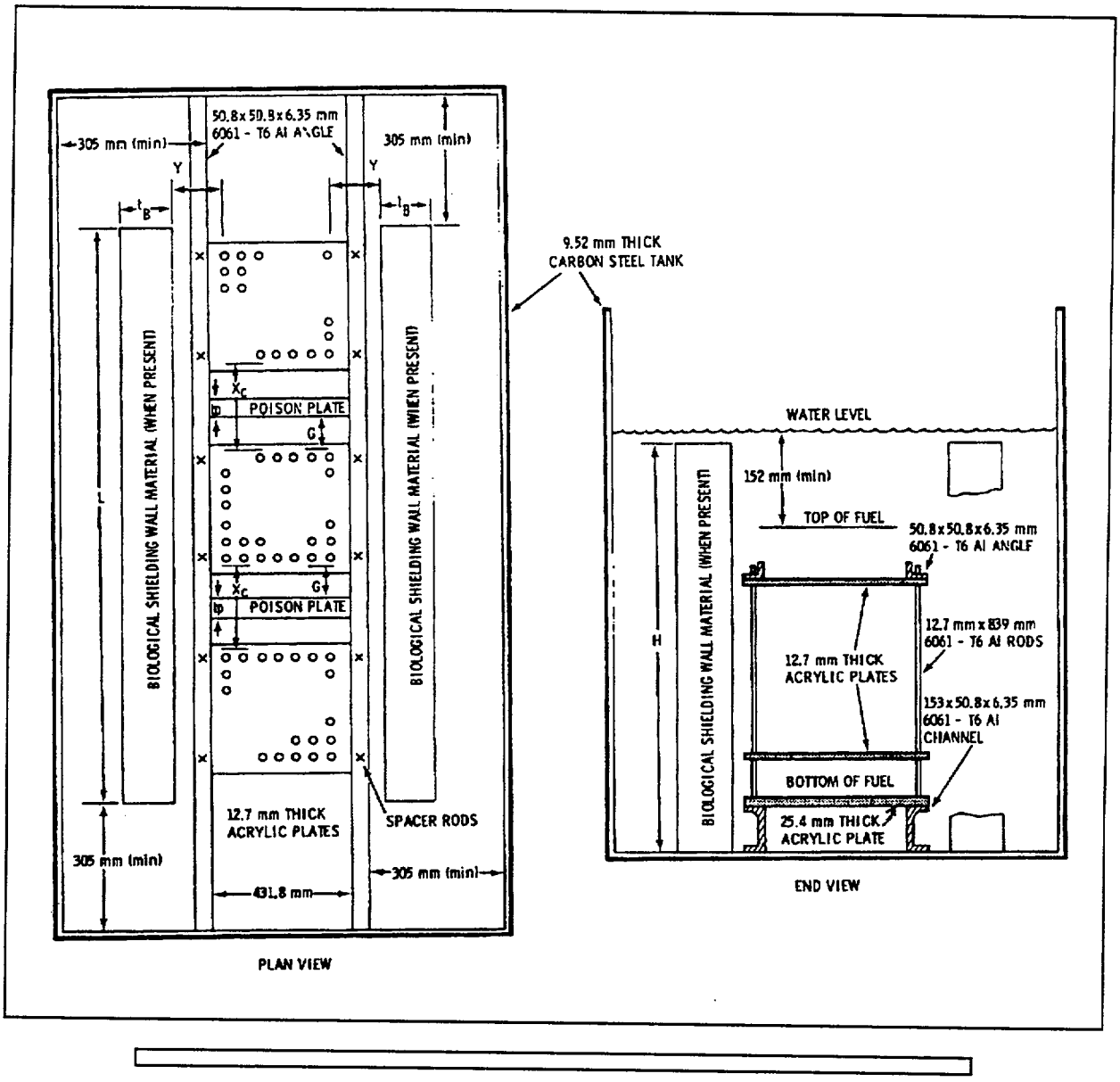

Figure 6.1 PNL Critical Experiment Layout (Reference 3)

Cases 001, 002, and 003 determine the critical size of one cluster. The critical size was interpolated based on experiments with integral numbers of rods per edge; the critical number had a fractional number of rods on one edge and either 8, 9, or 10 rods on the other edge. These three cases were modeled using cell-weighted cross sections. A suffix "x" on the case name was used to denote cases modeled with cell-weighted cross sections.

Table 6.2 Experimental Data on Clusters of 4.31 wt% ^{235}U Enriched UO_2 Rods in Water[1]

Fuel Clusters			
Number in Array[2]	**Length x Width 25.40 mm² Pitch (Fuel Rods)**	**Critical Separation Between Fuel Clusters[3] (Xc, mm)**	**Experiment Number**
1	10 x 11.51± 0.04	∞	001
1	9 x 13.35 ± 0.01	∞	003
1	8 x 16.37 ± 0.03	∞	002
3	15 x 8	106.4 ± 0.1	004
3	15 x 8	106.0 ± 0.1	032[4]

(1) Error limits shown are one standard deviation
(2) Clusters of fuel rods aligned in a single row
(3) Perpendicular distance between the cell boundaries of the fuel clusters
(4) Rerun of Experiment 004

Case 004 involved three 15x8 clusters with no absorber plates.

Cases 007, 008, 013, and 014 involved three clusters with 304L steel absorber plates. Two plate thicknesses and different absorber spacings from the central cluster were tested.

Cases 009, 010R, 011, and 012 are similar to the previous four except that the 304L steel contained either 1.05 or 1.62% Boron.

Cases 029 and 030 involved three clusters with Zircaloy-4 absorber plates.

The calculation results with the 27-group cross section library are included in Table 6.3. All cases used resonance parameters calculated by the CSAS modules. Most models included provisions for using different resonance parameters for interior and edge rods. The "latticecell" parameters were input for the interior rods and "more data" parameters equal to those resulting from the "latticecell" parameters were used for edge rods. The "x" suffix on the case name denotes cell-weighted cross-sections. Suffixes such as "a" are for explicitly-modeled rods.

The results indicate that cell-weighted calculations tend to yield higher k_{eff} values than explicit models.

Table 6.3 Reference 3 Cases Calculation Results with 27-Group Cross Sections

Case ID	k_{eff}	
	Avg.	Std. Dev.
b-c001x	1.00591	0.00264
b-c002x	0.99828	0.00274
b-c003x	1.00268	0.00234
b-c004	0.99853	0.00266
b-c005a	0.99882	0.00232
b-c006a	0.98996	0.0023
b-c007a	0.99063	0.00238
b-c007x	0.99789	0.00256
b-c008a	0.99818	0.00259
b-c008x	1.00177	0.00268
b-c009a	0.99613	0.00245
b-c010a	0.99444	0.00235
b-c011a	0.99382	0.00277
b-c012a	0.99103	0.00261
b-c013a	0.99776	0.0024
b-c013x	0.99306	0.0025
b-c014a	0.99352	0.00243
b-c014x	0.99708	0.0024
b-c029a	0.99366	0.0023
b-c030a	0.99241	0.00259
Avg.	0.99628	0.0025
Std.Dev.	0.00411	0.00015

6.3.5 Validation for Homogeneous (Powder) Calculations)

The Reference 5 experiments involve homogeneous uranium oxides. These benchmark experiments include 36 cases of moderated uranium oxides. They are, therefore, similar to the accident conditions evaluated in this CSE. The case numbers referenced below were taken from Reference 6.

Table 6.4 Reference 5 Cases Calculation Results with 27-Group Cross Sections

Case ID	k_{eff}	
	Avg.	Std. Dev.
b-bm01k	0.98692	0.00165
b-bmb02k	0.98884	0.00172
b-bmb03k	0.99144	0.00184
b-bmb04k	0.98744	0.00180
b-bmb05k	0.98923	0.00173
b-bmb06k	0.99066	0.00166
b-bmb07k	0.97997	0.00174
b-bmb08k	0.97807	0.00179
b-bmb09k	0.98459	0.00164
b-bmb10k	0.98508	0.00144
b-bmb11k	0.99483	0.00205
b-bmb12k	0.99376	0.00224
b-bmb13k	0.99885	0.00211
b-bmb14k	0.99882	0.00215
b-bmb15k	1.00076	0.00190
b-bmb16k	0.99117	0.00186
b-bmb017k	0.99516	0.00189
b-bmb18k	0.98864	0.00195
b-bmb19k	0.99137	0.00153
b-bmb20k	0.98407	0.00166
b-bmb21k	1.00545	0.00230
b-bmb22k	1.00369	0.00197
b-bmb23k	1.01063	0.00245
b-bmb24k	1.00429	0.00253

Case ID	k_{eff}	
	Avg.	Std. Dev.
b-bmb25k	1.00256	0.00244
b-bmb26k	1.01009	0.00220
b-bmb27k	1.00547	0.00241
b-bmb28k	1.00551	0.00243
b-bmb29k	1.00973	0.00225
b-bmb30k	1.01132	0.00233
b-bmb31k	1.01283	0.00229
b-bmb32k	1.00783	0.00234
b-bmb33k	0.99621	0.00221
b-bmb34k	1.00319	0.00253
b-bmb35k	0.99743	0.00237
b-bmb36k	0.99307	0.00254

6.3.6 Bias

The bias and its standard deviation were calculated using the methods described in Reference 4. These methods use standard analysis of variance principles. The average over all cases of the KENO k_{eff} and its variance (square of standard deviation) are calculated. The average of the average k_{eff} (grand average) is weighted by the reciprocal of its variance. Since all k_{eff} results have similar standard deviations, all 20 cases have nearly equal weights. The average value of the variance is taken as the "within class" variance. The variance of the average k_{eff} data, weighted as for the grand average, is taken as the "between class" variance. The "within class" variance is subtracted from the "between class" variance to yield the variance of the class effect. Since the true value for all cases is assumed to be 1.0 (critical), the class effect (the change in average k_{eff} from case to case) is also the bias and the variance of the class effect is the variance of the bias. A zero variance of the bias would mean that the bias is constant from case to case. The bias uncertainty may still be calculated and used if desired, but it should be recognized that the uncertainty of the bias uncertainty will be relatively large.

Based on the data in Table 6.3 and the methodology documented in Reference 4, the calculational bias has been determined to be 3.85 E-3 for heterogeneous (pellet) calculations. The bias is 5.69E-3 for homogeneous (powder) calculations and is based on the data in Table 6.4. These values for the bias are non-conservative and must therefore be added to the KENO.Va calculated k_{eff} +2σ when establishing upper limits on k_{eff}. In other words, the maximum allowed calculated k_{eff}+2σ is 0.9461 for homogeneous cases and 0.9443 for heterogeneous cases.

6.4 *Analysis*

6.4.1 Dry Uranium Oxide Powder Enriched to a Maximum 5.0 wt% in the ^{235}U Isotope

6.4.1.1 Powder shipment data from Application Dated March 1990

For a 0.2 minimum transport index, the number of packages per shipment (N) was taken as 250. The normal (undamaged) array (5N) modeled was 16x16x5 for 1,280 units. The damaged array (2N) modeled was 11x12x4 for 528 units. All units were placed edge-to-edge in all directions in a square-pitched array. Both arrays were approximately cubical, and were reflected by water at all six faces. The diameter and length of each damaged outer container was reduced by 2.0 inches; conservative relative to the actual damage observed during testing.

Note: The calculations for this section were completed in the 1980's and used SCALE 3.

The steel powder canister, the steel inner container, and the steel outer container were included in the KENO-Va model. The powder canister contained 1149 g H, and either 120, 100, 80, or 60 kg U as UO_2 with a density to completely fill the canister. Therefore, the H/U ratios are 2.26, 2.71, 3.39, and 4.52.

The data in Table 6.5 demonstrate that the normal array is subcritical with optimum interspersed moderation. The data in Table 6.6 demonstrate subcriticality for damaged arrays with optimum interspersed moderation. It is seen that for the fixed 1149 g H per package, the peak array k_{eff} occurs with the 120 kg U, and it decreases with decreasing uranium content despite the increasing H/U.

The data in Table 6.6 are based on the assumption that water will not enter the fissile material, and that up to 120 kg U may be loaded per package. Those data are retained for reference.

Table 6.5 (6.5.1 from CSE March 1990) - Normal Array (16x16x5 Units) Powder Shipments in Powder Canister KENO-Va Results

Interspersed Water Density (Vol%)	k_{eff}
120 kg U, 1149 g H	
0	0.8234 ± 0.0035
2	0.8844 ± 0.0044
4	0.8529± 0.0035
6	0.8100 ± 0.0031
100 kg U, 1149 g H	
0	0.8191 ± 0.0049
2	0.8625 ± 0.0045
4	0.8443 ± 0.0044
6	0.7896 ± 0.0037
80 kg U, 1149 g H	
0	0.7799± 0.0048
2	0.8320 ± 0.0043
4	0.8023 ± 0.0048
6	0.7544 ± 0.0046
60 kg U, 1149 g H	
0	0.7606 ± 0.0046
2	0.7907 ± 0.0043
4	0.7528 ± 0.0044
6	0.7227 ± 0.0040

Table 6.6 (6.5.2 from CSE March 1990) - Damaged Array (11x12x4 Units) Powder Shipments in Powder Canister KENO-Va Results

Interspersed Water Density (Vol%)	k_{eff}
120 kg U, 1149 g H	
0	0.7818 ± 0.0040
2	0.8477 ± 0.0046
4	0.8497± 0.0046
6	0.8373 ± 0.0045
100 kg U, 1149 g H	
0	0.7689 ± 0.0047
2	0.8270 ± 0.0043
4	0.8322 ± 0.0042
6	0.8046 ± 0.0044

Additional calculations were made with reduced amounts of powder per package, and also with the assumption that the powder may become fully moderated under hypothetical accident conditions. Four enrichments were modeled to justify the mass limits listed in Section 6.2.1. The models are identical to those used for the Table 6.6 data (model listings are included in Appendix 6A) with the following exceptions:

1. The powder insert was completely filled with UO_2 powder saturated with water (powder with 1149 g H was used in previous models). The powder volume per package is 58-95 liters (9.625" diameter x 49.44" long).

2. The array size was reduced to 8x7x2 (112 units) as appropriate for a transport index of 1.0.

3. The interspersed water density was set to zero. The k_{eff} of the damaged array with full-water reflection is listed in Table 6.7 for the UO_2 densities modeled.

Calculations were replicated using 16 and 27-group cross section libraries.

Table 6.7 (6.5.3 from the CSE March 1990) Damaged Array (8x7x2 Units) Fully Moderated UO_2 Powder KENO-Va Results

Powder Density (g UO_2/cm^3)	k_{eff} (16-Group)	k_{eff} (27-Group)
5.0% Enrichment, 36.9 kg U (41.8 kg UO_2) Per Package		
0.71	0.9406 ± 0.0043	0.9331 ± 0.004
4.6% Enrichment, 41.6 kg U (47.2 kg UO_2) Per Package		
0.80	0.9314 ± 0.0036	0.9305 ± 0.0037
3.8% Enrichment, 55.1 kg U (62.5 kg UO_2) Per Package		
1.06	0.9344 ± 0.0031	0.9408 ± 0.0046
3.4% Enrichment, 62.4 kg U (70.7 kg UO_2) Per Package		
1.20	0.9148 ± 0.0039	0.9250 ± 0.0034

The specified limits on uranium loadings assure criticality safety even with fully moderated fissile material.

6.4.1.2 Powder Shipment Data from Application Dated 1998 Evaluating Moderators in Powder Shipments

This section reviews the use of plastic in shipping urania powders and concludes that the use of PE bags with powder shipments has little impact on the peak k_{eff}.

The first step is to repeat the normal case with the highest k_{eff} for an undamaged powder shipping configuration reported in Section 6.4.1.1 (note that this case assumed powder is placed in the powder insert without any other containment.) This case consists of an array of 16x16x5 containers and each container has 100 kg U as UO_2 and 1149 g of H as water with 2 vol% interspersed moderation. The original k_{eff} for this condition is reported as 0.8625 ± 0.0045. The repeated calculation results are 0.8680 ± 0.0031 which is conservatively 0.0055 higher than the original calculation.

As discussed in Section 6.3, SPC currently uses the SCALE-4.2 system of codes to do criticality safety evaluations. This system of codes has been extensively used and validated by SPC for this use. Documentation of the majority of SPC's validation efforts is included in EMF-94-175, "Validation and Verification of KENO.Va". Based on 36 models of benchmark experiments involving homogeneous uranium oxides, the calculation bias has been

determined to be 5.69E-3. This bias is non-conservative and must therefore be added to the KENO calculated $k_{eff}+2\sigma$ when establishing upper limits on k_{eff}.

To review the impact of plastic moderator mixed with the powder, the conditions of Table 6.5 were repeated with the assumption that the 1149 grams of H are from PE. Table 6.8 reports the effects of PE, mass and density of urania powder and interspersed moderator on k_{eff} and shows that a 16x16x5 array of containers is acceptable at normal conditions.

Table 6.8 Undamaged Powder Container Arrays

Case	Description 16x16x5 Array	UO_2 DENSITY	k_{eff}		
			Ave.	σ	Ave. + 2σ
np120	120 kg U 1149 g H H/U=2.26 no interspersed moderator (IM)	2.308	.8141	.0032	.8205
np120.02	as above with 2 vol. % IM		.8692	.0030	.8752
np120.04	as above with 4 vol. % IM		.8435	.0035	.8505
np120.06	as above with 6 vol. % IM		.8036	.0032	.8099
np100	100 kg U 1149 g H H/U=2.71 no interspersed moderator (IM)	1.923	.7882	.0035	.7953
np100.02	as above with 2 vol. % IM		.8528	.0032	.8593
np100.04	as above with 4 vol. % IM		.8268	.0034	.8338
np100.06	as above with 6 vol. % IM		.7811	.0034	.7879
np80	80 kg U 1149 g H H/U=3.39 no interspersed moderator (IM)	1.539	.7821	.0035	.7892
np80.02	as above with 2 vol. % IM		.8320	.0032	.8385
np80.04	as above with 4 vol. % IM		.8008	.0025	.8058
np80.06	as above with 6 vol. % IM		.7449	.0034	.7518
np60	60 kg U 1149 g H H/U=4.52 no interspersed moderator (IM)	1.154	.7517	.0035	.7588
np60.02	as above with 2 vol. % IM		.7849	.0031	.7911
np60.04	as above with 4 vol. % IM		.7608	.0032	.7673
np60.06	as above with 6 vol. % IM		.7063	.0034	.7130

Table 6.7 provides the results for fully moderated powder, i.e. the powder was smeared throughout the inner container volume and then saturated with water. This condition does not represent optimum moderation. To demonstrate the consequences of flooding the inner powder container while powder is distributed inside the powder insert, the following considerations were made:

1. The powder contained 1149 g of hydrogen from PE before the powder container was flooded.

2. The initial choice of powder densities to be evaluated is based on data from ARH-600 to ensure the region is at or near optimum moderation. The fill volume was based on the allowed mass.

The results of this evaluation for various enrichments are reported in Tables 6.9.

It should be noted that the drop test data for the ANF-250 shows that the powder insert was undamaged and, although water is expected to enter the ANF-250 inner container, it is not expected to enter the powder insert.

Additional sensitivity studies to evaluate various powder densities, impact of wetting or loosing vermiculite are included in Tables 6.10-6.12.

Table 6.9 Damaged Container Evaluation For 5.0 wt% Enrichment

Case drdb-50.00*	Description	k_{eff}		
		Average	σ	Ave. + 2σ
31.4 kg UO_2 and 5.0 wt% enriched Optimum Saturated Powder Density Search				
10.314	8x7x1 array; 1.0 g UO_2/cc fill height =66.89cm; dry vermiculite	.9084	.0040	.9165
11.314	as above with 1.1 g UO_2/cc and fill height = 60.81	.9144	.0031	.9207
12.314	as above with 1.2 g UO_2/cc and fill height = 55.74	.9164	.0033	.9230
13.314	**as above with 1.3 g UO_2/cc and fill height = 51.45**	**.9162**	**.0039**	**.9230**
14.314	as above with 1.4 g UO_2/cc and fill height = 47.78	.9147	.0036	.9220
15.314	as above with 1.5 g UO_2/cc and fill height = 44.59	.9129	.0038	.9206
16.314	as above with 1.6 g UO_2/cc and fill height = 41.81	.9096	.0040	.9176
31.4 kg UO_2 and 5.0 wt% enriched Optimum Moderator Search For Missing Vermiculite				
drdb-50a.00.13.314	as case b-50av.0013.314 without vermiculite	.9107	.0036	.9179
*.01.13.314	as above with 1.0 vol% H_2O in place of vermiculite	.9081	.0039	.9158
***.02.13.314**	**as above with 2.0 vol% H_2O in place of vermiculite**	**.9130**	**.0036**	**.9201**
*.03.13.314	as above with 3.0 vol% H_2O in place of vermiculite	.9043	.0037	.9117
*.04.13.314	as above with 4.0 vol% H_2O in place of vermiculite	.9068	.0034	.9136
*.05.13.314	as above with 5.0 vol% H_2O in place of vermiculite	.9056	.0034	.9125
31.4 kg UO_2 and 5.0 wt% enriched Optimum Wetting of Vermiculite				
drdb-50av.00.13.314		.9162	.0039	.9230
50av.01.13.314	as above with 1.0 vol% H_2O in vermiculite	.9209	.0039	.9287
50av.02.13.314	**as above with 2.0 vol% H_2O in vermiculite**	**.9249**	**.0034**	**.9318**
50av.03.13.314	as above with 3.0 vol% H_2O in vermiculite	.9120	.0039	.9199
50av.04.13.314	as above with 4.0 vol% H_2O in vermiculite	.9096	.0037	.9170
50av.05.13.314	as above with 5.0 vol% H_2O in vermiculite	.9044	.0034	.9112
31.4 kg UO_2 and 5.0 wt% enriched Optimum Interspersed Moderator Search				
50av.00	**as case drdb-50av.02.13.314with 0 vol% H_2O as interspersed moderator**	**.9249**	**.0034**	**.9318**
50av.01	as above with 1 vol% H_2O as interspersed moderator	.9191	.0038	.9266
50av.03	as above with 3 vol% H_2O as interspersed moderator	.9144	.0036	.9215
50av.05	as above with 5 vol% H_2O as interspersed moderator	.9243	.0035	.9313
50av.07	as above with 7 vol% H_2O as interspersed moderator	.9202	.0034	.9270
50av.10	as above with 10 vol% H_2O as interspersed moderator	.9175	.0040	.9255
50av.20	as above with 20 vol% H_2O as interspersed moderator	.9072	.0036	.9143
50av.80	as above with 80 vol% H_2O as interspersed moderator	.8941	.0036	.9014
50av.90	as above with 90 vol% H_2O as interspersed moderator	.8958	.0033	.9024
50av.95	as above with 95 vol% H_2O as interspersed moderator	.9112	.0035	.9183

Table 6.10 Damaged Container Evaluation For 4.6 wt% Enrichment

Case drdb-46.00*	Description	k_{eff}		
		Average	σ	Ave. + 2σ
35.4 kg UO_2 and 4.6 wt% enriched Optimum Saturated Powder Density Search				
12.354	8x7x1 array; 1.2 g UO_2/cc fill height = 62.84 cm; dry vermiculite	.9065	.0030	.9126
13.354	as above with 1.3 g UO_2/cc and fill height = 58.00	.9130	.0029	.9187
14.354	**as above with 1.4 g UO_2/cc and fill height = 53.86**	**.9156**	**.0038**	**.9231**
15.354	as above with 1.5 g UO_2/cc and fill height = 50.27	.9116	.0035	.9186
16.354	as above with 1.6 g UO_2/cc and fill height = 47.13	.9113	.0036	.9184
35.4 kg UO_2 and 4.6 wt% enriched Optimum Moderator Search For Missing Vermiculite				
b-46a.00.14.354	as case b-46av.00.14.354 without vermiculite	.9034	.0032	.9097
*45.01.14.354	as above with 1.0 vol% H_2O in place of vermiculite	.9017	.0034	.9084
*45.02.14.354	as above with 2.0 vol% H_2O in place of vermiculite	.9016	.0034	.9084
*45.03.14.354	as above with 3.0 vol% H_2O in place of vermiculite	.9065	.0036	.9136
***45.04.14.354**	**as above with 4.0 vol% H_2O in place of vermiculite**	**.9068**	**.0042**	**.9152**
*45.05.14.354	as above with 5.0 vol% H_2O in place of vermiculite	.9050	.0034	.9117
35.4 kg UO_2 and 4.6 wt% enriched Optimum Wetting of Vermiculite				
	case b-46av.00.14.354	**.9156**	**.0038**	**.9231**
46av.01.354	as above with 1.0 vol% H_2O in vermiculite	.9148	.0030	.9208
46av.02.354	as above with 2.0 vol% H_2O in vermiculite	.9138	.0036	.9209
46av.03.354	as above with 3.0 vol% H_2O in vermiculite	.9086	.0034	.9154
46av.04.354	as above with 4.0 vol% H_2O in vermiculite	.9107	.0034	.9175
46av.05.354	as above with 5.0 vol% H_2O in vermiculite	.9089	.0038	.9165
35.4 kg UO_2 and 4.6 wt% enriched Optimum Interspersed Moderator Search				
46av.00	**as case drdb-46av.314with 0 vol% H_2O as interspersed moderator**	**.9156**	**.0038**	**.9231**
46av.01	as above with 1 vol% H_2O as interspersed moderator	.9130	.0032	.9193
46av.03	as above with 3 vol% H_2O as interspersed moderator	.9102	.0038	.9178
46av.05	as above with 5 vol% H_2O as interspersed moderator	.9135	.0039	.9212
46av.07	as above with 7 vol% H_2O as interspersed moderator	.9117	.0037	.9190
46av.10	as above with 10 vol% H_2O as interspersed moderator	.9119	.0036	.9191
46av.20	as above with 20 vol% H_2O as interspersed moderator	.9060	.0038	.9136
46av.80	as above with 80 vol% H_2O as interspersed moderator	.8961	.0038	.9038
46av.90	as above with 90 vol% H_2O as interspersed moderator	.9003	.0034	.9071
46av.95	as above with 95 vol% H_2O as interspersed moderator	.8943	.0039	.9020

Table 6.11 Damaged Container Evaluation For 3.8 wt% Enrichment

Case drdb-38av.00.*	Description	k_{eff}		
		Average	σ	Ave. + 2σ
46.5 kg UO_2 and 3.8 wt% enriched Optimum Saturated Powder Density Search				
12.465	8x7x1 array; 1.2 g UO_2/cc fill height = 82.55 cm; dry vermiculite	.8897	.0036	.8969
13.465	as above with 1.3 g UO_2/cc and fill height = 76.20	.9006	.0034	.9074
14.465	as above with 1.4 g UO_2/cc and fill height = 70.76	.9074	.0038	.9149
15.465	as above with 1.5 g UO_2/cc and fill height = 66.04	.9013	.0035	.9083
16.465	**as above with 1.6 g UO_2/cc and fill height = 61.91**	**.9124**	**.0035**	**.9193**
17.465	as above with 1.7 g UO_2/cc and fill height = 58.27	.9071	.0031	.9133
18.465	as above with 1.8 g UO_2/cc and fill height = 55.03	.8994	.0034	.9061
46.5 kg UO_2 and 3.8 wt% enriched Optimum Moderator Search For Missing Vermiculite				
drdb-38.00.16.465	as case b-38av.00.16.465 without vermiculite	.9000	.0031	.9057
***.01.16.465**	**as above with 1.0 vol% H_2O in place of vermiculite**	**.9011**	**.0033**	**.9076**
*.02.16.465	as above with 2.0 vol% H_2O in place of vermiculite	.8984	.0036	.9050
*.03.16.465	as above with 3.0 vol% H_2O in place of vermiculite	.8914	.0037	.8981
*.04.16.465	as above with 4.0 vol% H_2O in place of vermiculite	.8900	.0040	.8974
*.05.16.465	as above with 5.0 vol% H_2O in place of vermiculite	.8891	.0031	.8958
46.5 kg UO_2 and 3.8 wt% enriched Optimum Wetting of Vermiculite				
	case b-38av.00.16.465	**.9124**	**.0035**	**.9193**
*.01.16.465	as above with 1.0 vol% H_2O in vermiculite	.8988	.0032	.9051
*.02.16.465	as above with 2.0 vol% H_2O in vermiculite	.9009	.0036	.9081
*.03.16.465	as above with 3.0 vol% H_2O in vermiculite	.9015	.0034	.9082
*.04.16.465	as above with 4.0 vol% H_2O in vermiculite	.8995	.0041	.9064
*.05.16.465	as above with 5.0 vol% H_2O in vermiculite	.8976	.0034	.9034
46.5 kg UO_2 and 3.8 wt% enriched Optimum Interspersed Moderator Search				
*38av.01	as case drdb-38av.00.16.465 with 1 vol% H_2O as interspersed moderator	.8970	.0038	.9046
*38av.03	as above with 3 vol% H_2O as interspersed moderator	.9039	.0037	.9119
*38av.05	as above with 5 vol% H_2O as interspersed moderator	.8969	.0032	.9032
*38av.07	as above with 7 vol% H_2O as interspersed moderator	.9003	.0027	.9058

Table 6.12 Damaged Container Evaluation For 3.4 wt% Enrichment

Case	Description	k_{eff}		
		Average	σ	Ave. + 2σ
70.7 kg UO_2 and 3.4 wt% enriched Optimum Saturated Powder Density Search				
d34a	8x7x1 array; 1.2 g UO_2/cc full insert; dry vermiculite	.9009	.0026	.9061
1.5/d34a	as above with 1.5 g UO_2/cc and fill height = 100.40	.9224	.0030	.9283
1.75/d34a	as above with 1.75 g UO_2/cc and fill height = 86.06	.9242	.0032	.9306
1.8/d34a	as above with 1.8 g UO_2/cc and fill height = 83.67	.9257	.0032	.9322
1.9/d34a	as above with 1.9 g UO_2/cc and fill height = 79.27	.9254	.0035	.9324
2.0/d34a	as above with 2.0 g UO_2/cc and fill height = 75.31	.9242	.0032	.9305

This evaluation concludes that under the requested mass limits (see Table 6.13 below) and the assumption that the inner container floods with water until reactivity is maximized, k_{eff} remains less than 0.7461 for array sizes less than or equal to 8x7x1 (56 containers).

Table 6.13 Enrichment vs. Mass Limits for Powder Shipment

Maximum Enrichment (wt% ^{235}U)	Maximum Uranium (kg U/UO_2)	Maximum ^{235}U (kg ^{235}U)
3.4	62.4/70.7	2.12
3.8	41.0/46.5	1.56
4.6	31.2/35.4	1.44
5.0	27.7/31.4	1.38

TI = 50/28 = 1.8

6.4.2 Dry Uranium Oxide Pellets Enriched to a Maximum 5.0 wt% in the ^{235}U Isotope

6.4.2.1 Pellet Shipment Data from the Application Dated March 1990

Arrays of undamaged containers during pellet shipment

For the 0.4 minimum transport index, the number of packages per shipment (N) was taken as 125. The normal (undamaged) array (5N) modeled was 14x15x4 for 840 units. The damaged array (2N) modeled was 10x9x3 for 270 units.

All units were placed edge-to-edge in all directions in a square-pitched array. The optimum interspersed water density was determined for this array. The peak reactivity for other arrangements such as triangular-pitched arrays will be bounded by that for the square-pitched array, but the optimum water density may be slightly different for other arrangements. Both arrays (normal and damaged) were approximately cubical and were reflected by water at all six faces. The diameter and length of each damaged outer container was reduced by 2.0 inches (conservative relative to the actual damage observed during testing).

The steel pellet suitcase, the steel inner container, and the steel outer container were included in the KENO-Va model. Pellets are packaged in the suitcase as show on drawing EMF-

304,306. The suitcase is adapted to the cylindrical inner container using the insert (not modeled) shown on drawing EMF-305,176.

The suitcase was modeled at nominal dimensions for undamaged and damaged condition arrays. The only steel parts of the suitcase that were modeled are the 0.1519 cm thick cover and the 0.3048 cm thick base plate.

The pellet suitcases were modeled with at least 120 kg U and with at least 1149 g H except to explore potentially more reactive conditions. The 120 kg U is equivalent to about 136.1 kg UO_2 and, at 10.412 g UO_2 per cm^3, about 13.075 liters UO_2. The net volume of each suitcase is about 15.388 liters
(7.75"x4.87"x24.88"). With two suitcases per packages, the net volume per package is about 30.776 liters. With the maximum permitted U loading, the two suitcases per package will contain 13.075 liters UO_2 and up to 17.701 liters of moderation (Vw/Vf = 17.701/13.075 = 1.35).

For the undamaged array calculations, the maximum permitted H content (1149 gm) was assumed within the two suitcases and various degrees of interspersed moderation were tested to demonstrate safety at optimum interspersed moderation. The 1149 g H is equal to 10268.6 g water. For liquid water at 20°C, water will occupy 10.287 liters. Therefore, the volume available for fuel in the two suitcases is 20.489 liters. (Vw/Vf = 0.502) At 10.96 g UO_2/cm^3, the UO_2 mass is 213.3 kg versus the specified limit of 136.1 kg. Lesser UO_2 masses with the fixed 1149 g H were modeled by increasing the Vw/Vf ratio with corresponding reductions in the water density inside the suitcase. For example, for Vw/Vf ratios of 1.0 and 2.0, the water densities (in volume fraction used in CSAS input) are 0.6685 and 0.5014 respectively for 1149 g H in the suitcases.

For damaged array calculations, the suitcase contained optimally moderated UO_2 pellets while the interspersed moderation was conservatively taken as zero. Cases with low density interspersed moderation were also modeled to show that the array k_{eff} decreases with increasing interspersed moderation.

The results from calculations with undamaged and damaged arrays conservatively demonstrate criticality safety for a Transport Index of 0.4 for 5.0% enriched pellet shipments.

Suitcases were filled with a cell-weighted mixture representing a generic UO_2 pellet lattice with water to equal 1149 g H. The cell-weighted mixture was prepared using CSAS routines and BONAMI, NITAWL, and XSDRNPM. A 0.5" pellet diameter was modeled because previous calculations and the data of DP-1014 indicate that (for undermoderated pellets) this larger diameter will be slightly more reactive than smaller diameters. (Note: The calculations for this section were completed in the 1980's and used SCALE 3).

Various amounts of interspersed moderation were placed in and between the containers to assure safety with vermiculite with any moisture content.

A 14x15x4 array (5N=840) was modeled to justify a 0.3 transport index. Since all results are adequately subcritical, a smaller array was not modeled for a 0.4 transport index.

KENO results for the undamaged arrays are in Table 6.14.

Table 6.14 (6.6.1 from CSE March 1990) Undamaged ANF-250 Arrays, Pellet Shipment 14X15X4 Array (5N=840), 1149 g H Per Package, Pellet Diameter is 0.5"

Vw/Vf in Suitcase	Interspersed Water (Vol%)	k_{eff}
0.502	0	0.8371 ± 0.0044
0.502	1	0.8715 ± 0.0042
0.502	2	0.8685 ± 0.0036
0.502	4	0.8368 ± 0.0041
1.0	0	0.7378 ± 0.0032
1.0	1	0.7817 ± 0.0042
2.0	0	0.6761 ± 0.0035
2.0	1	0.7471 ± 0.0040

The undamaged array is subcritical with optimum interspersed moderation. Since the suitcases are undermoderated (1149 g H), interspersed moderation is beneficial in limited amounts. The results would be even lower with a 625 unit array (0.4 transport index). With the maximum 120 kg U content (Vw/Vf=1.35), the peak k_{eff} would be about 0.75 or less.

Arrays of Damaged Containers during Pellet Shipments

The damaged array was very conservative in assuming flooded suitcases (pellets) but potentially zero interspersed moderation. To achieve moderated suitcases, the vermiculite in the annulus would become wet and it would retain moisture if drained. This wet vermiculite would greatly reduce the array k_{eff}.

The suitcases were filled with cell-weighted mixtures simulating UO_2 pellet lattices with unlimited moderation. Since the suitcases are well moderated, interspersed moderation is not needed and it serves to decouple the fissile units. The KENO-Va results are in Table 6.15.

Table 6.15 (6.6.3 from CSE March 1990) Damaged ANF-250 Arrays, Pellet Shipment 9x10x3 Array (2N=270), Flooded Suitcases with 5.0% Enriched Pellets

Vw/Vf in Suitcase	Interspersed Water (Vol%)	k_{eff}
0.35" Pellet Diameter		
1.5	0	0.9343 ± 0.0033
2.0	0	0.9611 ± 0.0031
2.5	0	0.9560 ± 0.0030
3.0	0	0.9575 ± 0.0034
3.5	0	0.9503 ± 0.0033
0.50" Pellet Diameter		
1.5	0	0.9346 ± 0.0032
2.0	0	0.9532 ± 0.0036
2.5	0	0.9445 ± 0.0031
3.0	0	0.9439 ± 0.0034
3.5	0	0.9238 ± 0.0034

The damaged array is subcritical with optimally moderated suitcases and with optimum interspersed moderation. As for the unclad pellet data in DP-1014, the 0.35" pellet diameter is slightly more reactive than the 0.50" pellet diameter for well moderated pellets. For undermoderated pellets (normal conditions), larger pellets are most reactive. The damaged array data are adequate for justifying Fissile Class I shipments for enrichments up to 5.0% since unlimited moderation was assumed and since the array size exceeds 250 packages.

The data in Table 6.15 were generated to justify a minimum transport index of 0.4. Additional calculations were done to justify a minimum transport index of 0.5. The parameters employed in these calculations are:

- The damaged array was 8x9x3 (2N = 216) which exceeds the minimum size for N= 100.
- The pellet diameter was 0.35". The data in Table 6.16 demonstrate that this is the more reactive diameter.
- Cases with differential albedo reflectors and with biased water reflectors were calculated for comparison.
- Cases with 16 and 27 energy group cross sections were calculated for comparison. All 27-group cases used a biased water reflector.

The KENO-Va results for these cases are in Table 6.16.

Table 6.16 (6.4 from CSE March 1990) Damaged ANF-250 Arrays, Pellet Shipment 8x9x3 Array (2N = 216), Flooded Suitcases with 5.0% Enriched Pellets, 0.35" Pellet Diameter, Zero Interspersed Moderation, KENO-Va Results, 103 Generations of 300 Neutrons

Vw/Vf in Suitcase	k_{eff}
16 Group Cross Sections, Differential Albedo Reflector	
2.0	0.9300 ± 0.0041
2.5	0.9270 ± 0.0039
3.0	0.9273 ± 0.0042
3.5	0.9255 ± 0.0039
16 Group Cross Sections, Biased Water Reflector	
1.5	0.9007 ± 0.0046
2.0	0.9243 ± 0.0039
2.5	0.9350 ± 0.0038
3.0	0.9239 ± 0.0044
3.5	0.9237 ± 0.0040
27 Group Cross Sections, Biased Water Reflector	
1.5	0.9075 ± 0.0045
2.0	0.9316 ± 0.0044
2.1	0.9410 ± 0.0040
2.2	0.9419 ± 0.0045
2.2	0.9356 ± 0.0042 (Triang Pitch)
2.3	0.9413 ± 0.0039
2.4	0.9390 ± 0.0035
2.5	0.9433 ± 0.0038
3.0	0.9350 ± 0.0038
3.5	0.9398 ± 0.0045
4.0	0.9123 ± 0.0041

The data in Table 6.16 may be summarized as follows:

1) The differential albedo results are slightly different from those with a biased water reflector. The magnitude of the difference is of questionable significance.

2) The 27-group results are slightly higher than the 16-group results with a biased water reflector, but again, the difference is of questionable significance.

3) The one-sided 95% upper limit on the peak k_{eff} is 0.9496 (0.9433 ± 1.67*0.0038) which is less than 0.95. The actual peak k_{eff} will be much lower than the calculated value.

6.4.2.2 Pellet Shipment Data from the Application Dated 1998

The first step was to recalculate the worst case condition for pellet shipments documented in Section 6.4.2.1. This case assumed a V_{water}/V_{fuel} ratio of 2.0 and a pellet diameter of 0.35" and was calculated with 27-group cross sections. The case assumed damaged conditions and a

9x10x3 array size. The rev. 5 CSE reported a k_{eff} of 0.9611 ± 0.0031 for this condition. A repeat of this calculation produced a k_{eff} of 0.9603 ± 0.0035.

The results of this recalculation are statistically identical to those reported in Section 6.4.2.1. One can therefore conclude the base model correctly represents the model used in Section 6.4.2.1.

As described in Section 6.3, SPC currently uses the SCALE 4.2 system of codes to do criticality safety evaluations. This system of codes has been extensively used and validated by SPC for this use. Documentation of the majority of SPC's validation efforts is included in EMF-94-175, "Validation and Verification of KENO.Va." Based on 20 models of benchmark experiments involving 4.31 wt% enriched clusters of rods in water, the calculation bias has been determined to be 3.85E-3 (see Section 6.3.6). This bias is non-conservative and must therefore be added to the KENO calculated $k_{eff} + 2\sigma$ when establishing upper limits on k_{eff}.

Next, the sensitivity of k_{eff} to moderators other than water inside the suitcases is evaluated. Pellets shipped in the ANF-250 are placed on PS trays inside the suitcases. A suitcase full of PS trays and pellets contains about 2.5 kg of PS. This amount of PS conservatively results in less than 200 g H in each suitcase which results in less than 400 g H inside the inner vessel.

When the 1149 g H per inner container (574.5 g H per suitcase) limit is met, the maximum amount of moderator that may be present in each suitcase is shown in Table 6.17 along with the weight of water required to provide an equal hydrogen content.

Table 6.17 Hydrogen Density of Plastic

Moderator	Density	wt% Hydrogen	Grams Hydrogen	Total Grams of Moderator	Volume Fraction of Moderator Inside Suitcases
Polyethylene	0.92	14.37	574.5	3,997.9	0.2824
Polystyrene	1.06	7.74	574.5	7,422.5	0.4551
Water	1.0	11.19	574.5	5,139.0	0.3337

The effect of PS on k_{eff} with various V_{mod}/V_{fuel} ratios inside the suitcases is shown in Table 6.18. The array size for this evaluation is 9x10x3. The assumed container diameter is 20.5" which matches the damaged container array dimensions used in Section 6.4.2.1.

Table 6.18 k_{eff} For Various V_{mod}/V_{fuel} Ratios

Case ID	V_{mod}/V_{fuel}	k_{eff}		
		Ave.	σ	Ave. + 2σ
Polystyrene				
lbps15	1.5	.8459	.0038	.8534
lbps	2.0	.8752	.0038	.8828
lbps25	2.5	.8830	.0038	.8906
lbps30	3.0	.8836	.0036	.8908
lbps35	3.5	.8731	.0033	.8797

Comparison of the results given in Table 6.18, which uses PS as the moderator, with the reactivity of suitcases with optimum water moderator of the pellets (see Table 6.15) shows that suitcases moderated by PS are less reactive than the conditions (optimum water moderation) assumed in Section 6.4.2.1.

Small amounts of PE are used in the ANF-250 suitcases for cushioning and, optionally, for gasket material. A repeated case with 300 g of PE in each suitcase interspersed with water moderation was used to evaluate whether this amount of PE would have a reactivity less than or equal to the reactivity of a suitcase using only water as the moderator. The k_{eff} of this condition, case 300pwd9t3n, is 0.9553 ± 0.0036 compared to 0.9528 ± 0.0034 for the same condition without PE interspersed with the water moderator. The 0.0025 difference between these two cases is statistically insignificant. It is therefore concluded that a limit of 300 g PE in each of the two pellet suitcases within an ANF-250 container is acceptable and is bounded by this CSE.

6.4.3 Data Evaluating the Effect of Vermiculite on Reactivity from the Applications Dated 1998

This section evaluates the effect of vermiculite on k_{eff}. The ANF-250 is utilized with vermiculite in the annulus between the inner and outer container walls. The effect of the vermiculite on reactivity was evaluated by repeating some of the preceding cases and modeling dry vermiculite in the annular region of the models. The array size of this evaluation is 9x10x3. The assumed container diameter is 20.5" which matches the damaged container array dimensions used in Section 6.4.2.1. The results of this evaluation are reported in Table 6.19.

Table 6.19 The Effect of Vermiculite on k_{eff}

Case ID	Description	k_{eff}			delta-k of vermiculite
		Average	σ	Ave. + 2σ	
latbase	replicate from previous application- except suitcase dimensions increased per drawing EMF-304,306, rev.7 Model assumes optimum water moderation inside the suitcase	.9528	.0034	.9597	
latbasev	as above with dry vermiculite modeled	.9674	.0034	.9742	+0.0145
lbps	polystyrene moderation, but with no vermiculite in the array	.8752	.0038	.8828	
lbpsv	as above with dry vermiculite modeled	.9006	.0033	.9071	+0.0254

In both cases the inclusion of dry vermiculite caused k_{eff} to increase.

The impact of wetting the vermiculite and void spaces was evaluated next. Case latbasev was repeated at various array sizes and with differing densities of water added to the vermiculite. Table 6.20 evaluates these conditions and the effect of array size on k_{eff}. The addition of moderator either in the vermiculite or in the void spaces caused a decrease in reactivity.

Table 6.20 Worst Case Damaged Container Arrays

Case ID	Description	k_{eff}		
		Average	σ	Ave. + 2σ
Wet Vermiculite & Dry Voids Evaluation				
vt3.00	10x10x3 array with dry vermiculite	.9674	.0034	.9742
vt3.01	as above with 1 vol% water in vermiculite	.9760	.0033	.9826
vt3.10	as above with 10 vol% water in vermiculite	.8862	.0039	.8940
vt3.70	as above with 70 vol% water in vermiculite	.6749	.0032	.6812
Array Size Evaluation				
v883.00	as vt3.00 with 8x8x3 array	.9491	.0034	.9560
v873.00	as vt3.00 with 8x7x3 array	.9352	.0035	.9420
v773.00	as vt3.00 with 7x7x3 array	.9193	.0035	.9263
Dry Vermiculite & Wet Voids Evaluation				
v873.01	as v873 with 1 vol% water as interspersed moderator	.9344	.0029	.9402
v873.03	as v873 with 3 vol% water as interspersed moderator	.9202	.0035	.9273
v873.05	as v873 with 5 vol% water as interspersed moderator	.9036	.0034	.9105
v873.80	as v873 with 80 vol% water as interspersed moderator	.7681	.0037	.7756
v873.90	as v873 with 90 vol% water as interspersed moderator	.7623	.0032	.7687

Two times the number of containers allowed in a shipment must have a k_{eff} less than 0.9443 at damaged conditions. Based on this criterion, the maximum number of containers in a pellet shipment is 84.

Next, the allowed array size for undamaged containers was determined. Based on Table 6.14, 0.5" pellets, 574.5 g H in each suitcase (i.e., 1149 g H in the inner container) and a V_{water}/V_{fuel} ratio = 0.502 is used as the worst case normal condition. Table 6.21 evaluates the effect of array size for undamaged containers on k_{eff}.

Table 6.21 Undamaged Container Array Evaluation

Case	Description Array size and Vol% Interspersed Mod.	k_{eff}		
		Average	σ	Ave. + 2σ
No Vermiculite & Wet Voids Evaluation				
nc	Normal pellet array, 15x14x4 Pellet diameter is 0.5" V_{water}/V_{fuel} = 0.502 & no vermiculite	.8377	.0031	.8438
nc.01	As above with 1 vol% water in void spaces	.8520	.0030	.8579
nc.02	As above with 2 vol% water in void spaces	.8734	.0036	.8805
nc.03	As above with 3 vol% water in void spaces	.8659	.0026	.8710
nc.04	As above with 4 vol% water in void spaces	.8697	.0031	.8760
nc.05	As above with 5 vol% water in void spaces	.8702	.0030	.8762
nc.06	As above with 6 vol% water in void spaces	.8628	.0032	.8692
nc.10	As above with 10 vol% water in void spaces	.8188	.0028	.8245
Wet Vermiculite Evaluation				
ncv	Normal pellet array, 15x14x4 Pellet diameter is 0.5" V_{water}/V_{fuel} = 0.523 & dry vermiculite.	.8987	.0032	.9052
ncv.01	As case ncv with 1 vol% water in vermiculite	.8912	.0033	.8978
ncv.02	As case ncv with 2 vol% water in vermiculite	.9026	.0031	.9089
ncv.05	As case ncv with 5 vol% water in vermiculite	.8680	.0027	.8734
ncv.10	As case ncv with 10 vol% water in vermiculite	.8015	.0036	.8087
ncv.70	As case ncv with 70 vol% water in vermiculite	.5480	.0031	.5542

Five times the number of undamaged containers allowed in a shipment must have a k_{eff} less than 0.9443 at undamaged conditions. Based on this criterion, the maximum number of containers in a pellet shipment is 168.

Proposed TI for Shipping Pellets

The transport index for criticality safety is set such that five times the allowed number of containers at undamaged conditions and two times the allowed number of containers at damaged conditions must have a k_{eff} less than 0.9443.

Damaged conditions : array size = 8x7x3 = 168
Undamaged conditions : array size =15x14x4 = 840

TI=(50/84)=0.6

6.4.4 Pellets with Enrichments < 1.0 wt%

6.4.4.1 Arrays of Undamaged Packages for Pellet Shipment with Enrichments ≤1.0 wt%

Data from Application dated March 1980.

Suitcases were filled with a cell-weighted mixture representing a generic UO_2 pellet lattice with water to equal 1149 g H. The cell-weighted mixture was prepared using CSAS routines and BONAMI, NITAWL, and XSDRNPM. A 0.5" pellet diameter was modeled because previous

calculations and the data of DP-1014 indicate that (for undermoderated pellets) this larger diameter will be slightly more reactive than smaller diameters.

Calculations were performed for an infinite array of packages with 1.0% enriched pellets. The minimum Vw/Vf ratio modeled (0.102) is for edge-to-edge pellets in a triangular pitched array. The suitcase moderation was unlimited. The data for this Fissile Class I array are in Table 6.22.

Table 6.22 (6.6.2 from CSE March 1990) Undamaged ANF-250 Arrays, Pellet Shipment, Infinite Array Flooded Suitcases with 1.0% Enriched Pellets

Vw/Vf in Suitcase	Interspersed Water (Vol%)	k_{eff}
0.35" Pellet Diameter		
0.103	0	0.5302 ± 0.0030
0.103	1	0.5960 ± 0.0026
0.103	2	0.5939 ± 0.0028
1.0	0	0.8135 ± 0.0030
1.0	1	0.7429 ± 0.0034
2.0	0	0.7854 ± 0.0026
2.5	0	0.7572 ± 0.0025
3.0	0	0.7232 ± 0.0024
3.5	0	0.6980 ± 0.0023
0.50" Pellet Diameter		
0.102	0	0.5342 ± 0.0044
0.102	1	0.6057 ± 0.0022
1.0	0	0.8161 ± 0.0031
1.0	1	0.7473 ± 0.0026

Since the peak k_{inf} for an unclad 1.0% enriched rod lattice is only about 1.08, the infinite package array is expected to be subcritical even with unlimited moderation although the normal condition has very limited moderation; i.e., the model used for the data in Table 6.22 is very conservative.

6.4.4.2 Data for Arrays of Damaged Packages for Pellet Shipments with Enrichments ≤1.0 wt%.

The damaged array model used in Section 6.4.2.1 for 5.0 wt% enriched pellets was very conservative in assuming flooded suitcases (pellets) but potentially zero interspersed moderation.

The damaged array data presented in Section 6.4.2.1 are adequate for justifying Fissile Class I shipments for enrichments up to 5.0% since unlimited moderation was assumed and since the array size exceeds 250 packages, calculations for damaged arrays containing 1.0% enriched pellets were not needed.

6.4.5 Uranium Oxide Powder Enriched to a Maximum of 1 wt% in the ^{235}U Isotope

6.4.5.1 Undamaged Container Arrays

Tables 6.5 and 6.8 demonstrate acceptable k_{eff} for 16x16x5 (5N) array of undamaged containers filled with 120 kg U at 5.0 wt% ^{235}U. These data support a TI of 0.4 without additional calculations.

6.4.5.2 Damaged Container Arrays

Table 6.6 demonstrates an acceptable k_{eff} for an 11x12x4 (2N) array of damaged containers filled with 120 kg U at 5.0 wt% ^{235}U. These data support a TI of 0.4 when shipping UO_X powder limited to 1.0 wt% ^{235}U.

6.4.6 QA Review Description

1) Methodology used in this CSE is clearly defined and was verified to be applicable. The calculation methods including details on cross section preparation, atom densities assumed, and geometry models were reviewed and determined to be adequate. Each of these items was verified to be conservative.

2) Assumptions were reviewed for reasonableness and applicability to this analysis.

3) Modeling was reviewed and determined to conservatively model the actual system.

4) Referenced sources were reviewed and verified to be applicable to this CSE.

5) Input information was checked against referenced sources.

6) Inputs for computer calculations were checked for agreement with values used in the CSE.

7) Hand calculations were independently checked.

8) K_{eff} for worst case accident conditions is specifically stated in the text.

9) Comments are provided below and are referenced in the CSE text as QA-N, where N is the corresponding comment number.

10) Sample Computer Input Listings

Appendix 6A

KENO Model for Damaged Array, Powder Shipment

The most reactive damaged array model used in the March 1990 applications is listed.

```
POWDER SHIPMENTS IN ANF-250-, IIXI2X4 ARRAY, FIXED H, DAMAGED
READ PARAMETERS

THE-60.0 GEN-83 NPGn3OO LIB-41 TBA-2.0 FLX-YES FDN-YES XSI-YES NUB-YES PWT-YES PLT-NO

END PARAMETERS

READ MIXT SCT-1
MIX- I
' U02-WATER, 1149.1 GM H, 120 KG U PER ANF-250
92235 2.591910E-04
92238 4.862395E-03
8016  1.603187E-02
1001  1.157741E-02
MIX- 2
' CARBON STEEL
6012 3.921682E-03
26000 8.350009E-02
MIX- 3
' INTERSPERSED WATER, 4 VOL
8016 1.3352-3 1001 2.6704-3
MIX-4
' REFLECTOR WATER
8016 3.337967E-2
1001 6.675933E-2
END MIXT
READ GEOMETRY
' U.02 POWDER SHIPMENT WITH 1149 GM H, 120 KG U
' POWDER INSERT IS 50.130 LONG, INCLUDING 0.38" THK AL LID THE INNER
' CONTAINER IS 57.0- LONG (INSIDE)
' CENTER THE INSERT INSIDE THE INNER CONTAINER
' THUS, 3.435' SPACE TO BOTTOM & LID
UNIT I
COM=' POWDER INSERT, 49.06 INCH REGION BELOW FLANGE  '
'  ID - 9.5625 +/- 0.0625, USE 9.625'
CYLI 1 I  12.2238 2PG2.3062
' ADD 0.0750" THK CARBON STEEL WALL OF POWDER INSERT
CYLI 2 1 12.4143 2P62.3062
' ADD INTERSPERSED NODERATOR TO 11.380" FLANGE DIAM
CYLI 3 1 14.4526 2P62.3062
' ADD CAR  STL BOTTOM FLANGE OF POWDER INSERT, 0.19" THK
CYLI 2 1 14.4526 62.3062 -62.7888
' ADD INTERSPERSED MODERATION, 3.435n AT BOTTOM, DIAN TO 11.5"
CYLI 3 1 14.605 62.3062 -71.5137
' ADD 0.0598- CAR STL WALL, ALSO ADD 0.25- BOTTOM OF INNER CONTAINER
CYLI 2 1 14.7569 62.3062 -72.1487
' INTERSPERSED MOD TO 20.50 ID, ALSO ADD 3.125- AT -Z
CYLI 3 1 26.035 62.3062 -80.0862
' ADD 0.0598" CAR STL DRUM WALL & BOTTOM
CYLI 2 1 26.1869 62.3062 -80.2381
' ENCLOSE IN CUBOID
CUBO 3 1 4P26.1869 62.3062 -80.2381
UNIT 2
COM= ' POWDER INSERT, REGION NEAR INSERT UPPER FLANGE'
' POWDER ID-9.625a $ FLANGE THICKNESS - 0.38"
CYLI 1 12.2238 2PO.4826
```

```
' ADD CAR STL FLANGE TO 11.38- DIAM
CYLI 2 1 14.4526 2PO.4826
' ADD MODERATION TO 11.5" DIAM & TO BOTTOM
' OF INNER CONTAINER FLANGE, SPACE AT +Z - 3.435 - 0.5 2.935
' NOTE: THE ALUM LID OF THE POWDER INSERT NOT MODELED
CYLI 3 1 14.605 7.9375 -0.4826
' ADD 0.05980 CAR STL WALL
CYLI 2 1 14.7569 7.9375 -0.4826
' ADD MODERATION TO 20.5' DRUM ID
CYLI 3 1 26.035 7.9375 -0.4826
' ADD DRUM WALL
CYLI 2 1 28-7269 7.9375 .0.4826
' ENCLOSE IN MODERATION CUBOID
CUBO 3 1 4P28.7269 7.9375 -0.4826
UNIT 3
COM= " FLANGE & LID OF INNER CONTAINER"
' INTERSPERSED MODERATION IN INNER CONTAINER
CYLI 3 1 14.605 0.0 -1.27
' FLANGE OD-15.5', LID OD-14.75"t USE 14.750 FOR BOTH
CYLI 2 1 18.733 2P1.27
' INTERSPERSED MOD To 20.5"ID, ALSO ADD 6.50 AT +Z
CYLI 3 1 28.575 17.78 -1.27
' ADD 0.0598" CAR STL WALL & LID
CYLI 2 1 28-7269 17.9319 -1.27

' ENCLOSE IN CUBOID
CUBO 3 1 4P28.7269 17.3919 -1.27
UNIT 4
COM=' COMPLETE ANF-250 PACKAGE '
ARRAY 1 3RO.0
GLOBAL
UNIT 5
ARRAY 2 3RO.0
REPL 4 2 6R3.0 10
END GEOMETRY
READ ARRAY
ARA-1 NUX-1 NUY-1 NUZ-3
FILL 1 2 3 END FILL
ARA=2 NUX=11 NUY=12 NUZ=4
FILL F4 END FILL
END ARRAY
READ START
NST-1
END START
READ BOUNDS
ALL-VACUUM
```

Since oxygen is present in ' both the U02 pellet and the water between pellets, CSAS assigns #8016 to the first occurrence (in U02) and #4 (which is the sequence number) to the oxygen in water.

Since the Vw/Vf is 2.0 and since there is no gap or clad, the unit cell is 1/3 fuel and 2/3 water. The atom densities for the heterogeneous cell are weighted accordingly to yield the following homogeneous cell atom densities.

HOMOGENEOUS CELL ATOM DENSITIES

92235	3.91942E-04
92238	7.35280E-03
8016	1.5489SE-02
4	2.22532E-02
1001	4.45063E-02

The homogeneous cell atom densities are used in KENO along with cell weighted cross sections from XSDRNPH.Unweighted cross sections were used for the carbon steel, stainless steel, and interspersed water in the model.Unweighted H and 0 were designated by 100102 and 801602 in the KENO model. NITAWL was used to combine the weighted and unweighted cross sections into one working library read by KENO. An example of the input to this second NITAWL run is listed below.

NITAWL INPUT FOR FINAL-WORKING-LIBRARY

```
0$$ 6 7 8 11 18 19 9 0 20
1$$ 0 0 8 5 3R0 0 2R0 -1 0
T
2$$ 801602 100102 6012 26000 24304 25055 26304 28304
92235 92238 8016 4 1001
T
```

The KENO-VA model for the most reactive case is listed below.

```
PELLET SHIPMENTS IN ANF-250, S.O%ENR, DAMAGED ARRAY
READ PARAMETERS
TME=60.0 GEN=83   NPG=500 LIB=41 TBA-2.0
FLX=YES FDN=YES   XSI=YES NUB=YES PWT=YES
PLT=NO
END PARAMETERS
READ MIXT SCT=1
MIX=1
'HOMO MIXTURE, 0.350 DIM, Vw/Vf-2.0, 5.0% enr
92235 3.91942E-04
92238 7.352SOE-03
8016  1.5489SE-02
4   2.22532E-02
100   1 4.45063E-02
MIX=2
'CARBON STEEL
6012                3.921682E-03
26000               .8.350009E-02
MIX= 3
' SS304
24304               1.74295SE-02
25055               1.736443E-03
26304               5.935923E-02
28304               7.718178E-03
MIX= 4
'WATER BETWEEN SUITCASES, 0% 801602 3.337967E-12 100102
END MIXT
READ GEOMETRY
UNIT I
' 7.75" WIDE X 4.870 TALL X 24.88* LONG FUEL REGION IN SUITCASE
CUBO 1 1 2P9.8424 2P6.1848 2P31.5976
' ADD 0.0598" SS WALL EXCEPT AT -Y
REPL 3 1 3R0.1519 0.0 2R0.1519 I
' ADD MODERATION TO BASE OINS
CUBO 4 1 2PI1.9 6.3368 -6.1849 2P33.655
'  ADD STEEL FLANGE (16 GAGE) & 0.12- BASE PLATE
CUBO 3 1 2PI1.9 6.3368 -6.6416 2P33.655
UNIT 2
COM=' TWO EDGE-EDGE SUITCASES IN INNER CONTAINER'
ARRAY 1 -11.9 -6.6416 -67.31
'  INSIDE LENGTH OF INNER CONTAINER - 57.25'-O.25' - 57.0
' 0.5" IS IN THE UNIT WITH THE FLANGE
```

```
' LENGTH OF TWO SUITCASES – 53"
' CENTER THE SUITCASES IN THE 57" REGION
CYLI 4 1 14.605 71.12 -72.39
' ADD 0.05980 CAR STL WALL, ALSO ADD 0.250 BOTTOM OF INNER CONTAINER
CYLI 2 1 14.7569 71.12 -73.025
'  INTERSPERSED NOD TO 22.5 a ID, ALSO ADD 4.125" AT -Z
'  FOR DAMAGED CONDITIONS, USE 20.5' ID & 3.125"
CYLI 4 1 26.035 71.12 -80.9625
'  ADD 0.05980 CAR STL DRUM WALL & BOTTOM
CYLI 2 1 26.1869 71.12 -81.1144
' ENCLOSE IN CUBOID
CUBO 4 1 4P26.1869 71.12 -81.1144
UNIT 3
COM=' FLANGE & LID OF INNER CONTAINER'
'   INTERSPERSED MODERATION IN INNER CONTAINER
CYLI 4 1 14.605 0.0 -1.27
'  FLANGE OD-15.5@, LID OD-14.75', USE 14.75- FOR BOTH ,
CYLI  2 1 18.733 2P1.27
'  INTERSPERSED MOD TO 22.5"ID, ALSO ADD 6.5' AT +Z
'  FOR DAMAGED CONDITIONS, USE 20.5* ID & 5..5"
CYLI 4 1 26.035 15.24 -1.27 1
'  ADD 0.05980 CAR STL WALL & LID
CYLI 2 1 26.1869 15.3919 –1.27
' ENCLOSE IN CUBOID
CUBO 4 1 4P26.1869 15.3919 -1.27
UNIT 4
COM=" COMPLETE MF-250 PACKAGE"
ARRAY 2 3RO.0
GLOBAL
UNIT 5
ARRAY 3 3RO.0
END GEOMETRY
READ ARRAY
ARA=1 NUX=1 NUY=1 NUZ=2
FILL FI END FILL
ARA=2 NUX=1 NUY=1 NUZ=2
FILL 2 3 END FILL
ARA=3 NUX=9 NUY=10 NUZ=3
FILL F4 END FILL
END ARRAY
READ START
NST=1
END START
READ BOUNDS
ALL=WATER
END BOUNDS
END DATA
```

Sample computer inputs from the 1998 applications

Case ncv.01

```
=csas2x
'  parm=chk
ANF-250 normal cond. 14x15x6 array 0.5" pellets vw/vf=0.502
27group latt
'MIX=1
uo2  1  0.98 293  92235 5.0   92238 95.0  end
'MIX=2
'  CARBON STEEL
c    2  0  3.921682E-03  end
fe   2  0  8.350009E-02  end
'MIX= 3
'  SS304
crss   3 0  1.742958E-02  end
mn     3 0  1.736443E-03  end
fess   3 0  5.935923E-02  end
```

```
niss  3 0  7.718178E-03  end
' MIX= 4
'  WATER BETWEEN SUITCASES, 0%
o   4 0  3.337967E-6  end
h   4 0  6.675933E-6  end
'  END MIXT
' This case also contains  X% water in the void fractions of the vermic.
' add vermiculite # densities from arh-600
AL 5 0 .00023  end
Fe 5 0 .00009  end
H  5 0 .00081  end
K  5 0 .00012  end
Mg 5 0 .00042  end
o  5 0 .00242  end
Si 5 0 .00052  end
h2o 5 1.0E-2   end
' moderator for unit cell use water
' @ vm/vf=2.0
o   6 0  3.337967E-2  end
h   6 0  6.675933E-2  end
end comp
'  1149 g H = 10268.6 g h2o @ 20 C = 10.287L
'  Vm= 10.287/20.489=0.502
'  pellet 0D=.5" = 1.27cm pitch=1.389 cm
squa  1.3890   1.27   1  6  end
ANF-250 normal cond. 14x15x6 array 0.5" pellets vw/vf=0.502
READ PARAMETERS
TME=60.0 GEN=83 NPG=500
FLX=YES FDN=YES XS1=YES NUB=YES PWT=YES
PLT=NO  RUN=yes
END PARAMETERS
READ GEOMETRY
UNIT  1
'  8.375" WIDE X 5.25" TALL X 25.19" LONG FUEL REGION IN SUITCASE
CUBO  500 1  2P10.00125 2P6.19125 2P3175
'  ADD 0.0598" SS WALL EXCEPT AT -Y
REPL  3 1 3R0.1519 0.0 2R0.1519 1
'  ADD MODERATION TO BASE DIMS
CUBO  4 1 2P11.9 6.81940 -6.66750 2P33.655
'  ADD STEEL FLANGE (16 GAGE) & 0.12" BASE PLATE
CUBO  3 1 2P11.9 6.81940 -7.12420 2P33.655
UNIT 2
COM=" TWO EDGE-EDGE SUITCASES IN INNER CONTAINER  "
ARRAY 1 -11.9 -7.12420 -67.31
' INSIDE LENGTH OF INNER CONTAINER = 57.25"-0.25" = 57.0"
' 0.5 IS IN THE UNIT WITH THE FLANGE
' LENGTH OF TWO SUITCASES = 53"
' CENTER THE SUITCASES IN THE 57" REGION
CYLI  4 1 14.605 71.12 -72.39
' ADD 0.0598" CAR STL DRUM WALL & BOTTOM
CYLI  2 1 14.7569 71.12 -73.025
'INTERSPERSED MOD TO 22.5" ID, ALSO ADD 4.125" AT -Z
' FOR normal  CONDITIONS, USE 22.5" ID & 3.125
CYLI  5 1 28.575 71.12 -80.9625
' Add 0.0598" carbon stl drum wall & bottom
CYLI  2 1 28.7269 71.12 -81.1144
' ENCLOSE IN CUBOID
CUBO  4 1 4P28.7269 71.12 -81.1144
UNIT 3
COM=" FLANGE & LID OF INNER CONTAINER   "
' INTERSPERSED MODERATION IN INNER CONTAINER
CYLI  4 1 14.605 0.0 -1.27
'  FLANGE OD=15.5", LID OD=14.75", USE 14.75" FOR BOTH
CYLI  2 1 18.733 2P1.27
' INTERSPERSED MOD TO 22.5" ID, ALSO ADD 6.5" AT +Z
' FOR undamaged CONDITIONS, USE 20.5" ID & 6.5"
CYLI  4 1 28.575 16.51 -1.27
```

```
' ADD 0.0598" CAR STL WALL & LID
CYLI  2 1 28.7269 16.6619 -1.27
'  ENCLOSE IN CUBOID
CUBO  4 1 4P28.7269 16.6619 -1.27
UNIT 4
COM="  COMPLETE ANF-250 PACKAGE   "
ARRAY 2 3R0.0
GLOBAL
UNIT 5
ARRAY 3 3R0.0
END GEOMETRY
READ ARRAY
ARA=1 NUX=1 NUY=1 NUZ=2
FILL F1 END FILL
ARA=2
NUX=1 NUY=1 NUZ=2
FILL 2 3 END FILL
ARA=3 NUX=14 NUY=15 NUZ=4
FILL F4 END FILL
END ARRAY
READ START
NST=1
END START
READ BOUNDS
ALL=WATER
END BOUNDS
END DATA
END

Case  v873.00
=csas2x
'  parm=chk
-Va model for the ANF-250 most reactive case is listed below.
27group latt
'MIX=1
'  HOMO MIXTURE, 0.35" DIAM,  Vw/Bf=2.0, 5.0% enr
'  u-235 1 0  3.91942E-04  end
'  u-238 1 0  7.35280E-03  end
'  o  1 0   1.54895E-02    end
uo2  1  0.98 293  92235 5.0   92238 95.0  end
'MIX=2
'  CARBON STEEL
c     2  0  3.921682E-03  end
fe    2  0  8.350009E-02  end
'MIX= 3
'  SS304
crss   3 0  1.742958E-02  end
mn     3 0  1.736443E-03  end
fess   3 0  5.935923E-02  end
niss   3 0  7.718178E-03  end
' MIX= 4
'  WATER BETWEEN SUITCASES, 0%
o    4 0  3.337967E-6  end
h    4 0  6.675933E-6  end
'  END MIXT
' add vermiculite # densities from arh-600
' This case also contains  X% water in the void fractions of the vermic.
AL 5 0 .00023  end
Fe 5 0 .00009  end
H  5 0 .00081  end
K  5 0 .00012  end
Mg 5 0 .00042  end
o  5 0 .00242  end
Si 5 0 .00052  end
h2o 5 1.0E-6   end
'  water for unit cell
o    6 0  3.344E-02  end
```

```
H    6 0  6.689E-02  end
end comp
squa  1.36461  0.889  1  6  end
PELLET SHIPMENTS IN ANF-250, 5.0%ENR, DAMAGED ARRAY
READ PARAMETERS
TME=60.0 GEN=83 NPG=500
FLX=YES FDN=YES XS1=YES NUB=YES PWT=YES
PLT=NO  RUN=yes
END PARAMETERS
READ GEOMETRY
UNIT  1
'  8.375" WIDE X 5.25" TALL X 25.19" LONG FUEL REGION IN SUITCASE
CUBO  500 1  2P10.00125 2P6.19125 2P31.75
'  ADD 0.0598" SS WALL EXCEPT AT -Y
REPL  3 1 3R0.1519 0.0 2R0.1519 1
'  ADD MODERATION TO BASE DIMS
CUBO  4 1 2P11.9 6.81940 -6.66750 2P33.655
'  ADD STEEL FLANGE (16 GAGE) & 0.12" BASE PLATE
CUBO  3 1 2P11.9 6.81940 -7.12420 2P33.655
UNIT 2
COM=" TWO EDGE-EDGE SUITCASES IN INNER CONTAINER  "
ARRAY 1 -11.9 -7.12420 -67.31
' INSIDE LENGTH OF INNER CONTAINER = 57.25"-0.25" = 57.0"
' 0.5 IS IN THE UNIT WITH THE FLANGE
' LENGTH OF TWO SUITCASES = 53"
' CENTER THE SUITCASES IN THE 57" REGION
CYLI  4 1 14.605 71.12 -72.39
' ADD 0.0598" CAR STL DRUM WALL & BOTTOM
CYLI  2 1 14.7569 71.12 -73.025
'vermiculite to 22.5" ID
CYLI  5 1 26.035  71.12 -73.025
'INTERSPERSED MOD TO 22.5" ID, ALSO ADD 4.125" AT -Z
' FOR DAMAGED CONDITIONS, USE 20.5" ID & 3.125
CYLI  5 1 26.035 71.12 -80.9625
' Add 0.598" carbon stl drum wall & bottom
CYLI  2 1 26.1869 71.12 -81.1144
' ENCLOSE IN CUBOID
CUBO  4 1 4P26.1869 71.12 -81.1144
UNIT 3
COM=" FLANGE & LID OF INNER CONTAINER  "
' INTERSPERSED MODERATION IN INNER CONTAINER
CYLI  4 1 14.605 0.0 -1.27
'  FLANGE OD=15.5", LID OD=14.75", USE 14.75" FOR BOTH
CYLI  2 1 18.733 2P1.27
' INTERSPERSED MOD TO 22.5" ID, ALSO ADD 6.5" AT +Z
' FOR DAMAGED CONDITIONS, USE 20.5" ID & 5.5"
CYLI  4 1 26.035 15.24 -1.27
' ADD 0.0598" CAR STL WALL & LID
CYLI  2 1 26.1869 15.3919 -1.27
'  ENCLOSE IN CUBOID
CUBO  4 1 4P26.1869 15.3919 -1.27
UNIT 4
COM="  COMPLETE ANF-250 PACKAGE  "
ARRAY 2 3R0.0
GLOBAL
UNIT 5
ARRAY 3 3R0.0
END GEOMETRY
READ ARRAY
ARA=1 NUX=1 NUY=1 NUZ=2
FILL F1 END FILL
ARA=2
NUX=1 NUY=1 NUZ=2
FILL 2 3 END FILL
ARA=3 NUX=8 NUY=7 NUZ=3
FILL F4 END FILL
END ARRAY
```

```
READ START
NST=1
END START
READ BOUNDS
ALL=WATER
END BOUNDS
END DATA
END
```

Case b168v

```
=csas25
' parm=chk
-ANF-250 powder case damaged conditions 1.68 g/cc 3.8 wt.% u235 .
27grou infh
'MIX=1
' the uo2 density = 1.68 g/cc and is based on vol. for full can
' at flooded condtions for 71 kg uo2
' for 3.4 wt.% maximum mass is 62.4 kg u per container
' for this case use 3.8 wt% enriched and 71 kg uo2 per container
uo2 1 den=1.68 1.0 293 92235 3.8 92238 96.2 end
' add water to saturate the powder-pe mixture
' vf water = 1-0.153051 -0.00000 = 0.846949
h2o 1 0.846949 end

'MIX=2
' CARBON STEEL
c 2 0 3.921682E-03 end
fe 2 0 8.350009E-02 end
'MIX= 3
' interspersed moderator 0 vol%
h2o 3 1.0E-6 end

' MIX= 4
' reflector WATER
o 4 0 3.337967E-2 end
h 4 0 6.675933E-2 end
' END MIXT
' add vermiculite # densities from arh-600
' This case also contains 0% water in the void fractions of the vermic.
AL 5 0 .00023 end
Fe 5 0 .00009 end
H 5 0 .00081 end
K 5 0 .00012 end
Mg 5 0 .00042 end
o 5 0 .00242 end
Si 5 0 .00052 end
h2o 5 1.0E-6 end
'MIX=6
' CARBON STEEL for powder can use e-6 here
c 6 0 3.921682E-06 end
fe 6 0 8.350009E-06 end
end comp
-ANF-250 powder case damaged conditions 1.68 g/cc 3.8 wt.% u235 .
READ PARAMETERS
TME=60.0 GEN=83 NPG=500
FLX=YES FDN=YES XS1=YES NUB=YES PWT=YES
PLT=no RUN=yes
END PARAMETERS
READ GEOMETRY
' uo2 powder shipment with 1149 gm H,
' powder insert is 50.13" long including 0.38" tk al lid
' the inner container is 57.0" long (inside)
' center the insert inside the inner container
' thus, 3.435" space to bottom & lid
' powder can is 8-3/16" od- assume id here
' lid is 1/8" use .12" here
```

```
UNIT 1
com="  powder insert, 49.06 inche region below flange   "
' can for powder is cylinder that matches "B" pail dimensions
'  8-3/16" diameter  10.398 cm Radius
' for 5 wt.% maxium mass is 41.6 kg u assume 48. kg uo2  per container
' this volume =32,000.00
' for 3.8 wt.% maximum mass is 62.4 kg u assume 71 kg uo2  per container
' powder container volume =42,326.35
' @ 71 kg uo2 @ 1.68 g/cc fill height =42,326.35/339.664 =124.6124  cm
cyli  1  1  10.398   62.3062    -62.3062
'  add steel wall- assume im here .0598"
'  bottom is 1/8" ignore steel lid and bottom here
cyli  6  1  10.5500   2p62.3062
'add IM to wall of powder insert
'id= 9.5625 +/- 0.625, use 9.625
cyli  3  1  12.2238  2P62.3062
'  ADD 0.075" cS WALL of insert
cyli  2  1  12.4143  2P62.3062
'  add interspersed moderator to 11.38" flange diam
cyli  3  1  14.4526  2P62.3062
'  ADD cS bottom flange of powder insert, 0.19" thk
cyli  2  1  14.4526  62.3062  -62.7888
'  add interspersed moderation, 3.435" at bottom, diam to 11.5"
cyli  3  1  14.605   62.3062  -71.5137
'  ADD 0.0598" cS wall, also add 0.25" Bottom of inner container
cyli  2  1  14.7569  62.3062  -72.1487
'  interspersed mod to 20.5" id, also add 3.125" at -z
cyli  5  1  26.035   62.3062  -80.0862
'  ADD 0.0598" cS drum wall and Bottom
cyli  2  1 26.1869  62.3062  -80.2381
'  enclose in cuboid
CUBO  3  1 4P26.1869 62.3062 -80.2381

UNIT 2
COM=" powder insert, region near insert upper flange   "
'  powder ID=9.625", flange thickness = 0.38"
cyli  1  1  12.2238  2P0.4826
'  add cs to flange to 11.38" diam
cyli  2 1 14.4526  2p0.4826
'  add moderation to 11.5' diam & to bottom
'  of inner container flange, space at +z=3.435-0.5 = 2.935"
'  note:  the alum lid of the powder insert not modeled
cyli  3 1 14.605   7.9375  -0.4826
'  add 0.0598" cs wall
cyli  2 1 14.7569  7.9375  -0.4826
'  interspersed mod to 20.5" id, also add 4.125" at -z
cyli  5  1  26.035   7.9375  -0.4826
'  ADD 0.0598" cS drum wall and Bottom
cyli  2  1 26.1869  7.9375  -0.4826
'  enclose in cuboid
CUBO  3  1 4P26.1869 7.9375 -0.4826

UNIT 3
COM=" FLANGE & LID OF INNER CONTAINER   "
' INTERSPERSED MODERATION IN INNER CONTAINER
CYLI  3 1 14.605 0.0 -1.27
'  FLANGE OD=15.5", LID OD=14.75", USE 14.75" FOR BOTH
CYLI  2 1 18.733 2P1.27
'  interspersed mod to 20.5" id, also add 4.125" at -z
cyli  5  1  26.035   15.24  -1.27
'  ADD 0.0598" cS drum wall and Bottom
cyli  2  1 26.1869  15.3919  -1.27
'  enclose in cuboid
CUBO  3  1 4P26.1869 15.3919 -1.27

UNIT 4
COM="  COMPLETE ANF-250 PACKAGE   "
```

```
ARRAY 1 3R0.0
GLOBAL
UNIT 5
ARRAY 2 3R0.0
repl 4  2  6R3.0  10
END GEOMETRY
READ ARRAY
ARA=1 NUX=1 NUY=1 NUZ=3
FILL 1 2 3 END FILL
ARA=2
NUX=7 NUY=8 NUZ=2
FILL f4 END FILL
END ARRAY

read plot
nch=' fS.*v'
ttl='zx section at        '
xul=0.0 xlr=58. yul=26.18 ylr=26.18 zul=169.00 zlr=0.0
uax=1.0 wdn=-1.0 lpi=6 nax=120 end
ttl='yx section at z=30cm    '
xul=65.16  xlr=-15.0 yul=65.16 ylr=-15. zul=30.  zlr=30.
uax=1.0 vdn=1.0 lpi=6 nax=120 end
ttl='yx section at      cm'
xul=65.16  xlr=-15.0 yul=65.16 ylr=-15. zul=30.  zlr=30.
uax=1.0 vdn=1.0 lpi=6 nax=120 end
ttl='yx section at 60cm'
xul=58. xlr=-30.0 yul=58.16 ylr=-30. zul=60.  zlr=60.
uax=1.0 vdn=1.0 lpi=6 nax=120 end
nch=' 12345'
ttl='zx section at        '
xul=0.0 xlr=58. yul=26.18 ylr=26.18 zul=169.00 zlr=0.0
uax=1.0 wdn=-1.0 lpi=6 nax=140 end
ttl='zx section at        '
xul=0.0 xlr=58. yul=0.0 ylr=0.0 zul=169.00 zlr=0.0
uax=1.0 wdn=-1.0 lpi=6 nax=140 end
ttl='yx section at z=30cm    '
xul=65. xlr=-15.0 yul=65.16 ylr=-15. zul=30.  zlr=30.
uax=1.0 vdn=1.0 lpi=6 nax=140 end
ttl='yx section at      cm'
xul=65. xlr=-15.0 yul=65.16 ylr=-15. zul=30.  zlr=30.
uax=1.0 vdn=1.0 lpi=6 nax=140 end
ttl='yx section at 60cm'
xul=58. xlr=-30.0 yul=58.16 ylr=-30. zul=60.  zlr=60.
uax=1.0 vdn=1.0 lpi=6 nax=140 end
end plot
READ START
NST=1
END START
READ BOUNDS
ALL=WATER
END BOUNDS
END DATA
END
```

Sample input for Case drdb-50av.02.13.314

```
=csas25
'  parm=chk
-Va model for the ANF-250 most reactive normal powder case is listed below.
27grou  infh
'MIX=1
' 31.4 kg uo2 in 24,153 cc
' the uo2 density = 1.30 g/cc and is based on ARH-600 data for
' optimum at flooded condtions
uo2  1 den=1.30  1.0    293  92235  5.0  92238 95.0  end
'  the polyethelyene density for 1149 g H (7996 g PE) is 0.331045
'  @ vf 1.0  for ease of modeling
arbm-polyethylen 0.331045 2 0 1 0 6012 1
```

```
                    1001 2
  1  1.0 293  end
 ' add water to saturate the powder-pe mixture
 ' vf of water is 1-vf uo2 - vfpe; uo2=den/10.96 vfpe= den/.92
 ' vf water = 1-0.118613-0.359831 = 0.521556
 h2o 1 0.521556 end


 'MIX=2
 '  CARBON STEEL
 c    2  0  3.921682E-03  end
 fe   2  0  8.350009E-02  end
 'MIX= 3
 '  interspersed moderator 0 vol%
 'o    3 0  1.3352E-3  end
 'h    3 0  2.6704E-3  end
 h2o 3 1.0E-6   end


 ' MIX= 4
 '  reflector WATER
 o    4 0  3.337967E-2  end
 h    4 0  6.675933E-2  end
 '  END MIXT
 ' add vermiculite # densities from arh-600
 ' This case also contains  2% water in the void fractions of the vermic.
 AL 5 0 .00023  end
 Fe 5 0 .00009  end
 H  5 0 .00081  end
 K  5 0 .00012  end
 Mg 5 0 .00042  end
 o  5 0 .00242  end
 Si 5 0 .00052  end
  h2o 5 2.0E-2   end
 end comp
 -Va model for the ANF-250 most reactive normal powder case is listed below.
 READ PARAMETERS
 TME=60.0 GEN=83 NPG=500
 FLX=YES FDN=YES XS1=YES NUB=YES PWT=YES
 PLT=no  RUN=yes
 END PARAMETERS
 READ GEOMETRY
 '  powder insert is 50.13" long including 0.38" tk al lid
 '  the inner container is 57.0" long (inside)
 '  center the insert inside the inner container
 '  thus, 3.435" space to bottom & lid
 UNIT  1
 com="  powder insert, 49.06 inche region below flange   "
 'id= 9.5625 +/- 0.625, use 9.625
 ' 31.4 kg uo2 in 24,154 cc at 1.3 g/cc
 ' fill height is 51.45457 cm
 cyli  1  1  12.2238  -10.85163   -62.3062
 cyli  3  1  12.2238  2P62.3062
 '  ADD 0.075" cS WALL of insert
 cyli  2  1  12.4143  2P62.3062
 '  add interspersed moderator to 11.38" flange diam
 cyli  3  1  14.4526  2P62.3062
 '  ADD cS bottom flange of powder insert, 0.19" thk
 cyli  2  1  14.4526  62.3062  -62.7888
 '  add interspersed moderation, 3.435" at bottom, diam to 11.5"
 cyli  3  1  14.605   62.3062  -71.5137
 '  ADD 0.0598" cS wall, also add 0.25" Bottom of inner container
 cyli  2  1  14.7569  62.3062  -72.1487
 '  interspersed mod to 20.5" id, also add 3.125" at -z
 cyli  5  1  26.035   62.3062  -80.0862
 '  ADD 0.0598" cS drum wall and Bottom
 cyli  2  1 26.1869  62.3062  -80.2381
```

```
' enclose in cuboid
CUBO  3  1 4P26.1869 62.3062 -80.2381

UNIT 2
COM=" powder insert, region near insert upper flange   "
'  powder ID=9.625", flange thickness = 0.38"
cyli  1 1  12.2238  2P0.4826
'  add cs to flange to 11.38" diam
cyli  2 1 14.4526  2p0.4826
'  add moderation to 11.5' diam & to bottom
'  of inner container flange, space at +z=3.435-0.5 = 2.935"
'  note:  the alum lid of the powder insert not modeled
cyli  3 1 14.605   7.9375  -0.4826
'  add 0.0598" cs wall
cyli  2 1 14.7569  7.9375  -0.4826
'  interspersed mod to 20.5" id, also add 4.125" at -z
cyli  5  1  26.035   7.9375  -0.4826
'  ADD 0.0598" cS drum wall and Bottom
cyli  2  1 26.1869  7.9375  -0.4826
'  enclose in cuboid
CUBO  3  1 4P26.1869 7.9375 -0.4826

UNIT 3
COM=" FLANGE & LID OF INNER CONTAINER   "
' INTERSPERSED MODERATION IN INNER CONTAINER
CYLI  3 1 14.605 0.0 -1.27
'  FLANGE OD=15.5", LID OD=14.75", USE 14.75" FOR BOTH
CYLI  2 1 18.733 2P1.27
'  interspersed mod to 20.5" id, also add 4.125" at -z
cyli  5  1  26.035   15.24  -1.27
'  ADD 0.0598" cS drum wall and Bottom
cyli  2  1 26.1869  15.3919  -1.27
'  enclose in cuboid
CUBO  3  1 4P26.1869 15.3919 -1.27

UNIT 4
COM="  COMPLETE ANF-250 PACKAGE   "
ARRAY 1 3R0.0
GLOBAL
UNIT 5
ARRAY 2 3R0.0
repl 4  2  6R3.0  10
END GEOMETRY
READ ARRAY
ARA=1 NUX=1 NUY=1 NUZ=3
FILL 1 2 3 END FILL
ARA=2
NUX=8 NUY=7 NUZ=1
FILL f4 END FILL
END ARRAY

read plot
nch=' fS.*v'
ttl='zx section at         '
xul=0.0 xlr=58. yul=26.18 ylr=26.18 zul=169.00 zlr=0.0
uax=1.0 wdn=-1.0 lpi=6 nax=120 end
ttl='yx section at z=30cm    '
xul=65.16  xlr=-15.0 yul=65.16 ylr=-15.  zul=30.  zlr=30.
uax=1.0 vdn=1.0 lpi=6 nax=120 end
ttl='yx section at      cm'
xul=65.16  xlr=-15.0 yul=65.16 ylr=-15.  zul=30.  zlr=30.
uax=1.0 vdn=1.0 lpi=6 nax=120 end
ttl='yx section at 60cm'
xul=58.  xlr=-30.0 yul=58.16 ylr=-30.  zul=60.  zlr=60.
uax=1.0 vdn=1.0 lpi=6 nax=120 end
nch=' 12345'
ttl='zx section at         '
```

```
xul=0.0 xlr=58. yul=26.18 ylr=26.18 zul=169.00 zlr=0.0
uax=1.0 wdn=-1.0 lpi=6 nax=140 end
ttl='zx section at          '
xul=0.0 xlr=58. yul=0.0 ylr=0.0 zul=169.00 zlr=0.0
uax=1.0 wdn=-1.0 lpi=6 nax=140 end
ttl='yx section at z=30cm   '
xul=65. xlr=-15.0 yul=65.16 ylr=-15. zul=30.  zlr=30.
uax=1.0 vdn=1.0 lpi=6 nax=140 end
ttl='yx section at      cm'
xul=65. xlr=-15.0 yul=65.16 ylr=-15. zul=30.  zlr=30.
uax=1.0 vdn=1.0 lpi=6 nax=140 end
ttl='yx section at 60cm'
xul=58. xlr=-30.0 yul=58.16 ylr=-30. zul=60.  zlr=60.
uax=1.0 vdn=1.0 lpi=6 nax=140 end
end plot
READ START
NST=1
END START
READ BOUNDS
ALL=WATER
END BOUNDS
END DATA
END
```

7. Operating Procedures

7.1 *Container Handling*

Controls and precautions to be exercised during transport, loading, and handling of the shipment, and in the event of an accident or a delay, are described herein.

Nuclear safety hazards to personnel (radiation, contamination, criticality) are minimal during these operations. The hazards more likely to result in injury to personnel are those associated with the physical handling of the heavy containers and components. Appropriate material handling equipment and caution must be used to avoid injury and to avoid damage to the contents.

7.2 *Procedures for Loading and Unloading ANF-250 Containers*

Uranium oxide powder and pellets are loaded into powder jugs or pellet suitcases in the UO_2 Building. These containers are then transferred to the Traffic and Warehousing warehouse where ANF-250 shipping containers are both loaded and unloaded. The following describes the portions of the applicable procedures pertinent to safety. Unloading is done essentially in the reverse order of loading.

1) Remove the outer lid and ring, then remove the vermiculite bag(s) and inner lid. Remove the powder insert lid.

2) Notify HST to perform a survey for internal surface contamination.

3) Check the ANF-250 package for:

   - Conditions of inner and outer containers.
   - Condition of pellet suitcase "cage" or powder insert.
   - Condition of gaskets and gasket seating surfaces.
   - Condition of vermiculite bags.
   - Condition of closure hardware; lids, nuts, bolts, closure ring, etc.
   - Condition of container marking.

4) Repairs or replacement required for any of the above items shall be carried out per applicable procedure.

5) Select the powder jugs or pellet suitcases to be packed into ANF-250 shipping packages.

6) Confirm that the contents to be loaded do not exceed the limits in the Certificate of Compliance.

7) For powder shipments:

- Remove the lid for the powder insert and place the insert into the inner container.
- Load four powder jugs into the powder insert.
- Place the insert lid and gasket onto the insert.
- Apply a torque of 18 ft. lbs. ± 2 ft. lb. to each bolt on the powder insert in a crossing pattern.

8) For pellet shipments:

- Place the pellet suitcase cage into the inner container.
- Align the cage such that the lip on the inner side of the inner container lid will prevent the cage from rotating during shipment.
- Load two pellet suitcase into the cage.

9) Place the inner lid and gasket on the package and tighten the nuts. Torque the inner lid nuts to 35 ft. lbs. ± 3.5 ft. lbs. in a crossing pattern.

10) Place vermiculite bag(s) into the package to fill the void between the inner and outer lid.

11) Put on the outer lid, ring and bolt. The bolt should be located at 10 o'clock or 2 o'clock positions.

12) Torque the outer lid bolt to 45 ft. lbs. ± 4.5 ft. lbs. Use a rubber or plastic mallet, if needed, to help seat the lid ring.

13) Install a tamper indicating seal on the ring bolt.

14) Notify HST for the required contamination survey and radiation level measurements.

15) Affix proper radioactive and address labels to each outer container.

16) Load ANF-250 containers, two to a pallet, onto a truck bed or into a sea container and assure adequate tie down and/or shoring.

17) Notify HST for the required radiation level survey of the truck.

18) Assure proper placarding of the truck.

8. Acceptance Test and Maintenance Program

SPC's radioactive material shipping containers, including the ANF-250 container, are covered by the NRC-approved "Quality Assurance Manual," EMF-1. The scope of this QA program includes design, procurement, fabrication, assembly, maintenance, modification and repair of such shipping containers.

8.1 *Acceptance Tests*

SPC conducts quality inspections of ANF-250 containers prior to first use. The following steps are included in such inspections.

	Typical Characteristic Inspected	
• Outer Container	- Thickness	1
	- Closure ring and bolt	1
	- Vermiculite density	2
	- Material of Construction	2
	- Length	1
• Inner Container	- Wall thickness	1
	- Closure bolts	1
	- Material of construction	2
	- ID	1
	- Length	1
• Powder Insert	- Wall thickness	1
	- ID	1
	- Length	1
	- Material of construction	2
	- Closure bolts	1
• Pellet Suitcase	- Cover dimensions	1
	- Latches	1
	- Material of construction	2
• Container Insert (Suitcase)	- Length	1
	- Height/width of suitcase holder	1
	- Material of construction	2
• The containment vessel is essentially centered and supported by spring steel rods welded to the containment vessel at the top flange and near the bottom of the vessel. Perform at vendor's shop prior to filling with vermiculite or by removal of vermiculite and/or the inner container as necessary.		Visual
• The void space between the containment vessel and the outer container is filled with vermiculite. Remove pipe plugs to perform inspection.		Visual

Typical Characteristic Inspected	
• Outer container shall be properly marked.	Visual
• Visually inspect container welds to insure that parent metals are fused, free of cracks, burn-outs, etc.	100%

1 – Measurement based on approved drawings

2 – Certificate of Conformance from vendor

Note: The "approved drawings" mentioned above are those listed in the current NRC Certificate of Compliance.

8.2 *Maintenance*

ANF-250 containers are maintained and repaired at SPC. The following steps are included in such maintenance and repair and are carried out under the terms of a formal maintenance procedure.

- Inner and outer gaskets shall be replaced when damaged or deteriorated.
- When replacing vermiculite after maintenance or repair, pipe plug seams and seams between inner and outer containers must be sealed with silicone to prevent vermiculite leakage.
- Replace damaged studs and nuts.
- Repaint and mark as required.
- Repair dents 1 inch deep or greater.

9. References

1) SCALE Standardized Computer Analyses for Licensing Evaluation, NUREG/CR-2000 ORNL/NUREG/CSD-2, Volumes 1, 2, and 3.

2) "Application for Use of the ANF-250 Shipping Container for Transport of Radioactive Materials," Revision 5, March 1990.

3) "Critical Separation Between Subcritical Clusters of 4.29 wt% Enriched UO_2 Rods in Water with Fixed Neutron Poisons", NUREG/CR-0073.

4) Nuclear Criticality Safety Experiments Volume 35", pages 278-279, W. Marshall, T.D. Clemson, and G. Walker, ANS TRANSACTIONS (attached).

[1] 10 CFR §71 regulations as of January 1, 1986.

[1] IAEA Regulations for the Safe Transport of Radioactive Materials 1973 Revised Edition (As Amended).

[1] IAEA Regulations for the Safe Transport of Radioactive Materials 1985 Edition with Supplement 1986.

[1] Based upon IAEA 1973 - The requirements may be classified differently in IAEA 1985.

[1] Temperature range is a condition of evaluation in 10 CFR §71.71(c)(1)-38°C and §71(c)(2)-40°C.